REGULATION OF NRF2 BY A KEAP1-DEPENDENT E3 UBIQUITIN LIGASE

A Dissertation presented to

The Faculty of the Graduate School

at the University of Missouri-Columbia

In Partial Fulfillment

of the Requirements for the Degree

Doctor of Philosophy

by

SHIH-CHING (JOYCE) LO

Dr. Mark Hannink, Dissertation Adviser

DECEMBER 2007

The undersigned, appointed by the Dean of the Graduate School, have examined the dissertation entitled

REGULATION OF NRF2 BY A KEAP1-DEPENDENT E3 UBIQUITIN LIGASE

Presented by Shih-Ching (Joyce) Lo

A candidate for the degree of Doctor of Philosophy

And hereby certify that in their opinion it is worthy of acceptance.

Mark Hannink

———————————————————————

Thomas Guilfoyle

———————————————————————

David Pintel

———————————————————————

Grace Sun

———————————————————————

Richard Tsika

———————————————————————

DEDICATION

Okay. Mom, I got you the Ph.D. you asked, at the place you picked. Can I now please do something else? Dad, this is to you, too… you accomplice!

ACKNOWLEDGEMENTS

Dr. Mark Hannink. This work would never have been possible without his guidance, criticism and encouragement. His sheer enthusiasm and critical thinking of science are the most valuable lessons that I could ever obtain during my graduate studies.

I should also extend my appreciation to my committee members, Drs. Thomas Guilfoyle, David Pintel, Grace Sun and Richard Tsika, as well as Drs. Lesa Beamer, Joan Conaway, Beverly DaGue, Marc Johnson, Alan Diehl and Michael Henzl, for their insightful advice and thoughtful comments on this work.

I thank the present and previous members in Dr. Hannink's laboratory, including Drs. Donna Zhang, Rick Sachdev, Sang-Hyun Lee, Xuchu Li, as well as Brittany Angle, Carolyn Eberle, Zheng Sun, Jordan Wilkins, Marquis Patrick, Xiaofang Jin, Casey Williams, Joel Pinkston, Julie Unverferth, and Benjamin Creech. They provided me with technical help and inspiring discussions on this work.

Toward completion of my graduate study, I have also received copious amounts of help and encouragement from friends and colleagues both on campus and elsewhere. While it is not possible to list all the names due to space constraint, I would like to express my appreciation to them all.

TABLES OF CONTENTS

CHAPTER

   A. A snapshot of the ubiquitin/proteasome system (UPS)

   B. General features of cullin-RING ligases (CRLs)

   B.1. The cullin family

   B.2. The RING finger proteins in cullin-RING ligases

   B.3. Substrate adaptors of cullin-RING ligases

   B.4. Recognition of degradation signals in substrates by substrate adaptors

   B.5. Architecture of cullin-RING ligases and the 'positioning' model

   B.6. Polygamy among substrates and substrate adaptors, and the 'processivity' model

   B.7. Cyclic assembly and disassembly of cullin-RING ligase complex, and the major

      mediator CAND1

   C. Modulation of cullin-RING ligase activity toward substrates

   C.1. Modulation of substrate binding events

   C.2. Dimerization of culiin-RING ligases

   C.3. Dynamic subcellular localization of cullin-RING ligases: circuit riders in CRL

      systems.

LIST OF TABLES

LIST OF FIGURES

REGULATION OF NRF2 BY A KEAP1-DEPENDENT E3 UBIQUITIN LIGASE

Shih-Ching (Joyce) Lo

Dr. Mark Hannink, Dissertation Advisor

ABSTRACT

Oxidative damage to biological macromolecules has been implicated in diverse pathophysiological processes, including cancer, neurodegeneration, aging and cardiovascular disease. The Nrf2 transcription factor regulates expression of ROS (reactive oxygen species)-scavenging enzymes and enables mammalian cells to counteract oxidative stress and maintain redox homeostasis. The Keap1 protein functions as a substrate adaptor for a Cul3-RING dependent E3 ubiquitin ligase complex and targets Nrf2 for proteasome-mediated degradation under homeostatic conditions. The Keap1-Cul3-RING ubiquitin ligase is inactivated following exposure of cells to oxidative stress or electrophilic chemicals, resulting in accumulation of Nrf2 and activation of Nrf2-dependent cytoprotective gene expression.

The Keap1-Cul3-RING ubiquitin ligase complex is modulated at multiple levels, such that steady-state levels of Nrf2 are finely tuned in response to cellular redox conditions. The experiments presented in this dissertation have demonstrated that both neddylation of Cul3 on Lys 712 and CAND1-dependent cyclical assembly and disassembly of the Keap1-Cul3-RING ubiquitin ligase are required for optimal activity of the ligase. To achieve inhibition of Nrf2 turnover, quinone-induced oxidative stress

stimulates autoubiquitination and self-degradation of the substrate adaptor Keap1, while sulforaphane, an electrophilic isothiocyanate, interferes with binding of Keap1 to Cul3

Keap1 contains an N-terminal BTB domain and a C-terminal Kelch domain. The BTB domain of Keap1 mediates homodimerization while the Kelch domain binds substrate proteins such as Nrf2. A number of critical amino acid residues located within the substrate-binding pocket of Kelch β-propeller domain of Keap1 make key contacts with the conserved (D/N)xE(T/S)GE motifs in the substrate protein. The two Kelch domains within the Keap1 dimer bind substrate independently, allowing one Keap dimer to simultaneously bind two different substrate proteins.

Phosphoglycerate mutase 5 (PGAM5) is a newly identified Keap1-binding protein. Under normal tissue culture conditions, PGAM5 is predominantly localized at the outer membrane of mitochondria via an intrinsic mitochondrial-targeting sequence at the N-terminus. PGAM5 nucleates formation of a mitochondrial ternary complex consisting of one PGAM5, one Keap1 homodimer, and one Nrf2. As a result, a distinct subpopulation of the Keap1-Nrf2 complex is anchored at mitochondria and may facilitate communication between the nuclear anti-oxidant genes that are regulated by Nrf2 and ROS produced by mitochondria. Our studies have provided valuable insights into how Nrf2-dependent anti-oxidant gene expression is modulated in response to changes in cellular physiology and have provided a mechanistic framework for the development of novel therapeutic strategies to counteract the pathophysiological consequences of oxidative stress.

I.   INTRODUCTION

A. A snapshot of the ubiquitin/proteasome system (UPS)

Modulation of the steady-state levels of regulatory proteins in a timely and selective manner is employed to switch regulatory circuits from one state to another in many cellular and organismal processes. As important as protein synthesis, protein degradation has emerged as a critical mechanism in control of protein abundance by abruptly eliminating regulatory proteins. In eukaryotes, the bulk protein degradation is achieved by the ubiquitin/26S proteasome system in the cytoplasm and nucleus.

The 26S proteasome is the main self-compartmentalized protease of eukaryotes. This enzyme utilizes the energy of ATP to drive the translocation of a protein substrate into a chamber where proteolysis is accomplished rapidly and completely. The 26S proteasome is assembled from the proteolytic 20S and the regulatory 19S complexes. The 20S complex consists of ~28 subunits that are arranged into four rings (α, β, β, and α), and form a barrel-shaped structure. The subunits in β rings harbor proteolytic sites that are sequestered within the "barrel" and catalyze polypeptide hydrolysis. The 19S regulatory complex consists of at least 18 subunits that are arranged into a base and a lid subcomplex. One of the major functions of the 19S regulatory complex is to recognize the proteolytic signals of a protein substrate. Unlike conventional proteases, which recognize amino acid chains near the cleavage sites in the substrate, the 26S proteasome targets substrates that are covalently modified with the ubiquitin protein. In particular, the

1

19S subcomplex binds with the highest affinity to a polymer comprised of four or more ubiquitins that are conjugated through lysine 48 of each ubiquitin (for full review, see [1]).

Ubiquitin is a 76-amino acid protein and is highly conserved among eukaryotes. Ubiquitination is a reaction in which the carboxyl group of Gly76 in ubiquitin forms an isopeptide bond with the ε-amino group of a lysine residue in a substrate protein. Polyubiquitination is carried out when additional ubiquitin molecules are conjugated in sequence through linkage between Gly76 of the succeeding ubiquitin and a lysine residue of the preceding ubiquitin, such that a substrate protein is modified by a polymer of branched ubiquitin chain. Ubiquitin contains seven conserved lysine residues, all of which can potentially be used for formation of polyubiquitin chain. However, the extent of a polyubiquitin chain and the type of ubiquitin-ubiquitin linkage can confer distinct fates for substrate proteins. A polyubiquitin chain of at least four ubiquitin molecules linked via Lys48 is essential for efficient degradation by 26S proteasome [2].

Each ubiquitination reaction is mediated by a three-enzyme cascade: (1) an activating E1 enzyme forms a thiol ester bond between its reactive cystein residue and the carboxyl group of Gly76 in an ubiquitin; (b) a conjugating E2 enzyme inherits the thio-ester-bonded ubiquitin from the E1 enzyme; (3) an E3 ligase facilitates transfer of the activated ubiquitin from the E2 to the lysine residue in a substrate, or a substrate-bound ubiquitin (for full review, see [3]). This ubiquitination machinery is highly hierarchical. In human, there is only one E1 enzyme that activates the entire pool of ubiquitin

molecules; a handful of E2 ubiquitin conjugating enzymes, each of which functions in several E3 ubiquitin ligases; and a large number of E3 ubiquitin ligases. In addition to their ability to bind E2, E3 ubiquitin ligases contain diverse modules that recognize specific degradation motifs in substrates, and thereby dictate the specificity of ubiquitination reactions. Moreover, productive ubiquitination depends on successful interaction and positioning of E3 ubiquitin ligases with E2 enzymes and cognate substrates. Thus, modulation of E3 activity and E3-substrate interaction has merged as key mechanisms in regulation of ubiquitin-dependent protein degradation.

E3 ubiquitin ligases are classified into two major groups, HECT-domain and RING-finger E3s, based on the domains that mediate E2 binding (for full review, see [4]). The HECT domain contains a strictly conserved cysteine residue that forms a catalytic intermediate with ubiquitin via a thiol ester bond, whereas the RING-finger does not. Instead, the RING E3s function as molecular scaffolds that bring ubiquitin-charged E2s and the lysine residues of cognate substrates into close proximity to facilitate nucleophilic attack in ubiquitin transfer. RING E3s can either function as a single subunit, or assemble with other protein members in a multi-subunit complex. Multisubunit RING E3s are often assembled on a cullin scaffold protein, and therefore termed cullin-RING ligases (CRL). Cullin-RING complexes are found throughout eukaryotes, and constitute the largest known class of E3 ubiquitin ligases to date. We herein describe the general composition, properties and function of cullin-RING ligases, and discuss the potential mechanisms underlying the regulation of CRL activity.

B. General features of cullin-RING ligases (CRLs)

A typical cullin-RING ligase is generally comprised of a handful of subunit proteins that contain functionally conserved modules. In the following sections, we first describe the domain organization and properties of each CRL subunit. We then describe a signature architecture that is widely adopted in cullin-RING ligases to arrange the assembly of these subunits. Finally, we discuss several characteristics of CRL that lie at the heart of CRL kinetics, and shape CRL's efficacy toward ubiquitination of cognate substrates.

B.1. The cullin family

Members in the cullin family are structurally related proteins that are defined by the presence of an evolutionarily conserved cullin domain. Cullin domains are characterized by a long N-terminal curved stalk and a distinct C-terminal globular domain. The N-terminal domain consists of three copies of a five-helix bundle, and is termed cullin repeats. The C-terminal domain contains multiple structure units that are organized by a four-helix bundle (4HB) and form a V-shaped groove, and is termed cullin-homology domain [5].

Yeast genomes encode three cullins: Cul1 and Cul3 orthologs (Cdc53 and Cul3/Ygr003w), and Cul8 (Rtt101/Yjl047c) in *Saccharomyces cerevisiae*; Cul1, Cul3 and Cul4 orthologs in *Schizosaccharomyces pombe* (Pcu1, Pcu3, and Pcu4). Worm and

fruit fly genomes each encode at least six cullins. In humans and rodents, seven different cullin proteins have been identified and studied (Cul1, 2, 3, 4A, 4B, 5 and 7). Each is capable of nucleating a three to five subunit complex that exhibits E3 ubiquitin ligase activity. In addition, the APC2 protein contains a cullin-homology domain, and functions as a molecular scaffold in the multi-subunit RING E3 ubiquitin ligase APC/C (Anaphase-promoting complex/ cyclosome). However, the core complex of APC/C is composed of thirteen different subunits that are organized and operate in an exceptionally complicated manner. Thus, APC/C is functionally analogous with, yet architecturally divergent from the typical cullin-RING ligases.

B.2. The RING finger proteins in cullin-RING ligases

RING finger proteins comprise a large family, in which members contain a cysteine and histidine-featured fold that accommodates two zinc ions in a cross-brace structure, termed RING finger [6]. These zinc ions and their ligands are catalytically inert. Instead, their characteristic lies in a highly conserved spacing between zinc ligands, such that RING finger proteins often function as molecular modules in protein complex scaffolding, rather than chemical catalysts. An increasing number of RING finger proteins have been identified as bona fide single subunit E3 ubiquitin ligases that mediate assembly of E2 ubiquitin conjugating enzymes and cognate substrates. On the other hand, three members in RING-H2 subfamily, Rbx1 (Roc1/Hrt1), Rbx2, and Apc11, are essential components of multi-subunit E3 ubiquitin ligases, in which they constitute core complexes with cullins.

Rbx1 is a small RING-H2 protein that shares high sequence identity among orthologues in eukaryotes. It binds to Cul1, 2, 3, 4A, 4B, and 7, and appears to be the most commonly utilized RING finger module in cullin-RING ligases. Rbx1 contains an N-terminal β-strand, and a C-terminal RING domain that is stabilized by zinc ions. On one hand, the E2 ubiquitin conjugating enzymes are recruited to Rbx1 via a hydrophobic groove in the RING domain of Rbx1. On the other hand, Rbx1 assembles with cullins via extensive interactions in between. In the primary interactions, an intermolecular β-sheet is formed by the N-terminal β-strand of Rbx1 and several structure units in the C-terminal domain of cullins. In the secondary interactions, the C-terminal RING domain of Rbx1 slightly packs into a V-shaped groove on the cullin-homology domain of cullins [5].

B.3. Substrate adaptors of cullin-RING ligases

A key feature of cullin-RING ligases is that each cullin can assemble with a number of different substrate adaptor proteins, each of which recruits different substrates for degradation. A substrate adaptor protein contains a substrate-binding domain and a cullin-binding module that can be present on the same or different polypeptide. The cullin-binding modules display considerable structural homology, including BTB (Broad-complex, Tramtrack and Bric-a-brac) domains and BTB folds. In contrast, the substrate-binding domains come in great variety that in turn allows recruitment of a broad range of substrates for cullin-RING ligases. Based on the protein-protein interaction motifs, it is estimated that in humans, there are ~600 putative substrate adaptor units for the various

known CRLs. Among these, approximately 50 have been shown to assemble and function in CRLs. Three well-characterized examples are described below.

Skp1:F-box protein complex. In Cul1-based and Cul7-based cullin-RING ligases, the substrate adaptors function as a two-subunit complex that consists of the Skp1 protein and a F-box protein (FBP). The BTB fold-containing Skp1 protein binds simultaneously to Cul1 and an F-box protein. The F-box proteins bind to Skp1 through the F-box motif, and to substrates through C-terminal specialized protein-protein interaction domains. F-box proteins are found in all eukaryotes. Mouse and human genomes each contain more than a hundred F-box proteins. As defined by their substrate-binding domains, the mammalian F-box proteins are further classified into three groups [7]: (1) the FBW proteins, such as Cdc4 (Fbw7) and β−TrCP1, which contain WD-40 repeats that form a β-propellar structure [8, 9]; (2) the FBL proteins, such as Skp2, which contain leucine-rich repeats (LRRs) that form a curved blade structure of α−helix/β−strand repeats [5]; (3) the FBX proteins which contain neither WD-40 repeats nor leucine-rich repeats, but often have distinct substrate-binding domains, such as CASH (carbohydrate binding and sugar hydrolysis) and zinc-finger domains.

Elongin B/C:SOCS-box protein complex. In Cul2-based and Cul5-based cullin-RING ligases, the substrate adaptors function as a three-subunit complex that consists of the Elongin C/B dimer and a SOCS-box containing protein [10]. In a similar fashion to Skp1:F-box module, Elongin C bridges the interaction between Cul2/5 and the SOCS-box proteins, while the SOCS-box proteins recruit various substrates through additional

protein-protein interaction domains, such as SH2 domain and ankyrin repeats. Although the function of Elongin B in CRLs is not understood, the assembly of Elongin B significantly stabilizes the otherwise labile Elongin C:SOCS-box protein complex.

BTB domain proteins. In Cul3-based cullin-RING ligases, the function of substrate adaptors is carried out by a single protein that contains both a BTB domain and a substrate-binding domain. Mouse and human genomes each encode ~400 BTB domain proteins that contain additional protein-protein interaction domains, such as ankyrin repeats, Kelch repeats, MATH, and zinc finger domains [11]. The BTB-Kelch double domain containing proteins in particular, have a growing list of physiological substrates identified, raising the possibilities that BTB-Kelch proteins may in general function as substrate adaptors in Cul3-based cullin-RING ligases.

B.4. Recognition of degradation signals in substrates by substrate adaptors

Binding of substrates by substrate adaptors is a critical determinant in CRL-mediated protein degradation. Effective binding requires presentation of degradation motifs in substrates that can subsequently be recognized by the corresponding substrate adaptors. Degradation signals can be present intrinsically as a stretch of specific amino acid sequences in substrates, and result in otherwise constitutive degradation of substrates. This will be discussed later in this chapter, in the section of Nrf2 degradation by a Keap1-dependent CRL. On the other hand, degradation signals are in many cases formed via post-translational modifications, resulting in inducible degradation of substrates. Three

common post-translational modifications that govern degradation signals are listed below, each provided with a well-studied example.

Proline-hydroxylation. HIF-1 (hypoxia-inducible factor-1) is a transcriptional complex that activates expression of a genetic program to cope with hypoxic conditions in cells. HIF-1α subunit undergoes rapid degradation by a pVHL(von Hippel-Lindau)-dependent Cul2-RING ligase in the presence of oxygen. Under normoxic conditions, critical proline residues in HIF-1α subunit are subjected to hydroxylation by a group of 2-oxoglutarate-dependent, non-heme dioxygenases. These hydroxylations trigger direct interaction of HIF-1α with a conserved hydroxyl proline-binding pocket in pVHL, hence lead to efficient degradation of HIF-1α [12, 13].

Phosphorylation. Cyclin E functions to promote transition from G1 to S phase. Protein abundance of Cyclin E oscillates during a normal cell cycle. Stringent controls of cyclin E degradation are in part achieved by Fbw7-dependent Cul1-RING ligases in response to phosphorylation of cyclin E. Cyclin E can be phosphorylated in vivo at four sites, including a cluster of C-terminal sites, S372, T380, and S384, and a N-terminal site, T62. Although phosphorylation at T380 of cyclin E alone presents a high-affinity binding motif for the substrate adaptor Fbw7, efficient degradation of cyclin E requires phosphorylation at multiple sites [14, 15]. It is likely that phosphorylation at multiple sites reorients Fbw7-bound cyclin E in a way that allows better presentation of the susceptible lysine residues for ubiquitin transfer.

Glycosylation. N-linked glycosylation of proteins occurs in the endoplasmic reticulum (ER) and, in part, functions to facilitate chaperone-mediated protein folding and degradation. Glycoproteins that fail to fold correctly are retrotranslocated from ER and degraded in cytoplasm by the ubiquitin/proteasome system. Fbx2-dependent Cul1-RING ligases can target glycoproteins for degradation in an N-glycan-dependent manner [16]. Immediately downstream of the F-box motif, the N-terminal module of Fbx2 (Fbs1) forms a β-sandwich structure that contain a small hydrophobic pocket. This hydrophobic pocket primarily binds $Man_3GlcNAc_2$, and thereby enables Fbx2 to target high mannose N-linked glycoproteins for degradation [17]. Given the broad range of glycoproteins that are attached to high mannose oligosaccharides, Fbx2 may play a significant role in protein quality control.

B.4. Architecture of cullin-RING ligases (CRLs) and the 'positioning' model

The typical cullin-RING ubiquitin ligases share strikingly similar architecture (Figure I-1). In general, cullins serve as the complex organizational center. The C-terminal globular domains of cullins bind to the RING finger protein Rbx1 (Roc1/Hrt1), or Rbx2 in the case of Cul5-based CRL. The N-terminal stalk regions of cullins bind to either a substrate adaptor subcomplex, or a single substrate adaptor protein in the case of Cul3-based CRL. The RING finger proteins recruit ubiquitin-charged E2 conjugating enzymes, while the substrate adaptor proteins recruit the cognate substrates. As revealed by three-dimensional X-ray crystallography studies, the cullin-RING ligases have a rigid structural organization with no obvious flexible hinge regions or rotatable domains [5, 9].

The overall rigidity of CRLs provides productive positioning of the substrates, such that the effective concentration of the substrate lysine residues is increased in the vicinity of the E2, and theses lysines are optimally presented to the E2 active site to favor ubiquitin transfer.

A paradoxical issue to consider though is that there is generally a 50-60 Å gap between the substrate-binding site of a substrate adaptor and the thiol ester bond of Ub~E2 in a CRL (Figure I-2) [5, 9]. It is not known how this 50-60 Å gap is bridged. However, this spatial gap may accommodate larger-scaled movement of a substrate's lysine residues that in turn enables productive positioning of Lys48 in the distal ubiqutin as a poly-ubiquitin chain grows. The structural data in support of this tentative notion is still awaited.

B.5. Polygamy among substrates and substrate adaptors, and the 'processivity' model

Mutual polygamy is a common feature in cullin-RING ligase system, in that one substrate can be targeted by different CRLs, and one substrate adaptor in a CRL can target diverse substrates for degradation. On one hand, various degradation signals can be formed in the same substrate upon different stimuli, and thereby allow recognition of one substrate by different substrate adaptors. For example, cyclin E can be targeted for degradation by an Fbw7-dependent Cul1-RING ligase and a Cul3-RING ligase (the BTB domain substrate adaptor is yet to be identified). The Fbw7-dependent turnover of cyclin

E requires phosphorylation at T380 and multiple other sites, in which association of cyclin E with Cdk2 kinase is a prerequisite. Conversely, degradation of cyclin E by Cul3-RING ligase does not require phosphorylation at T380, nor does it require association with Cdk2. In fact, assembly with Cdk2 prevents cyclin E from Cul3-mediated ubiquitination [18-20]. It is likely that these two distinct CRLs may complement to control levels of free cyclin E as well as Cdk2-bound cyclin E.

On the other hand, versatility is enhanced as a single substrate adaptor in cullin-RING ligase can target multiple substrate proteins for degradation. For example, β-TrCP in Cul1-RING ligase is responsible for ubiquitination of IκBα and β-catenin [21]; Fbw7 in Cul1-RING ligase is responsible for degradation of cyclin E, c-Jun, c-Myc, and Notch [22-25]; Keap1 in Cul3-RING ligase is responsible for ubiquitination of Nrf2 and PGAM5 [26, 27]; gigaxonin (GAN) in Cul3-RING ligase is responsible for degradation of MAP1B light chain, and TBCB (tubulin folding cofactor B) [28, 29]. It is intriguing how CRLs have evolved with such delicate mechanisms whereby one substrate adaptor is able to juggle among multiple substrates in response to diverse cellular signaling.

A 'processivity' model was proposed to explain how one cullin-RING ligase discriminates between different substrates in order to execute their destruction at different timing and with different kinetics. In this model, processivity is defined as the number of ubiquitin molecules that are conjugated into polyubiquitin chains on a substrate during one single binding event [30, 31]. (One binding event is defined as the episode starting at association of one substrate with a CRL and ending at the following dissociation of this

substrate from the CRL.) Highly processive substrates might obtain polyubiquitin chains sufficient for degradation during one timet binding with CRLs, while less processive substrates would require multiple rounds of binding with CRLs to achieve full polyubiquitination. In between substrate binding events, these suboptimal ubiquitin chains that are not susceptible to 26S proteasome are instead prone to de-ubiquitination enzymes. De-ubiquitination enzymes trim down these ubiquitin chains with their isopeptidase activity, and further amplify the differences in kinetics of substrate ubiquitination. Thus, by exploiting differences in processivity, CRLs are able to mediate degradation of substrates with varying degrees of preference.

For example, the ubiquitin E3 ligase APC/C coordinates mitosis and G1 by promoting a number of cell cycle regulators for degradation in a temporal order [32]. The APC/C is activated in early mitosis by the activator Cdc20, and during anaphase by a second activator Cdh1. Shortly after APC/C is assembled with the activator Cdh1 in anaphase, the first activator Cdc20 is degraded. Subsequently, PlK1 and Aurora A are degraded after they have functioned in telophase and cytokinesis, and following that, UbcH10 E2 enzyme is degraded. Finally, at low levels of UbcH10, cyclin A is no longer degraded, whereas another substrates, such as securin and geminin, are still degraded by APC/C-Cdh1. A series of *in vitro* studies showed a striking correlation between the processivity of these substrates and the relative timing of their degradation in cell cycle: the higher processivity a substrate displays, the earlier it is degraded relatively to the other substrates [31]. Although the determinants of processivity remain elusive, differences in substrate processivity may allow APC/C-Cdh1 to carry out degradation of

13

multiple substrates at a defined temporal sequence, and therefore ensure the orderly progression of cell cycle.

B.6. Cyclic assembly and disassembly of cullin-RING ligase complexes, and the major mediator CAND1

Given the large number of substrate adaptors and a limited amount of cullin proteins in vivo, the complex-cycling model was proposed to explain how multiple substrate adaptors compete for access to a common cullin-RING subcomplex [33, 34]. In this model, a cullin protein dissociates from one substrate adaptor that has accomplished its (temporal) mission, and subsequently associates with the next substrate adaptor to carry out another round of ubiquitination on the bound substrate. A key feature in this model is that continuous cycles of association and disassociation between cullins and substrate adaptors are essential to sustain CRL activity towards diverse substrates.

CAND1 (TIP120A) is a cullin-binding protein, and has merged as an important player in the process of cyclic assembly and disassembly of CRLs. CAND1 forms a U-shaped double-layer structure that consists of 27 consecutively stacked HEAT repeats of antiparallel helices. The hallmark of CAND1 structure is an additional curvature on each end, in which N-terminal and C-terminal halves are further twisted 90° and form two superhelical strucutures facing toward the same side. As a result, this concave side of CAND1 creates a ~ 40 Å x 80 Å x 40 Å space that is able to accommodate an elongated molecule, such as cullin proteins. Three-dimensional X-ray crystallography studies show

that CAND1 assembles with Cul1 by utilizing multiple binding sites that extend throughout both proteins. The N-terminal curvature of CAND1 grasps the C-terminal globular domain of Cul1, while its central and C-terminal curvatures clasp around the N-terminal stalk of Cul1 [35].

In particular, a long β hairpin structure protruding from the 25th HEAT repeat of CAND1 directly interacts with α helices in the first cullin repeat of Cul1 that are otherwise involved in binding of the substrate adaptor Skp1. Consistently, when CAND1:Cul1 structure and Skp1:Cul1 structure are superimposed, this β hairpin of CAND1 significantly collides with the BTB fold of Skp1 that mediates interaction with Cul1 [35]. These spatial conflicts suggest a competitive relationship between CAND1 and Skp1 for binding of Cul1. Indeed, binding of CAND1 with Cul1 causes dissociation of Skp1, and release of CAND1 from Cul1 enables assembly of Skp1 into an active Cul1-RING ligase [36, 37]. In CRL systems, a general role for CAND1 is to control assembly and disassembly of substrate adaptors with cullins. Thus, dynamic association and disassociation between CAND1 and cullins can sway the kinetics of CRL complex cycling, and in turn modulate CRL activities. We will discuss key regulators in CAND1-dependent cycles of CRL assembly and disassembly in the later sections.

C. Modulation of cullin-RING ligase activity toward substrates

The cullin-RING ligase activity is regulated at multiple levels through various modes. The versatility in regulation of CRLs enables destruction of substrates to be

efficiently fine-tuned in response to diverse cellular signaling. In this section, we discuss featured regulatory mechanisms and key regulators in CRL systems.

C.1. Modulation of substrate binding events

Following recognition and delivery of substrates to CRLs, the interaction between substrates and CRLs can further be modulated. As a result, the overall binding affinity of a substrate that is situated in a CRL for ubiquitination differs from the site-specific binding affinity that initially triggers substrate recognition. This allows a secondary control to guard the threshold for ubiquitination, or to set changes in substrate processivity. Below are listed several detailed mechanisms that modulate substrate binding events within CRLs in a post-recognition manner.

Increased stability of binding by additional contacts. Certain substrate proteins in Cullin-RING ligase systems contain additional CRL-binding motifs that are distinct from degradation signal motifs. A degradation signal motif is first utilized for recognition of a substrate by its cognate substrate adaptors via specific binding. Once the substrate is delivered to the CRL, distinct motifs within the substrate are further utilized to make extra contacts with subunits of the CRL as the substrate reorients, such that the overall substrate binding is stabilized by these extended interactions. Importantly, the efficiency of substrate ubiquitination can be increased in accordance to its binding stability.

For example, securin (Pds1) is an inhibitor for mitotic sister chromatid segregation. During anaphase, securin undergoes ubiquitin-dependent degradation by APC/C E3 ligases to promote cell cycle progression. Securin proteins are highly processive substrates for APC/C, and contain two consensus sequence motifs that are required for their rapid degradation. These two motifs are termed D box (destruction box), and KEN box respectively. Recognition of securin by APC/C-Cdh1 is mediated through specific binding between KEN box of securin and the activator Cdh1, a process that does not require D box. Subsequently within the APC/C-Cdh1-securin complex, the D-box of securin further makes direct interaction with APC/C-Cdh1, and thereby increases stability of this complex assembly. Interestingly, when replaced with a cryptic D box from a low processive substrate of APC/C-Cdh1, securin is converted to a low processive substrate. Thus, additional interaction between substrates and APC/C-Cdh1 that is mediated by D box presents a critical determinant for processivity of substrate ubiquitination [31, 38].

Reinforced binding by accessory proteins. In some cases of CRLs, accessory proteins participate in substrate binding events through simultaneous association with a substrate and a substrate adaptor, and consequently contribute to substrate ubiquitination. For example, the cyclin-dependent kinase (CDK) inhibitor $p27^{Kip1}$ is subject to ubiquitin-mediated proteolysis during G1/S transition in cell cycle. Phosphorylation at Thr187 in $p27^{Kip1}$ triggers its recognition by a Skp2-dependent Cul1-RING ligase, but is insufficient for productive ubiquitination. In *in vitro* reconstituted systems, addition of purified Cks proteins markedly increases ubiquitin conjugation onto $p27^{Kip1}$ without affecting its phosphorylation kinetics. Further in vitro and in vivo studies show that Cks causes a

dramatic increase in association between substrate p27^{Kip1} and substrate adaptor Skp2 in a phosphor-Thr187-dependent manner, suggesting that Cks may function to reinforce binding of phospho-p27^{Kip1} with Skp2 for efficient ubiquitination [39, 40]. Indeed, pull-down analysis has shown direct binding of the accessory protein Cks with the substrate phospho-p27^{Kip1}, and with the substrate adaptor Skp2. In agreement with this, crystal structure studies further revealed interactions between Cks, Skp2 proteins, and a p27^{Kip1}-derived 10-mer phospho-peptide (a.a. 181-190) [41]. The substrate-binding LRR domain of Skp2 forms a curved blade structure of ten α-helix/β-strand repeats. The concaved surface presented by the ten β-strand repeats on the top face of LRR domain provides an interaction platform for Cks and phospho- p27^{Kip1}. Cks is a small protein that consists of a four-stranded β sheet, and two α helices. It binds to the concaved surface of the Skp2 LRR domain via extensive hydrophobic bondings and Van der Waals contacts. On the other hand, the p27^{Kip1}-derived phosphopeptide displays a partially extended conformation, and spans around Cks and the LRR domain of Skp2 in a bipartite manner: (1) residues 181-184 in p27^{Kip1} pack with Skp2; (2) Glu185 of p27^{Kip1} inserts in between Cks and Skp2 and forms bifurcated hydrogen bonds with both proteins; (3) residues 186-190 in p27^{Kip1} turn back to Cks whose β-sheet forms a shallow pocket to bind the phosphate group of phospho-Thr187 in p27^{Kip1}. An intriguing indication here is that the phospho-Thr187 in p27^{Kip1} may function in two independent processes: first to initiate Skp2-dependent recognition, and secondly to fortify Cks-mediated stabilization in binding of p27^{Kip1} with Skp2.

The mechanisms underlying the ordered assembly of the ternary complex p27^{Kip1}-Spk2-Cks remain obscure. As the binding of Cks does not cause any significant conformational change in Skp2 [41], it is likely that Cks binding triggers rearrangement in the orientation and interaction contacts among the p27^{Kip1}, Spk2, and Cks, and results in tighter association of the trio. The three-dimensional structural analysis of complexes consisting of either two members from the trio will further address this hypothesis.

Increased binding probability by 'allovalency'. The 'allovalent' model was proposed to explain how a Cullin-RING ligase may increase binding probability toward a substrate of otherwise poor binding affinity, in order to promote ubiquitination efficiency [8]. In this model, one single substrate contains multiple degradation signal motifs, each of which can bind weakly to a single substrate-binding site within a substrate adaptor. Upon initial recognition of the substrate by the substrate adaptor, local concentration of degradation signal motifs is increased in proximity of the substrate-binding site. Even though the substrate might be dissociated due to its low affinity-binding motif, re-association can readily occur through another nearby binding motif in the substrate, such that the substrate would not diffuse away. In a sense, the overall binding probability between the substrate and the substrate adaptor is increased via this mode of allovalent binding.

The hallmark in this model is that the overall binding probability increases exponentially with the number of degradation signal motifs present in a substrate. For example, ubiquitin-dependent degradation of the cyclin-dependent kinase (CDK)

inhibitor Sic1 is required for cyclin B-CDK activity and DNA replication in cell cycle in yeast. Ubiquitination of Sic1 is accomplished by a Cdc4-dependent Cul1-RING ligase following phosphorylation of Sic1. There are nine threonine- or serine-containing consensus motifs in Sic1 that, once phosphorylated, can be recognized by Cdc4, and are termed Cdc4 phospho-degron (CPD). However, due to electrostatic repulsion generated from basic residues in the CPDs of Sic1 and in the CPD-binding pocket within Cdc4, each of the CPDs in Sic1 binds to Cdc4 only with low affinity, and is not sufficient for degradation of Sic1. Remarkably, phosphorylation on any six of its nine sites results in efficient binding of Sic1 with Cdc4 and productive polyubiquitination onto Sic1 [8]. Consistent with allovalent model, a series of suboptimal CPDs in Sic1 modulates binding probability with Cdc4. Thus, phosphosrylation of CPDs of Sic1 sets the threshold for Sic1 degradation.

Binding affinity guard by pseudo-substrates. The idea of pseudosubstrate was introduced into CRL systems for certain substrate-like proteins that assemble into CRLs in a manner resembling substrate-substrate adaptor binding, but are not subject to productive ubiquitination for proteasome-dependent degradation. Instead, by using their suboptimal binding affinity for substrate adaptors, these pseudosubstrates likely function to guard the threshold for 'true' substrate binding with CRLs [42]. That is, pseudosubstrate proteins do not interfere with high affinity binding between degradation signal motifs present in substrates and substrate adaptors, but they interfere with premature bindings of substrates or nonspecific bindings of irrelevant proteins onto substrate adaptors.

For example, ribonucleoprotein hnRNP-U is an abundant phospho-protein that stably associates with a large pool of the F-box protein β-TrCP1/E3RS *in vivo* [42]. hnRNP-U directly binds residues within WD-repeats of β-TrCP1/E3RS that are also utilized to recruit the phosphorylated substrate IκBα. Unlike IκBα however, hnRNP-U does not contain a classic DSGxxS motif that, upon phosphorylation, binds β-TrCP/E3RS with high affinity. As a result, hnRNP-U can assemble into β-TrCP1/E3RS-dependent Cul1-RING ligases through substrate-binding site, yet undergoes very little ubiquitin conjugation. Furthermore, despite its seemingly stable association with β-TrCP1/E3RS, hnRNP-U can be readily replaced by fully phosphorylated DSGxxS peptides, but not semi-phosphorylated ones. Thus, hnRNP-U is a suitable pseudosubstrate. Interestingly, pre-incubation of β-TrCP1/E3RS-dependent Cul1-RING ligases with hnRNP-U proteins significantly increases polyubiquitination of phospho-IκBα substrates, suggesting that hnRNP-U may play an active role in CRLs to facilitate subsequent ubiquitination of bona fide substrates. An intriguing notion is that, in addition to serving as an affinity guard, pseudosubstrates function in pre-production of highly active forms of CRLs, such that once engaged with true substrates, these CRLs are ready to mediate substrate destruction with high efficiency. A plausible mechanism underlying this active role of psedosubstrates will be discussed in detail in the later sections.

C.2. Dimerization of cullin-RING ligases

Components in Cullin-RING ligases, including substrate adaptors and cullins, have each been shown to form a dimeric complex that can often enhance CRL activity. Computational modeling of the whole CRL complexes indicates that homotypic dimerization of substrate adaptors can lead to assembly of a super-complex containing two sets of CRLs. In this section, we will discuss the putative conformation of this dimeric CRL supercomplex and its biochemical impact on processivity of the bound substrates. In addition, new studies suggest that cullins can form homotypic dimers independently of substrate adaptors. We will also discuss what is known about cullin dimerization in this section.

Dimerization of substrate adaptors. A number of substrate adaptors in CRLs are able to form homotypic dimers, including the F-box proteins Cdc4, Fbw7 and β-TrCP, the BTB domain protein Keap1, and the SOCS-box protein pVHL [43-47]. A thorough characterization of Cdc4-dependent Cul1-RING ligases demonstrated that dimerization of Cdc4 significantly promotes degradation of weakly-associated substrates, such as phosphorylated Sic1 (phospho-Sic1), but has little effect on tightly-associated substrates [48]. In vitro quantitative binding assays showed equal affinities between monomeric and dimeric Cdc4 for binding of phospho-Sic1 [43], suggesting that dimerization of Cdc4 does not cause conformation change in Cdc4 that might otherwise stimulate substrate recognition. On the other hand, a series of *in vitro* ubiquitination assays over a time course revealed that the time period required for dimeric Cdc4 to generate long polyubiquitin chains onto phospho-Sic1 was dramatically decreased [43], suggesting that dimerization of Cdc4 may function to enhance processivity of substrate Sic1.

Dimerization of Cdc4 is mediated by the N-terminal conserved region preceding the F-box within Cdc4, termed the D domain [44, 48]. The D domains are each comprised of three α helices, and form a parallel dimer via hydrophobic bindings within the D domain dimer interface. A structure model of the entire Cdc4-dependent Cul1-RING ligase complex containing this D domain dimer was constructed by computational modeling. In this model, dimerization of D domains results in the assembly of a super-complex consisting of two sets of Cdc4:Skp1-dependent Cul1-RING ligase complexes. This dimeric Cul1-RING ligase supercomplex is oriented in a suprafacial configuration (side-by-side manner), such that the two substrate-binding sites in Cdc4 are facing to the same general direction yet with a slight tilt. The two substrate-binding sites are apart from each other by ~65 Å. The predicted distance between one substrate-binding site to the E2 active site in the neighboring CRL is 102 Å, while a 64 Å gap is lying between the substrate binding site and the E2 active site within the same CRL (Figure I-3) [48].

This overall geometry of the dimeric CRL supercomplex situates two adjacent substrate-binding sites in between the two E2 catalytic sites. The substantial differences in the substrate-to-catalytic site distances, namely 102 Å for inter-CRL and 64 Å for intra-CRL, may provide further flexibility for CRLs to accommodate polyubiquitin chains of various length and diverse geometry during chain elongation. In addition, two models were proposed to explain how this dimeric CRL supercomplex promotes processivity of weakly-associated substrate Sic1 [43, 48].When one substrate is recruited, greater stability of substrate binding can be achieved through divalent binding, in which

two CPDs (degrons) in the same Sic1 are held by two CDC4. Better stabilized substrate binding in turn leads to higher processivity in ubiquitination. On the other hand, irrespective of whether one or two substrates are recruited, additional lysine residues in bound substrates can be well presented for ubiquitin transfer as alternative E2 active sites are now available. Thus, dimeric CRL supercomplex can promote substrate processivity either by stabilizing substrate binding, or by facilitating ubiquitination of additional lysine residues within substrates.

Besides homotypic dimerization, substrate adaptors seem to mix-and-match among different isoforms, resulting in heterodimers, such as yeast F-box protein Pop1-Pop2 dimer, mammalian F-box protein βTrCP1-βTrCP2 dimer, and Fbw7α-Fbw7γ [44, 45, 49, 50]. Heterotypic dimerization of substrate adaptor isoforms has been shown to enable shuttling of complexes between different subcellular compartments. Details in dimerization-mediated substrate adaptor shuttling will be discussed in the section C.3. On the other hand, an interesting hypothesis is that heterodimerization of substrate adaptors may expand substrate repertoire for a CRL through combinatorial assembly among various substrate adaptors [51]. Indeed, heterotypic dimerization of substrate adaptors is a newly appreciated molecular aspect of CRL systems, yet its biological relevance remains poorly understood. Nonetheless, further in-depth analysis is likely to uncover the multiplicity in biochemical functions of heterotypic dimerization among substrate adaptors, and allow exploration of a whole new level in modulation of CRL activities.

Dimerization of cullins. Among cullin family members, Cul1, Cul3, and Cul4A can exist as homotypic dimer in vivo, whereas homodimers of Cul2 or Cul5 have not been observed [52]. Formation of a dimeric Cul3-Cul3 complex did not seem to rely on dimerization of BTB domain proteins, but rather, requires the C-terminal WH-B domains of Cul3 and a small ubiquitin-like protein Nedd8 [53]. Details of the interaction interface within this dimeric Cul3 complex will be describe in the section of Nedd8. Interestingly, the Cul3-Cul3 dimers can assemble with substrate-bound BTB domain proteins and with RING-finger Rbx1 proteins [53], suggesting that Cul3-Cul3 dimers may function in CRLs to regulate substrate ubiquitination. This Cul3-Cul3 dimer-based CRL complex is likely to adopt a very distinct conformation from that of a dimeric CRL supercomplex, as the latter is assembled via dimerization of substrate adaptors near the N-terminal regions of cullins, while the former is assembled around the C-termini of.a Cul3-Cul3 dimer. Three-dimensional structural analysis of this Nedd8-dependent Cul3-Cul3 dimer will provide insights into a novel regulatory mode in CRL systems, in which assembly of a CRL supercomplex via distinct architectures can modulate processivity of substrate ubiquitination by situating bound substrates in different orientations.

C.3. Dynamic subcellular localization of cullin-RING Ligases: circuit-riders in CRL systems.

Ubiquitin-dependent degradation of substrates can be regulated in a spatial manner by increasing local concentration of cognate CRLs in specific subcellular compartments, where destruction of substrates is desired. One major way to achieve a

timely increase in CRL abundance at specific subcellular locations is through massive relocalization of CRLs. Indeed, a number of cullin-RING ligases have each been found to occupy multiple loci in the cell, and to shuttle in the midst following cellular cues. On the other hand, many substrate proteins of CRLs also exhibit dynamic distributions in cells, in performing their regular tasks in cellular processes. Thus, four-dimensional colocalization of CRLs and cognate substrates becomes sophisticatedly controlled in order to selectively terminate substrate proteins as they are no longer needed at specific sites.

Spatial relationship between substrates and CRLs can be highly dynamic, yet exquisitely orchestrated at the same time. For example, cyclin B is a major player in the entry of mitosis in the cell cycle, while its destruction by ubiquitin/proteasome system is crucial for the exit from mitosis. In Drosophila embryos, cyclin B is localized mainly in cytoplasm in interphase, with a small fraction at centrosomes. In early prophase, cyclin B starts accumulating at centromeres, and then significantly stores up in nucleus. As nuclear envelope breaks down, the bulk of nuclear cyclin B relocates onto mitotic spindles. Subsequently, mitotic spindle-bound cyclin B moves toward mid-spindles at the plus-ends of interpolar microtubules in metaphase. Immediately prior to anaphase, destruction of cyclin B takes place over a period of approximately 1-2 minutes. Strikingly, a series of time-lapse analysis revealed a spatially-ordered disappearance of cyclin B during this period, starting from spindle poles and sequentially spreading toward spindle equator [54], suggesting that degradation of cyclin B can be subjected temporal regulation according to its relative locations on mitotic spindles. Ubiquitin-dependent

degradation of cyclin B is carried out by APC/C E3 ligases. Importantly, there seems to be a spatial correlation between APC/C and cyclin B over the course of cell cycle, in that APC/C is excluded from nucleus during interphase, but largely shifts into nucleus prior to the entry of mitosis in Drosophila embryos [55]. In addition, APC/C can accumulate in centrosomes and spindles under certain circumstances [56]. Further studies have suggested that subpopulations of APC/C may be differentially localized in mitosis. For instance, the Apc3(Cdc27) subunit-containing APC/C was found associated with mitotic chromatin, whereas the Apc6(Cdc16) subunit-containing APC/C was not [55]. An intriguing notion is that these subpopulations of APC/C shuttle to various subdomains in mitotic apparatus, where each confers distinct kinetics for ubiquitination of cyclin B. As a result, the overall cyclin B destruction is finely modulated in a temporal and spatial manner.

Shuttling of CRLs can be cooperatively managed by intrinsic and extrinsic localization modes. That is, individual subgroups of a CRL have their intrinsically-determined courses and directions to specific loci, but can readjust these regular routes when extrinsically complexed with one another. In particular, heterotypic dimerization of substrate adaptor isoforms has been shown to potentiate such cooperative mode of CRL shuttling. For example, the F-box protein Fbw7 functions as a substrate adaptor in Cul1-RING ligases that mediates ubiquitin-dependent degradation of cyclin E during S phase in the cell cycle. The human Fbw7 contains three widely-expressed isoforms, Fbw7α, Fbw7β, and Fbw7γ, that are derived from alternative splicing. Each splice variant mRNA consists of a single unique 5' exon, and ten common 3' exons. The ten common 3' exons

encode three C-terminal domains, D domain, F box, and WD40 repeats, that are critical for CRL functioning. As a result, Fbw7 isoform proteins are all capable of mediating cyclin E destruction, but each presents discrete *cis*-acting signals that divert isoforms to different subcellular compartments [57, 58]. Fbw7α is generally nucleoplasmic and absent from nucleolus; Fbw7β is localized to membrane compartments through its N-terminal transmembrane domain; Fbw7γ predominantly occupies nucleolus, with small amount in nucleoplasm and cytoplasm. *In vivo* studies have shown complex formation of heterotypic dimers composed of either two of the Fbw7 isoforms, and the consequent relocalization of the dimeric complexes between these compartments [44], suggesting that CRLs can be transported to distinct subcellular domains via extrinsic association with other subgroups of CRLs.

When ectopically expressed in vivo, the heterotypic dimer of nucleoplasmic Fbw7α and nucleolar Fbw7γ constitutes a remarkably prevalent dimer fashion among both Fbw7 homotypic and heterotypic dimmers [44]. In an interesting correlation, a bulk of the substrate cyclin E, that is able to shuttle between nucleoplasm and cytoplasm, switches to a bivariate distribution between nucleolus and nucleoplasm prior to its destruction by Fbw7-dependent Cul1-RING ligases in S phase of the cell cycle [59, 60]. Furthermore, abnormal accumulation of cyclin E in nucleoli was observed throughout the cell cycle in a number of carcinoma cells, in which cyclin E destruction was blocked [60]. Thus, it is likely that dynamic nucleoplasmic-nucleolar distribution for both cyclin E and Fbw7 promotes efficient cyclin E turnover, whereas static localization hinders it. It is interesting to note that isoform-mediated heterodimerization of CRLs may be a

regulatory mechanism only in higher ordered metazoans, as Fbw7 exits only in a single isoform in *S. cerevisiae*, *C. elegans,* and *Drosophila*.

C.4. Degradation of substrate adaptors

The cullin-RING ligase activity can be rapidly and thoroughly turned off via degradation of its own subunit proteins. Substrate adaptor proteins amongst all are most prone to ubiquitin-dependent degradation. Ubiquitination of substrate adaptors is generally carried out *in cis* within their own assembled CRLs. It is therefore termed 'auto-ubiquitination' or 'self-ubiquitination'. However, certain substrate adaptors are subject to ubiquitination *in trans* by other cullin-RING ligases. Further details in each mechanism are described below, providing with well-studied examples.

Auto-ubiquitination. Cullin-Ring ligases often exhibit strong autoubiquitination activities in vitro, in that they spontaneously mediate intramolecular ubiquitin conjugation onto their own substrate adaptors. However, in the *in vivo* milieu, autoubiquitination of substrate adaptors occurs in two different modes: either continually or in a timely manner. First, some substrate adaptors constitutively undergo autoubiquitination and subsequent degradation, such that they are intrinsically short-lived proteins. An important characteristic of these substrate adaptors is that they often clean themselves out from cullin-RING subcomplexes soon after degradation of cognate substrates. This mode of autoubiquitination allows rapid alteration among different substrate adaptors to assemble into a CRL. Thus, constitutive autoubiquitination serves as

an alternative mechanism to CRL complex cycling, in order to sustain activity of a CRL toward diverse substrates. For example, the yeast F-box proteins Cdc4 and Grr1 function in Cul1-RING ligases to target a number of cell cycle regulators for degradation in G1/S transition. Interestingly, Cdc4 and Grr1 are subject to constant autoubiquitination and self-degradation irrespective of different phases in the cell cycle [61, 62]. This consistent instability of Cdc4 and Grr1 ensures a dynamic equilibrium between multiple Cul1-RING ligases, and thereby enables rapid response to environmental changes throughout the cell cycle.

Conversely, some substrate adaptors undergo autoubiquitination and degradation in a specific timely manner, such that their half-lives can vary depending on the state of cellular physiology. Levels of these substrate adaptors fluctuate dramatically under different conditions, and thereby influence the degradation rate of their cognate substrates. For example, the mammalian F-box protein Skp2 functions in a Cul1-RING ligase to target several CDK inhibitors for degradation in cell cycle. Skp2 plays an important role in driving cell cycle progression, but is kept inactive during G0/G1 phase (quiescence). Corresponding to its activity, levels of Skp2 fluctuate periodically throughout cell cycle: they can be first detected as cells enter the cell cycle; start rising at G1/S transition; accumulate during S/G2; drop through M phase; and diminish as cells exit the cell cycle [63]. Indeed, studies have shown that Skp2 is subject to autoubiquitination-mediated degradation in quiescent cells, but not in rapidly-dividing cells [64]. Thus, autoubiquitination of Skp2 may in part function to suppress its CRL activity during G0/G1 phases in the cell cycle. Further identification of the molecular switches for Skp2

30

autoubiquitination will provide tremendous insights into mechanisms of how CRLs sense cellular signals and redirect ubiquitin transfer inwardly.

Ubiquitination in *trans* by non-cognate CRLs. Some substrate adaptor proteins can be individually recruited into a noncognate CRL by this CRL's substrate-recognition module, in which they switch roles into substrates, and become susceptible to ubiquitination and subsequent degradation. As a result, their cognate substrates are let to escape the destruction by these substrate adaptors. For example, in cells that are progressing immediately from prometaphase, knockdown of Cdh1 blocks degradation of F-box protein Skp2 and delays recover of $p27^{Kip1}$ and $p21^{Cip1}$ levels, suggesting that Cdh1-dependent APC/C controls ubiquitin-mediated degradation of Skp2 during late M/early G1 in the cell cycle [65, 66]. Indeed, Skp2 directly binds to Cdh1, and is subjected to ubiquitin conjugation by APC/C-Cdh1 complexes. These processes do not require the F-box motif in Skp2 that otherwise mediates assembly of Skp2 as a substrate adaptor into Cul1-RING ligases. Contrarily, Skp2 contains a putative D-box (destruction box) motif that is often present in conventional substrate proteins for APC/C-typed CRLs. Consistent with these D-box containing substrates of APC/C-Cdh1, this putative D-box in Skp2 is essential for efficient degradation by APC/C-Cdh1, yet dispensable for recognition by Cdh1.

In addition to well-defined substrate-binding domains and cullin-binding modules, substrate adaptors in CRL systems often contain other cryptic motifs that may potentially convert to degradation signal sequences. By selective use of these motifs and modules, it

is likely a common theme for many substrate adaptors to serve in certain CRLs, and to be served in others according to cellular demands.

C.5. Nedd8, and regulation of cullin-RING ligases via neddylation

Nedd8 (Neuronal precursor cell-Expressed Developmentally Down-regulated) is an 81-amino acid protein that is highly conserved among eukaryotes. It shares 57% sequence identity with ubiquitin. Furthermore, three-dimensional structures of Nedd8 and ubiquitin display high resemblance with each other [67]. Like other members of the ubiquitin-like protein family, Nedd8 can be covalently linked to other polypeptides via an isopeptide bond between the C-terminal glycine residue of Nedd8 and the ε-amino group of a lysine residue in a target protein. In the process of neddylation, Nedd8 is first activated by a heterodimeric E1-like enzyme consisting of Uba3 and APP-BP1 (Ula1); the activated Nedd8 is then transferred to an E2-like conjugating enzyme Ubc12; lastly, Ubc12 transfers Nedd8 to substrates possibly with the assist of RING-finger protein Rbx1 [68, 69]. The best known substrates for neddylation are cullin proteins, all of which seem to be modified by Nedd8 on a highly conserved lysine residue near C-termini.

Nedd8 conjugation of cullin proteins primarily functions to enhance the efficacy of CRLs in mediating substrate ubiquitination. Several mechanisms have been demonstrated in regard to the biochemical roles of cullin neddylation in regulation of CRL activities. First, in vitro studies have shown that Nedd8 conjugation of Cul1 increases association of a β-TrCP-dependent Cul1-RING ligase with ubiquitin-

conjugating E2 enzyme Ubc4, suggesting that cullin neddylation may facilitate recruitment of ubiquitin-charged E2 enzymes to CRLs [70]. Secondly, an in vivo study suggested that Nedd8 can mediate dimerization of Cul3, resulting in a heterodimeric complex composed of one neddylated and one unneddylated Cul3, which directly associate via hydrophobic binding between the Nedd8 protein covalently attached to one Cul3 molecule and the C-terminal WH-B motif within the unneddylated Cul3 molecule [53]. In addition, studies in *Drosophila melanogaster* indicated that cullin neddylation may promote degradation of neddylated Cul1 and Cu3 proteins [71]. However, this was not observed in mammalian cells [52]. Lastly and most importantly, neddylation of Cul1 causes dissociation of CAND1 from Cul1 and concomitant re-assembly of Skp1 with Cul1 [36, 37]. Thus, cullin neddylation may regulate CRL complex cycling by reducing the binding affinity of CAND1 for cullins. Details in this mechanism will be discussed in the next section.

C.6. COP9 signalosome (CSN), and its role in regulation of CRLs

COP9 signalosome (CSN) is a multisubunit complex consisting of eight subunits, CSN1-CSN8. CSN functions in an array of diverse biological processes by virtue of its pleiotropic role as a key regulator in the ubiquitin/proteasome system (UPS). One major biochemical function of CSN in UPS is its ability to cleavage Nedd8 conjugates from cullins. The CSN5 (Jab1) subunit contains a metalloprotease motif that, in coordination with other subunits in CSN, manifests the isopeptidase activity toward Nedd8 conjugates.

This deneddylation activity of CSN has been observed in cleavage of Nedd8 from various cullin proteins, and is widely conserved in eukaryotes (for full review, see [33, 72]).

In vitro biochemical studies showed that CSN negatively regulates CRL activity upon removal of Nedd8 from cullins. However, general genetic studies have demonstrated that CSN promotes CRL-dependent substrate degradation *in vivo*. This perplexing paradox thus indicates that CSN may be tightly coupled with neddylation machinery to regulate the status of cullin neddylation, and consequently the dynamic bindings of CAND1 with cullins that ultimately governs CRL complex cycling and activity. A tentative model was proposed to illustrate how cyclic neddylation and deneddylation of cullins may regulate cyclic assembly and disassembly of a Cul1-RING ligase. In this model, the events that occur in a hypothetical sequence include: (1) CSN is recruited to an active Cul1-RING ligase complex as the bound substrate is successfully degraded; (2) CSN cleaves Nedd8 conjugates from Cul1, and subsequently enables CAND1 to bind unneddylated Cul1; (3) binding of CAND1 with Cul1 dislodges the F-box protein-Skp1 from Cul1, and temporarily inactivates this Cul1-RING ligase from degrading substrates; (4) E2-like enzyme Ubc12 mediates conjugation of Nedd8 onto Cul1, which weakens binding affinity of CAND1 for Cul1; (5) upon release of CAND1 from Cul1, another F-box protein-Skp1 re-associates with Cul1 and activates this Cul1-RING ligase for degradation of the bound substrate (Figure I-4) [33, 72].

Several critical links in this scheme remain elusive. For example, what triggers association of CSN with CRLs? How is deneddylation activity of CSN regulated? How

does E2-like enzyme Ubc12 gain access to CAND1-bound Cul1? How does a neddylated cullin-RING subcomplex select the next immediate substrate adaptors for assembly? And how does dimerization of cullins play a role, if it does, in CRL complex cycling? In addition to these missing links, there are innate caveats in this scheme. For instance, although CAND1 shows competition relationship with BTB domain proteins for binding of Cul3 [73], it binds to both neddylated and unneddylated Cul3 without significant differentiation (our unpublished data), suggesting that CAND1 is a common player that drives dissociation of substrate adaptors from cullins, while neddylation of cullins is not necessarily involved in direct binding between CAND1 and other cullin proteins. It is likely that variations on the CAND1-dependent complex cycling theme are utilized by distinct cullin proteins to regulate CRL activity.

C.7. Multilateral interplay among regulatory factors in CRLs

A number of recent studies have suggested a more convoluted profile in regulation of CRLs, in that several regulatory factors cross-talk, and result in interdependent relationship among distinct regulatory modes. Rather than functioning in parallel lines, these regulatory mechanisms form an intertwined network, such that they can operate to complement one another, in a feedback manner, or to cause cumulative effects. In this section, we describe several examples, and discuss their provocative suggestions and the questions left to be answered.

CSN executes deubiquitination through Ubp12. Independently from its deneddylation activity in CRL complex cycling, CSN confers deubiquitination activity through associated Ubp12 proteins [74]. Ubp12 is a cysteine protease that contains isopeptidase activity toward ubiquitin conjugates. One major *in vivo* targets of the deubiquitination enzyme Ubp12 are substrate adaptor proteins in CRLs. Studies have shown that Ubp12 is recruited to cullins by CSN, and CSN-bound Ubp12 neutralizes polyubiquitination mediated by cullin-RING ligases. In particular, substrates adaptors in CRLs, such as the F-box protein Pop1, and the BTB domain protein Btb3, are rescued by Ubp12-CSN from autoubiquitination-dependent self-destruction [74]. It has been proposed that Ubp12-CSN complexes function to antagonize spurious autoubiquitination of substrate adaptors. On the other hand, it is likely that Ubp12-CSN complexes enable CRLs to bypass the routine of substrate adaptor alteration, such that they can carry out degradation of cognate substrate pools quickly and intensively at certain junctures upon cellular demands.

Feedback regulation of autoubiquitination by substrates. Autoubiquitination of substrate adaptors can also be regulated in a feedback manner based on availability of their cognate substrates. It was proposed that substrate adaptors are accelerated into self-destruction when levels of bound-substrates are diminished, while protected from self-degradation when levels of degradable substrates are high. For example, the F-box protein β-TrCP2/HOS (the homologue of Slimb) functions in Cul1-RING ligases to mediate ubiquitin-dependent degradation of IκB proteins upon phosphorylation of IκB by IKK kinases. The HOS proteins are unstable substrate adaptors that undergo

autoubiquitination and self-degradation within Cul1-RING ligases. However, studies have shown that addition of phosphorylated IκBα inhibit HOS autoubiquitination *in vitro*, whereas non-phosphorylated IκBα did not. In addition, *in vivo* studies showed that sustained phosphorylation of IκBα by constitutive activation of IKKβ resulted in stabilization of HOS [75], further supporting the notion that HOS stability can be modulated to meet cellular demands for substrate degradation.

In a similar tone, it has been demonstrated that the substrate adaptor β-TrCP1/E3RS, that is free from bound substrates, requires association of the pseudosubstrate hnRNP-U to maintain its own stability [42], suggesting that the actual occupancy of substrate-like macromolecules on substrate adaptors is likely the very essence of this feedback regulatory mode. Although the molecular mechanism underlying the (pseudo)substrate-dependent inhibition of autoubiquitination is not clear, it is possible that bound (pseudo)substrates may physically shield substrate adaptors from ubiquitin transfer.

Modulation of autoubiquitination by regulators in CRL complex cycling. Several regulators in cyclic process of CRL assembly and disassembly have been shown to affect autoubiquitination and self-degradation of substrate adaptors. First, impaired deneddylation activity of CSN caused hyper-neddylation of cullins, and promoted autoubiquitination and self-degradation of substrate adaptors, such as Btb3 and Skp2 [76]. Secondly, abrogation of cellular Nedd8 conjugation resulted in decreased self-destruction of substrate adaptors, such as F-box protein Skp2 [77]. Thirdly, knockdown of CAND1

led to tighter association between BTB domain protein Keap1 and Cul3, and stimulated autoubiquitination and degradation of the substrate adaptor Keap1 [73]. Seemingly intricate, these independent studies all point to another level of regulation for autoubuquitination of substrate adaptors, in which players in CRL complex cycling regulate mobility of substrate adaptors on or off cullins, and the mobility of a substrate adaptor in turn determines its self-destruction. The lower the mobility, the higher the autoubiquitination, and vice versa. As a result, any substrate adaptor that is free of substrates or pseudosubstrates but still bound to cullins, is destined for self-destruction. This phenomenon likely refers back to the fundamental notion that autoubiquitination mechanism and CRL complex cycling scheme complement each other to ensure proper alteration of substrate adaptors on cullins, and thereby sustain CRL activity for various substrates.

Feedback regulation of cullin neddylation and deneddylation by substrates and substrate adaptors. Chemical reactions and the enzymes directly involved in neddylation and deneddylation of cullins are well understood now. Biochemical functions of cullin neddylation and deneddylation in regulation of CRL activity have been extensively studied for almost a decade. However, our understanding of how neddylation and deneddylation of cullins are regulated remains in its infancy. It has been observed that association of CAND1 with Cul1 renders partial inhibitory effect on neddylation of Cul1, possibly due to the steric hinderance at the neddylation site [78]. Following up to this observation, a number of intriguing findings in a recent study have demonstrated a

feedback regulatory model, in which substrates and substrate adaptors, based on their levels, synergistically regulate neddylation and deneddylation of cullins.

In this study, primary substrate adaptor Skp1, secondary substrate adaptor Skp2, and its cognate substrate p27^{Kip1} were examined for their functional interactions with CAND1, CSN, or neddylation enzymes in altering neddylation status of Cul1 [79]. First, the presence of Skp2 and Skp1 together was found to cause substantial dissociation of CAND1 from Cul1 *in vitro*, while Skp1 alone was not, suggesting that F-box proteins may transform Skp1 into a stronger competitor than CAND1 for binding to Cul1. Furthermore, addition of *in vitro* reconstitute neddylation system along with Skp1-Skp2 complexes was found to cause greater dissociation of CAND1 from Cul1, consistent with the current paradigm that neddylation of Cul1 prevents re-binding of CAND1 onto Cul1. As inhibitory effect of CAND1 on Cul1 neddylation was diminished upon CAND1 dissociation, Skp1-Skp2 complexes were also found to enhance Cul1 neddylation in this system. As expected, the presence of CSN in this system offsets the increase in Cul1 neddylation resulted from Skp1-Skp2 complexes. Strikingly, further addition of substrate protein phospho-p27^{Kip1} was found to counteract the effect of CSN and recover Cul1 neddylation, suggesting that bound substrates may prevent CSN-mediated deneddylation of Cul1.

Overall, these findings suggest that high levels of substrates and substrate adaptors may cooperatively up-regulate neddylation of cullins, which in turn promotes efficacy of CRLs in substrate destruction. In support of this notion, *in vivo* Skp2-

39

dependent Cul1-RING ligases are highly active at G1/S transition, and indeed, levels of Skp2 and its degradable substrate phospho-p27^{Kip1} increase markedly at this stage of the cell cycle. Thus, for those CRLs containing substrate adaptors whose levels surge upon elevation of degradable substrates, the mechanism underlying the interdependent relationship between substrates, substrate adaptors, and neddylation status of cullins can be further refined as following: (1) upon an increase in their levels, F-box proteins assemble with Skp1, and together replace CAND1 from Cul1; (2) E2-like enzyme Ubc12 acquires better access to Cul1 to mediate Cul1 neddylation, whereby it obstructs re-binding of CAND1 with Cul1; (3) bound-substrates in CRLs repress CSN-mediated deneddylation of Cul1; (4) resultant culmination of Cul1 neddylation promotes productive ubiquitination and degradation of substrates; (5) as substrates are eliminated, substrate adaptors are submit to autoubiquitination and degradation; (6) also, CSN-mediated deneddylation of Cul1 is de-repressed upon substrate elimination, and increases unneddylated pool of Cul1; (7) CAND1 re-gains higher affinity for binding with unneddylated Cul1, and temporarily keeps CRLs inactive. As cyclic neddylation and deneddylation of cullins is intimately involved in cyclic assembly and disassembly of CRL complexes, this newly-refined model also represents a probable generality that illustrates how episodic changes in levels of substrates and/or substrate adaptors can influence the dynamic complex cycling of Cul1-RING ligases in a feedback manner.

It remains enigmatic in this model how substrates antagonize CSN-mediated deneddylation of Cul1. Nevertheless, an independent study of pseudosubstrates indicated that serving as a transient deneddylation antagonist may be a common feature for

substrates and/or substrate-like proteins in CRL systems. In this study, pseudosubstrate hnRNP-U was found assembled with Cul1 that is predominantly neddylated and exhibits hyper activity toward subsequently recruited substrate phospho-IκBα [42], suggesting that, in sequence, pseudosubstrates and true substrates may additively inhibit cullin deneddylation. It is tempting to envision that binding of substrate-like macromolecules with substrate adaptors renders sterical blockage against association of CSN with CRLs, hence prevents cleavage of Nedd8 conjugates from cullins. Further comprehensive analysis of protein-protein interactions and comparison of three-dimensional structures of CRL-substrate and CRL-CSN complexes will provide tremendous insights into molecular mechanisms underlying the inhibition of cullin deneddylation by substrates and substrate-like proteins.

D. Nrf2 and Keap1

The transcription factor Nrf2 controls a genetic program that protects cells from oxidative damage and maintains cellular redox homeostasis. Nrf2 regulates both constitutive and inducible expression of a large number of detoxifying and antioxidant genes. The modular protein Keap1 directly binds Nrf2, and functions as a substrate adaptor in a Cul3-RING ligase that mediates ubiquitin-dependent degradation of Nrf2. In the following sections, we describe the domain structures, interaction partners, and biochemical properties of Nrf2 and Keap1 proteins.

D.1. The transcription factor Nrf2

Nrf2 belongs to CNC (Cap' n' collar) family of transcription factors. Members in CNC family are structurally-related proteins that are defined by the presence of CNC-type bZIP (basic leucine zipper) domain. The CNC-type bZIP domains are utilized to bind DNA via simultaneous heterotypic dimerization with small Maf transcription factors, such as MafF, MafG, and MafK. In humans, six members in CNC family identified to date include p45 NF-E2, Nrf1, Nrf2, Nrf3, Bach1, and Bach2. *In vivo* transcription analysis and mouse genetic studies have demonstrated that among these family members, Nrf2 is the most potent transcriptional activator in gene expression of phase II detoxifying enzymes and ROS (reactive oxygen species)-scavenging antioxidants [80-84].

Nrf2 governs transcription of target genes through direct binding to their *cis*-acting elements, termed ARE (antioxidant response element). The ARE motifs contain the consensus sequences (A/G)TGACnnnGC, that are present in the promoter and/or enhancer regions of Nrf2-regulated detoxifying and antioxidant genes, such as glutathione S-transferases (GSTs), NAD(P)H:qinone oxidoreductase (NQO-1), γ-glutamylcysteine synthetase (γGCS), heme oxygenase-1 (HO-1), and peroxiredoxin 1 [82, 84-90]. Several microarray studies have suggested that Nrf2 may regulate expression of a wider array of approximately 200 genes that include detoxifying and antioxidant genes and differently-categorized genes, such as genes that encode 26S proteasome subunits, heat shock proteins, and metabolic enzymes [91-94]. Expression of these genes is maintained constitutively at low basal levels, while can be activated to various degrees in an inducible manner upon exposure of cells to stress signals, including ROS, electrophilic

chemicals, heavy metals, and mitochondrial toxins [95]. The non-elderly Nrf2-null mice display no significant phenotype under normal conditions, but carry high susceptibility and develop severer symptoms to various environmental stresses [96-100], suggesting that the critical functionality of Nrf2 is subject to modulation under different conditions. On the other hand, the aged female Nrf2-null mice developed lupus erythematosus-like systematic autoimmunity, resulting in glomerular nephritis and a shortened lifespan [101-103]. Taken together, it is now established that Nrf2 plays a crucial role in protection against pathophysiological consequences of both chronic and acute oxidative stress from endogenous as well as exogenous sources.

The characteristic domain organization of Nrf2 protein enables Nrf2 to coordinate the upstream signaling regulators and the downstream transcriptional outcomes. Nrf2 protein consists of six conserved domains, termed Neh1-Neh6, each of which has unique roles for biochemical actions of Nrf2 (Figure I-5). First, the C-terminal Neh1 and Neh3 domains function in nuclear localization, DNA binding, and heterodimerization with small Maf proteins [104]. Secondly, the Neh4 and Neh5 domains in the central region of Nrf2 function to recruit transcriptional co-activators, such as CBP (CREB-binding protein) [105, 106]. Lastly, the Neh6 and Neh2 domains independently function to control ubiquitin-dependent proteolysis of Nrf2 [107]. The Neh6 is located in the central region of Nrf2, and renders moderate instability of Nrf2 independently of stress signals. However, the mechanism underlying Neh6-mediated degradation of Nrf2 is not known. On the other hand, the N-terminal Neh2 domain directly binds to the modular protein

Keap1, whereby it mediates massive degradation of Nrf2 in a manner that is highly sensitive to stress signals.

D.2. The modular protein Keap1, and its sensor system

Keap1 (Kelch-like ECH-associated protein 1) was first identified by virtue of its association with the N-terminal Neh2 domain of Nrf2 [108]. Subsequent in vivo and in vitro studies have demonstrated that Keap1 functions to repress transcriptional activity of Nrf2, in large part, by mediating constitutive degradation of Nrf2. This function of Keap1 is conditionally disrupted in response to various stress signals, such that Nrf2 can be stabilized and carry out transcriptional activation of target genes. In a sense, Keap1 presents itself as a delicate molecular switch that launches Nrf2-based cytoprotective mechanisms only when certain stress signals are present.

Indeed, a unique feature of Keap1 is its high cysteine content, in which the sulfhydryl groups are potentially prone to alkylation or oxidation by environmental stresses in the forms of highly reactive chemicals. In theory, the reactivity of the sulfhydryl groups of Keap1 with selected electrophilic molecules endows Keap1 with the ability to directly sense these stress signals. Consequently, the local conformational change within Keap1 caused by adduction or modification of particular sulfhydryl groups enables Keap1 to further transduce stress signals onto bound Nrf2. In reality, Keap1 contains twenty-five cysteine residues that are conserved between human and mouse. *In vitro* studies have identified ten cysteine residues in Keap1 that can be directly modified

by chemical inducers of Nrf2-dependent gene expression. These cysteine residues are Cys 151, Cys196, Cys226, Cys241, Cys257, Cys273, Cys288, Cys297, Cys319, and Cys613 [109-111]. Mutational studies have highlighted the *in vivo* significance of three cysteine residues among these ten, Cys151, Cys273, and Cys288 (Figure I-5) [112]. The thiol in residue Cys151 is dispensable for Keap1 to repress Nrf2, but is vital for Keap1 to sense sulforaphane and quinone-induced stress signals in order to de-repress Nrf2 [112]. On the other hand, the thiols in residues Cys273 and Cys288 are crucial for Keap1 to repress Nrf2 perhaps due to their binding of zinc. It has been proposed that Cys273 and Cys288 may sense chemical inducers that abrogate the zinc-thiol interaction [113].

Another key feature of Keap1 is its modular characteristic that allows Keap1 to nucleate a signaling complex for cooperative regulation of Nrf2 stability. Keap1 belongs to the BTB-Kelch subgroup within the BTB (POZ) super-family of modular proteins that typically contain a BTB domain and one or two other types of domains, such as Kelch domain in the case of BTB-Kelch subgroup. The BTB (bric-a'-brac, tramtrack and broad) domains in the family members share a secondary structure topology in the core BTB fold, and differ in their periphery secondary structure elements [11]. As a result, BTB domain proteins often function as a versatile adaptor in various cellular processes, in that the core BTB folds mediate family-specific complex assembly, while the peripheral elements participate in different types of protein-protein interaction. Several BTB domain-mediated interaction modes include homotypic dimerization, homotypic oligomerization, heterotypic dimerization among members in the BTB family, and heterotypic dimerization between BTB domain proteins and non-BTB domain proteins

[114-117]. In particular, many BTB domains exist as obligate homodimers via formation of intermolecular anti-parallel β-sheets. Disruption of the interface within homodimers often results in unfolded or misfolded proteins, such that these BTB domain proteins can only exist and function in homodimeric forms [118-120].

Keap1 contains an N-terminal BTB domain, a linker domain (IVR, or BACK) in the central region, and a C-terminal Kelch domain (Figure I-5). The BTB domain accounts for formation of Keap1 homotypic dimer [46]. *In vivo* studies have shown that majority, if not all, of the Keap1 proteins exist and function as BTB domain-mediated homodimers [121]. The linker domain harbors a leucine-rich nuclear export sequence (NES) that accounts for mass cytoplasmic localization of Keap1 [122]. Additionally, the linker domain contains several sequence clusters that are conserved among orthologues and paralogues, and are predicted to form a non-canonical BTB folds [11]. Both BTB domain and linker domain are required for Keap1 to assemble into Cul3-RING ligases, although the three-dimensional structure of a BTB domain-Cul3 complex is yet to be identified [123, 124]. A number of reactive cysteine residues are located in BTB domain and linker domain, raising a tempting possibility that Keap1 may utilize an adjustable Cul3-binding mode to sense and transduce stress signals. Lastly, the Kelch domain of Keap1 consists of six kelch repeats of β- strands, and forms a β-propellar structure [106]. It mainly functions to mediate protein-protein interaction between Keap1 homodimer and a diverse array of proteins, such as Nrf2, actins, FAC1 (fetal Alz clone 1), PGAM5, p62 (SQSTM1), and possibly Prothymosin and DJ-1 [125-127]. Among these Kelch domain-binding proteins, Nrf2 is a well-characterized substrate protein that is subject to

repression by Keap1, whereas others have appeared as secondary regulators for Keap1-dependent repression of Nrf2, via either simultaneous binding with Nrf2-bound Keap1, or the competitive binding for Keap1 that in turn triggers dissociation of Nrf2.

E. Regulations of Nrf2 by Keap1

Investigation of mechanisms underlying the regulation of Nrf2 by Keap1 started out with a simple and elegant model that soon became the established dogma. This early model was based on experiments performed in 1999 by the Yamamoto laboratory and proposed that first, Keap1 is a cytoplasmic protein, and it represses Nrf2-dependent gene expression by physically sequestering of Nrf2 in cytoplasm; secondly, Keap1 discharges Nrf2 upon stress signals due to conformational changes that cripple Keap1 from binding Nrf2 [108]. However, starting in 2003, a series of papers were published that challenged this dogma, leading to a more refined view in which first, Keap1 is a bona fide nuclear-cytoplasmic shuttling protein; secondly, it represses Nrf2 mainly by mediating ubiquitin-dependent degradation of Nrf2; and thirdly, the stress signals do not abrogate the ability of Keap1 to bind Nrf2, but rather the efficiency to catalyze degradation of Nrf2 [27, 123, 124, 128]. In the following sections, we describe in detail the mechanisms of how Keap1 mediates degradation of Nrf2. Furthermore, we describe the three-dimensional structure of Nrf2-Keap1 complex characterized to date. Two tentative models regarding to the binding stoichiometry of Nrf2 and Keap1 homodimer, and their functional implication will also be discussed. Lastly, we describe dynamic localization of Keap1 at multiple

subdomains in cells, and discuss the potential impacts it might have on regulation of Nrf2-dependent gene expression.

E1. Ubiquitination and degradation of Nrf2 by Keap1-dependent Cul3-RING ligases

It is now established that Keap1 functions as a substrate adaptor in Cul3-RING ligases, and collectively targets multiple substrate proteins of various processivities for polyubiquitination and subsequent 26S proteasome-dependent degradation [26, 27]. Keap1 assembles into Cul3-RING subcomplexes via cooperative binding of its BTB domain and linker domain with N-terminal stalk region within Cul3, while recruits cognate substrates for productive ubiquitin transfer via its Kelch domain. Consistent with the observation that Keap1 functions as homodimers in vivo, computational modeling suggested that the Keap1-dependent Cul3-RING ligase likely forms a super-complex that consists of two sets of CRLs via a Keap1 homodimer [11]. Unlike most of the substrates in Cul1-RING ligases whose degradation signals are extrinsically generated upon post-translational modification, the substrates of Keap1-dependent Cul3-RING ligases possess intrinsic degradation signals that are encoded in the consensus sequence (D/N)xE(T/S)GE [26, 129]. These intrinsic degradation signal sequences enable facile association between substrates and Keap1, such that the substrates are subject to constitutive degradation, unless the degradation process is perturbed upon cellular demands for substrate proteins to cope with stress.

Nrf2 contains a DxETGE motif within Neh2 domain that is highly conserved among orthologues. The DxETGE motif in Nrf2 directly binds Keap1 with high affinity, and innately signals Nrf2 for Keap1-mediated destruction. Seven lysine residues within Neh2 domain appear to be the most effective targets in Nrf2 for Keap1-mediated ubiquitin conjugation [27]. Under normal conditions, the Keap1-dependent Cul3-RING ligases readily bind Nrf2, and target it for constitutive ubiquitination and degradation, such that the steady-state levels of Nrf2 remain barely detectable, and Nrf2-dependent gene expression is kept at low basal levels. As cells are challenged by the environmental stresses, including ROS and electrophilic chemicals, ubiquitination and degradation of Nrf2 by Keap1-dependent Cul3-RING ligases is marketed reduced. As a result, stabilization of Nrf2 and concomitant activation of detoxifying and antioxidant genes can be achieved, and enable cells to combat the stresses encountered [27, 130]. Such failure of Keap1-dependent Cul3-RING ligases to mediate effective ubiquitination of substrate Nrf2 is not due to its failure to bind Nrf2. Rather, I suggest that altered processivity of bound Nrf2 by the Keap1-dependent Cul3 RING ligase is the key determinant responsible for stabilization of Nrf2 following exposure of cells to oxidative stress or electrophilic chemicals.

Although the exact mechanism of how processivity of Nrf2 decreases in response to the stress signals remains to be identified, it is likely that Cys151 within Keap1, when modified by electrophilic chemicals, subtly causes rearrangement in local intermolecular interaction between two BTB domains within Keap1 homodimer. The idea is that small changes in space between these BTB domains could lead to big spatial changes between

two Kelch domains within Keap1 homodimer, such that the optimal positioning of bound Nrf2 toward ubiquitin-charged E2 enzyme is no longer maintained. Consequently, the kinetics of ubiquitin transfer onto lysine residues in Neh2 domain of Nrf2 become a fiasco.

This notion is consistent with the observation that electrophilic chemicals from distinct structure classes can interfere with Keap1-mediated ubiquitination and degradation of Nrf2, but each cause different molecular behaviors of substrate adaptor Keap1 [109, 110]. Intuitively, modification of cysteine residues in Keap1 with electrophilic chemicals of distinct structure is likely to reorient Keap1 homodimer differently, hence its biochemical property. However, as long as the reorientation of Keap1 homodimer causes deviation of bound Nrf2 from optimal range in space that allows productive ubiquitin transfer, a reduction of Nrf2 processivity would naturally occur. For example, *tert*-butylhydroquinone (tBHQ) in quinone subclass and sulforaphane in isothiocyanate class are both potent inducers for Nrf2-dependent gene expression. Neither chemicals interfere physical binding of Keap1 with Nrf2, but both depend on the thiol group of Cys151 in Keap1 to block Nrf2 ubiquitination and degradation [27, 112]. Interestingly, tBHQ often promotes autoubiquitination and self-destruction of substrate adaptor Keap1, whereas sulforaphane does not [131]. In a model that had been proposed for the substrate-mediated feedback regulation of autoubiquitination, the cognate substrates, when bind to substrate adaptors in an optimal position, can sterically shield substrate adaptors from ubiquitin transfer, and thereby inhibit autoubiquitination. In a similar tone, it is likely that modification of Keap1 with

tBHQ causes suboptimal repositioning of Nrf2 in a way that no longer shields Keap1 from autoubiquitination, while modification of Keap1 with sulforaphane leads to repositioning of Nrf2 in a different way that ultimately excuses both Nrf2 and Keap1 from ubiquitin transfer. Three-dimensional structure of Keap1 homodimers that are modified with either tBHQ or sulforaphane will provide validation for this differential intra-CRL repositioning model.

Like most of the CRLs in metazoans, the Keap1-dependent Cul3-RING ligases undergo CAND1-dependent complex cycling process. Binding of CAND1 with Cul3 causes dissociation of Keap1, and release of CAND1 from Cul3 enables assembly of Keap1 into Cul3-RING ligases that then mediate ubiquitination of Nrf2. Cyclic assembly and disassembly of Cul3-RING ligases by CAND1 is essential to alternate various BTB-Kelch proteins that function as substrate adaptors in Cul3-RING ligases, such as Keap1,GAN (gigaxonin), and potentially sarcosin and others [73]. Additionally, optimal dynamics in physical interaction between CAND1 and Cul3 appeared crucial for specifically-tuned destruction of Nrf2, as sustained dissociation of CAND1 from Keap1-bound Cul3 resulted in increased autoubiquitination and self-destruction of Keap1, and led to defective degradation of Nrf2 [73]. Furthermore, Nedd8, another player in complex cycling of Cul1-RING ligases, is required for efficient degradation of Nrf2 by Keap1 [73]. However, CAND1 binds to neddylated Cul3 as well as to unneddylated Cul3, suggesting that Nedd8-mediated regulation of Nrf2 turnover is not accomplished via dynamic association and disassociation between CAND1 and Cul3. It is possible that Nedd8-dependent dimerization of Cul3 nucleates formation of a Keap1-dependent Cul3-RING

ligase super-complex that displays different architecture, and exhibits higher catalysis in Nrf2 ubiquitination.

E2. Structure of Nrf2-Keap1 complex, and its binding stoichiometry

Three dimensional structures of the Kelch domain of Keap and the complexes of the Kelch domains bound with several different Nrf2-derived peptides have been characterized. We describe the details of these structures in this section. In addition, we describe two proposed binding modes in Nrf2-Keap1 system, and discuss how these two binding modes may determine processivity of Nrf2 ubiquitination by Keap1 under different cell physiological conditions.

Structure of the Kelch domain. The Kelch domain of Keap1 forms a highly symmetric, six-bladed β-propeller structure, in which each blade of the propeller (I-VI) is comprised of four β-strands (A-D). The β-strands are connected by loops of varying lengths that project from the central core of the β-propeller. By convention, the short loops that connect either β-strands A and B (A-B), or β-strands C and D (C-D) define the bottom face of the β-propeller, whereas the longer loops that connect either β-strands D and A (D-A) or β-strands B and C (B-C) define the top face of the β-propeller. The D-A and B-C loops form a shallow pocket at the top face that contains significant patches of positive charge, where the DxETGE degradation signal motif in Nrf2 binds with high affinity (Figure I-6) [106].

Structure of DxETGE motif-Kelch complex. The DxETGE motif, amino acids 77 - 82 in Nrf2, mediates binding between the Neh2 domain of Nrf2 and the Kelch domain of Keap1 with a remarkably high affinity at a binding constant (Ka) of $2*10^8$ M^{-1} [132]. The DxETGE motif forms a β-hairpin structure, in which two anti-parallel β-strands are connected by a turn region comprised of two overlapping type I β-turns. The turn region is stabilized by hydrogen bonding between Asp77 and Thr80 within the DxETGE motif. This β-hairpin moiety fits into the binding pocket on top face of β-propeller of Kelch domain via extensive hydrogen bondings and van der Waals interactions. Eight residues in the Kelch domain of Keap1 that are involved in these interactions include Arg380 and Arg415 near the bottom of the binding pocket, and Tyr334, Asn382, His436, Arg483, Tyr525, and Tyr572 deployed on the side of the binding pocket (Figure I-6) [82, 133].

Structure of DLG motif-Kelch complex. In addition to the DxETGE motif, Nrf2 contains a DLG (LxxQDxDLG) motif from amino acids 23 to 31 within Neh2 domain. This motif is also conserved among orthologues and has been demonstrated as the second site in Nrf2 for Keap1 binding [107, 134]. The DLG motif mediates binding between the Neh2 domain of Nrf2 and the Kelch domain of Keap1 at a binding constant (Ka) of $1*10^6$ M^{-1}. This is a rather low binding affinity that is about two orders of magnitude weaker than DxETGE motif, suggesting that the DLG motif participates in minor, if any, binding events for Nrf2-Keap1 complex [132]. The DLG motif forms a tight β-hairpin structure that is stabilized by two intra-molecular hydrogen bonds. The β-hairpin of DLG motif packs into the binding pocket of β-propeller of Kelch domain in a

manner that is similar with DxETGE motif, in that the β-hairpins of both motifs make contacts with three common residues in the binding pocket of Kelch domain, including Asn382, Arg415, and Arg483. However, consistent with the differences in binding affinities, the weak-binding DLG motif is partially buried in the pocket through only eight electrostatic interactions, while the strong-binding DxETGE motif is deeply entrenched via thirteen electrostatic interactions [135].

Binding stoichiometry of Nrf2-Keap1 complex. Given the biochemical properties that (1) Keap1 functions as homodimers and presents two substrate-binding pockets in a super-complex of Cul3-RING ligase, and that (2) the Neh2 domain of substrate Nrf2 contains two unique motifs that can each directly occupy one binding pocket in Kelch domain *in vitro*, two models were proposed to explain how Nrf2-Keap1 complex may be formed *in vivo*. In one model, only the DxETGE motif in Neh2 domain is utilized for binding of Keap1, while DLG motif is completely 'spared' as it is unable to compete with DxETGE motifs in other Nrf2 molecules. Consequently, two Nrf2 molecules are concurrently recruited to one Keap1 homodimer, resulting in a hetero-tetramer of Nrf2-Keap1 complex at 2:2 stoichiometry [133]. Furthermore, the seven critical lysine residues that are all located preceding DxETGE motif in Neh2 domain is now able to stick out toward E2 enzymes for productive ubiquitin transfer. In the second model, both DLG motif and DxETGE motif in Neh2 domain are utilized for binding to Keap1, such that one Nrf2 molecule occupies one Keap1 homodimer, resulting in a hetero-trimer of Nrf2-Keap1 complex at 1:2 stoichiometry [121, 132, 135]. As all the seven lysine residues in Neh2 domain are located in between DLG motif and DxETGE

motif, these lysine residues are now confined on the top faces between two binding pockets in β-propellers, in which one pocket grasps the DLG motif, and the other grasps the DxETGE motif. Given that a featured 50-60 Å gap lies between the substrate-binding site of a substrate adaptor and the thiol ester bond of Ub~E2 in a CRL, it is likely that ubiquitin would now be transferred at an inefficient rate onto these restrained seven lysine residues in Neh2 domain. Thus, a poor processivity is predicted for substrate Nrf2 that binds Keap1 homodimer at a 1:2 stoichiometry [121, 132, 135].

Seemingly contradictory with each other, these two models nevertheless raise the possibility that Keap1 homodimer may adopt either mode of complex formation under different conditions in order to switch between high and low processivity of Nrf2 ubiquitination. As the binding affinities between Keap1 and these two motifs in Nrf2 do not appear to be modulated by post-translational modifications, binding of Nrf2 to Keap1 is not likely to be the critical determinant of high versus low processivity. Rather, the distance between two substrate binding pockets in Kelch domains may play a critical factor in directing Keap1 homodimer to form a complex with one or two Nrf2 molecules. Solution NMR spectroscopic studies have shown that Neh2 domain of Nrf2 is highly disordered [132]. Given that the mean path length for a disordered polypeptide of ~60 residues, such as the segment stretching from DLG motif to DxETGE motif in Neh2 domain, is approximately 20 Å, two binding pockets in β-propellers of Kelch domains would have to be close enough to generate a ~20 Å distance for simultaneous binding of these two distinct motifs within one Neh2 domain. On the other hand, it would require a larger distance between two substrate-binding pockets to accommodate two Neh2

domains that both dock in via DxETGE motifs. The mechanisms of how Keap1 homodimer may modulate this critical distance is not known, yet it is likely achieved via the relative orientation of two Kelch domains, in that a slight tilt of Kelch domains away from each other results in a larger distance, while a tilt toward each other gives rise to a smaller distance. An attractive notion is that modification of Cys151 in BTB domains of Keap1 homodimer by electrophilic chemicals rearranges the interaction interface within BTB domains, which in turn modulates orientation of Kelch domains to tilt toward each other, and thus constrains the space for binding of only one Nrf2 molecule with expected low processivity.

E3. Dynamic subcellular localization of Nrf2-Keap1 system

Both Keap1 and Nrf2 shuttle between nucleus and cytoplasm. Furthermore, inhibition of nuclear export of Keap1 often leads to deregulation of Nrf2-dependent gene expression, suggesting that Keap1 carries out cytoplasm-specific tasks that are crucial for regulation of Nrf2 [122, 136]. Indeed, studies have shown that Keap1 can be localized to multiple subdomains in cytoplasm, such as actins, specialized adherens junctions and focal adhesions, mitochondria, and protein inclusion bodies that are often enriched in ubiquitin-modified proteins [137, 138]. Different subcellular compartments exhibit different redox potentials, have different oxidant-generating complexes, and provide platforms for different signaling events that function to sense both cellular physiology and external stimuli [139, 140]. It is likely that localization of Keap1 to multiple subcellular loci may enable activation of Nrf2 in response to different types of cellular

stress. One intriguing notion is that dynamic localization of Keap1 among various subcellular loci may potentiate the ability of Keap1 to function as a signal sensor at one location and a transducer at others. In this section, we describe (1) mitochondrial localization of Keap1 via physical interaction with mitochondrial protein PGAM5, (2) localization of Keap1 at specific protein inclusion bodies through binding with SQSTM1/p62 proteins, and their functional implications on regulation of Nrf2-dependent gene expression.

PGAM5-mediated mitochondrial localization of Keap1. PGAM5 belongs to phosphoglycerate mutase family, in which members share a structurally-related PGAM domain that may confer putative phosphatase or kinase activities. However, neither phosphatase nor kinase activities have been confirmed for PGAM5. Nonetheless, PGAM5 contains an N-terminal mitochondrial targeting sequence that functions to deliver PGAM5 to outer membrane of mitochondria [141]. In addition, PGAM5 contains a conserved NxE(S/T)GE motif that binds Kelch domain of Keap1 in a manner that highly resembles how the DxETGE motif in Neh2 domain of Nrf2 binds Keap1 [26]. Studies have shown that PGAM5, when present in cytoplasm, is a highly processive substrate that undergoes Keap1-mediated ubiquitination and degradation. On the other hand, once delivered onto mitochondrial outer membrane, PGAM5 becomes a low processive substrate that is, however, still associated with Keap1 [141]. Interestingly, PGAM5 can recruit Nrf2 and Keap1 to mitochondria, where it forms a ternary complex with one Keap1 homodimer and one Nrf2 molecule. Studies have suggested that this ternary complex may contribute to repression of Nrf2-dependent gene expression [141],

It is likely that PGAM5, by localizing the Keap1-Nrf2 complex to mitochondria, enables facile coordination between mitochondrial signaling and regulation of Nrf2-dependent gene expression.

SQSTM1/p62-mediated localization of Keap1 at sequestosome bodies. SQSTM1/p62 (sequestosome 1/ZIP/STAP/A170) is a multi-domain protein and functions as molecular scaffold for assembly of multi-protein signaling complexes, including complexes that regulate NFκB activation. SQSTM1/p62 consists of an N-terminal PB1 (Phox and Bem1p) domain, a ZZ type zinc finger domain, two PEST sequences containing putative phosphrylation sites, and a C-terminal UBA domain that forms noncovalent binding with polyubiquitin chains [142, 143]. SQSTM1/p62 shuttles between nucleus and cytoplasm, and has been found to partially reside in late endosomes and lysosomes [142, 144, 145]. In addition, SQSTM1/p62 is a common component of protein aggregates that contain abundant polyubiquitinated proteins [146, 147], and represent morphological hallmarks in protein aggregation diseases, such as neurodegenerative diseases, alcoholic liver diseases, and hepatocellular carcinoma [146, 148-152].

Under tissue culture conditions, SQSTM1/p62 proteins are enriched in numerous round speckles and punctae, termed sequestosome bodies (SQSTM1/p62 bodies) [153]. Sequestosome bodies come in different sizes with a diameter ranging from 0.1 μm to 2 μm. Immunocytochemistry and real-time confocal microscopic studies have classified these bodies into two subtypes: (1) a high number of faint, 0.1-to-0.2-μm-diameter bodies

that exhibit high mobility; and (2) a low number of intense, 0.5-to-2-µm-diameter bodies that exhibit lower mobility [154]. Further electron microscopic studies revealed that the smaller-sized subtype of sequestosome bodies is membrane-confined vesicles, while the larger-sized subtype is membrane-free protein aggregates [154]. It is possible that SQSTM1/p62 carries out distinct functions at different subtypes of sequestosome bodies, likely via association with distinct functional protein partners and nucleating different multi-protein complexes. Alternatively, given that SQSTM1/p62 can form homo-polymers via its N-terminal PB1 domain [153], SQSTM1/p62 may mediate 'fusion' of high-mobile, small-sized bodies with low-mobile, larger-sized bodies, and enable the functional communications in between [154, 155].

SQSTM1/p62 is a bona fide Keap1-binding protein via association with Kelch domain of Keap1 [156]. However, SQSTM1/p62 does not contain a (D/N)xE(T/S)GE motif, suggesting a low-affinity interaction between SQSTM1/p62 and Keap1. Thus, unlike DxETGE motif in Nrf2 that is deeply buried in the substrate-binding pocket, SQSTM1/p62 only binds to one side on the outer rim region of the binding pocket in Kelch domain of Keap1 [156]. Consistently, it was not observed that SQSTM1/p62 could be subjected to Keap1-dependent ubiquitination and degradation. Despite weaker interaction, a substantial amount (a subpopulation) of Keap1 is colocalized with SQSTM1/p62 proteins in the larger-sized sequestosome bodies [156]. Moreover, this subpopulation of Keap1 that partners with SQSTM1/p62 shuttles between nucleus and cytoplasm along with larger-sized sequestosome bodies, suggesting that this discrete compartment provides critical arena for the functionality of nuclear and cytoplasmic

Keap1-SQSTM1/p62 complexes. Interestingly, a high-throughput genomic screen for activators of ARE-dependent gene expression revealed SQSTM1/p62 as a top candidate [157]. Followed-up studies showed that overexpression of SQSTM1/p62 led to increased expression of detoxifying enzymes in an Nrf2-dependent manner, suggesting that SQSTM1/p62 may function as upstream regulator of Nrf2 [157]. Although the mechanism underlying SQSTM1/p62-mediated activation of Nrf2 functionality is unknown, it is likely that SQSTM1/p62 functions as a modulator for regulation of Nrf2 in a Keap1-dependent fashion.

F. A preview of the following chapters in this dissertation

The overall objective of the research presented in this dissertation was to understand the mechanisms of how Keap1 regulates Nrf2 by utilizing an array of biochemical, molecular and cell biological approaches. In chapter II, a set of experiments was carried out in collaboration with Dr. Donna D. Zhang, a previous postdoctoral fellow in Dr. Hannink's laboratory, in which we demonstrated that Keap1 functions as a substrate adaptor for a Cul3-RING ubiquitin ligase, and collectively targets Nrf2 for proteasome-mediated degradation. In addition, we demonstrated that both quinone-induced oxidative stress and sulforaphane, a chemopreventive isothiocyanate compound, inhibit Keap1-dependent Cul3-RING ligases, resulting in reduction of Nrf2 ubiquitination, accumulation of Nrf2 proteins and activation of Nrf2-dependent gene expression.

In chapter III, another set of experiments was carried out in collaboration with Dr. Donna D. Zhang, in which we demonstrated that the substrate adaptor Keap1 is subjected to auto-ubiquitination that requires the catalytic Cul3-RING subcomplex. Furthermore, we showed that quinone-induced oxidative stress promotes autoubiquitination and resultant degradation of Keap1, whereas sulforaphane does not. Thus, we revealed important differences between inducers of Nrf2-dependent transcription in terms of the regulatory mechanisms of how the Keap1-dependent Cul3-RING ligase can be modulated.

In chapter IV, I examined how the Keap1-dependent Cul3-RING ligase complex is regulated by both neddylation of the Cul3 protein, and by a CAND1 protein that competes with Keap1 for binding to Cul3. These experimental data suggested that dynamic cycles of assembly and disassembly of the Keap1-dependent Cul3-RING ligase are crucial for efficient degradation of Nrf2.

In chapter V, another set of experiments was carried out in collaboration with a previous graduate student, Xuchu Li, in which we determined the interaction interface within the Nrf2-Keap1 complex. In particular, I carried out a number of biochemical and mutational experiments that provided functional validation of Xuchu's crystallographic data. Additionally, these experimental data demonstrated that Keap1 and Nrf2 form a hetero-tetrameric complex with a 2:2 stoichiometry.

In chapter VI, I used a proteomic approach to identify the PGAM5 protein as a novel binding partner of Keap1. I carried out a set of experiments in which I

demonstrated that a cytoplasmic form of the PGAM5 protein is subjected to ubiquitin-dependent degradation by the Keap1-dependent Cul3-RING ligase.

In chapter VII, I carried out another set of experiments, in which I revealed a mitochondrial form of the PGAM5 protein. Interestingly, these experimental data demonstrated that unlike the cytoplasmic pools of PGAM5, the mitochondrial-localized PGAM5 proteins are not subjected to Keap1-mediated degradation. Instead, they function to recruit Keap1 and Nrf2 to mitochondria and form a ternary complex containing one PGAM5, one Keap1 homodimer, and one Nrf2 at the outer membrane of mitochondria.

In chapter VIII, a set of experiments are proposed for further investigations on the biochemical role of the mitochondrial PGAM5-Keap1-Nrf2 complex in regulation of Nrf2-dependent gene expression.

Figure I-1
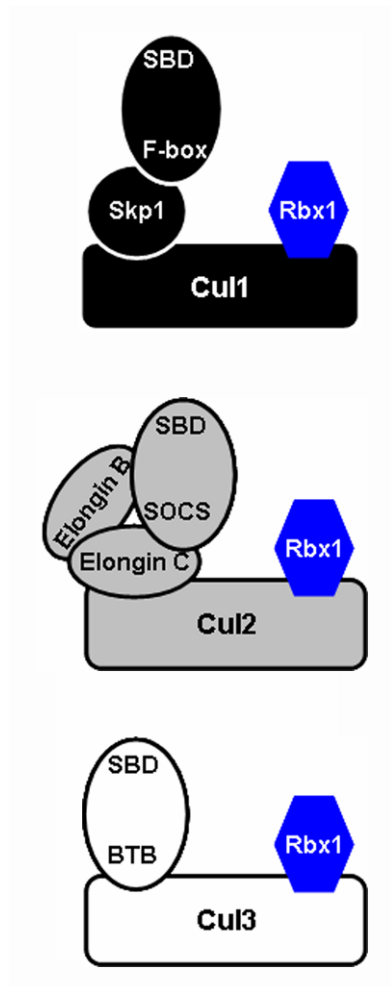
Figure I-1. Architecture of cullin-RING ligases. The typical cullin-RING ubiquitin ligases share strikingly similar architecture. In general, cullins serve as the complex organizational center. The C-terminal domains of cullins bind to the RING finger protein Rbx1 (Roc1/Hrt1), or Rbx2 in the case of Cul5-based CRL. The N-terminal regions of cullins bind to either a substrate adaptor subcomplex, or a single substrate adaptor protein in the case of Cul3-based CRL. The RING finger proteins recruit ubiquitin-charged E2 conjugating enzymes, while the substrate adaptor proteins recruit the cognate substrates via the substrate-binding domains (SBD). The general subunit components and architectures of a Cul1-RING ligase, a Cul2-RING ligase, and a Cul3-RING ligase are shown in this figure.

Figure I-2
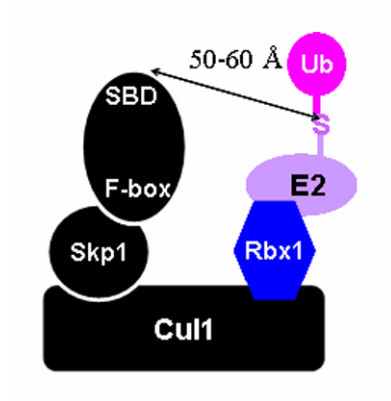
Figure I-2. The conundrum of a 50-60 Å gap in cullin-RING ligases. A paradoxical issue to consider though is that there is generally a 50-60 Å gap between the substrate-binding site of a substrate adaptor and the thiol ester bond of Ub~E2 in a CRL. It is not known how this 50-60 Å gap is bridged. However, this spatial gap may accommodate larger-scaled movement of a substrate's lysine residues that in turn enables productive positioning of Lys48 in the distal ubiqutin as a poly-ubiquitin chain grows.

Figure I-3
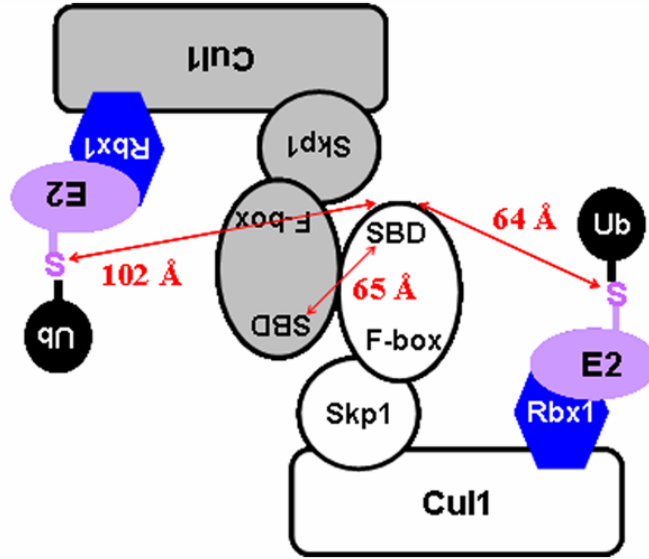
Figure I-3. A dimeric CRL supercomplex. Dimerization of the F-box proteins results in the assembly of a super-complex consisting of two sets of F-box protein:Skp1-dependent Cul1-RING ligase complexes. This dimeric Cul1-RING ligase supercomplex is oriented in a suprafacial configuration (side-by-side manner), such that the two substrate-binding sites (SBDs) in the F-box proteins are facing to the same general direction (sticking out perpendicularly from the paper in this figure). The two substrate-binding sites (SBDs) are apart from each other by ~65 Å. The predicted distance between one substrate-binding site (SBD) to the E2 active site in the neighboring CRL is 102 Å, while a 64 Å gap is lying between the substrate binding site (SBD) and the E2 active site within the same CRL

Figure I-4
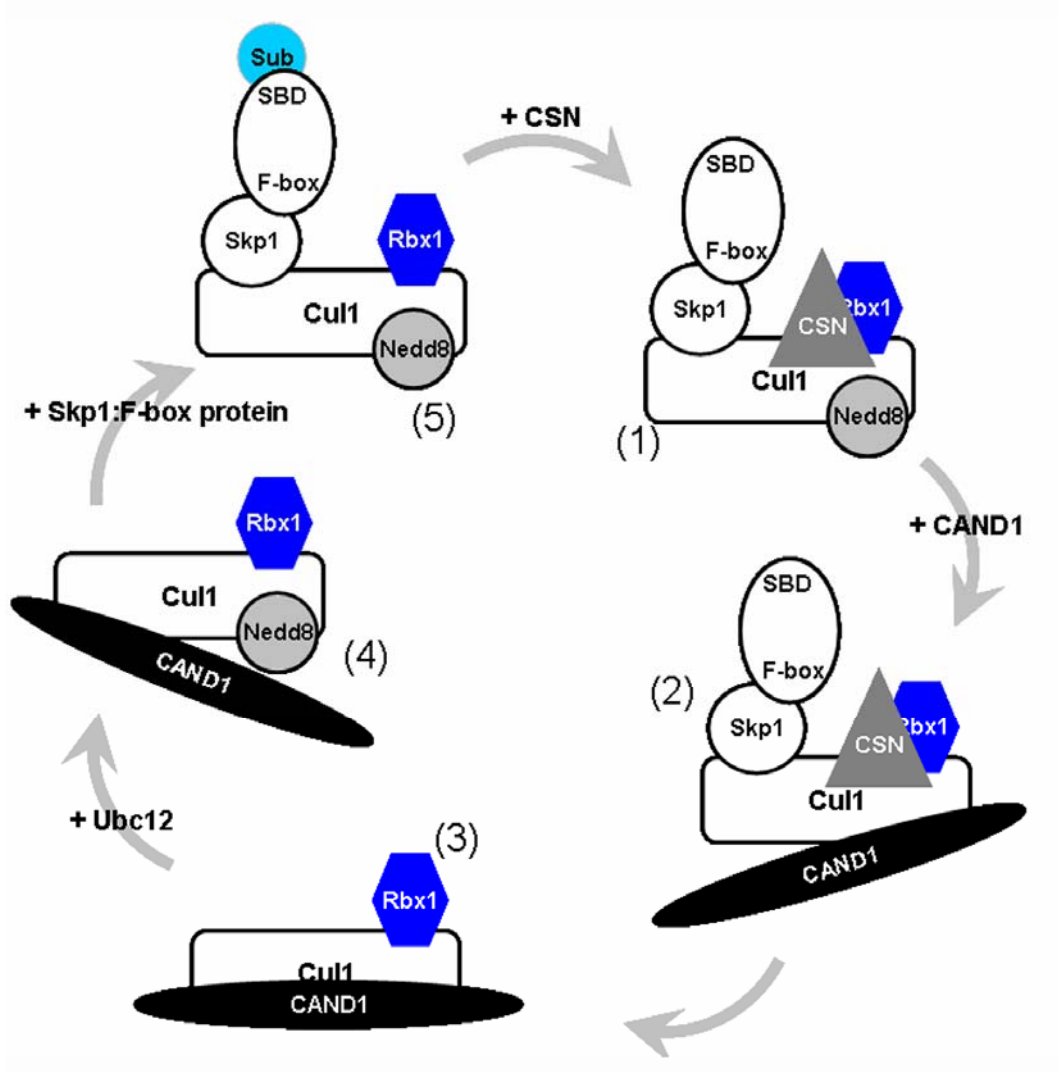
Figure I-4. A tentative model for the cyclic assembly and disassembly of a Cul1-RING ligase by neddylation and deneddylation of Cul1. (1) CSN is recruited to an active Cul1-RING ligase complex as the bound substrate is successfully degraded; (2) CSN cleaves Nedd8 conjugates from Cul1, and subsequently enables CAND1 to bind unneddylated Cul1; (3) binding of CAND1 with Cul1 dislodges FBP-Skp1 from Cul1, and temporarily inactivates this Cul1-RING ligase from degrading substrates; (4) E2-like enzyme Ubc12 mediates conjugation of Nedd8 onto Cul1, which weakens binding affinity of CAND1 for Cul1; (5) upon release of CAND1 from Cul1, another FBP-Skp1 re-associates with Cul1 and activates this Cul1-RING ligase for degradation of the bound substrate.

Figure I-5
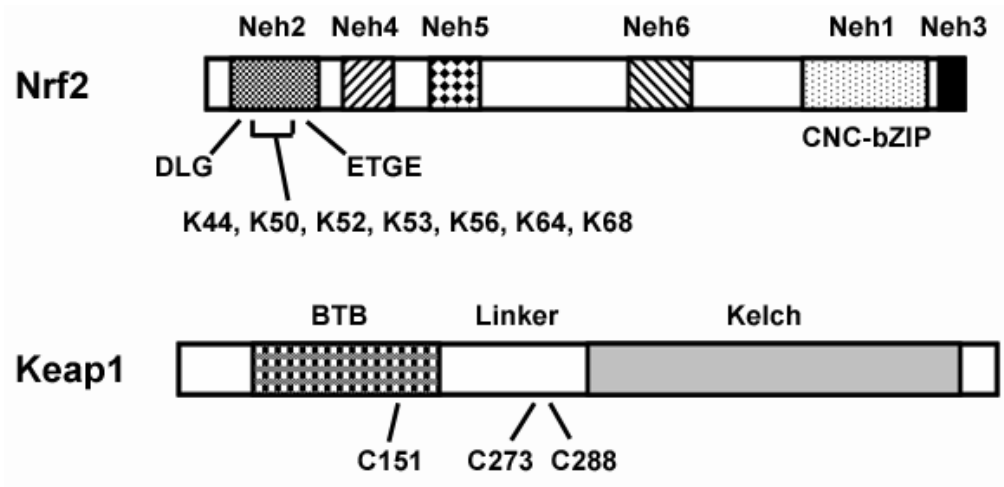
Figure I-5. Domain structures and motifs of Nrf2 and Keap1. Nrf2 consists of six conserved domains, termed Neh1-Neh6, each of which has unique roles for biochemical actions of Nrf2. First, the C-terminal Neh1 and Neh3 domains function in nuclear localization, DNA binding, and heterodimerization with small Maf proteins. Secondly, the Neh4 and Neh5 domains in the central region of Nrf2 function to recruit transcriptional co-activators, such as CBP (CREB-binding protein). Lastly, the Neh6 and Neh2 domains independently function to control ubiquitin-dependent proteolysis of Nrf2. The Neh6 is located in the central region of Nrf2, and renders moderate instability of Nrf2 independently of stress signals. The N-terminal Neh2 domain directly binds to the modular protein Keap1, whereby it mediates degradation of Nrf2 in a manner that is highly sensitive to stress signals. Keap1 contains an N-terminal BTB domain, a linker domain (IVR, or BACK) in the central region, and a C-terminal Kelch domain. The BTB domain accounts for formation of Keap1 homotypic dimer. The linker domain harbors a leucine-rich nuclear export sequence (NES) that accounts for mass cytoplasmic localization of Keap1. Both BTB domain and linker domain are required for Keap1 to assemble into Cul3-RING ligases. Lastly, the Kelch domain of Keap1 mainly functions to mediate protein-protein interaction between Keap1 homodimer and a diverse array of proteins, such as Nrf2, actins, PGAM5, and p62 (SQSTM1).

Figure I-6
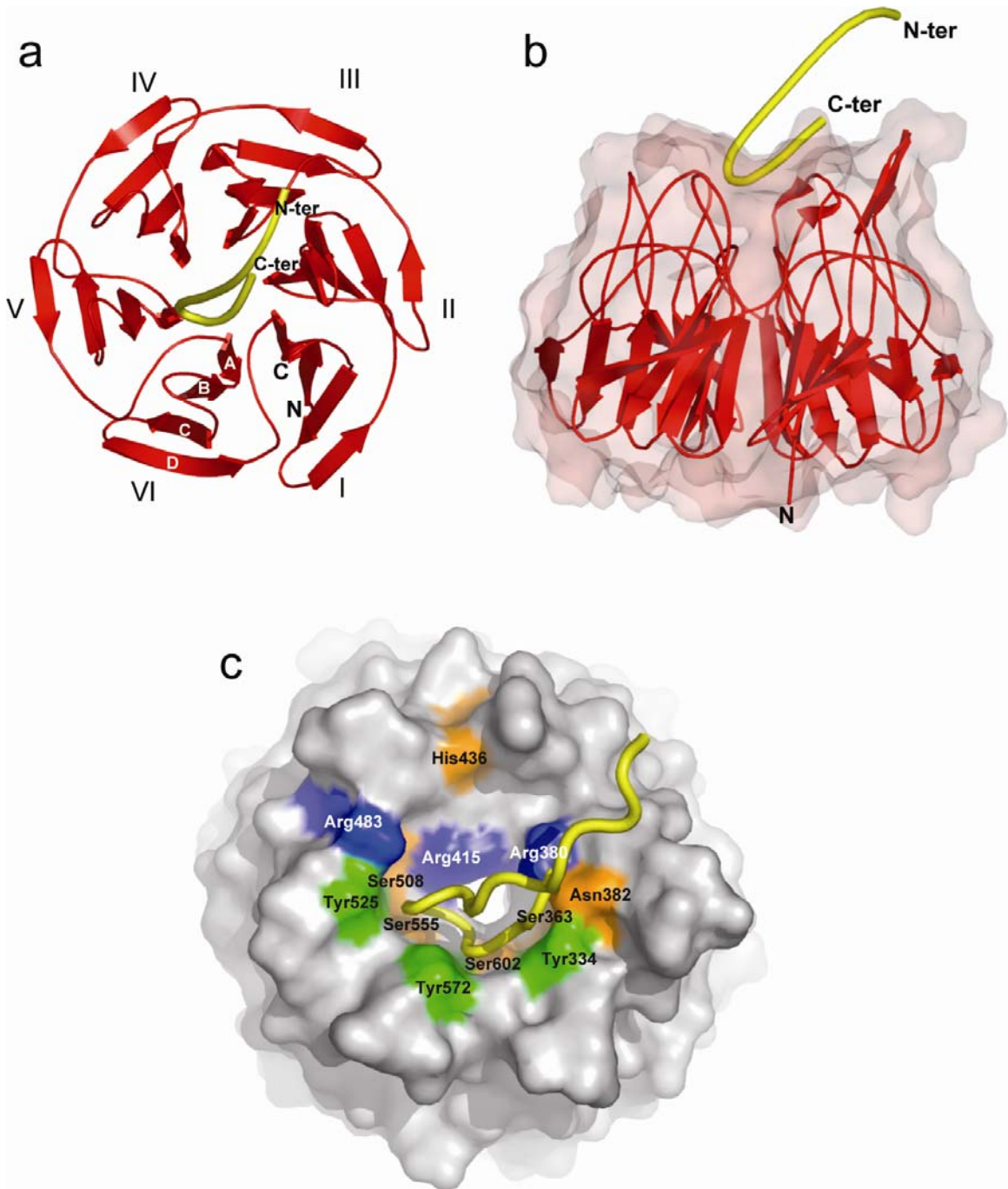
Figure I-6. Three-dimensional structures of the Kelch β-propeller bound with the Nrf2-derived peptide. (**A**) A ribbon diagram of the Kelch β-propeller (red) and bound Nrf2 peptide (yellow tube). The termini of the peptide are labeled N-ter and C-ter; those of the Kelch domain are labeled N and C. The six blades of the β-propeller are labeled I-VI and the four β-strands found in each blade are labeled A-D (white font) on blade VI. (**B**) Side view of the Kelch domain, with a surface representation of the β-propeller. (**C**) A surface representation of the Kelch propeller (gray) and peptide (yellow tube). Selected residues are shown in blue (basic), orange (polar), and green (apolar).

REFERENCE

1. Voges, D., P. Zwickl, and W. Baumeister, *The 26S proteasome: a molecular machine designed for controlled proteolysis.* Annu Rev Biochem, 1999. **68**: p. 1015-68.

2. Chau, V., et al., *A multiubiquitin chain is confined to specific lysine in a targeted short-lived protein.* Science, 1989. **243**(4898): p. 1576-83.

3. Hershko, A. and A. Ciechanover, *The ubiquitin system.* Annu Rev Biochem, 1998. **67**: p. 425-79.

4. Pickart, C.M., *Mechanisms underlying ubiquitination.* Annu Rev Biochem, 2001. **70**: p. 503-33.

5. Zheng, N., et al., *Structure of the Cul1-Rbx1-Skp1-F boxSkp2 SCF ubiquitin ligase complex.* Nature, 2002. **416**(6882): p. 703-9.

6. Borden, K.L., *RING domains: master builders of molecular scaffolds?* J Mol Biol, 2000. **295**(5): p. 1103-12.

7. Cardozo, T. and M. Pagano, *The SCF ubiquitin ligase: insights into a molecular machine.* Nat Rev Mol Cell Biol, 2004. **5**(9): p. 739-51.

8. Orlicky, S., et al., *Structural basis for phosphodependent substrate selection and orientation by the SCFCdc4 ubiquitin ligase.* Cell, 2003. **112**(2): p. 243-56.

9. Wu, G., et al., *Structure of a beta-TrCP1-Skp1-beta-catenin complex: destruction motif binding and lysine specificity of the SCF(beta-TrCP1) ubiquitin ligase.* Mol Cell, 2003. **11**(6): p. 1445-56.

10. Bullock, A.N., et al., *Crystal structure of the SOCS2-elongin C-elongin B complex defines a prototypical SOCS box ubiquitin ligase.* Proc Natl Acad Sci U S A, 2006. **103**(20): p. 7637-42.

11. Stogios, P.J., et al., *Sequence and structural analysis of BTB domain proteins.* Genome Biol, 2005. **6**(10): p. R82.

12.   Jaakkola, P., et al., *Targeting of HIF-alpha to the von Hippel-Lindau ubiquitylation complex by O2-regulated prolyl hydroxylation.* Science, 2001. **292**(5516): p. 468-72.

13.   Hon, W.C., et al., *Structural basis for the recognition of hydroxyproline in HIF-1 alpha by pVHL.* Nature, 2002. **417**(6892): p. 975-8.

14.   Nash, P., et al., *Multisite phosphorylation of a CDK inhibitor sets a threshold for the onset of DNA replication.* Nature, 2001. **414**(6863): p. 514-21.

15.   Welcker, M., et al., *Multisite phosphorylation by Cdk2 and GSK3 controls cyclin E degradation.* Mol Cell, 2003. **12**(2): p. 381-92.

16.   Yoshida, Y., et al., *E3 ubiquitin ligase that recognizes sugar chains.* Nature, 2002. **418**(6896): p. 438-42.

17.   Mizushima, T., et al., *Structural basis for the selection of glycosylated substrates by SCF(Fbs1) ubiquitin ligase.* Proc Natl Acad Sci U S A, 2007. **104**(14): p. 5777-81.

18.   Clurman, B.E., et al., *Turnover of cyclin E by the ubiquitin-proteasome pathway is regulated by cdk2 binding and cyclin phosphorylation.* Genes Dev, 1996. **10**(16): p. 1979-90.

19.   Singer, J.D., et al., *Cullin-3 targets cyclin E for ubiquitination and controls S phase in mammalian cells.* Genes Dev, 1999. **13**(18): p. 2375-87.

20.   Winston, J.T., C. Chu, and J.W. Harper, *Culprits in the degradation of cyclin E apprehended.* Genes Dev, 1999. **13**(21): p. 2751-7.

21.   Winston, J.T., et al., *The SCFbeta-TRCP-ubiquitin ligase complex associates specifically with phosphorylated destruction motifs in IkappaBalpha and beta-catenin and stimulates IkappaBalpha ubiquitination in vitro.* Genes Dev, 1999. **13**(3): p. 270-83.

22.   Koepp, D.M., et al., *Phosphorylation-dependent ubiquitination of cyclin E by the SCFFbw7 ubiquitin ligase.* Science, 2001. **294**(5540): p. 173-7.

23. Yada, M., et al., *Phosphorylation-dependent degradation of c-Myc is mediated by the F-box protein Fbw7.* Embo J, 2004. **23**(10): p. 2116-25.

24. Nateri, A.S., et al., *The ubiquitin ligase SCFFbw7 antagonizes apoptotic JNK signaling.* Science, 2004. **303**(5662): p. 1374-8.

25. Tsunematsu, R., et al., *Mouse Fbw7/Sel-10/Cdc4 is required for notch degradation during vascular development.* J Biol Chem, 2004. **279**(10): p. 9417-23.

26. Lo, S.C. and M. Hannink, *PGAM5, a Bcl-XL-interacting protein, is a novel substrate for the redox-regulated Keap1-dependent ubiquitin ligase complex.* J Biol Chem, 2006. **281**(49): p. 37893-903.

27. Zhang, D.D., et al., *Keap1 is a redox-regulated substrate adaptor protein for a Cul3-dependent ubiquitin ligase complex.* Mol Cell Biol, 2004. **24**(24): p. 10941-53.

28. Allen, E., et al., *Gigaxonin-controlled degradation of MAP1B light chain is critical to neuronal survival.* Nature, 2005. **438**(7065): p. 224-8.

29. Wang, W., et al., *Gigaxonin interacts with tubulin folding cofactor B and controls its degradation through the ubiquitin-proteasome pathway.* Curr Biol, 2005. **15**(22): p. 2050-5.

30. Carroll, C.W. and D.O. Morgan, *The Doc1 subunit is a processivity factor for the anaphase-promoting complex.* Nat Cell Biol, 2002. **4**(11): p. 880-7.

31. Rape, M., S.K. Reddy, and M.W. Kirschner, *The processivity of multiubiquitination by the APC determines the order of substrate degradation.* Cell, 2006. **124**(1): p. 89-103.

32. Peters, J.M., *The anaphase-promoting complex: proteolysis in mitosis and beyond.* Mol Cell, 2002. **9**(5): p. 931-43.

33. Cope, G.A. and R.J. Deshaies, *COP9 signalosome: a multifunctional regulator of SCF and other cullin-based ubiquitin ligases.* Cell, 2003. **114**(6): p. 663-71.

34.   Serino, G. and X.W. Deng, *The COP9 signalosome: regulating plant development through the control of proteolysis.* Annu Rev Plant Biol, 2003. **54**: p. 165-82.

35.   Goldenberg, S.J., et al., *Structure of the Cand1-Cul1-Roc1 complex reveals regulatory mechanisms for the assembly of the multisubunit cullin-dependent ubiquitin ligases.* Cell, 2004. **119**(4): p. 517-28.

36.   Liu, J., et al., *NEDD8 modification of CUL1 dissociates p120(CAND1), an inhibitor of CUL1-SKP1 binding and SCF ligases.* Mol Cell, 2002. **10**(6): p. 1511-8.

37.   Zheng, J., et al., *CAND1 binds to unneddylated CUL1 and regulates the formation of SCF ubiquitin E3 ligase complex.* Mol Cell, 2002. **10**(6): p. 1519-26.

38.   Burton, J.L., V. Tsakraklides, and M.J. Solomon, *Assembly of an APC-Cdh1-substrate complex is stimulated by engagement of a destruction box.* Mol Cell, 2005. **18**(5): p. 533-42.

39.   Ganoth, D., et al., *The cell-cycle regulatory protein Cks1 is required for SCF(Skp2)-mediated ubiquitinylation of p27.* Nat Cell Biol, 2001. **3**(3): p. 321-4.

40.   Spruck, C., et al., *A CDK-independent function of mammalian Cks1: targeting of SCF(Skp2) to the CDK inhibitor p27Kip1.* Mol Cell, 2001. **7**(3): p. 639-50.

41.   Hao, B., et al., *Structural basis of the Cks1-dependent recognition of p27(Kip1) by the SCF(Skp2) ubiquitin ligase.* Mol Cell, 2005. **20**(1): p. 9-19.

42.   Davis, M., et al., *Pseudosubstrate regulation of the SCF(beta-TrCP) ubiquitin ligase by hnRNP-U.* Genes Dev, 2002. **16**(4): p. 439-51.

43.   Hao, B., et al., *Structure of a Fbw7-Skp1-cyclin E complex: multisite-phosphorylated substrate recognition by SCF ubiquitin ligases.* Mol Cell, 2007. **26**(1): p. 131-43.

44.   Welcker, M. and B.E. Clurman, *Fbw7/hCDC4 dimerization regulates its substrate interactions.* Cell Div, 2007. **2**: p. 7.

45.   Suzuki, H., et al., *Homodimer of two F-box proteins betaTrCP1 or betaTrCP2 binds to IkappaBalpha for signal-dependent ubiquitination.* J Biol Chem, 2000. **275**(4): p. 2877-84.

46.   Zipper, L.M. and R.T. Mulcahy, *The Keap1 BTB/POZ dimerization function is required to sequester Nrf2 in cytoplasm.* J Biol Chem, 2002. **277**(39): p. 36544-52.

47.   Chung, J., et al., *Homotypic association between tumour-associated VHL proteins leads to the restoration of HIF pathway.* Oncogene, 2006. **25**(21): p. 3079-83.

48.   Tang, X., et al., *Suprafacial orientation of the SCFCdc4 dimer accommodates multiple geometries for substrate ubiquitination.* Cell, 2007. **129**(6): p. 1165-76.

49.   Kominami, K., I. Ochotorena, and T. Toda, *Two F-box/WD-repeat proteins Pop1 and Pop2 form hetero- and homo-complexes together with cullin-1 in the fission yeast SCF (Skp1-Cullin-1-F-box) ubiquitin ligase.* Genes Cells, 1998. **3**(11): p. 721-35.

50.   Wolf, D.A., F. McKeon, and P.K. Jackson, *F-box/WD-repeat proteins pop1p and Sud1p/Pop2p form complexes that bind and direct the proteolysis of cdc18p.* Curr Biol, 1999. **9**(7): p. 373-6.

51.   Petroski, M.D. and R.J. Deshaies, *Function and regulation of cullin-RING ubiquitin ligases.* Nat Rev Mol Cell Biol, 2005. **6**(1): p. 9-20.

52.   Chew, E.H., et al., *Characterization of cullin-based E3 ubiquitin ligases in intact mammalian cells--evidence for cullin dimerization.* Cell Signal, 2007. **19**(5): p. 1071-80.

53.   Wimuttisuk, W. and J.D. Singer, *The Cullin3 ubiquitin ligase functions as a Nedd8-bound heterodimer.* Mol Biol Cell, 2007. **18**(3): p. 899-909.

54.   Huang, J. and J.W. Raff, *The disappearance of cyclin B at the end of mitosis is regulated spatially in Drosophila cells.* Embo J, 1999. **18**(8): p. 2184-95.

55.   Huang, J.Y. and J.W. Raff, *The dynamic localisation of the Drosophila APC/C: evidence for the existence of multiple complexes that perform distinct functions and are differentially localised.* J Cell Sci, 2002. **115**(Pt 14): p. 2847-56.

56.   Tugendreich, S., et al., *CDC27Hs colocalizes with CDC16Hs to the centrosome and mitotic spindle and is essential for the metaphase to anaphase transition.* Cell, 1995. **81**(2): p. 261-8.

57.   Welcker, M., et al., *A nucleolar isoform of the Fbw7 ubiquitin ligase regulates c-Myc and cell size.* Curr Biol, 2004. **14**(20): p. 1852-7.

58.   Ye, X., et al., *Recognition of phosphodegron motifs in human cyclin E by the SCF(Fbw7) ubiquitin ligase.* J Biol Chem, 2004. **279**(48): p. 50110-9.

59.   Jackman, M., et al., *Cyclin A- and cyclin E-Cdk complexes shuttle between the nucleus and the cytoplasm.* Mol Biol Cell, 2002. **13**(3): p. 1030-45.

60.   Juan, G. and C. Cordon-Cardo, *Intranuclear compartmentalization of cyclin E during the cell cycle: disruption of the nucleoplasm-nucleolar shuttling of cyclin E in bladder cancer.* Cancer Res, 2001. **61**(3): p. 1220-6.

61.   Galan, J.M. and M. Peter, *Ubiquitin-dependent degradation of multiple F-box proteins by an autocatalytic mechanism.* Proc Natl Acad Sci U S A, 1999. **96**(16): p. 9124-9.

62.   Zhou, P. and P.M. Howley, *Ubiquitination and degradation of the substrate recognition subunits of SCF ubiquitin-protein ligases.* Mol Cell, 1998. **2**(5): p. 571-80.

63.   Lisztwan, J., et al., *Association of human CUL-1 and ubiquitin-conjugating enzyme CDC34 with the F-box protein p45(SKP2): evidence for evolutionary conservation in the subunit composition of the CDC34-SCF pathway.* Embo J, 1998. **17**(2): p. 368-83.

64.   Wirbelauer, C., et al., *The F-box protein Skp2 is a ubiquitylation target of a Cul1-based core ubiquitin ligase complex: evidence for a role of Cul1 in the suppression of Skp2 expression in quiescent fibroblasts.* Embo J, 2000. **19**(20): p. 5362-75.

65.   Bashir, T., et al., *Control of the SCF(Skp2-Cks1) ubiquitin ligase by the APC/C(Cdh1) ubiquitin ligase.* Nature, 2004. **428**(6979): p. 190-3.

66. Wei, W., et al., *Degradation of the SCF component Skp2 in cell-cycle phase G1 by the anaphase-promoting complex.* Nature, 2004. **428**(6979): p. 194-8.

67. Whitby, F.G., et al., *Crystal structure of the human ubiquitin-like protein NEDD8 and interactions with ubiquitin pathway enzymes.* J Biol Chem, 1998. **273**(52): p. 34983-91.

68. Kerscher, O., R. Felberbaum, and M. Hochstrasser, *Modification of proteins by ubiquitin and ubiquitin-like proteins.* Annu Rev Cell Dev Biol, 2006. **22**: p. 159-80.

69. Hochstrasser, M., *There's the rub: a novel ubiquitin-like modification linked to cell cycle regulation.* Genes Dev, 1998. **12**(7): p. 901-7.

70. Kawakami, T., et al., *NEDD8 recruits E2-ubiquitin to SCF E3 ligase.* Embo J, 2001. **20**(15): p. 4003-12.

71. Wu, J.T., et al., *Neddylation and deneddylation regulate Cul1 and Cul3 protein accumulation.* Nat Cell Biol, 2005. **7**(10): p. 1014-20.

72. Wei, N. and X.W. Deng, *The COP9 signalosome.* Annu Rev Cell Dev Biol, 2003. **19**: p. 261-86.

73. Lo, S.C. and M. Hannink, *CAND1-mediated substrate adaptor recycling is required for efficient repression of Nrf2 by Keap1.* Mol Cell Biol, 2006. **26**(4): p. 1235-44.

74. Zhou, C., et al., *Fission yeast COP9/signalosome suppresses cullin activity through recruitment of the deubiquitylating enzyme Ubp12p.* Mol Cell, 2003. **11**(4): p. 927-38.

75. Li, Y., et al., *Stability of homologue of Slimb F-box protein is regulated by availability of its substrate.* J Biol Chem, 2004. **279**(12): p. 11074-80.

76. Wee, S., et al., *CSN facilitates Cullin-RING ubiquitin ligase function by counteracting autocatalytic adapter instability.* Nat Cell Biol, 2005. **7**(4): p. 387-91.

77.   Cope, G.A. and R.J. Deshaies, *Targeted silencing of Jab1/Csn5 in human cells downregulates SCF activity through reduction of F-box protein levels.* BMC Biochem, 2006. **7**: p. 1.

78.   Hwang, J.W., et al., *TIP120A associates with unneddylated cullin 1 and regulates its neddylation.* FEBS Lett, 2003. **541**(1-3): p. 102-8.

79.   Bornstein, G., D. Ganoth, and A. Hershko, *Regulation of neddylation and deneddylation of cullin1 in SCFSkp2 ubiquitin ligase by F-box protein and substrate.* Proc Natl Acad Sci U S A, 2006. **103**(31): p. 11515-20.

80.   Jaiswal, A.K., *Nrf2 signaling in coordinated activation of antioxidant gene expression.* Free Radic Biol Med, 2004. **36**(10): p. 1199-207.

81.   Kensler, T.W., N. Wakabayashi, and S. Biswal, *Cell survival responses to environmental stresses via the Keap1-Nrf2-ARE pathway.* Annu Rev Pharmacol Toxicol, 2007. **47**: p. 89-116.

82.   Padmanabhan, B., et al., *Structural basis for defects of Keap1 activity provoked by its point mutations in lung cancer.* Mol Cell, 2006. **21**(5): p. 689-700.

83.   Motohashi, H., et al., *Integration and diversity of the regulatory network composed of Maf and CNC families of transcription factors.* Gene, 2002. **294**(1-2): p. 1-12.

84.   Nguyen, T., P.J. Sherratt, and C.B. Pickett, *Regulatory mechanisms controlling gene expression mediated by the antioxidant response element.* Annu Rev Pharmacol Toxicol, 2003. **43**: p. 233-60.

85.   Alam, J., S. Camhi, and A.M. Choi, *Identification of a second region upstream of the mouse heme oxygenase-1 gene that functions as a basal level and inducer-dependent transcription enhancer.* J Biol Chem, 1995. **270**(20): p. 11977-84.

86.   Friling, R.S., et al., *Xenobiotic-inducible expression of murine glutathione S-transferase Ya subunit gene is controlled by an electrophile-responsive element.* Proc Natl Acad Sci U S A, 1990. **87**(16): p. 6258-62.

87.   Kim, Y.C., et al., *Hemin-induced activation of the thioredoxin gene by Nrf2. A differential regulation of the antioxidant responsive element by a switch of its binding factors.* J Biol Chem, 2001. **276**(21): p. 18399-406.

88.   Mulcahy, R.T., et al., *Constitutive and beta-naphthoflavone-induced expression of the human gamma-glutamylcysteine synthetase heavy subunit gene is regulated by a distal antioxidant response element/TRE sequence.* J Biol Chem, 1997. **272**(11): p. 7445-54.

89.   Rushmore, T.H., M.R. Morton, and C.B. Pickett, *The antioxidant responsive element. Activation by oxidative stress and identification of the DNA consensus sequence required for functional activity.* J Biol Chem, 1991. **266**(18): p. 11632-9.

90.   Itoh, K., et al., *An Nrf2/small Maf heterodimer mediates the induction of phase II detoxifying enzyme genes through antioxidant response elements.* Biochem Biophys Res Commun, 1997. **236**(2): p. 313-22.

91.   Kwak, M.K., et al., *Modulation of gene expression by cancer chemopreventive dithiolethiones through the Keap1-Nrf2 pathway. Identification of novel gene clusters for cell survival.* J Biol Chem, 2003. **278**(10): p. 8135-45.

92.   Li, J., J.M. Lee, and J.A. Johnson, *Microarray analysis reveals an antioxidant responsive element-driven gene set involved in conferring protection from an oxidative stress-induced apoptosis in IMR-32 cells.* J Biol Chem, 2002. **277**(1): p. 388-94.

93.   Thimmulappa, R.K., et al., *Identification of Nrf2-regulated genes induced by the chemopreventive agent sulforaphane by oligonucleotide microarray.* Cancer Res, 2002. **62**(18): p. 5196-203.

94.   Lee, J.M., et al., *Identification of the NF-E2-related factor-2-dependent genes conferring protection against oxidative stress in primary cortical astrocytes using oligonucleotide microarray analysis.* J Biol Chem, 2003. **278**(14): p. 12029-38.

95.   Shih, A.Y., et al., *Induction of the Nrf2-driven antioxidant response confers neuroprotection during mitochondrial stress in vivo.* J Biol Chem, 2005. **280**(24): p. 22925-36.

96.   Kitamura, Y., et al., *Increased susceptibility to hepatocarcinogenicity of Nrf2-deficient mice exposed to 2-amino-3-methylimidazo[4,5-f]quinoline.* Cancer Sci, 2007. **98**(1): p. 19-24.

97.   Ramos-Gomez, M., et al., *Interactive effects of nrf2 genotype and oltipraz on benzo[a]pyrene-DNA adducts and tumor yield in mice.* Carcinogenesis, 2003. **24**(3): p. 461-7.

98.   Ramos-Gomez, M., et al., *Sensitivity to carcinogenesis is increased and chemoprotective efficacy of enzyme inducers is lost in nrf2 transcription factor-deficient mice.* Proc Natl Acad Sci U S A, 2001. **98**(6): p. 3410-5.

99.   Burton, N.C., T.W. Kensler, and T.R. Guilarte, *In vivo modulation of the Parkinsonian phenotype by Nrf2.* Neurotoxicology, 2006. **27**(6): p. 1094-100.

100.   Chan, K. and Y.W. Kan, *Nrf2 is essential for protection against acute pulmonary injury in mice.* Proc Natl Acad Sci U S A, 1999. **96**(22): p. 12731-6.

101.   Ma, Q., L. Battelli, and A.F. Hubbs, *Multiorgan autoimmune inflammation, enhanced lymphoproliferation, and impaired homeostasis of reactive oxygen species in mice lacking the antioxidant-activated transcription factor Nrf2.* Am J Pathol, 2006. **168**(6): p. 1960-74.

102.   Morito, N., et al., *Nrf2 deficiency improves autoimmune nephritis caused by the fas mutation lpr.* Kidney Int, 2004. **65**(5): p. 1703-13.

103.   Yoh, K., et al., *Nrf2-deficient female mice develop lupus-like autoimmune nephritis.* Kidney Int, 2001. **60**(4): p. 1343-53.

104.   Nioi, P., et al., *The carboxy-terminal Neh3 domain of Nrf2 is required for transcriptional activation.* Mol Cell Biol, 2005. **25**(24): p. 10895-906.

105.   Katoh, Y., et al., *Two domains of Nrf2 cooperatively bind CBP, a CREB binding protein, and synergistically activate transcription.* Genes Cells, 2001. **6**(10): p. 857-68.

106.   Shen, G., et al., *Regulation of Nrf2 transactivation domain activity. The differential effects of mitogen-activated protein kinase cascades and synergistic*

stimulatory effect of Raf and CREB-binding protein. J Biol Chem, 2004. **279**(22): p. 23052-60.

107.   McMahon, M., et al., *Redox-regulated turnover of Nrf2 is determined by at least two separate protein domains, the redox-sensitive Neh2 degron and the redox-insensitive Neh6 degron.* J Biol Chem, 2004. **279**(30): p. 31556-67.

108.   Itoh, K., et al., *Keap1 represses nuclear activation of antioxidant responsive elements by Nrf2 through binding to the amino-terminal Neh2 domain.* Genes Dev, 1999. **13**(1): p. 76-86.

109.   Dinkova-Kostova, A.T., et al., *Direct evidence that sulfhydryl groups of Keap1 are the sensors regulating induction of phase 2 enzymes that protect against carcinogens and oxidants.* Proc Natl Acad Sci U S A, 2002. **99**(18): p. 11908-13.

110.   Hong, F., et al., *Specific patterns of electrophile adduction trigger Keap1 ubiquitination and Nrf2 activation.* J Biol Chem, 2005. **280**(36): p. 31768-75.

111.   Eggler, A.L., et al., *Modifying specific cysteines of the electrophile-sensing human Keap1 protein is insufficient to disrupt binding to the Nrf2 domain Neh2.* Proc Natl Acad Sci U S A, 2005. **102**(29): p. 10070-5.

112.   Zhang, D.D. and M. Hannink, *Distinct cysteine residues in Keap1 are required for Keap1-dependent ubiquitination of Nrf2 and for stabilization of Nrf2 by chemopreventive agents and oxidative stress.* Mol Cell Biol, 2003. **23**(22): p. 8137-51.

113.   Dinkova-Kostova, A.T., W.D. Holtzclaw, and N. Wakabayashi, *Keap1, the sensor for electrophiles and oxidants that regulates the phase 2 response, is a zinc metalloprotein.* Biochemistry, 2005. **44**(18): p. 6889-99.

114.   Espinas, M.L., et al., *The N-terminal POZ domain of GAGA mediates the formation of oligomers that bind DNA with high affinity and specificity.* J Biol Chem, 1999. **274**(23): p. 16461-9.

115.   Katsani, K.R., M.A. Hajibagheri, and C.P. Verrijzer, *Co-operative DNA binding by GAGA transcription factor requires the conserved BTB/POZ domain and reorganizes promoter topology.* Embo J, 1999. **18**(3): p. 698-708.

116. Hoatlin, M.E., et al., *A novel BTB/POZ transcriptional repressor protein interacts with the Fanconi anemia group C protein and PLZF*. Blood, 1999. **94**(11): p. 3737-47.

117. Takenaga, M., et al., *Bcl6-dependent transcriptional repression by BAZF*. Biochem Biophys Res Commun, 2003. **303**(2): p. 600-8.

118. Ahmad, K.F., et al., *Mechanism of SMRT corepressor recruitment by the BCL6 BTB domain*. Mol Cell, 2003. **12**(6): p. 1551-64.

119. Melnick, A., et al., *In-depth mutational analysis of the promyelocytic leukemia zinc finger BTB/POZ domain reveals motifs and residues required for biological and transcriptional functions*. Mol Cell Biol, 2000. **20**(17): p. 6550-67.

120. Ahmad, K.F., C.K. Engel, and G.G. Prive, *Crystal structure of the BTB domain from PLZF*. Proc Natl Acad Sci U S A, 1998. **95**(21): p. 12123-8.

121. McMahon, M., et al., *Dimerization of substrate adaptors can facilitate cullin-mediated ubiquitylation of proteins by a "tethering" mechanism: a two-site interaction model for the Nrf2-Keap1 complex*. J Biol Chem, 2006. **281**(34): p. 24756-68.

122. Velichkova, M. and T. Hasson, *Keap1 regulates the oxidation-sensitive shuttling of Nrf2 into and out of the nucleus via a Crm1-dependent nuclear export mechanism*. Mol Cell Biol, 2005. **25**(11): p. 4501-13.

123. Kobayashi, A., et al., *Oxidative stress sensor Keap1 functions as an adaptor for Cul3-based E3 ligase to regulate proteasomal degradation of Nrf2*. Mol Cell Biol, 2004. **24**(16): p. 7130-9.

124. Cullinan, S.B., et al., *The Keap1-BTB protein is an adaptor that bridges Nrf2 to a Cul3-based E3 ligase: oxidative stress sensing by a Cul3-Keap1 ligase*. Mol Cell Biol, 2004. **24**(19): p. 8477-86.

125. Clements, C.M., et al., *DJ-1, a cancer- and Parkinson's disease-associated protein, stabilizes the antioxidant transcriptional master regulator Nrf2*. Proc Natl Acad Sci U S A, 2006. **103**(41): p. 15091-6.

126.   Karapetian, R.N., et al., *Nuclear oncoprotein prothymosin alpha is a partner of Keap1: implications for expression of oxidative stress-protecting genes.* Mol Cell Biol, 2005. **25**(3): p. 1089-99.

127.   Strachan, G.D., et al., *Fetal Alz-50 clone 1 interacts with the human orthologue of the Kelch-like Ech-associated protein.* Biochemistry, 2004. **43**(38): p. 12113-22.

128.   Furukawa, M. and Y. Xiong, *BTB protein Keap1 targets antioxidant transcription factor Nrf2 for ubiquitination by the Cullin 3-Roc1 ligase.* Mol Cell Biol, 2005. **25**(1): p. 162-71.

129.   Kobayashi, M., et al., *Identification of the interactive interface and phylogenic conservation of the Nrf2-Keap1 system.* Genes Cells, 2002. **7**(8): p. 807-20.

130.   Kobayashi, A., et al., *Oxidative and electrophilic stresses activate Nrf2 through inhibition of ubiquitination activity of Keap1.* Mol Cell Biol, 2006. **26**(1): p. 221-9.

131.   Zhang, D.D., et al., *Ubiquitination of Keap1, a BTB-Kelch substrate adaptor protein for Cul3, targets Keap1 for degradation by a proteasome-independent pathway.* J Biol Chem, 2005. **280**(34): p. 30091-9.

132.   Tong, K.I., et al., *Keap1 recruits Neh2 through binding to ETGE and DLG motifs: characterization of the two-site molecular recognition model.* Mol Cell Biol, 2006. **26**(8): p. 2887-900.

133.   Lo, S.C., et al., *Structure of the Keap1:Nrf2 interface provides mechanistic insight into Nrf2 signaling.* Embo J, 2006. **25**(15): p. 3605-17.

134.   Katoh, Y., et al., *Evolutionary conserved N-terminal domain of Nrf2 is essential for the Keap1-mediated degradation of the protein by proteasome.* Arch Biochem Biophys, 2005. **433**(2): p. 342-50.

135.   Tong, K.I., et al., *Different Electrostatic Potentials Define ETGE and DLG Motifs as Hinge and Latch in Oxidative Stress Response.* Mol Cell Biol, 2007.

136.   Sun, Z., et al., *Keap1 controls postinduction repression of the Nrf2-mediated antioxidant response by escorting nuclear export of Nrf2.* Mol Cell Biol, 2007. **27**(18): p. 6334-49.

137. Kang, M.I., et al., *Scaffolding of Keap1 to the actin cytoskeleton controls the function of Nrf2 as key regulator of cytoprotective phase 2 genes.* Proc Natl Acad Sci U S A, 2004. **101**(7): p. 2046-51.

138. Velichkova, M. and T. Hasson, *Keap1 in adhesion complexes.* Cell Motil Cytoskeleton, 2003. **56**(2): p. 109-19.

139. Terada, L.S., *Specificity in reactive oxidant signaling: think globally, act locally.* J Cell Biol, 2006. **174**(5): p. 615-23.

140. Hansen, J.M., Y.M. Go, and D.P. Jones, *Nuclear and mitochondrial compartmentation of oxidative stress and redox signaling.* Annu Rev Pharmacol Toxicol, 2006. **46**: p. 215-34.

141. Lo, S.-C., M. Hannink, *PGAM5 anchors Keap1-Nrf2 complex at mitochondria, and regulates Nrf2-dependent gene expression. (submitted).* 2007.

142. Geetha, T. and M.W. Wooten, *Structure and functional properties of the ubiquitin binding protein p62.* FEBS Lett, 2002. **512**(1-3): p. 19-24.

143. Vadlamudi, R.K., et al., *p62, a phosphotyrosine-independent ligand of the SH2 domain of p56lck, belongs to a new class of ubiquitin-binding proteins.* J Biol Chem, 1996. **271**(34): p. 20235-7.

144. Sanchez, P., et al., *Localization of atypical protein kinase C isoforms into lysosome-targeted endosomes through interaction with p62.* Mol Cell Biol, 1998. **18**(5): p. 3069-80.

145. Samuels, I.S., et al., *Nerve growth factor stimulates the interaction of ZIP/p62 with atypical protein kinase C and targets endosomal localization: evidence for regulation of nerve growth factor-induced differentiation.* J Cell Biochem, 2001. **82**(3): p. 452-66.

146. Zatloukal, K., et al., *p62 Is a common component of cytoplasmic inclusions in protein aggregation diseases.* Am J Pathol, 2002. **160**(1): p. 255-63.

147. Donaldson, K.M., et al., *Ubiquitin-mediated sequestration of normal cellular proteins into polyglutamine aggregates.* Proc Natl Acad Sci U S A, 2003. **100**(15): p. 8892-7.

148.   Kuusisto, E., A. Salminen, and I. Alafuzoff, *Early accumulation of p62 in neurofibrillary tangles in Alzheimer's disease: possible role in tangle formation.* Neuropathol Appl Neurobiol, 2002. **28**(3): p. 228-37.

149.   Nakaso, K., et al., *Transcriptional activation of p62/A170/ZIP during the formation of the aggregates: possible mechanisms and the role in Lewy body formation in Parkinson's disease.* Brain Res, 2004. **1012**(1-2): p. 42-51.

150.   Nagaoka, U., et al., *Increased expression of p62 in expanded polyglutamine-expressing cells and its association with polyglutamine inclusions.* J Neurochem, 2004. **91**(1): p. 57-68.

151.   Stumptner, C., et al., *Analysis of intracytoplasmic hyaline bodies in a hepatocellular carcinoma. Demonstration of p62 as major constituent.* Am J Pathol, 1999. **154**(6): p. 1701-10.

152.   Stumptner, C., et al., *Mallory body--a disease-associated type of sequestosome.* Hepatology, 2002. **35**(5): p. 1053-62.

153.   Lamark, T., et al., *Interaction codes within the family of mammalian Phox and Bem1p domain-containing proteins.* J Biol Chem, 2003. **278**(36): p. 34568-81.

154.   Bjorkoy, G., et al., *p62/SQSTM1 forms protein aggregates degraded by autophagy and has a protective effect on huntingtin-induced cell death.* J Cell Biol, 2005. **171**(4): p. 603-14.

155.   Pankiv, S., et al., *p62/SQSTM1 binds directly to Atg8/LC3 to facilitate degradation of ubiquitinated protein aggregates by autophagy.* J Biol Chem, 2007. **282**(33): p. 24131-45.

156.   Lo, S.-C., M. Hannink, *Characterization of physical and functional interactions between Keap1 and SQSTM1/p62. (unpublished work).* 2007.

157.   Liu, Y., et al., *A genomic screen for activators of the antioxidant response element.* Proc Natl Acad Sci U S A, 2007. **104**(12): p. 5205-10.

II. KEAP1 IS A REDOX-REGULATED SUBSTRATE ADAPTOR PROTEIN FOR A CUL3-DEPENDENT UBIQUITIN LIGASE COMPLEX

ABSTRACT

The bZIP transcription factor Nrf2 controls a genetic program that protects cells from oxidative damage and maintains cellular redox homeostasis. Keap1, a BTB-Kelch protein, is the major upstream regulator of Nrf2 and controls both the subcellular localization and steady-state levels of Nrf2. In this report, we demonstrate that Keap1 functions as a substrate adaptor protein for a Cul3-dependent E3 ubiquitin ligase complex. Keap1 assembles into a functional E3 ubiquitin ligase complex with Cul3 and Rbx1 that targets multiple lysine residues located in the N-terminal Neh2 domain of Nrf2 for ubiquitin conjugation both in vivo and in vitro. Keap1-dependent ubiquitination of Nrf2 is inhibited following exposure of cells to quinone-induced oxidative stress and sulforaphane, a cancer-preventive isothiocyanate. A mutant Keap1 protein containing a single cysteine to serine substitution at residue 151 within the BTB domain of Keap1 is markedly resistant to inhibition by either quinone-induced oxidative stress or sulforaphane. Inhibition of Keap1-dependent ubiquitination of Nrf2 correlates with decreased association of Keap1 with Cul3. Neither quinone-induced oxidative stress nor sulforaphane disrupt association between Keap1 and Nrf2. Our results suggest that the ability of Keap1 to assemble into a functional E3 ubiquitin ligase complex is the critical determinant that controls steady-state levels of Nrf2 in response to cancer-preventive compounds and oxidative stress.

INTRODUCTION

Eukaryote cells are exposed to both intrinsic and extrinsic sources of reactive oxygen species (ROS) and other chemically reactive molecules that can damage biological macromolecules including DNA, proteins and lipids (22). Oxidative damage to biological macromolecules can have profound effects on cellular functions and has been implicated in cancer, inflammation, cardiovascular and neurodegenerative diseases and aging (2, 3, 9, 21, 39, 45). Eukaryote cells have evolved multiple mechanisms to provide protection from oxidative damage. One major mechanism for protection against oxidative damage involves the coordinated induction of a group of cytoprotective genes that enable cells to neutralize reactive molecules and restore cellular redox homeostasis (14, 41). These cytoprotective genes, which include classical Phase 2 genes such as the glutathione-S-transferases, NAD(P)H oxidoreductase (NQO1), and γ-glutamylcysteinesynthase (γGCS), are regulated at the transcriptional level by cis-acting DNA sequences termed Anti-oxidant Response Elements (AREs) or Electrophilic Response Elements (EpREs) (14, 41, 54).

The bZIP transcription factor Nrf2 is the major regulator of the cytoprotective ARE-dependent transcriptional program (27, 41). Nrf2 is a member of the Cap n' Collar (CNC) subclass of bZIP proteins, which share a conserved dimerization and DNA binding domain (38). Nrf2 binds DNA as a heterodimer with one of several small Maf proteins and is a potent activator of ARE-dependent transcription. The absence of Nrf2 results in impaired basal and inducible expression of genes that encode a diverse array of proteins, including the classical phase 2 proteins, protein chaperones, anti-oxidant

enzymes, and proteins involved in ubiquitin-dependent proteolysis, cell growth and apoptosis (23, 33, 34, 36, 51). The absence of Nrf2 does not impair normal development in mice but results in increased sensitivity to chemical-induced stresses (4, 10, 13, 18), hyperoxia (11), autoimmune-like nephritis (59), and chemical-induced carcinogenesis (44). Conversely, increased expression of Nrf2 protects against neurotoxic agents (35, 47). Activation of Nrf2-dependent gene expression by plant-derived phytochemicals contributes to their cancer-preventive properties (50).

Genetic and biochemical evidence have implicated the Keap1 protein as the major upstream regulator of Nrf2. Keap1 was first identified in a yeaste two-hybrid screen by virtue of its ability to bind the N-terminal Neh2 regulatory domain of Nrf2 (15, 25). Mice that lack Keap1 develop normally during embryogenesis, but die soon after birth due to hyperkeratotic constrictions of the esophagus and forestomach (53). The absence of Keap1 results in constitutive activation of Nrf2-dependent genes, while the postnatal lethality seen in Keap1-deficient mice is reversed in mice that lack both Nrf2 and Keap1 (53).

The cytoplasmic Keap1 protein is a potent repressor of Nrf2-dependent transcription (25). Keap1 contains an N-terminal BTB domain, a conserved linker domain and a C-terminal Kelch domain. The Kelch domain of Keap1 binds to the Neh2 domain of Nrf2 and, together with sequences located within the linker domain, enables Keap1 to sequester Nrf2 in the cytoplasm (25, 60). The Kelch domain of Keap1 is also able to bind actin and an intact actin-based cytoskeleton is required for cytoplasmic sequesteration of Nrf2 by Keap1 (29).

Keap1 also regulates steady-state levels of Nrf2. Consistent with several reports that Nrf2 is degraded by the proteosome in a Keap1-dependent manner (26, 37, 40, 49, 60), we have previously demonstrated that Keap1 is able to target Nrf2 for ubiquitination (60). In this report, we demonstrate that Keap1 associates with Cul3 and Rbx1 to form a functional E3 ubiquitin ligase complex that targets Nrf2 for ubiquitination both in vivo and in vitro. Our results provide the first direct evidence that a human BTB-Kelch protein can function as a substrate adaptor protein for a Cul3-dependent E3 ubiquitin ligase complex. Our results support the emerging view that proteins with BTB domains can function as substrate adaptors for Cul3-dependent E3 ubiquitin ligase complexes (19, 20, 43, 55, 58).

The ability of increased Nrf2 expression to protect cells from oxidative damage suggests that small molecules that increase Nrf2-dependent gene expression may have broad therapeutic benefits. Indeed, chemical inducers of Nrf2-dependent gene expression are promising cancer-preventive agents (32, 50). A large number of small molecule inducers of Nrf2-dependent gene expression, of both natural and synthetic origins, have been identified, and the ability of these structurally diverse molecules to react with thiols correlates with their ability to activate Nrf2-dependent transcription (17). In this report, we demonstrate that two well-characterized inducers of Nrf2-dependent transcription, quinone-induced oxidative stress and sulforaphane, a plant-derived isothiocyanate with chemopreventive properties, inhibit Keap1-dependent ubiquitination of Nrf2. A single cysteine-to-serine substitution at Cys 151 in the BTB domain of Keap1 confers significant resistance to inhibition by either oxidative stress or sulforaphane. Exposure of cells to these chemical inducers decreased association of Keap1 with Cul3. However,

these chemical inducers do not disrupt association between Keap1 and Nrf2. Regulation of ubiquitin ligase activity by a single redox-sensitive amino acid of the substrate adaptor protein represents a novel paradigm for regulation of cullin-dependent E3 ubiquitin ligases.

MATERIALS AND METHODS

Construction of recombinant DNA molecules. Plasmids expressing wild type Keap1, Nrf2, or Gal4-Neh2 proteins have been previously described (60). The CBD-tagged version of wild type Keap1 was generated by insertion of a PCR-generated DNA fragment encoding the chitin binding domain of *B. Circulans* chitinase A1 gene upstream of the stop codon for Keap1. The Keap1 mutants described in this study were generated by oligonucleotide-directed mutagenesis (46). Plasmids containing the individual cullin cDNAs were purchased from ATCC (American Type Culture Collection). A PCR-generated DNA containing the coding region of each cullin protein was cloned into the Sma1/Not1 sites of a HA-tagged pCI vector (Clontech). A Cul3 cDNA containing a stop codon at amino acid 381 was constructed by a PCR-based approach. The Myc-Rbx1 expression vector was obtained from Dr. Joan Conaway (28). The integrity of all of the plasmids used in this study was confirmed by sequence analysis.

Cell culture, transfections, indirect immunofluorescence and reporter gene assays. COS-1 and MDA-MB-231 cells were purchased from ATCC. Cells were maintained in either Dulbecco's modified Eagle's medium (DMEM) or Eagle's minimal essential medium (EMEM) in the presence of 10% fetal bovine serum (FBS). Transfections were performed with Lipofectamine Plus (Gibco BRL) according to the manufacturer's instructions. DNA amounts in each transfection were kept constant by addition of empty pcDNA3 plasmid. The ARE TATA-Inr luciferase reporter plasmid pARE-Luc was obtained from Dr. Bill Fahl (54). A plasmid encoding Renilla luciferase was included in

95

all samples to control for transfection efficiency. Reporter assays were performed using the Promega Dual-Light assay system as previously described (60).

Antibodies, immuprecipitation, and immunoblot analysis. The anti-Keap1 antibody has been described (60). Antibodies against Nrf2 (Santa Cruz), Gal4 (SantaCruz), ubiquitin (Sigma), Chitin binding domain (New England Biolabs) and the Myc and HA epitopes (Covance) were purchased from commercial sources.

For detection of protein expression in total cell lysates, cells were lysed in sample buffer (50 mM Tris-HCl [pH 6.8], 2% SDS, 10% Glycerol, 100 mM DTT, 0.1% bromophenol blue) at 48 hr post-transfection. For immunoprecipitation assays, cells were lysed in RIPA buffer (10 mM sodium phosphate pH [8.0], 150 mM NaCl, 1% Triton X-100, 1% sodium deoxycholate, 0.1% SDS) containing 1 mM dithiothreitol (DTT), 1 mM phenylmethylsulfonyl fluoride (PMSF) and protease inhibitor cocktail (Sigma). Cell lysates were pre-cleared with protein A beads and incubated with 2 μg of affinity-purified antibodies for 2 hr at 4 °C, followed by incubation at 4 °C with protein A-agarose beads for 2 hr. Immunoprecipitated complexes were washed four times with RIPA buffer and eluted in sample buffer by boiling for 4 minutes, electrophoresed through SDS-polyacrylamide gels, transferred to nitrocellulose membranes and subjected to immunoblot analysis.

Pulse-chase analyses. Transfected MDA-MB-231 cells in 35 mm dishes were labeled with DMEM containing 100 μCi of ^{35}S-methionine and ^{35}S-cysteine supplemented with 10% dialyzed FBS for 15 minutes. The labeled cells were either collected in RIPA buffer

or the labeling medium was replaced with complete growth medium. Cell lysates were collected in RIPA buffer following the indicated chase periods and subjected to immunoprecipitation with anti-HA antibodies. The immunoprecipitated proteins were electrophoresed through a 7.5 % SDS-polyacrylamide gel and visualized by fluorography. The relative intensities of immunoprecipitated Nrf2 were quantified by phosphor-imager analysis (BioRad FXImager).

Ubiquitination of Nrf2. For detection of ubiquitinated Nrf2 in vivo, cells were transfected with expression vectors for HA-ubiquitin, HA-Cul3, myc-Rbx1, Keap1, and Gal4-Neh2. The transfected cells were exposed to MG132 (Boston Biochem) for 5 hours. Cells were lysed by boiling in a buffer containing 2% SDS, 150 mM NaCl, 10 mM Tris-Hcl and 1 mM DTT. This rapid lysis procedure inactivates cellular ubiquitin hydrolases and therefore preserves ubiquitin-Nrf2 conjugates present in cells prior to lysis. Protein-protein interactions, including association of Nrf2 with Keap1, are also disrupted by this lysis procedure. For immunoprecipitation, these lysates were diluted five-fold in buffer lacking SDS and incubated with anti-Gal4 antibodies (8). Immunoprecipitated proteins were analyzed by immunoblot with antibodies directed against the HA epitope.

For ubiquitination of Nrf2 in vitro, COS-1 cells were transfected with expression vectors for HA-Nrf2, Keap1-CBD, HA-Cul3 and myc-Rbx1. The transfected cells were lysed in Buffer B (15 mM Tris-HCL [pH 7.4], 500 mM NaCl, and 0.25% NP40) containing 1 mM DTT, 1mM PMSF, and protease inhibitor cocktail. The lysates were pre-cleared with protein A beads prior to incubation with chitin beads (New England

Biolabs) for four hours at 4 °C. Chitin beads were washed twice with Buffer B, twice

with buffer A (25 mM Tris-HCl [pH 7.5], 10% (v/v) glycerol, 1 mM EDTA, 0.01% NP-

40 and 0.1 M NaCl), and twice with Reaction Buffer (50 mM Tris-HCl [pH 7.5], 5 mM

$MgCl_2$, 2 mM NaF and 0.6 mM DTT). The pellets were incubated with ubiquitin (300

pmol), E1 (2 pmol), E2-UbcH5a (10 pmol), and ATP (2 mM) in 1X Reaction Buffer in a

total volume of 30 μl for 1 hr at 37 °C. Ubiquitin, E1 and E2-UbcH5a were purchased

from Boston Biochem. The chitin beads were centrifuged at 3,000 x g, resuspended in

2% SDS, 150 mM NaCl, 10 mM Tris-Hcl [pH 8.0] and 1 mM DTT and boiled for 5 min

to release bound proteins, inactivate any contaminating ubiquitin hydrolases and disrupt

protein-protein interactions. The supernatant was diluted five-fold with buffer lacking

SDS prior to immunoprecipitation with anti-Nrf2 antibodies. Immunoprecipitated

proteins were subjected to immunoblot analysis with anti-ubiquitin antibodies.

RESULTS

Association of Keap1 with Cul3 mediates Keap1-dependent ubiquitination of Nrf2.
The N-terminal BTB domain of Keap1 is required for efficient repression of Nrf2-dependent gene expression (29, 60) (Fig. 1). The well-characterized Skp1 protein, which bridges the Cul1 protein and F-box-containing substrate adaptor proteins, contains a BTB-like fold (61). Several BTB-domain-containing proteins have been reported to function as substrate adaptor proteins for Cul3-dependent E3 ubiquitin ligase complexes (19, 20, 43, 58). To determine if Keap1 is able to associate with one or more of the cullin proteins, expression vectors for several HA-tagged cullin proteins were constructed and transfected into COS1 cells along with an expression vector for Keap1. Expression of Keap1 and the individual cullin proteins was confirmed by immunoblot analysis of total cell lysates (Figure 2A, top and middle panels). Equivalent amounts of cell lysates were immunoprecipitated with anti-Keap1 antibodies and the presence of the HA-tagged cullin proteins in the anti-Keap1 immunoprecipitates was determined by immunoblot analysis. In agreement with a recent report by Yamamoto and coworkers (31), both Cul2 and Cul3 were able to associate with Keap1 (Fig. 2A, lower panel).

To examine the functional relevance of association between the cullin proteins and Keap1, the ability of the cullin proteins to increase Keap1-dependent ubiquitination of Nrf2 was determined. For these experiments, a Gal4-Neh2 fusion protein containing the N-terminal Neh2 domain of Nrf2 was co-expressed in MDA-MB-231 cells along with HA-ubiquitin, Keap1 and the cullin proteins. Consistent with our previous results (60), the Neh2 domain of Nrf2 is efficiently ubiquitinated by Keap1 in a dose-dependent manner (Fig. 2B, lanes 2-5). Expression of Cul3, but neither Cul1 nor Cul2, increased

99

Keap1-dependent ubiquitination of Gal4-Neh2 in a dose-dependent manner (Fig. 2B, lanes 6-17). Ectopic expression of Cul3 was most effective at increasing Keap1-dependent ubiquitination of Gal4-Neh2 when Keap1 was expressed at submaximal levels (Fig. 2B and data not shown), consistent with the notion that Keap1 competes with other BTB-domain-containing proteins for Cul3.

To confirm that Keap1 utilizes Cul3 to target Nrf2 for ubiquitination, the ability of a dominant-negative Cul3 protein to block Keap1-dependent degradation of Nrf2 was determined. A stop codon was introduced at amino acid 381 in Cul3 to construct a truncated protein lacking the C-terminal Rbx1-binding domain of Cul3. Expression of this dominant-negative Cul3 protein in MDA-MB-231 cells inhibited both the ability of Keap1 to target the Gal4-Neh2 protein for ubiquitination (Fig. 2C) and to decrease the steady-state levels of the full-length Nrf2 protein (Fig. 2D) in a dose-dependent manner.

Keap1 functions as a substrate adaptor protein for a Cul3/Rbx1 E3 ubiquitin ligase complex. Cullin proteins function as molecular scaffolds to bring together a substrate adaptor protein and the RING protein, Rbx1 (42). Specific substrate(s) are brought into the complex by the substrate adaptor protein, while the Rbx1 protein recruits a ubiquitin-charged E2 protein. To further define the role of Cul3 in Keap1-dependent ubiquitination of Nrf2, we first determined if Keap1 is able to assemble into a ternary complex with Cul3 and Rbx1. To facilitate purification of Keap1, a chitin-binding domain was fused to the C-terminus of Keap1 (Keap1-CBD). The presence of the C-terminal chitin binding domain did not alter the ability of Keap1 to associate with either Cul3 or Nrf2 or alter the responsiveness of Keap1 to chemical inducers of Nrf2 (data not

shown). Expression vectors for Keap1-CBD, Cul3 and Rbx1 were transfected into COS1 cells and Keap1 was purified using chitin beads. Both Cul3 and Rbx1 co-purified with Keap1, as determined by either immunoblot analysis (Fig. 3A) or by silver stain (data not shown). Co-purification of Rbx1 with Keap1-CBD was markedly enhanced in the presence of co-expressed Cul3 (Fig. 3A, lane 4) consistent with the notion that Cul3 functions as a molecular scaffold to assemble both Keap1 and Rbx1 into an E3 ubiquitin ligase complex.

The ability of the Keap1-Cul3-Rbx1 complex to target Nrf2 for ubiquitination and subsequent proteosome-mediated degradation was determined. In one set of experiments, steady-state levels of Nrf2 were determined in MDA-MB-231 cells transfected with expression vectors for Nrf2, Keap1, Rbx1 and one of several cullin proteins. The input amounts of the various plasmid DNAs were carefully titrated so that submaximal repression of Nrf2 steady state levels by expression of Keap1 alone was achieved. Under these conditions, a marked reduction in steady-state levels of Nrf2 was achieved by coexpression of Cul3 and Rbx1 (Fig. 3B, lane 5). Treatment of the transfected cells with MG132 prior to cell lysis restored steady-state levels of Nrf2 (Fig. 3B, lane 6). Coexpression of Cul3 and Rbx1 also markedly increased Keap1-dependent ubiquitination of the Gal4-Neh2 fusion protein (Fig. 3C, compare lanes 2 and 4). In contrast, co-expression of Rbx1 with either Cul1 or Cul2 did not alter steady-state levels of Nrf2 (Fig. 3B, lanes 7 and 8) or Keap1-dependent ubiquitination of Gal4-Neh2 (data not shown).

To confirm that the Keap1-Cul3-Rbx1 complex assembles into an active E3 ubiquitin ligase complex, the ability of the Keap1-Cul3-Rbx1 complex to target Nrf2 for ubiquitination in vitro was determined. Expression vectors for Nrf2, Keap-CBD, Cul3

and Rbx1 were transfected into COS1 cells and the complex was purified using chitin beads (Fig. 3D, lower panel). As expected, co-expression of Cul3 and Rbx1 along with Keap1 resulted in decreased levels of Nrf2 that were restored by treatment of the transfected cells with MG132 prior to cell lysis (Fig. 3D, lower panel, compare lanes 2 and 3). The chitin beads were mixed with purified E1, E2-UbcH5a, and ubiquitin in the presence of ATP. The ubiquitination reactions were terminated by boiling to release proteins from the chitin beads. The samples were immunoprecipitated under stringent denaturing conditions using anti-Nrf2 antibodies. The immunoprecipitated proteins were subjected to immunoblot analysis using anti-ubiquitin antibodies. Ubiquitination of Nrf2 was markedly enhanced in the presence of both Cul3 and Rbx1 (Fig. 3D, compare lanes 1 and 3). Importantly, very low levels of ubiquitinated Nrf2 proteins were observed if purified E1 was not included in the reaction (Fig 3D, lane 4), confirming that conjugation of ubiquitin onto Nrf2 occurred in vitro. Although the Keap1-Cul3-Rbx1 complex is also able to target Nrf2 for ubiquitination in vivo (Fig. 3C, lane 4), the ubiquitin-Nrf2 conjugates formed in vivo are likely removed by ubiquitin hydrolases during cell lysis and purification of the complex. Alternatively, ubiquitination of Nrf2 by the purified Keap1-Cul3-Rbx1 complex may simply be more efficient in vitro, perhaps due to the absence of proteins that compete with Keap1 for binding to Cul3.

Mutations within the BTB domain of Keap1 decrease ubiquitination of Nrf2 but increase ubiquitination of Keap1. Molecular contacts between the cullin proteins and their cognate BTB domain-containing substrate adaptor proteins are highly conserved, as the crystal structure of the Skp1-Cul1-Rbx1 complex has been used to

predict amino acids required for association of MEI-26 with the *C. elegans* Cul3 protein (58, 61). The corresponding residues in Keap1 are residues 123-127 and 160-164. Two mutant Keap1 proteins, containing alanine substitutions for amino acids 125-127 (Keap1-125A3) and for amino acids 162-164 (Keap1-162A3) were constructed and characterized for their ability to assemble with Cul3 and Rbx1 into a functional E3 complex that targets Nrf2 for ubiquitination. The mutant Keap1 proteins were not impaired in their ability to associate with Nrf2 (data not shown). In the presence of ectopic Cul3 and Rbx1, the mutant Keap1 proteins were expressed at reduced levels in COS1 cells as compared to the wild-type Keap1 protein (Fig. 4A, top panel). Therefore, to compare the ability of the wild-type and mutant Keap1 proteins to associate with Cul3 and Rbx1, the amount of cell lysate used in the affinity purification experiments was normalized such that the input levels of the wild-type and mutant Keap1 proteins were approximately equivalent (Fig. 4A, 4th panel from top). To our surprise, assocation of Cul3 with the mutant Keap1 proteins was not reduced. Rather, increased levels of Cul3 and Rbx1 were observed to copurify with the mutant Keap1 proteins as compared to the wild-type protein (Fig. 4A, bottom panels, compare lane1 with lanes 2 and 3). Increased association of the mutant Keap1 proteins with Cul3 and Rbx1 was reflected in increased ubiquitination onto the mutant Keap1 proteins (Fig. 4B, compare lanes 3 and 4 with lanes 5-8). However, these mutant Keap1 proteins were unable to cooperate with Cul3 for ubiquitination of the Gal4-Neh2 protein (Fig. 4C, compare lane 4 with lanes 6 and 8) and repression of steady-state levels of Nrf2 (Fig. 4D). In addition, the mutant Keap1 proteins were impaired in their ability to down-regulate Nrf2-dependent gene expression (Fig. 4E). Thus, contrary to our expectation based on published reports (58, 61), mutation of conserved residues within

the BTB domain of Keap1 did not disrupt association with Cul3. Nevertheless, these mutations disrupt the ability of the Keap1-Cul3-Rbx1 complex to efficiently target Nrf2 for ubiquitination and subsequent proteosome-mediated degradation.

Identification of lysine residues in Nrf2 targeted for ubiquitination by Keap1. The N-terminal Neh2 domain of Nrf2 contains seven lysine residues (Fig. 5A). The full-length Nrf2 protein contains an additional 32 lysine residues that are potential candidates for Keap1-dependent ubiquitination. To determine if the seven lysine residues in the Neh2 domain are the major determinants of Keap1-dependent ubiquitination, a mutant Nrf2 protein was constructed in which these lysine residues were replaced by arginine residues (Nrf2-R7). The presence of these seven arginine substitutions did not alter the ability of the Nrf2-R7 protein to co-immunoprecipitate with Keap1 from co-transfected COS1 cells or associate with Keap1 in vitro (data not shown). However, in the presence of co-expressed Keap1, steady-state levels of the Nrf2-R7 protein were markedly increased relative to the wild-type Nrf2 protein (Fig. 5B). To confirm that the observed difference in steady-state levels reflected differences in the stability of the wild-type and mutant Nrf2 proteins, the half-lives of the respective Nrf2 proteins were determined by pulse-chase analysis. The half-life of the wild-type Nrf2 protein in the presence of coexpressed Keap1 was slightly more than 1 hour, while the half-life of the Nrf2-R7 protein in the presence of coexpressed Keap1 was nearly three hours (Table 1). Furthermore, ubiquitination of the Gal4-Neh2-R7 protein in the presence of co-expressed Keap1 was markedly reduced relative to the wild-type Gal4-Neh2 protein, both in vivo (Fig. 5C, lane 11) and in vitro (data not shown). Taken together, these experiments

demonstrate that one or more lysine residues in the Neh2 domain of Nrf2 are the major determinants of Keap1-dependent ubiquitination of Nrf2.

The Nrf2-R7 cDNA was used to construct "add-back" mutant Nrf2 proteins containing single lysine residues within the Neh2 domain. The steady-state levels of these mutant Nrf2 proteins in the presence of Keap1 were intermediate between the wild-type Nrf2 and the Nrf2-R7 proteins (Fig. 5B). Pulse-chase analysis confirmed that the half-lives of the Nrf2 proteins containing single lysine residues were intermediate between that of the wild-type and Nrf2-R7 proteins (data not shown). The ability of Keap1 to target these "add-back" mutant Nrf2 proteins for ubiquitination in vivo was also determined. In all cases, the presence of a single lysine residue within the Neh2 domain resulted in increased levels of ubiquitination of the Gal4-Neh2 fusion protein as compared to the Gal4-Neh2-R7 fusion protein, particularly for lysine residues 52 and 53 (Fig. 5C, lanes 6 and 7). These results indicate that Keap1 targets multiple lysine residues within the Neh2 domain of Nrf2 for ubiquitination.

Keap1-dependent ubiquitination of Nrf2 is inhibited by oxidative stress. The ability of Keap1 to function as a substrate adaptor protein for Cul3 and thereby target Nrf2 for ubiquitin conjugation provides an efficient mechanism for repression of Nrf2 steady-state levels and of Nrf2-dependent transcription. However, exposure of cells to a wide variety of thiol-reactive chemicals results in elevated steady-state levels of Nrf2 and transcriptional activation of the cytoprotective Nrf2-dependent genetic program (1, 26, 49, 60). For example, we have previously demonstrated that both quinone-induced oxidative stress and sulforaphane, a chemopreventive isothiocyanate, increase the

stability of Nrf2 and activate Nrf2-dependent gene expression (60). Furthermore, we have previously reported that a single cysteine to serine substitution at Cys 151, located within the BTB domain of Keap1, specifically blocked activation of Nrf2-dependent transcription in response to both quinone-induced oxidative stress and sulforaphane (60).

To determine if oxidative stress and sulforaphane inhibit the ability of Keap1 to target Nrf2 for ubiquitination, levels of Keap1-dependent ubiquitin conjugation onto the Gal4-Neh2 protein were determined in cells exposed to either t-butylhydroquinone (tBHQ) or sulforaphane prior to cell lysis. Exposure of cells to either tBHQ or sulforaphane markedly decreased levels of ubiquitinated Gal4-Neh2 protein (Fig. 6A, lanes 1-3). A four-hour exposure of cells to tBHQ resulted in maximal inhibition of Keap1-dependent ubiquitination of Gal4-Neh2 (data not shown). In contrast, the ability of the Keap1-C151S protein to target the Gal4-Neh2 protein for ubiquitination was not inhibited by either tBHQ or sulforaphane (Fig. 6A, lanes 4-6).

To confirm that tBHQ and sulforaphane inhibit the ability of Keap1 to function as a substrate adaptor protein for Cul3, ubiquitination onto the Gal4-Neh2 protein was examined in the presence of both Keap1 and Cul3. Input ratios of Keap1 and Cul3 expression vectors were carefully titrated to achieve maximal ubiquitination onto the Gal4-Neh2 protein in the presence of both Cul3 and Keap1 (Fig. 6B, lanes 1-3). Exposure of the transfected cells to either sulforaphane or tBHQ decreased ubiquitination onto the Gal4-Neh2 protein in the presence of Cul3 and the wild-type Keap1 protein (Fig. 6B, lanes 4 and 5). The Keap1-C151S protein was largely resistant to inhibition by either sulforaphane or tBHQ, although a slight decrease in ubiquitination of the Gal4-Neh2 protein was observed following sulforaphane treatment (Fig. 6B, lanes 8 and 9).

The ability of Keap1 to associate with Cul3 was assessed following treatment of cells with either tBHQ or sulforaphane. Treatment of cells with either tBHQ or sulforaphane decreased the level of Cul3 that copurified with the wild-type Keap1-CBD protein following affinity purification (Fig. 6C, lanes 2-4). Association of the Keap1-C151S protein with Cul3 was not significantly affected by either tBHQ or sulforaphane treatment (Fig. 6C, lanes 5-7). Importantly, the amount of Cul3 that co-purified with the Keap1-C151S protein was greater than the amount of Cul3 that co-purified with the wild-type Keap1 protein following treatment with either tBHQ or sulforaphane (Fig, 6C, compare lanes 3 and 6 and lanes 4 and 7), in agreement with the increased ability of the Keap1-C151S protein to target Nrf2 for ubiquitination in cells exposed to either tBHQ or sulforaphane (Figs. 6A and 6B).

The ability of Nrf2 to associate with Keap1 was assessed following exposure of cells to either tBHQ or sulforaphane. In one experiment, MDA-MB-231 cells transfected with expression vectors for Keap1-CBD and HA-Nrf2 were treated with either tBHQ or sulforaphane for five hours and the levels of Keap1-associated HA-Nrf2 was assessed by immunoblot analysis following affinity purification using chitin beads. The level of Keap1-associated HA-Nrf2 following treatment with either tBHQ or sulforaphane was markedly increased, in parallel with increased levels of HA-Nrf2 in total cell lysates (Fig. 7A, lanes 2-4, compare top and middle panels). In a second experiment, cells were transfected with an expression vector for Keap1-CBD and levels of endogenous Nrf2 protein associated with Keap1-CBD were measured following affinity purification of Keap1-CBD (Fig. 7B). As expected, endogenous Nrf2 co-purified with Keap1 from MG132-treated cells (Fig. 7B, middle panel, lane 3). Endogenous Nrf2 also co-purified

with Keap1 from both tBHQ and sulforaphane-treated cells (Fig. 7B, middle panel, lanes 4 and 5). In a third experiment, levels of endogenous Nrf2 associated with the endogenous Keap1 protein was determined by immunoblot analysis following immunoprecipitation with anti-Keap1 antibodies. As expected, elevated levels of Nrf2 in total lysates was observed in cells treated with tBHQ, sulforaphane or MG132, either individually or in combination (Fig. 7C, upper panel). The level of endogenous Nrf2 present in anti-Keap1 immunoprecipitates was markedly increased in cells treated with tBHQ, sulforaphane, or MG132 (Fig. 7C, lower panel, lanes 3-8). Taken together, these results suggest that the ability of Keap1 to assemble into a functional E3 ubiquitin ligase complex, not the ability of Nrf2 to associate with Keap1, is the critical step that is perturbed by these chemical inducers of Nrf2-dependent transcription.

DISCUSSION

In this report, we demonstrate that Keap1 functions as a substrate adaptor protein for a Cul3-dependent E3 ubiquitin ligase complex to target Nrf2 for proteosome-mediated degradation under normal culture conditions. Upon exposure to chemical inducers of Nrf2-dependent transcription, Keap1-dependent ubiquitination of Nrf2 is inhibited, leading to accumulation of Nrf2 and allowing subsequent activation of Nrf2-dependent transcription. Mutation of a single cysteine residue in the BTB domain of Keap1 markedly reduces inhibition of Keap1-dependent ubiquitination of Nrf2 by oxidative stress or sulforaphane. The ability of Keap1 to function as a redox-sensitive substrate adaptor protein for an E3 ubiquitin ligase complex constitutes a novel mechanism by which cells are able to sense and respond to electrophilic chemicals and oxidative stress.

Keap1 is one of more than 50 human proteins that share an N-terminal BTB domain, a central linker domain and a C-terminal Kelch domain. BTB-Kelch proteins appear to have diverse biological roles in regulation of the cytoskeleton (7, 30, 48). In *D. melanogaster*, the Kelch protein, which is the founding member of the BTB-Kelch family, binds actin and regulates the cross-linking of actin filaments at ring canals that form between cells in the *D. melanogaster* oocyte (30). In humans, mutations within the GAN1 gene cause giant axonal neuropathy, an autosomal recessive disease characterized by defects in intermediate filament organization in sensorimotor neurons (6). Our results provide direct biochemical evidence that Keap1 assembles into a functional E3 ubiquitin ligase complex with Cul3 and Rbx1. Several other BTB-Kelch proteins are able to

associate with Cul3, including GAN1 (19). Furthermore, residues within the BTB domain of Keap1 that are conserved in other BTB-Kelch proteins, including a highly conserved serine residue within the BTB domain, S104, are required for ubiquitination of Nrf2 (S. – C. L. and M. H., unpublished data) and repression of Nrf2-dependent transcription (62). A glycine subsitution at the corresponding residue in GAN1 has been reported in a patient with giant axonal neuropathy (6). We suggest that ability of BTB-Kelch proteins to function as substrate adaptors for Cul3-dependent E3 ubiquitin ligase complexes reflects a conserved biochemical function that underlies their diverse biological functions.

The Skp1 protein, which functions as a linker between Cul1 and F-box substrate adaptor proteins, contains a BTB domain fold (61). The crystal structure of the Skp1-Cul1-Rbx1 complex has been used to predict amino acids required for association of MEI-26, a *C. elegans* BTB domain protein, with the *C. elegans* Cul3 protein (58, 61). Therefore, we constructed two mutant Keap1 proteins that contained alanine substitutions in place of the corresponding residues in Keap1. To our surprise, these mutant Keap1 proteins displayed increased ability to associate with Cul3 and Rbx1. Our results suggest that Keap1 interacts with Cul3 in a manner distinct from the way in which Skp1 interacts with Cul1. In other experiments, we find that the BTB domain of Keap1 is not sufficient to associate with Cul3 (data not shown), in agreement with a recent report by Yamamoto and coworkers suggesting that the linker domain of Keap1 is critically required for association with Cul3 (31). Nevertheless, the BTB domain of Keap1 is required for efficient down-regulation of steady-state levels of Nrf2 (31, 60). Furthermore, mutations within the BTB domain of Keap1, as reported in this manuscript, can result in increased

association with Cul3 and increased levels of auto-ubiquitination. Importantly, these mutant Keap1 proteins are impaired in their ability to efficiently target Nrf2 for ubiquitination and subsequent proteosome-mediated degradation. These results suggest that the balance between ubiquitination of substrate (Nrf2) and substrate adaptor (Keap1) may contribute to regulation of the Keap1-Cul3-Rbx1 E3 ubiquitin ligase complex, perhaps by regulating steady-state levels of Keap1.

Substrate ubiquitination by cullin-dependent E3 ubiquitin ligase complexes is often tightly regulated by changes in cell physiology induced by environmental signals or cell cycle progression. For example, the well-characterized F-box protein βTrCP, which functions as a substrate adaptor protein for Cul1, only recognizes substrate proteins that are phosphorylated on two serine residues embedded within a conserved sequence motif of DSGφXS (57). As a result, the activity of the SCF1$^{\beta TrCP}$ E3 ubiquitin ligase towards its substrates, which include IκBα and β-catenin, is regulated at the level of substrate binding. We find that inducers of Nrf2, including sulforaphane and quinone-induced oxidative stress, result in accumulation of Nrf2 but do not abolish the ability of Nrf2 to bind to Keap1. Thus, the Keap1-dependent E3 ubiquitin ligase complex, in contrast to other cullin-dependent E3 ubiquitin ligase complexes typified by the SCF1$^{\beta TrCP}$ complex, is not regulated at the level of substrate binding.

Recent experiments suggest that E3 ubiquitin ligase complexes that assemble around cullin scaffolds undergo cycles of assembly and disassembly that enable exchange of the core Cullin-Rbx1 complex between different substrate adaptor proteins (12, 56). Substrate adaptor exchange is likely to be an important mechanism by which a new substrate molecule is brought into the complex. This substrate adaptor exchange model

provides an attractive paradigm for understanding how Keap1-dependent ubiquitination of Nrf2 is regulated by oxidative stress or sulforaphane. Our results demonstrate that both sulforaphane and quinone-induced oxidative stress result in reduced association between Keap1 and Cul3. In contrast, association between Cul3 and the Keap1-C151S mutant protein, which is markedly resistant to inhibition by both sulforaphane and quinone-induced oxidative stress, is not significantly perturbed by either inducer of Nrf2. We propose that exposure of cells to sulforaphane or oxidative stress, by altering the redox state of Cys 151, reduces the ability of Nrf2-bound Keap1 proteins to associate with the Cul3-Rbx1 core complex. As a result, fewer Nrf2 molecules will be targeted for ubiquitination and subsequent degradation, leading to increased accumulation of Nrf2.

Nrf2 must also escape Keap1-mediated cytoplasmic sequesteration in order to accumulate in the nucleus and activate gene expression. Keap1 binds to actin via its Kelch repeat domain and pharmacological disruption of the actin cytoskeleton enables Nrf2 to escape Keap1-mediated sequesteration in the cytoplasm (29). Inducers of Nrf2 may perturb the ability of Keap1 to associate with the actin cytoskeleton and thus enable release of Nrf2 into the nucleus. However, our results indicate that neither sulforaphane nor quinone-induced oxidative stress results in quantitative release of Nrf2 from Keap1. An alternative possibility is suggested by the observation that ongoing protein synthesis is required for accumulation of Nrf2 in the nucleus (24, 26). We propose that, under normal conditions, a single Keap1 protein is able to target multiple Nrf2 proteins for destruction. However, when the ability of Keap1 to efficiently target Nrf2 proteins for degradation is inhibited, each Keap1 protein (or Keap1 dimer (62)), is only able to sequester a single Nrf2 protein. Thus, newly synthesized Nrf2 proteins will no longer be

bound by Keap1 proteins and, instead, accumulate in the nucleus following transport from the cytoplasm. Consistent with this "saturation" model, overexpression of a Neh-GFP fusion protein enables nuclear accumulation of endogenous Nrf2 (5).

The ability of structurally diverse chemicals to activate Nrf2-dependent gene expression correlates closely with their reactivity toward thiols (17). Talalay and co-workers have identified four cysteine residues in Keap1 (Cys 257, Cys 273, Cys 288, and Cys 297) that are preferentially labeled following in vitro exposure of purified Keap1 to a cysteine-reactive alkylating agent (16, 52). Mutant Keap1 proteins containing serine substitutions for two of these residues (Cys 273 and Cys 288) are impaired in their ability to target Nrf2 for ubiquitination and to repress Nrf2-dependent gene expression in transfected cells (52, 60). In our previous work, we demonstrated that Cys 151 is required for both a novel redox-dependent alteration in Keap1 in cells exposed to oxidative stress and the ability of oxidative stress to activate Nrf2-dependent gene expression (60). In our present work, we demonstrate that Cys 151 is required for inhibition of Keap1-dependent ubiquitination of Nrf2 by both sulforaphane and oxidative stress. Taken together, our results and those reported by Talalay's group suggest that multiple cysteine residues in Keap1 are capable of undergoing redox-dependent alterations. Identification of redox-dependent biochemical modifications that occur on the endogenous Keap1 protein will further our understanding of how cells sense the presence of reactive molecules and activate an Nrf2-dependent transcription program that protects sensitive biological molecules from chemical and oxidative damage.

113

This chapter was reproduced with the expressed written permission of the American Society for MicroBiology.

Table II-1

Table 1

Nrf2 Protein[a]	$t_{1/2}$ (h)[b]
WT-Nrf2	1.23
R7-Nrf2	2.96

[a]MDA-MB-231 cells were transfected with expression vectors for wild type Keap1 and either WT-Nrf2 or R7-Nrf2. The ratio of expression vectors for Keap1 and Nrf2 in the transfection was 1:4.

[b]The half-life of HA-Nrf2 was determined by pulse-chase labeling.

Figure II-1
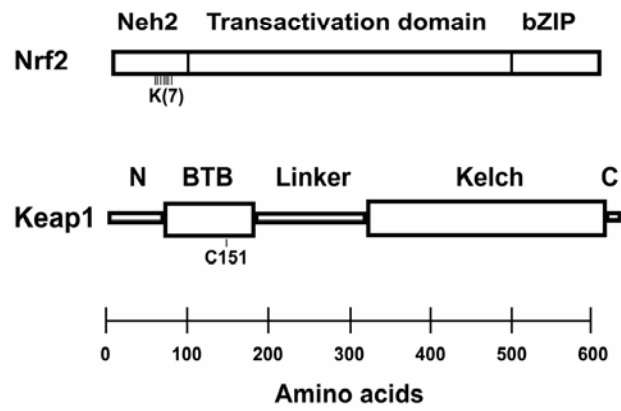
Figure II-1. Domain structures of Nrf2 and Keap1. Nrf2 contains three discrete domains, including an N-terminal Neh2 domain, a central transactivation domain and a C-terminal bZIP domain. The N-terminal Neh2 domain interacts with the Kelch domain of Keap1. The location of seven lysine residues that are candidate sites for ubiquitination within the Neh2 domain is indicated. Keap1 contains five discrete domains that are designated as N, BTB, Linker, Kelch, and C. The location of Cys 151 in the BTB domain of Keap1 is indicated.

Figure II-2
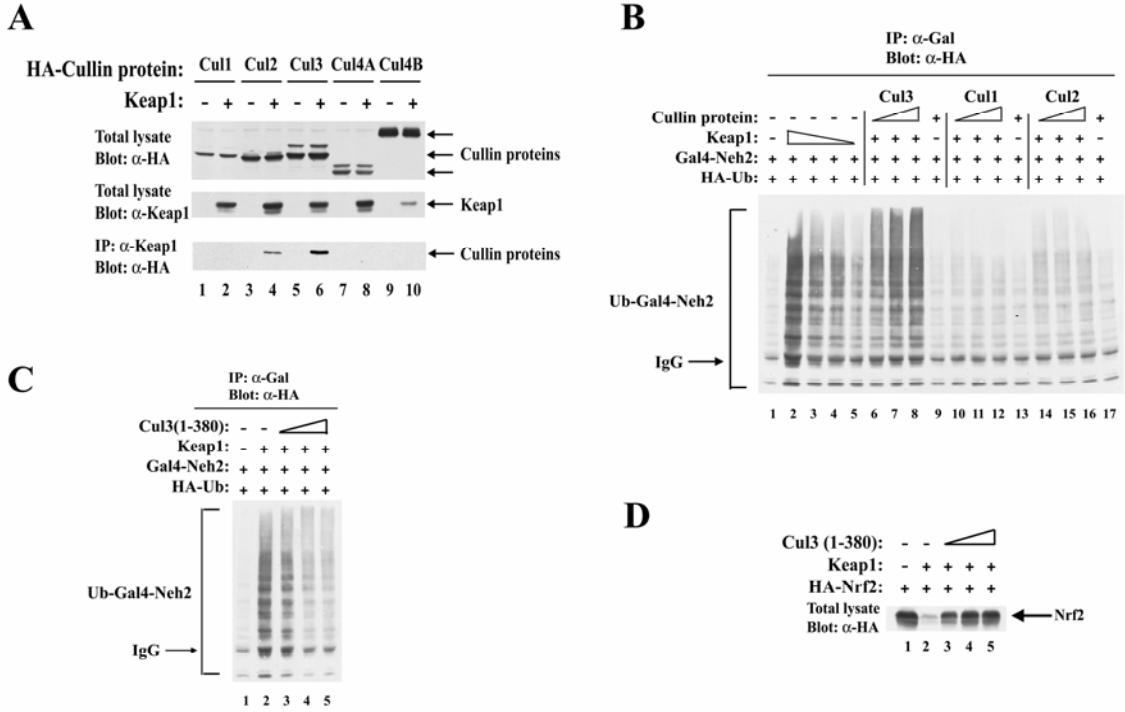
Figure II-2. Association of Keap1 with Cul3 mediates Keap1-dependent ubiquitination of Nrf2. (A). COS-1 cells were cotransfected with expression vectors for wild-type Keap1 and the indicated Cullin proteins. Total cell lysates were immunoblotted with anti-HA antibodies (top panel) and anti-Keap1 antibodies (middle panel). Anti-Keap1 immunoprecipitates were subjected to immunoblot analysis using anti-HA antibodies (lower panel). (B). 60 mm dishes of MDA-MB-231 cells were transfected with expression vectors for HA-Ub, Gal4-Neh2, Keap1, and each of the Cullin proteins as indicated. Constant amounts of expression vectors for HA-ubiquitin (0.6 μg) and Gal4-Neh2 (0.6 μg) were included in all samples. The Keap1 expression vector was either omitted from some samples (lanes 1, 9, 13, 17), titrated down from 0.6 to 0.038 μg (lanes 2-5), or kept constant at 0.038 μg per dish (lanes 6-8, 10-12, 14-16). Increasing amounts of each Cullin expression vector, from 0.1 to 0.6 μg, were added to some samples (lanes 6-17). Anti-Gal4 immunoprecipitates were analyzed by immunoblot analysis with anti-HA antibodies. (C). 60 mm dishes of MDA-MB-231 cells were transfected with expression vectors for HA-Ub (0.6 μg), Gal4-Neh2 (0.6 μg), Keap1 (0.3 μg, lanes 2-5) and Cul3 (1-380) (from 0.1 to 0.5 μg, lanes 3-5). Anti-Gal4 immunoprecipitates were analyzed by immunoblot analysis with anti-HA antibodies. (D). 24 well plates of MDA-MB-231 cells were transfected with expression vectors for HA-Nrf2 (0.18 μg, lanes 1-5), Keap1 (0.02μg, lanes 2-5) and Cul3(1-380) (from 0.02 to 0.18 μg, lanes 3-5). Total cell lysates were subjected to immunoblot analysis with anti-HA antibodies.

Figure II-3
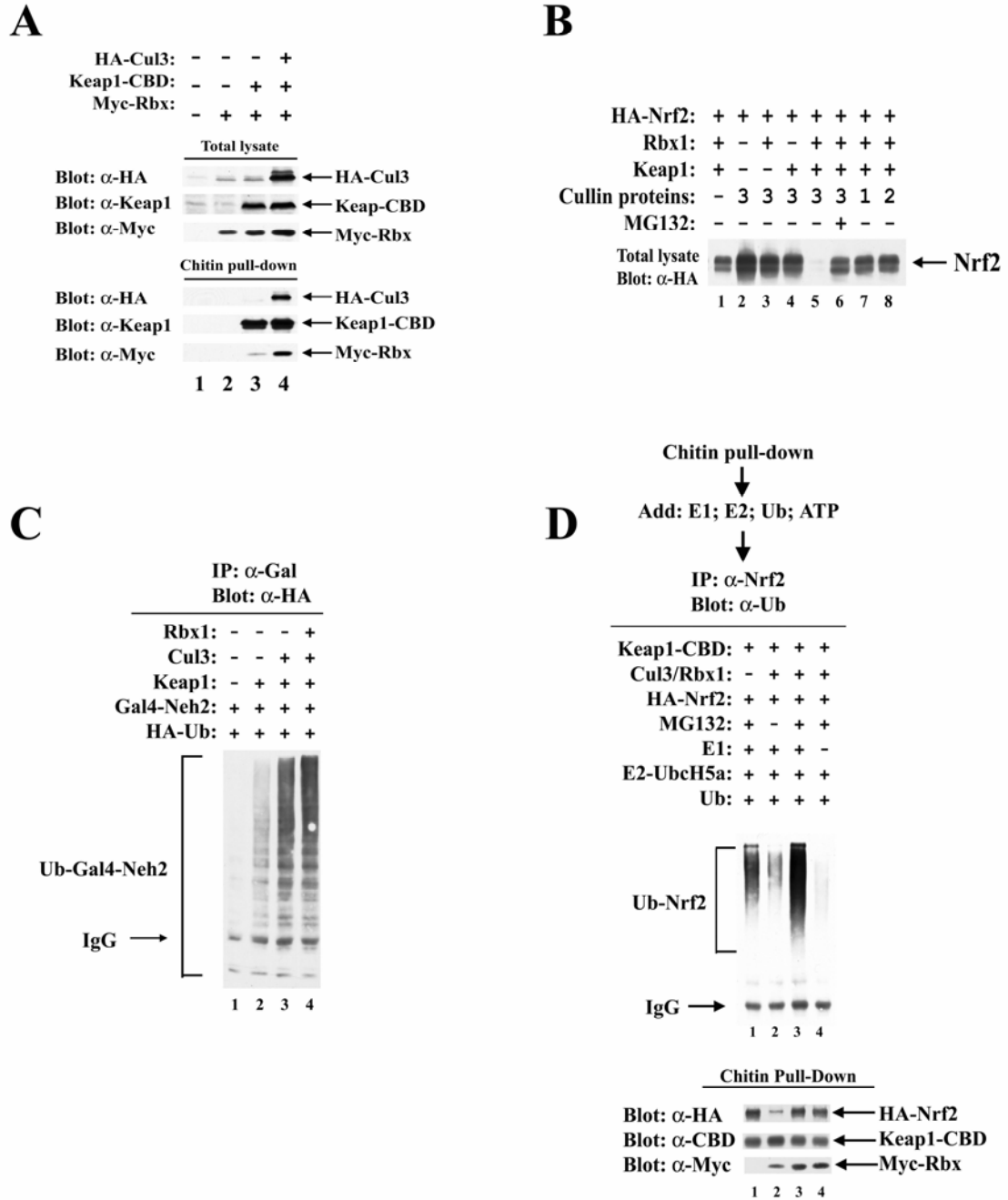
Figure II-3. Keap1 functions as a substrate adaptor for a Cul3-Rbx1 E3 ubiquitin ligase complex. (A). COS-1 cells were mock-transfected (lane 1) or cotransfected with expression vectors for Myc-Rbx1 (lanes 2-4), Keap1 (lanes 3 and 4) and HA-Cul3 (lane 4). Total cell lysates were analyzed by immunoblot with anti-HA, anti-Myc, and anti-Keap1 antibodies (upper three panels). The lysates were incubated with chitin beads, pelleted by centrifugation (3000 x g) and washed three times in RIPA buffer. Proteins that remained associated with the chitin beads were analyzed by immunoblot with anti-HA, anti-Myc, and anti-Keap1 antibodies (lower three panels). (B). MDA-MB-231 cells were cotransfected with expression vectors for HA-Nrf2, Myc-Rbx1 (lanes 1, 3, 5-8), Keap1 (lanes 1, 4-8), and each of the Cullin proteins as indicated (lanes 2-8). The cells were either untreated (lanes 1-5, 7, 8) or treated with 10 μM MG132 (lane 6) for five hours prior to analysis of total cell lysates by immunoblot with anti-HA antibodies. (C). MDA-MB-231 cells were transfected with expression vecotors for HA-Ub, Gal4-Neh2, Keap1 (lanes 2-4), Cul3 (lanes 3-4) and the myc-Rbx1 expression plasmid (lane 4). Anti-Gal4 immunoprecipitates were analyzed by immunoblot analysis with anti-HA antibodies (top panel). (D). COS1 cells were transfected with expression vectors as indicated. Lysates were pooled for each sample and incubated with chitin beads. After washing, the chitin beads were incubated with E1, E2-UbcH5a, ubiquitin and ATP. Subsequently, the chitin beads were pelleted, washed and proteins that eluted from the beads after boiling were split into two sets of samples. One set was immunoprecipitated with anti-Nrf2 antibodies followed by immunoblot analysis with anti-ubiquitin antibodies (upper panel). The other set was subjected to immunoblot analysis using anti-HA, anti-CBD and anti-Myc antibodies (bottom three panels).

Figure II-4
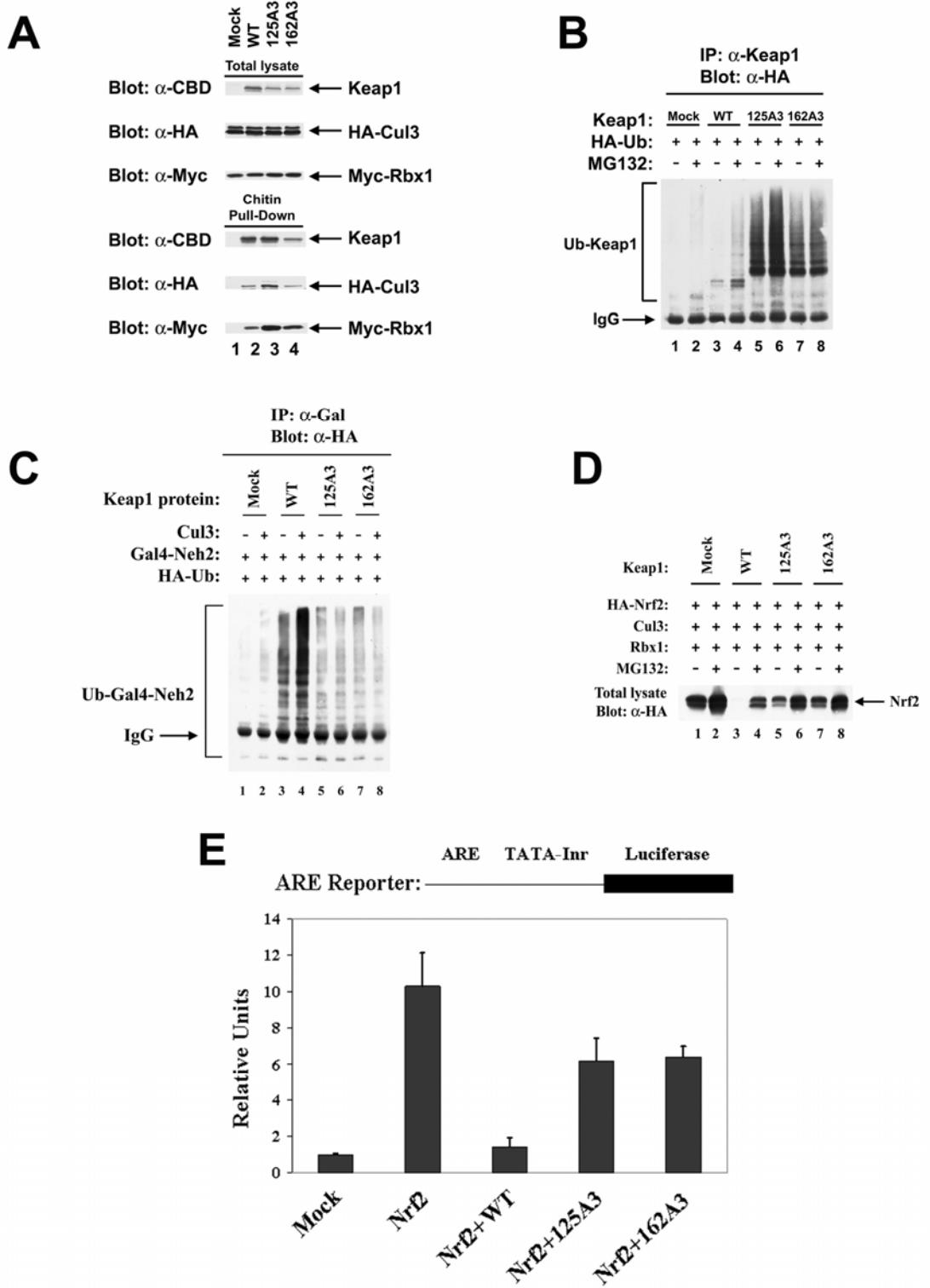
Figure II-4. Mutations within BTB domain of Keap1 decrease ubiquitination of Nrf2 but increase ubiquitination of Keap1. (A). COS1 cells were transfected with equal amounts of expression vectors for the indicated Keap1-CBD proteins, HA-Cul3 and Myc-Rbx1. Cell lysates were collected and immunoblotted with the indicated antibodies (top three panels) or incubated with chitin beads. Proteins that remained bound to the chitin beads after extensive washing were analyzed by immunoblot with the indicated antibodies (bottom three panels). (B). MDA-MB-231 cells were transfected with expression vectors for HA-Ub and the indicated Keap1 proteins and either left untreated (odd numbered lanes) or treated with MG132 for five hours (even numbered lanes) prior to collection of cell lysates. Anti-Keap1 immunoprecipitates were analyzed by immunoblot with anti-HA antibodies. (C). MDA-MB-231 cells were transfected with expression vectors as indicated. Anti-Gal4 immunoprecipitates were analazed by immunoblot analysis with anti-HA antibodies. (D). MDA-MB-231 cells were transfected with expression vectors for HA-Nrf2, Cul3, myc-Rbx1 and the wild-type or mutant Keap1 proteins (as indicated in lanes 3-8). The transfected cells were either untreated (odd-numbered lanes) or treated with MG132 for five hours (even-numbered lanes) prior to collection of cell lysates and determination of HA-Nrf2 levels by immunoblot analysis. (E). MDA-MB-231 cells were transfected in duplicate with an ARE-dependent firefly luciferase reporter gene construct and expression plasmids for Nrf2 and the wild-type or mutant Keap1 proteins. A plasmid encoding Renilla luciferase was included as control for transfection efficiency. Lysates were collected at 48 h post-transfection and both firefly and Renilla luciferase activities in cell lysates were analyzed. Data shown represent the mean and standard error from three independent experiments.

Figure II-5

A

Neh2 domain of Nrf2

```
            10              20              30              40              50
            |               |               |               |               |
MMDLELPPPG  LPSQQDMDLI  DILWRQDIDL  GVSREVFDFS  QRRKEYELEK
                                                          ↓        ↓
                                                          R        R

            60              70              80              90
            |               |               |               |
QKKLEKERQE  QLQKEQEKAF  FAQLQLDEET  GEFLPIQPAQ  HTQSETSG
    ↓↓  ↓       ↓       ↓
    RR  R       R       R
```

B

Total lysate
Blot: α-HA

Keap1:	−	◁	+
HA-Nrf2:	+ + + +
MG132:	− − − +

WT
R7
R44K
R50K
R52K
R53K
R56K
R64K
R68K

1 2 3 4

C

IP: α-Gal
Blot: α-HA

Gal4-Neh2:	WT	R7	WT	R44K	R50K	R52K	R53K	R56K	R64K	R68K	R7
Keap1:	−	−	+	+	+	+	+	+	+	+	+
HA-Ub:	+	+	+	+	+	+	+	+	+	+	+

Ub-Gal4-Neh2

IgG →

1 2 3 4 5 6 7 8 9 10 11

124
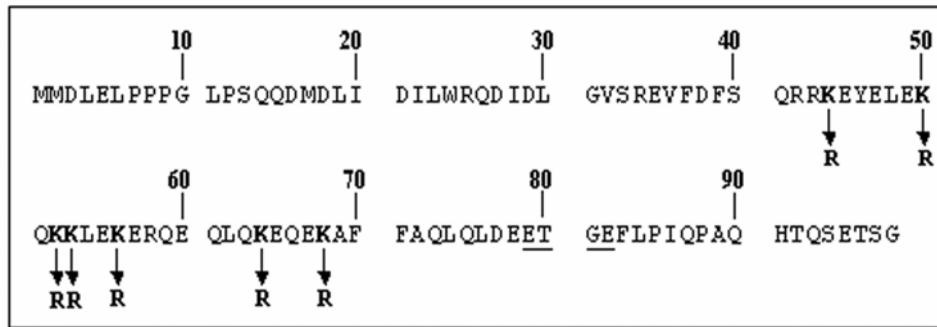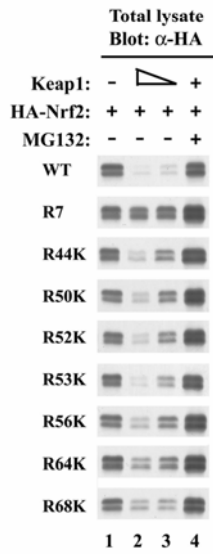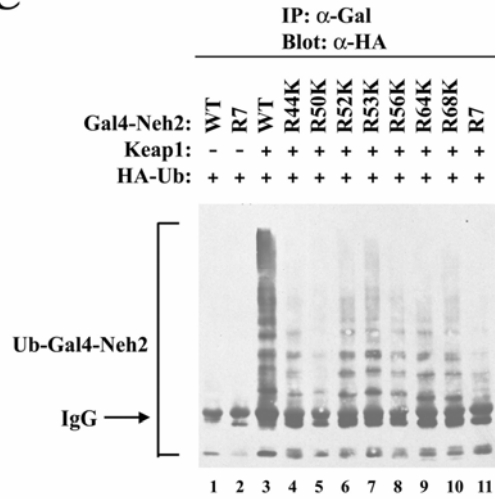
Figure II-5. Identification of lysine residues in Nrf2 targeted for ubiquitination by Keap1. (A). Seven lysine residues in the Neh2 domain of Nrf2 (bold) were substituted with arginine residues. A conserved ETGE motif (underlined) is required for association of Nrf2 with Keap1. (B). 24-well plates of MDA-MB-231 cells were transfected with expression vectors for wild-type or mutant HA-Nrf2 proteins (0.2 µg each, lane 1) and with different amounts of the expression vector for Keap1 (0.1 µg, lanes 2 and 4 or 0.025 µg, lane 3). The transfected cells were either untreated or treated with 10 µM MG132 (lane 4) for 4 hours prior to analysis by immunoblot using anti-HA antibodies. (C). 60 mm dishes of MDA-MB-231 cells were transfected with expression vectors for HA-ubiquitin (0.6 µg), either wild-type Nrf2 or each of mutant Nrf2 proteins as indicated (0.7 µg), and Keap1 (0.7 µg, lanes 3-11). The cells were treated with 10 µM MG132 for four hours prior to lysis. Anti-Gal4 immunoprecipitates were analyzed by immunoblot with anti-HA antibodies.

Figure II-6
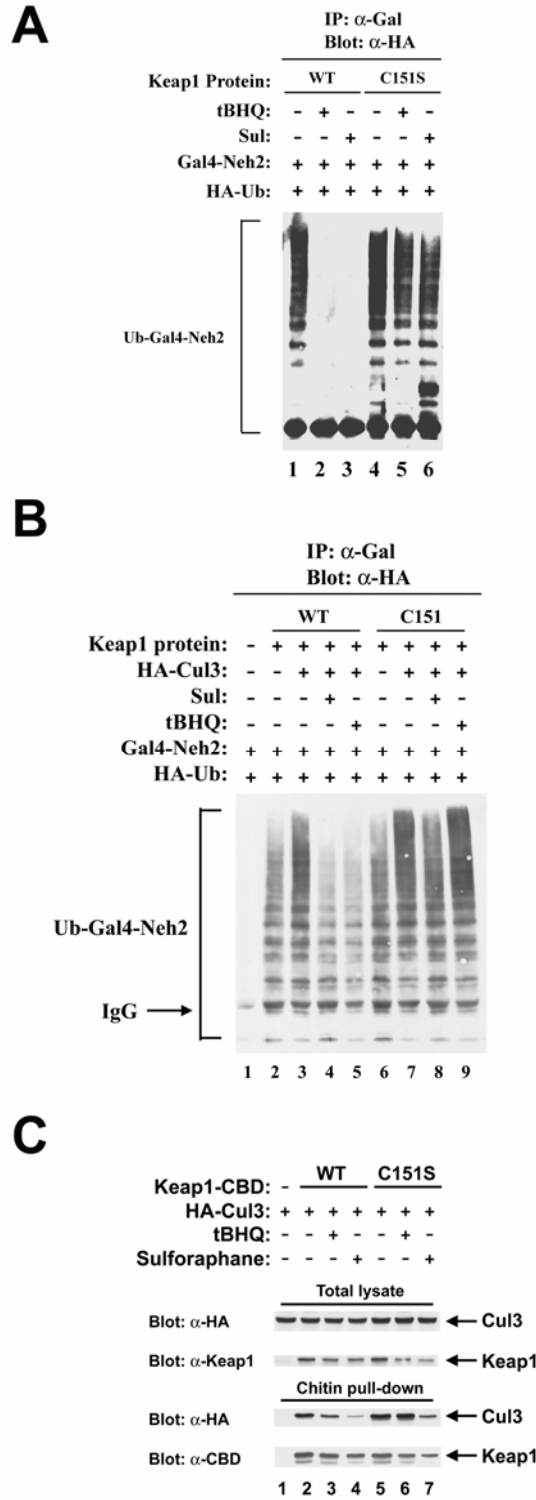
Figure II-6. Oxidative stress results in reduced ubiquitination of Nrf2 by a Keap1-dependent Cul3-RING ligase. (A). 60 mm dishes of MDA-MB-231 cells were transfected with expression vectors for HA-Ub (0.6 µg) and Gal4-Neh2 (0.7 µg) and for either wild-type Keap1 (0.7 µg, lanes 1-3) or Keap1-C151S (0.7 µg, lanes 4-6). The cells were either untreated (lanes 1 and 4), treated with 50 µM tBHQ (lanes 2 and 5) or 20 µM sulforaphane (lanes 3 and 6) for 4 hours prior to cell lysis. Anti-Gal4 immunoprecipitates were analyzed by immunoblot analysis with anti-HA antibodies. (B). 60 mm dishes of MDA-MB-231 cells were transfected with expression vectors for HA-Ub (0.6 µg), Gal4-Neh2 (0.7 µg), Cul3 (0.3 µg, lanes 3-5 and 7-9) and either wild-type Keap1 (0.4 µg, lanes 2-5) or Keap1-C151S (0.4 µg, lanes 6-9). The cells were either untreated (lanes 1-3, 6, 7), treated with 50 µM tBHQ (lanes 5 and 9) or 20 µM sulforaphane (lanes 4 and 8) for 4 hours prior to cell lysis. Anti-Gal4 immunoprecipitates were analyzed by immunoblot analysis with anti-HA antibodies. (C). 35 mm dishes of MDA-MB-231 cells were transfected with expression vectors for HA-Cul3 (0.5 ug) and either CBD-tagged wild-type Keap1 (0.5 ug, lanes 2-4) or CBD-tagged Keap1-C151S (0.5 ug, lanes 5-7). The cells were either left untreated (lanes 1, 2, and 5) or treated with 50 µM tBHQ (lanes 3 and 6) or 25 µM sulforaphane (lanes 4 and 7) for five hours. Cell lysates were collected in ELB and immunoblotted with the indicated antibodies (top two panels) or incubated with chitin beads. Proteins that remained bound to the chitin beads after extensive washing were analyzed by immunoblot with the indicated antibodies (bottom two panels).

Figure II-7
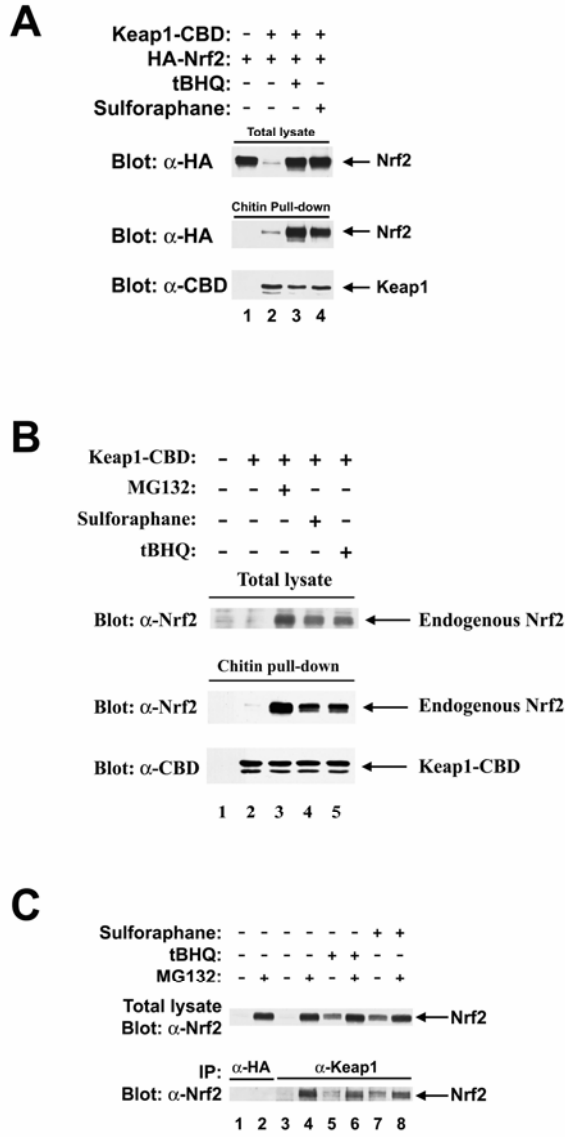
Figure II-7. Oxidative stress does not cause dissociation of Nrf2 from Keap1. (A). 60 mm dishes of MDA-MB-231 cells were transfected with of expression vectors for HA-Nrf2 (0.32 ug, lanes 1-4) and Keap1-CBD (0.16 ug, lanes 2-4). The cells were either left untreated (lanes 1 and 2) or treated with 50 μM tBHQ (lane 3) or 25 μM sulforaphane (lane 4) for five hours. Cell lysates were collected in ELB and immunoblotted with anti-HA antibodies (top panel) or incubated with chitin beads. Proteins that remained bound to the chitin beads after extensive washing were analyzed by immunoblot with either anti-HA antibodies (middle panel) or anti-CBD (bottom panel). (B). 60 mm dishes of MDA-MB-231 cells were transfected with an expression vector for Keap1-CBD (2 μg, lanes 2-5) and treated with 10 μM MG132 (lane 3), 20 μM sulforaphane (lane 4) or 50 μM tBHQ (lane 5) for five hours. Total cell lysates were subjected to immunoblot analysis with anti-Nrf2 antibodies (top panels) or incubated with chitin beads (middle and bottom panels). Proteins that remained bound to the chitin beads after extensive washing were analyzed by immunoblot analysis using either anti-Nrf2 antibodies (middle panel) or anti-CBD antibodies (bottom panel). (C). 100 mm dishes of MDA-MB-231 cells were either untreated (lanes 1 and 3), treated for five hours with 10 μM MG132 (lanes even-numbered lanes), 50 μM tBHQ (lanes 5 and 6) or 25 μM sulforaphane (lanes 7 and 8). Total cell lysates were collected and 2% of the cell lysate was subjected to immunoblot analysis with anti-Nrf2 antibodies (top panel). The remainder of the lysate was subjected to immunoprecipitation with anti-HA antibodies (bottom panel, lanes 1 and 2) or affinity-purified anti-Keap1 antibodies (bottom panel, lanes 3-8). The immunoprecipated proteins were analyzed by immunoblot using anti-Nrf2 antibodies.

REFERENCES

1. **Alam, J., E. Killeen, P. Gong, R. Naquin, B. Hu, D. Stewart, J. R. Ingelfinger, and K. A. Nath.** 2003. Heme activates the heme oxygenase-1 gene in renal epithelial cells by stabilizing Nrf2. Am J Physiol Renal Physiol **284:**F743-52.

2. **Ames, B. N., and M. K. Shigenaga.** 1993. DNA and Free Radicals, p. 1-15. *In* B. Halliwell and O. I. Aruoma (ed.), Oxidants are a major contributor to cancer and aging. Ellis Horwood, New York, NY.

3. **Andreassi, M. G.** 2003. Coronary atherosclerosis and somatic mutations: an overview of the contributive factors for oxidative DNA damage. Mutat Res **543:**67-86.

4. **Aoki, Y., H. Sato, N. Nishimura, S. Takahashi, K. Itoh, and M. Yamamoto.** 2001. Accelerated DNA adduct formation in the lung of the Nrf2 knockout mouse exposed to diesel exhaust. Toxicol Appl Pharmacol **173:**154-60.

5. **Bloom, D. A., and A. K. Jaiswal.** 2003. Phosphorylation of Nrf2S40 by PKC in response to antioxidants leads to the release of Nrf2 from INrf2 but not required for Nrf2 stabilization/accumulation in the nucleus and transcriptional activation of ARE-mediated NQO1 gene expression. J Biol Chem.

6. **Bomont, P., L. Cavalier, F. Blondeau, C. Ben Hamida, S. Belal, M. Tazir, E. Demir, H. Topaloglu, R. Korinthenberg, B. Tuysuz, P. Landrieu, F. Hentati, and M. Koenig.** 2000. The gene encoding gigaxonin, a new member of the cytoskeletal BTB/kelch repeat family, is mutated in giant axonal neuropathy. Nat Genet **26:**370-4.

7. **Bomont, P., and M. Koenig.** 2003. Intermediate filament aggregation in fibroblasts of giant axonal neuropathy patients is aggravated in non dividing cells and by microtubule destabilization. Hum Mol Genet **12:**813-22.

8. **Buschmann, T., S. Y. Fuchs, C. G. Lee, Z. Q. Pan, and Z. Ronai.** 2000. SUMO-1 modification of Mdm2 prevents its self-ubiquitination and increases Mdm2 ability to ubiquitinate p53. Cell **101:**753-62.

9. **Butterfield, D. A., B. J. Howard, and M. A. LaFontaine.** 2001. Brain oxidative stress in animal models of accelerated aging and the age-related neurodegenerative disorders, Alzheimer's disease and Huntington's disease. Curr Med Chem **8:**815-28.

10. **Chan, K., and Y. W. Kan.** 1999. Nrf2 is essential for protection against acute pulmonary injury in mice. Proc Natl Acad Sci U S A **96:**12731-6.

11. **Cho, H. Y., A. E. Jedlicka, S. P. Reddy, T. W. Kensler, M. Yamamoto, L. Y. Zhang, and S. R. Kleeberger.** 2002. Role of NRF2 in protection against hyperoxic lung injury in mice. Am J Respir Cell Mol Biol **26:**175-82.

12. **Cope, G. A., and R. J. Deshaies.** 2003. COP9 signalosome: a multifunctional regulator of SCF and other cullin-based ubiquitin ligases. Cell **114:**663-71.

13. **Cullinan, S. B., D. Zhang, M. Hannink, E. Arvisais, R. J. Kaufman, and J. A. Diehl.** 2003. Nrf2 Is a Direct PERK Substrate and Effector of PERK-Dependent Cell Survival. Mol Cell Biol **23:**7198-7209.

14. **Dalton, T. P., H. G. Shertzer, and A. Puga.** 1999. Regulation of gene expression by reactive oxygen. Annu Rev Pharmacol Toxicol **39:**67-101.

15. **Dhakshinamoorthy, S., and A. K. Jaiswal.** 2001. Functional characterization and role of INrf2 in antioxidant response element-mediated expression and antioxidant induction of NAD(P)H:quinone oxidoreductase1 gene. Oncogene **20:**3906-17.

16. **Dinkova-Kostova, A. T., W. D. Holtzclaw, R. N. Cole, K. Itoh, N. Wakabayashi, Y. Katoh, M. Yamamoto, and P. Talalay.** 2002. Direct evidence that sulfhydryl groups of Keap1 are the sensors regulating induction of phase 2 enzymes that protect against carcinogens and oxidants. Proc Natl Acad Sci U S A **99:**11908-13.

17. **Dinkova-Kostova, A. T., M. A. Massiah, R. E. Bozak, R. J. Hicks, and P. Talalay.** 2001. Potency of Michael reaction acceptors as inducers of enzymes that protect against carcinogenesis depends on their reactivity with sulfhydryl groups. Proc Natl Acad Sci U S A **98:**3404-9.

18. **Enomoto, A., K. Itoh, E. Nagayoshi, J. Haruta, T. Kimura, T. O'Connor, T. Harada, and M. Yamamoto.** 2001. High sensitivity of Nrf2 knockout mice to acetaminophen hepatotoxicity associated with decreased expression of ARE-regulated drug metabolizing enzymes and antioxidant genes. Toxicol Sci **59:**169-77.

19. **Furukawa, M., Y. J. He, C. Borchers, and Y. Xiong.** 2003. Targeting of protein ubiquitination by BTB-Cullin 3-Roc1 ubiquitin ligases. Nat Cell Biol **5:**1001-7.

20. **Geyer, R., S. Wee, S. Anderson, J. Yates, and D. A. Wolf.** 2003. BTB/POZ domain proteins are putative substrate adaptors for cullin 3 ubiquitin ligases. Mol Cell **12:**783-90.

21. **Golden, T. R., D. A. Hinerfeld, and S. Melov.** 2002. Oxidative stress and aging: beyond correlation. Aging Cell **1:**117-23.

22. **Imlay, J. A.** 2003. Pathways of oxidative damage. Annu Rev Microbiol **57:**395-418.

23. **Ishii, T., K. Itoh, S. Takahashi, H. Sato, T. Yanagawa, Y. Katoh, S. Bannai, and M. Yamamoto.** 2000. Transcription factor Nrf2 coordinately regulates a group of oxidative stress-inducible genes in macrophages. J Biol Chem **275:**16023-9.

24. **Itoh, K., K. I. Tong, and M. Yamamoto.** 2004. Molecular mechanism activating nrf2-keap1 pathway in regulation of adaptive response to electrophiles. Free Radic Biol Med **36:**1208-13.

25. **Itoh, K., N. Wakabayashi, Y. Katoh, T. Ishii, K. Igarashi, J. D. Engel, and M. Yamamoto.** 1999. Keap1 represses nuclear activation of antioxidant responsive elements by Nrf2 through binding to the amino-terminal Neh2 domain. Genes Dev **13:**76-86.

26. **Itoh, K., N. Wakabayashi, Y. Katoh, T. Ishii, T. O'Connor, and M. Yamamoto.** 2003. Keap1 regulates both cytoplasmic-nuclear shuttling and degradation of Nrf2 in response to electrophiles. Genes Cells **8:**379-91.

27. **Jaiswal, A. K.** 2004. Nrf2 signaling in coordinated activation of antioxidant gene expression. Free Radic Biol Med **36:**1199-207.

28. **Kamura, T., D. M. Koepp, M. N. Conrad, D. Skowyra, R. J. Moreland, O. Iliopoulos, W. S. Lane, W. G. Kaelin, Jr., S. J. Elledge, R. C. Conaway, J. W.**

Harper, and J. W. Conaway. 1999. Rbx1, a component of the VHL tumor suppressor complex and SCF ubiquitin ligase. Science **284:**657-61.

29. **Kang, M. I., A. Kobayashi, N. Wakabayashi, S. G. Kim, and M. Yamamoto.** 2004. Scaffolding of Keap1 to the actin cytoskeleton controls the function of Nrf2 as key regulator of cytoprotective phase 2 genes. Proc Natl Acad Sci U S A **101:**2046-51.

30. **Kelso, R. J., A. M. Hudson, and L. Cooley.** 2002. Drosophila Kelch regulates actin organization via Src64-dependent tyrosine phosphorylation. J Cell Biol **156:**703-13.

31. **Kobayashi, A., M. I. Kang, H. Okawa, M. Ohtsuji, Y. Zenke, T. Chiba, K. Igarashi, and M. Yamamoto.** 2004. Oxidative stress sensor Keap1 functions as an adaptor for Cul3-based E3 ligase to regulate proteasomal degradation of Nrf2. Mol Cell Biol **24:**7130-9.

32. **Kwak, M. K., P. A. Egner, P. M. Dolan, M. Ramos-Gomez, J. D. Groopman, K. Itoh, M. Yamamoto, and T. W. Kensler.** 2001. Role of phase 2 enzyme induction in chemoprotection by dithiolethiones. Mutat Res **480-481:**305-15.

33. **Kwak, M. K., N. Wakabayashi, K. Itoh, H. Motohashi, M. Yamamoto, and T. W. Kensler.** 2003. Modulation of gene expression by cancer chemopreventive dithiolethiones through the Keap1-Nrf2 pathway. Identification of novel gene clusters for cell survival. J Biol Chem **278:**8135-45.

34. **Lee, J. M., M. J. Calkins, K. Chan, Y. W. Kan, and J. A. Johnson.** 2003. Identification of the NF-E2-related factor-2-dependent genes conferring protection against oxidative stress in primary cortical astrocytes using oligonucleotide microarray analysis. J Biol Chem **278:**12029-38.

35. **Lee, J. M., A. Y. Shih, T. H. Murphy, and J. A. Johnson.** 2003. NF-E2-related factor-2 mediates neuroprotection against mitochondrial complex I inhibitors and increased concentrations of intracellular calcium in primary cortical neurons. J Biol Chem **278:**37948-56.

36. **McMahon, M., K. Itoh, M. Yamamoto, S. A. Chanas, C. J. Henderson, L. I. McLellan, C. R. Wolf, C. Cavin, and J. D. Hayes.** 2001. The Cap'n'Collar basic leucine zipper transcription factor Nrf2 (NF-E2 p45-related factor 2) controls both constitutive and inducible expression of intestinal detoxification and glutathione biosynthetic enzymes. Cancer Res **61:**3299-307.

37. **McMahon, M., K. Itoh, M. Yamamoto, and J. D. Hayes.** 2003. Keap1-dependent proteasomal degradation of transcription factor Nrf2 contributes to the negative regulation of antioxidant response element-driven gene expression. J Biol Chem **278:**21592-600.

38. **Motohashi, H., T. O'Connor, F. Katsuoka, J. D. Engel, and M. Yamamoto.** 2002. Integration and diversity of the regulatory network composed of Maf and CNC families of transcription factors. Gene **294:**1-12.

39. **Nathan, C.** 2002. Points of control in inflammation. Nature **420:**846-52.

40. **Nguyen, T., P. J. Sherratt, H. C. Huang, C. S. Yang, and C. B. Pickett.** 2003. Increased protein stability as a mechanism that enhances Nrf2-mediated transcriptional activation of the antioxidant response element. Degradation of Nrf2 by the 26 S proteasome. J Biol Chem **278:**4536-41.

41. **Nguyen, T., P. J. Sherratt, and C. B. Pickett.** 2003. Regulatory mechanisms controlling gene expression mediated by the antioxidant response element. Annu Rev Pharmacol Toxicol **43:**233-60.

42. **Pickart, C. M.** 2001. Mechanisms underlying ubiquitination. Annu Rev Biochem **70:**503-33.

43. **Pintard, L., J. H. Willis, A. Willems, J. L. Johnson, M. Srayko, T. Kurz, S. Glaser, P. E. Mains, M. Tyers, B. Bowerman, and M. Peter.** 2003. The BTB protein MEL-26 is a substrate-specific adaptor of the CUL-3 ubiquitin-ligase. Nature **425:**311-6.

44. **Ramos-Gomez, M., M.-K. Kwak, P. M. Dolan, K. Itoh, M. Yamamoto, P. Talalay, and T. W. Kensler.** 2001. Sensitivity to carcinogenesis is increased and chemopreventive efficacy of enzyme inducers is lost in nrf2 transcription factor-deficient mice. Proc. Nat. Acad. Sci USA **98:**3410-3415.

45. **Rao, A. V., and B. Balachandran.** 2002. Role of oxidative stress and antioxidants in neurodegenerative diseases. Nutr Neurosci **5:**291-309.

46. **Sambrook, J., and D. W. Russell.** 2001. Molecular Cloning: A Lab Manual, 3rd edition ed. Cold Spring Harbor Press, Cold Spring Harbor, NY.

47. **Shih, A. Y., D. A. Johnson, G. Wong, A. D. Kraft, L. Jiang, H. Erb, J. A. Johnson, and T. H. Murphy.** 2003. Coordinate regulation of glutathione biosynthesis and release by Nrf2-expressing glia potently protects neurons from oxidative stress. J Neurosci **23:**3394-406.

48. **Spence, H. J., I. Johnston, K. Ewart, S. J. Buchanan, U. Fitzgerald, and B. W. Ozanne.** 2000. Krp1, a novel kelch related protein that is involved in pseudopod elongation in transformed cells. Oncogene **19:**1266-76.

49. **Stewart, D., E. Killeen, R. Naquin, S. Alam, and J. Alam.** 2003. Degradation of transcription factor Nrf2 via the ubiquitin-proteasome pathway and stabilization by cadmium. J Biol Chem **278:**2396-402.

50. **Talalay, P., and J. W. Fahey.** 2001. Phytochemicals from cruciferous plants protect against cancer by modulating carcinogen metabolism. J Nutr **131:**3027S-33S.

51. **Thimmulappa, R. K., K. H. Mai, S. Srisuma, T. W. Kensler, M. Yamamoto, and S. Biswal.** 2002. Identification of Nrf2-regulated genes induced by the chemopreventive agent sulforaphane by oligonucleotide microarray. Cancer Res **62:**5196-203.

52. **Wakabayashi, N., A. T. Dinkova-Kostova, W. D. Holtzclaw, M. I. Kang, A. Kobayashi, M. Yamamoto, T. W. Kensler, and P. Talalay.** 2004. Protection against electrophile and oxidant stress by induction of the phase 2 response: fate of cysteines of the Keap1 sensor modified by inducers. Proc Natl Acad Sci U S A **101:**2040-5.

53. **Wakabayashi, N., K. Itoh, J. Wakabayashi, H. Motohashi, S. Noda, S. Takahashi, S. Imakado, T. Kotsuji, F. Otsuka, D. R. Roop, T. Harada, J. D. Engel, and M. Yamamoto.** 2003. Keap1-null mutation leads to postnatal lethality due to constitutive Nrf2 activation. Nat Genet.

54. **Wasserman, W. W., and W. E. Fahl.** 1997. Functional antioxidant responsive elements. Proc Natl Acad Sci U S A **94:**5361-6.

55. **Wilkins, A., Q. Ping, and C. L. Carpenter.** 2004. RhoBTB2 is a substrate of the mammalian Cul3 ubiquitin ligase complex. Genes Dev **18:**856-61.

56. **Wolf, D. A., C. Zhou, and S. Wee.** 2003. The COP9 signalosome: an assembly and maintenance platform for cullin ubiquitin ligases? Nat Cell Biol **5:**1029-33.

57. **Wu, G., G. Xu, B. A. Schulman, P. D. Jeffrey, J. W. Harper, and N. P. Pavletich.** 2003. Structure of a beta-TrCP1-Skp1-beta-catenin complex: destruction motif binding and lysine specificity of the SCF(beta-TrCP1) ubiquitin ligase. Mol Cell **11:**1445-56.

58. **Xu, L., Y. Wei, J. Reboul, P. Vaglio, T. H. Shin, M. Vidal, S. J. Elledge, and J. W. Harper.** 2003. BTB proteins are substrate-specific adaptors in an SCF-like modular ubiquitin ligase containing CUL-3. Nature **425:**316-21.

59. **Yoh, K., K. Itoh, A. Enomoto, A. Hirayama, N. Yamaguchi, M. Kobayashi, N. Morito, A. Koyama, M. Yamamoto, and S. Takahashi.** 2001. Nrf2-deficient female mice develop lupus-like autoimmune nephritis. Kidney Int **60:**1343-53.

60. **Zhang, D. D., and M. Hannink.** 2003. Distinct cysteine residues in Keap1 are required for Keap1-dependent ubiquitination of Nrf2 and for stabilization of Nrf2 by chemopreventive agents and oxidative stress. Mol Cell Biol **23:**8137-51.

61. **Zheng, N., B. A. Schulman, L. Song, J. J. Miller, P. D. Jeffrey, P. Wang, C. Chu, D. M. Koepp, S. J. Elledge, M. Pagano, R. C. Conaway, J. W. Conaway, J. W. Harper, and N. P. Pavletich.** 2002. Structure of the Cul1-Rbx1-Skp1-F boxSkp2 SCF ubiquitin ligase complex. Nature **416:**703-9.

62. **Zipper, L. M., and R. T. Mulcahy.** 2002. The Keap1 BTB/POZ Dimerization Function Is Required to Sequester Nrf2 in Cytoplasm. J Biol Chem **277:**36544-52.

III. UBIQUITINATION OF KEAP1, A BTB-KELCH SUBSTRATE ADAPTOR PROTEIN FOR CUL3, TARGETS KEAP1 FOR DEGRADATION BY A PROTEOSOME-INDEPENDENT PATHWAY

ABSTRACT

Keap1 is a BTB-Kelch protein that functions as a substrate adaptor protein for a Cul3-dependent E3 ubiquitin ligase complex. Keap1 targets its substrate, the Nrf2 transcription factor, for ubiquitination and subsequent degradation by the 26S proteosome. Inhibition of Keap1-dependent ubiquitination of Nrf2 increases steady-state levels of Nrf2 and enables activation of cytoprotective Nrf2-dependent genes. In this report, we demonstrate that Keap1 and three other BTB-Kelch proteins, including GAN1, ENC1 and Sarcosin, are ubiquitinated by a Cul3-dependent complex. Ubiquitination of Keap1 is markedly increased in cells exposed to quinone-induced oxidative stress, occurs in parallel with inhibition of Keap1-dependent ubiquitination of Nrf2, and results in decreased steady-state levels of Keap1, particularly in cells that are unable to synthesize glutathione. Degradation of Keap1 is independent of the 26S proteosome, as inhibitors of the 26S proteosome do not prevent loss of Keap1 following exposure of cells to quinone-induced oxidative stress. Our results suggest that a switch from substrate to substrate adaptor ubiquitination is a critical regulatory step that controls steady-state levels of both BTB-Kelch substrate adaptor proteins and their cognate substrates.

INTRODUCTION

Oxidative stress results from an imbalance between the production and removal of reactive oxygen species and has been implicated in numerous pathophysiological settings, including cancer, neurodegeneration, aging, and cardiovascular disease (1-5). The induction of proteins that increase the anti-oxidant capacity of cells and enable restoration of intracellular redox homeostasis is a major protective mechanism against the damaging consequences of oxidative stress. The expression of many anti-oxidant and cytoprotective proteins, including classical phase 2 detoxification enzymes, chaperone proteins, antioxidant proteins, and proteins in the proteasomal degradation pathway is regulated by Nrf2, a bZIP transcription factor (6-9). Induction of Nrf2-dependent genes occurs in response to chemical inducers of oxidative stress, including redox-cycling quinones and heavy metals (9-11). In additon, the cancer-protective properties of structurally diverse natural and synthetic anticarcinogens derive, in large part, from induction of an Nrf2-dependent transcriptional program (6,7,12-14).

Nrf2 is controlled at the post-translational level by the cytoplasmic Keap1 protein (15-17). Keap1 is member of the large BTB-Kelch protein family, more than 40 of which are encoded by the human genome (18). Recent reports by several groups have demonstrated that Keap1 functions as a substrate adaptor protein for a Cul3-Rbx1 E3 ubiquitin ligase complex (19-22). The N-terminal BTB domain and central linker region of Keap1 bind Cul3, while the C-terminal Kelch domain of Keap1 binds Nrf2 via residues located within loops that extend out from the bottom of the Kelch domain (20,21,23). Under conditions of homeostatic cell growth, Keap1 brings Nrf2 into the

Cul3-Rbx1 complex and enables ubiquitin conjugation onto specific lysine residues located within the N-terminal Neh2 domain of Nrf2 (21). However, following exposure of cells to a wide variety of chemical inducers of Nrf2-dependent transcription, Keap1-dependent ubiquitination of Nrf2 is blocked, enabling Nrf2 to accumulate in the nucleus and activate expression of Nrf2-dependent genes (21,24).

The molecular definition of Keap1 as a substrate adaptor protein for Cul3 provides a conceptual framework for understanding how Keap1-dependent ubiquitination of Nrf2 is regulated. In general, the six cullin proteins encoded by the human genome function as scaffold proteins that bring together a substrate protein and a ubiquitin-charged E2 ubiquitin conjugation (Ubc) protein (25,26). The E2 protein does not associate directly with the cullin protein but is brought into the complex by the cullin-associated Rbx1 protein. Likewise, the substrate does not typically associate directly with the cullin protein but is brought into the complex by a substrate adaptor protein. Once the entire E3 ubiquitin ligase complex is assembled, the ubiquitin molecule is transferred from a conserved cysteine residue in the Ubc protein to one or more lysine residues in the substrate protein. Cullin-based E3 ubiquitin ligases typically catalyze the addition of a multi-ubiquitin chain onto the substrate protein and thereby target the substrate protein for proteosome-mediated degradation.

Cullin-based E3 ubiquitin ligase complexes are dynamic complexes that undergo cycles of assembly and disassembly (27,28). The ability of cullin-based E3 ubiquitin ligase complexes to undergo facile substrate adaptor exchange is a critical functional property, as each cullin protein supports the ability of a large number of substrate adaptor proteins to target their substrates for degradation. Several mechanisms have been

suggested to account for facile exchange of substrate adaptor proteins by cullin-based E3 ubiquitin ligase complexes. In yeast, several well-characterized F-box-containing substrate adaptor proteins, including Grr1, cdc4p and Met30, all of which function as substrate adaptors for Cul1, are labile proteins that are subject to auto-ubiquitination by the same Cul1-Rbx1 complex that directs ubiquitination of their substrates (29,30). As F-box proteins play critical roles in the cell cycle and in the response of cells to environmental conditions, rapid degradation of a specific substrate adaptor protein may enable timely accumulation of its substrate protein. Rapid degradation of a substrate adaptor protein will also minimize competition for limiting amounts of the cullin-Rbx1 complex and provides a mechanism for substrate adaptor exchange (27). In mammalian cells, which contain numerous substrate adaptor proteins that specifically utilize individual cullin proteins, only two F-box proteins, Skp2 and βTrCP, are known to be regulated at the level of ubiquitination and proteosome-mediated degradation (31-34). Additional mechanisms have been uncovered that contribute to substrate adaptor exchange in mammalian cells. For example, the CAND1 protein has been proposed to displace a substrate adaptor protein from Cul1 following deneddylation of the Cul1 protein by the COP9 signalosome (28,35,36).

In this report, we demonstrate that Keap1 is ubiquitinated in vivo and in vitro by the same Cul3-Rbx1 complex that ubiquitinates its substrate, Nrf2. Other members of the BTB-Kelch protein family are also able to assemble into functional E3 ubiquitin ligase complexes with Cul3 that support ubiquitination of the respective BTB-Kelch protein, providing evidence that the ability to function as a substrate adaptor protein for Cul3 is a conserved property of this large family of proteins. Quinone-induced oxidative stress

enhances ubiquitination of Keap1 and decreases steady state levels of Keap1, resulting in a corresponding increase in steady-state levels of Nrf2. However, in contrast to Nrf2 degradation, which is blocked by inhibitors of the 26S proteosome, proteasome inhibitors do not block degradation of Keap1. Keap1 ubiquitination and proteosome-independent degradation of Keap1 following exposure to quinone-induced oxidative stress is markedly enhanced in glutathione-deficient cells. The isothiocyanate sulforaphane, a well-characterized cancer-preventive inducer of Nrf2-dependent transcription, inhibits Keap1-dependent ubiquitination of Nrf2 but does not induce Keap1 ubiquitination, indicating that Keap1 differentially responds to inducers of Nrf2-dependent transcription. Our results indicate that ubiquitination targets BTB-Kelch proteins for degradation by a proteosome-independent pathway and suggest that a switch from substrate to substrate adaptor ubiquitination is a critical regulatory step that controls steady-state levels of both BTB-Kelch substrate adaptor proteins and their cognate substrates.

MATERIALS AND METHODS

Construction of recombinant DNA molecules. Plasmids expressing wild type Keap1, Nrf2, Cul3, Cul3DN, Rbx1 and HA-Ub proteins have been previously described (21). cDNA clones of GAN1, ENC1, and sarcosin were purchased from ATCC (American Type Culture Collection). The CBD-tagged versions of GAN1, ENC1 and sarcosin were generated by insertion of a PCR-generated DNA fragment encoding the chitin binding domain of *B. Circulans* chitinase A1 gene upstream of the stop codon. The integrity of all of the plasmids used in this study was confirmed by sequence analysis.

Cell culture and transfections. COS-1 and MDA-MB-231 cells were purchased from ATCC. Cells were maintained in either Dulbecco's modified Eagle's medium (DMEM) or Eagle's minimal essential medium (EMEM) in the presence of 10% fetal bovine serum (FBS). The GCS-2 cell line was a gift from Dr. Lieberman (37). GCS-2 cells were grown in knock-out DMEM medium supplemented with 15% ES-cell qualified bovine serum, 2.5 mM glutathione, and 100 μM β-mercaptoethanol. Transfections were performed with Lipofectamine Plus (Gibco BRL) according to the manufacturer's instructions.

Antibodies, immuprecipitation, and immunoblot analysis. The anti-Keap1 antibody has been described (24). Antibodies against Nrf2 and Myc (Santa Cruz), ubiquitin (Sigma), chitin binding domain (New England Biolabs), and HA (Covance) were purchased from commercial sources.

For detection of protein expression in total cell lysates, cells were lysed in sample buffer (50 mM Tris-HCl [pH 6.8], 2% SDS, 10% Glycerol, 100 mM DTT, 0.1% bromophenol blue) at 48 hr post-transfection. For immunoprecipitation assays, cells were lysed in RIPA buffer (10 mM sodium phosphate pH [8.0], 150 mM NaCl, 1% Triton X-100, 1% sodium deoxycholate, 0.1% SDS) containing 1 mM dithiothreitol (DTT), 1 mM phenylmethylsulfonyl fluoride (PMSF) and protease inhibitor cocktail (Sigma). Cell lysates were pre-cleared with protein A beads and incubated with 2 μg of affinity-purified antibodies for 2 hr at 4 °C, followed by incubation at 4 °C with protein A-agarose beads for 2 hr. Immunoprecipitated complexes were washed four times with RIPA buffer and eluted in sample buffer by boiling for 4 minutes, electrophoresed through SDS-polyacrylamide gels, transferred to nitrocellulose membranes and subjected to immunoblot analysis.

In vivo ubiquitination. For detection of ubiquitinated proteins in vivo, cells were transfected with expression vectors for HA-ubiquitin and the indicated proteins. Expression vectors for HA-Cul3 and Myc-Rbx1 were included in some of experiments, as indicated. Cells were rapidly lysed by boiling in a buffer containing 2% SDS, 150 mM NaCl, 10 mM Tris-Hcl and 1 mM DTT. This rapid lysis procedure inactivates cellular ubiquitin hydrolases and therefore preserves ubiquitin-protein conjugates present in cells prior to lysis. Protein-protein interactions, including association of Nrf2 with Keap1, are also disrupted by this lysis procedure. For immunoprecipitation, these lysates were diluted five-fold in buffer lacking SDS and incubated with anti-Keap1, anti-Nrf2, or anti-

CBD antibodies accordingly. Immunoprecipitated proteins were analyzed by immunoblot with antibodies directed against the HA epitope.

In vitro ubiquitination. For ubiquitination of the BTB-Kelch proteins in vitro, COS-1 cells were transfected with expression vectors for the individual CBD-tagged BTB-Kelch protein, HA-Cul3 and Myc-Rbx1. The transfected cells were lysed in buffer B (15 mM Tris-HCL [pH 7.4], 500 mM NaCl, and 0.25% NP40) containing 1 mM DTT, 1 mM PMSF, and protease inhibitor cocktail. The lysates were pre-cleared with protein A beads prior to incubation with chitin beads (New England Biolabs) for four hours at 4 $^{\circ}$C. Chitin beads were washed twice with buffer B, twice with buffer A (25 mM Tris-HCl [pH 7.5], 10% (v/v) glycerol, 1 mM EDTA, 0.01% NP-40 and 0.1 M NaCl), and twice with reaction buffer (50 mM Tris-HCl [pH 7.5], 5 mM $MgCl_2$, 2 mM NaF and 0.6 mM DTT). The pellets were incubated with ubiquitin (300 pmol), E1 (2 pmol), E2-UbcH5a (10 pmol), and ATP (2 mM) in 1X reaction buffer in a total volume of 30 µl for 1 hr at 37 $^{\circ}$C. Ubiquitin, E1 and E2-UbcH5a were purchased from Boston Biochem. The chitin beads were centrifuged at 3,000 x g, resuspended in 2% SDS, 150 mM NaCl, 10 mM Tris-Hcl [pH 8.0] and 1 mM DTT and boiled for 5 min to release bound proteins, inactivate any contaminating ubiquitin hydrolases, and disrupt protein-protein interactions. The supernatant was diluted five-fold with buffer lacking SDS prior to immunoprecipitation with anti-CBD antibodies. Immunoprecipitated proteins were subjected to immunoblot analysis with anti-ubiquitin antibodies.

RESULTS

Assembly into a functional ubiquitin ligase complex is a conserved property of BTB-Kelch protein. The major function of substrate adaptor proteins is to target specific substrate proteins for ubiquitination. However. ubiquitination of substrate adaptor proteins may also play an important role in cellular physiology. For example, autoubiquitination of several yeast F-box proteins is responsible for their rapid turnover during progression through the cell cycle (29,30).

To examine the possibility that Keap1 is ubiquitinated by a Cul3-Rbx1 complex in vitro, the Keap1-Cul3-Rbx1 complex was purified from COS-1 cells transfected with expression vectors for Keap1, Cul3 and Rbx1. To facilitate purification of Keap1 and Keap1-associated proteins, an expression vector encoding a Keap1 protein containing a C-terminal chitin binding domain (CBD) was utilized in this experiment. Proteins that bound to the chitin beads were incubated with purified E1, E2-UbcH5a, ubiquitin and ATP. Subsequently, anti-Keap1 immunoprecipitates were prepared under strongly denaturing conditions and subjected to immunoblot analysis using anti-ubiquitin antibodies (Fig. 1A, top panel). Keap1-ubiquitin conjugates were readily observed in the presence of both Cul3 and Rbx1 (Fig. 1A, top panel, lane 5), and required the addition of ubiquitin, E1 and E2-UbcH5a to the in vitro reaction (Fig 2C, top panel, lanes 2-4). Immunoblot analysis of anti-Keap1 immunoprecipitates confirmed the presence of equivalent levels of Keap1-CBD in all reactions (Fig. 1A, bottom panel).

Keap1 is one of more than 40 BTB-Kelch proteins that are encoded by the human genome (18,38). The members of the BTB-Kelch family share both a common domain

organization and approximately 25% sequence identity, when compared on a one-to-one basis with each other. The biochemical functions of this family of proteins are, in general, not known, although the ability of Keap1 to function as a substrate adaptor protein suggests a common function for these proteins. To determine if other BTB-Kelch proteins may function as substrate adaptor proteins for Cul3, the ability of several different BTB-Kelch proteins to associate with Cul3 and Rbx1 to form a functional ubiquitin ligase complex was determined. The three BTB-Kelch proteins used for these experiments, GAN1, ENC1 and sarcosin, were selected because of their known or suspected roles in cancer and neurodegenerative diseases (39-43).

To facilitate purification and detection of these BTB-Kelch proteins, fusion proteins containing a C-terminal chitin binding domain (CBD) were constructed. Expression vectors for the CBD-tagged BTB-Kelch proteins were transfected into COS-1 cells alone or with expression vectors for HA-Cul3 and Myc-Rbx1. Cell lysates were subjected to affinity purification using chitin beads. Neither Cul3 nor Rbx1 purified with the chitin beads in the absence of a CBD-tagged BTB-Kelch protein (Fig. 1B). Each of these BTB-Kelch proteins was able to associate with both Cul3 and Rbx1, as determined by immunoblot analysis of the purified complexes using anti-HA or anti-Myc antibodies (Fig. 1C, middle and bottom panels, respectively).

The ability of the complexes formed between the respective BTB-Kelch proteins, Cul3 and Rbx1 to support ubiquitin conjugation onto the BTB-Kelch protein was determined. The chitin beads containing the purified complexes were incubated with E1, E2-UbcH5a, ubiquitin and ATP. Subsequently, anti-CBD immunoprecipitates prepared under strongly denaturing conditions were subjected to immunoblot analysis with anti-

ubiquitin antibodies. Ubiquitin conjugation onto each of the BTB-Kelch proteins that was dependent upon the addition of E1 into the in vitro reaction was observed (Fig. 1D). The presence of ubiquitin conjugation onto Keap1 and GAN1 in the absence of co-expressed Cul3 and Rbx1 proteins presumably represents co-purification of endogenous Cul3 and Rbx1 proteins with these two BTB-Kelch proteins (Fig. 1D, lanes 3 and 6).

Keap1 is ubiquitinated by a Cul3-Rbx1 complex in vivo. To determine if Keap1 is ubiquitinated in vivo, MDA-MB-231 cells were cotransfected with expression vectors for HA-ubiquitin, HA-Cul3, and Keap1 and increasing amounts of the expression vector for Myc-Rbx1. Cells were lysed under denaturing conditions and subjected to immunoprecipitation with Keap1 antibodies. The presence of ubiquitin-conjugated Keap1 proteins was assessed by immunoblot analysis of anti-Keap1 immunoprecipitates with anti-HA antibodies. Ubiquitin conjugation onto ectopically expressed Keap1 was readily observed and was increased by coexpression of Cul3 (Fig. 2A, top panel, lanes 1-3). Low levels of co-expressed Rbx1 slightly increased the levels of ubiquitin conjugation onto Keap1 (Fig. 2A, top panel, lane 4). Increased Rbx1 expression did not further increase Keap1 ubiquitination, but markedly decreased steady-state levels of Keap1 in a dose-dependent manner (Fig. 2A, lanes 5-8).

To confirm that Keap1 is ubiquitinated in vivo, cell lysates from 293T cells transfected with expression vectors for Keap1 and HA-ubiquitin were immunoprecipitated with anti-HA antibodies. The presence of Keap1 in anti-HA immunoprecipitates was confirmed by immunoblot analysis with anti-Keap1 antibodies (Fig. 2B).

To define the role of Cul3 in ubiquitination of Keap1 in vivo, we determined the ability of a dominant-negative Cul3 protein lacking the C-terminal Rbx1 binding domain to block Keap1 ubiquitination. Cell lysates were collected from MDA-MB-231 cells transfected with expression vectors for Keap1 and either wild-type or dominant-negative Cul3. As expected, co-expression of Keap1 with the wild-type Cul3 protein increased ubiquitination onto Keap1 (Fig. 2C, top panel, lanes 3-6). Co-expression of Keap1 with the dominant-negative Cul3 protein decreased levels of ubiquitin-conjugated Keap1 (Fig. 2C, top panel, lanes 7 and 8). Treatment of the transfected cells with MG132 prior to collection of cell lysates enhanced ubiquitin conjugation onto Keap1 (Fig 2C, top panel, compare even and odd lanes), but did not alter steady-state levels of Keap1 (Fig. 2C, bottom panel, compare even and odd lanes). Taken together, these results indicate that ubiquitination of Keap1 is mediated by an E3 ubiquitin ligase complex that contains Cul3 and Rbx1.

A panel of mutant ubiquitin proteins containing a single lysine residue was evaluated for their ability to participate in multi-ubiquitination onto Keap1. Prominent ubiquitin conjugation onto Keap1 was only observed in the presence of either wild-type ubiquitin (Fig. 2D, lane 1) or a mutant ubiquitin protein containing only lysine 63 (Fig. 2D, lane 7).

Increased ubiquitination results in proteosome-independent degradation of Keap1.
In our previous work, we have identified several Keap1 mutants that display increased association with Cul3 (21). To determine if increased association with Cul3 correlates with increased autoubiquitination of Keap1, one of these mutant Keap1 proteins, Keap1-

125A3, which contains three alanine substitutions for conserved residues located within the BTB domain of Keap1, was further characterized. In MDA-MB-231 cells, ubiquitin conjugation onto the Keap1-125A3 protein was markedly elevated relative to the wild-type Keap1 protein (Fig. 3A, top panel) and correlated with reduced steady-state levels of the Keap1-125A3 protein (Fig. 3A, bottom panel). Surprisingly, steady-state levels of the Keap1-125A3 protein were not increased following treatment with MG132, a well-characterized proteosome inhibitor. (Fig. 3A, bottom panel, compare lanes 4 and 5). To extend this observation, several other proteosome inhibitors, including clasto-lactacystin β-lactone and epoxomicin, were tested for their ability to increase steady-state levels of the Keap1-125A3 protein. None of these proteosome inhibitors increased steady-state levels of the wild-type or Keap1-125A3 proteins (Fig. 3B). Taken together, these observations indicate that ubiquitination of Keap1 targets Keap1 for degradation in a proteosome-independent manner.

Quinone-induced oxidative stress increases ubiquitination and decreases steady-state levels of Keap1. The ability of Keap1 to function as a substrate adaptor protein that targets Nrf2 for ubiquitination is perturbed by chemically diverse compounds, resulting in stabilization of Nrf2 and activation of Nrf2-dependent transcription. For example, both the chemopreventive isothiocyanate sulforaphane and oxidative stress induced by redox cycling of tert-butylhydroquinone (tBHQ) inhibit Keap1-dependent ubiquitination of Nrf2 (21,24). To determine if ubiquitination of Keap1 is altered under conditions that inhibit Keap1-dependent ubiquitination of Nrf2, the presence of ubiquitin-Keap1 conjugates was assessed in MDA-MB-231 cells transfected with an expression vector for

Keap1 and exposed to either tBHQ or sulforaphane. Treatment of cells with tBHQ increased ubiquitin conjugation onto Keap1 in a time-dependent manner (Fig. 4A, top panel, lanes 4 and 5). In parallel, decreased steady-state levels of Keap1 were observed in tBHQ-treated cells (Fig. 4A, bottom panel, lanes 4 and 5). In contrast, ubiquitin conjugation onto Keap1 was not increased in sulforaphane-treated cells, with no alteration in steady state levels of Keap1 (Fig. 4A, top and bottom panels, lanes 6 and 7). These results indicate that quinone-induced oxidative stress, but not sulforaphane, increases ubiquitination onto Keap1, resulting in decreased steady-state levels of Keap1.

To determine if oxidative stress increases ubiquitination conjugation or steady-state levels of the endogenous Keap1 protein, we first determined if ubiquitin conjugation onto the endogenous Keap1 protein could be detected. The endogenous Keap1 protein was immunoprecipitated by anti-Keap1 antibodies conjugated onto sepharose beads after cells were lysed under strongly denaturing conditions. Anti-Keap1 immunoprecipitates were subjected to immunoblot analysis with anti-ubiquitin antibodies to detect ubiquitin-Keap1 conjugates. Multiple slowly migrating bands representing the ubiquitin-conjugated forms of Keap1 were readily detected in untreated cells (Fig. 4B, top panel, lane 2). The high molecular weight bands were specific to anti-Keap1 immunoprecipitates, as low background levels of cross-reactivity in immunoblot analysis using the anti-ubiquitin antibody was observed with anti-HA immunoprecipitates (Fig. 4B, top panel, lane 1). Anti-Keap1 immunoprecipitates from MDA-MB-231 cells exposed to tBHQ were analyzed in parallel. Comparable amounts of ubiquitin conjugation onto Keap1 were observed in anti-Keap1 immunoprecipitates from either untreated cells or cells treated with tBHQ for 16 hours (Fig. 4B, top panel, compare lane

2 with lane 3). However, the steady-state level of the endogenous Keap1 protein was markedly reduced in lysates from cells exposed to tBHQ (Fig. 4B, bottom panel, compare lane 2 with lane 3).

A series of Keap1 deletion mutants were used to localize the domains of Keap1 required for ubiquitin conjugation. A Keap1 mutant lacking the N-terminal BTB domain (Keap1-ΔBTB) contained high levels of ubiquitin conjugation that was slightly increased following tBHQ treatment (Fig. 4C, top panel, lanes 5 and 6). Deletion of the central linker domain (Keap1-ΔL) reduced both basal and tBHQ-induced ubiquitination (Fig. 4C, top panel, lanes 7 and 8). Deletion of the C-terminal Kelch domain (Keap1-ΔK) increased both basal and tBHQ-induced ubiquitination (Fig. 4C, top panel, lanes 9 and 10). Finally, deletion of the C-terminal fifteen amino acids of Keap1 (Keap1-ΔC) did not alter basal levels of Keap1 ubiquitination, although tBHQ-induced ubiquitination was increased slightly (Fig. 4C, top panel, lanes 11 and 12). Taken together, these results suggest that one or more of the six lysine residues located in the central linker domain of Keap1 are the likely site(s) of ubiquitin conjugation in vivo.

Quinone-induced degradation of Keap1 is enhanced in cells deficient in glutathione biosynthesis. Intracellular levels of glutathione, a major intracellular reductant, are reduced following exposure of cells to oxidative stress. In an effort to restore an intracellular reducing environment, synthesis of glutathione is enhanced following exposure of eukaryote cells to oxidative stress. The rate-limiting enzyme for glutathione biosynthesis is γ-glutamyl cysteine synthase (γGCS), composed of a large subunit (GCLM), which carries out catalysis, and a small regulatory subunit (GCLC). In

vertebrates, Nrf2 regulates transcription of both the GCLM and GCLC genes (44,45). Thus, oxidative stress, by acting on Keap1, activates an autoregulatory feedback mechanism that counteracts the damaging effects of oxidative stress.

To determine if reduced levels of glutathione would, by itself, be sufficient to inactivate Keap1-dependent ubiquitination of Nrf2, we characterized the ability of Keap1 to regulate Nrf2 in GCS-2 cells that are nullizygous for the large subunit of γGCS (37). GCS-2 cells were derived from blastocysts of mice in which both copies of the GCLM gene were disrupted by homologous recombination. Although mice that lack GCLM are unable to complete embryonic development due to increased apoptosis, GCS-2 cells are able to proliferate in culture when the culture media is supplemented with 2.5 mM glutathione. However, the intracellular gluthathione level in the GCS-2 cells grown in the presence of 2.5 mM glutathione is approximately 2% of that found in normal cells (37).

We first characterized the ability of Keap1 to regulate Nrf2 in GCS-2 cells. Expression of the endogenous Nrf2 or Keap1 proteins could not be detected in GCS-2 cells (data not shown). However, ectopic expression of both Nrf2 and Keap1 in GCS-2 cells was readily accomplished by transient transfection. Despite the reduced levels of glutathione, Keap1 was able to efficiently down-regulate steady-state levels of Nrf2 in GCS-2 cells (Fig. 5A, compare lanes 1 and 2). Steady-state levels of Nrf2 were restored by treatment with the proteosome inhibitor MG132, confirming the ability of Keap1 to target Nrf2 for proteosome-mediated degradation in GCS-2 cells despite low intracellular levels of glutathione (Fig. 5B, bottom panel, compare lanes 1 and 2). Consistent with this observation, inhibition of γGCS function by buthionine sulfoximine treatment of MDA-

MB-231 cells did not increase steady-state levels of Nrf2, either in the absence or presence of co-expressed Keap1 (data not shown). Taken together, these results indicate that reduced levels of glutathione are not sufficient to inhibit the ability of Keap1 to target Nrf2 for ubiquitination and proteosome-mediated degradation.

To determine if chemical inducers of Nrf2-dependent transcription are able to inhibit Keap1-mediated regulation of Nrf2 in GCS-2 cells, GCS-2 cells transfected with expression vectors for Keap1 and HA-Nrf2 were exposed to tBHQ or sulforaphane prior to cell lysis. Steady state levels of Nrf2 or Keap1 were determined by immunoblot analysis with anti-HA or anti-Keap1 antibodies, respectively. Steady-state levels of Nrf2 were markedly increased when cells were treated with either tBHQ or sulforaphane for 4 hours (Fig. 5B, bottom panel, lanes 3 and 5), or for 16 hours (Fig. 5C, bottom panel, lanes 3 and 5). As was observed in MDA-MB-231 cells, sulforaphane did not alter the steady-state levels of Keap1 (Figs. 5B and 5C, top panels, lanes 5 and 6). In contrast, and in agreement with the previous observations in MDA-MB-231 cells, treatment of GCS-2 cells with tBHQ markedly reduced steady-state levels of Keap1, particularly following prolonged exposure to tBHQ (Figs. 5B and 5C, top panels, lanes 3 and 4).

As expected, Keap1-dependent degradation of Nrf2 was blocked by treatment of cells with the proteasome inhibitor MG132 prior to cell lysis (Figs. 5B and 5C, bottom panels, lanes 1 and 2). However, MG132 treatment did not restore steady-state levels of Keap1 following exposure of transfected cells to tBHQ (Figs. 5B and 5C, top panels, lanes 3 and 4). Several other proteasome inhibitors, including 2-Leu-Leu-Leu-B(OH)2, clasto-lactacystin β-lactone and epoxomicin were also tested for their ability to block tBHQ-induced degradation of Keap1. None of these inhibitors were able to restore

steady state levels of Keap1 in tBHQ-treated cells (data not shown), indicating that tBHQ-induced degradation of Keap1 is not mediated by the proteasome.

Oxidative stress induces ubiquitination and degradation of multiple BTB-Kelch proteins. The ability of three other BTB-Kelch proteins to associate with Cul3 and Rbx1 into a functional complex that is competent for ubiquitin conjugation onto the respective BTB-Kelch protein in vitro suggests that these BTB-Kelch proteins may function as substrate adaptor proteins in a manner similar to Keap1. To further explore functional similarities between Keap1 and the other BTB-Kelch proteins, the ability of quinone-induced oxidative stress to decrease steady-state levels of these proteins was determined in GCS-2 cells. Reduced levels of Keap1, ENC1 and sarcosin, but not GAN1, were detected in response to tBHQ treatment (Fig. 5D, even-numbered lanes). As observed for Keap1, quinone-induced oxidative stress increased ubiquitin conjugation onto both ENC1 and sarcosin in GCS-2 cells (data not shown).

Quinone-induced oxidative stress induces a switch from substrate to substrate adaptor ubiquitination. To determine the relationship between quinone-induced ubiquitination of Keap1 and the ability of Keap1 to target Nrf2 for ubiquitination, levels of ubiquitin conjugation onto both Keap1 and Nrf2 were measured in GCS-2 cells following exposure to tBHQ. As prolonged exposure of cells to quinone-induced oxidative stress markedly decreases the steady-state levels of Keap1, levels of ubiquitin conjugation onto both Keap1 and Nrf2 were measured following a four-hour exposure to tBHQ. At this time point, substantial Keap1 protein is still present in tBHQ-treated cells

152

(Fig. 5B, top panel, lanes 3 and 4). As ubiquitinated Nrf2 proteins are rapidly degraded by the 26S proteosome, MG132 was added to cells prior to cell lysis to enable detection of ubiquitinated forms of Nrf2 (Fig. 6A, compare lanes 1 and 2). Exposure of GCS-2 cells to tBHQ for four hours markedly decreased ubiquitin conjugation onto full length Nrf2 (Fig. 6A, compare lanes 2 and 4). In parallel, a marked increase in ubiquitination of Keap1 was observed (Fig. 6B, compare lanes 2 and 4). In contrast, although sulforaphane completely blocked ubiquitination of Nrf2, no increase in ubiquitin conjugation onto Keap1 was observed (Figs. 6A and 6B, compare lanes 2 and 6). Thus, quinone-induced oxidative stress perturbs the Keap1-Cul3-Rbx1 E3 ubiquitin ligase complex such that Keap1, but not Nrf2, becomes the target for ubiquitin conjugation. Furthermore. This switch in the ubiquitin ligase activity of the Keap1-dependent E3 ubiquitin ligase complex is specific to quinone-induced oxidative stress and not to sulforaphane.

DISCUSSION

BTB-Kelch proteins comprise a large and evolutionarily conserved protein family present in all metazoan organisms, ranging from 5 members in flies to more than 40 family members in humans (18,38). BTB-Kelch proteins are defined by the presence of an N-terminal BTB domain, a central linker domain and a C-terminal Kelch domain. The BTB-Kelch proteins share modest sequence identity, approximately 25%, when compared on a one-to-one basis within the same species. Thus, it has not been clear if these proteins share a common biochemical function or, alternatively, if the conserved domains simply function as protein-protein interaction domains that enable each BTB-Kelch protein to assemble into different macromolecular complexes, each with a unique function. In this report, we demonstrate that four human BTB-Kelch proteins are each able to assemble with Cul3 and Rbx1 into a functional ubiquitin ligase complex capable of autoubiquitination of the BTB-Kelch protein. Our results support the hypothesis that BTB-Kelch proteins share a common biochemical function as substrate adaptor proteins that target specific proteins for ubiquitination.

The biological functions of only a small number of BTB-Kelch proteins have been defined. A unifying theme appears to be the ability of the BTB-Kelch proteins to regulate the formation of actin filaments or other components of the cytoskeleton. Thus, for example, the Kelch protein of *D. melanogaster*, is required for proper cross-linking of actin filaments at ring canals that enable macromolecular transport between the nurse cells and the oocyte during oogenesis (46,47). Mutations in the human GAN1 protein, which are the cause of a sensorimotor neuropathy termed giant axonal neuropathy, result

in the accumulation of disorganized intermediate filaments in affected neurons (48,49). Sarcosin associates with a muscle-specific isoform of N-RAP and may play a role in regulation of myofibril assembly and pseudopod formation in fibroblasts (43,50). In the case of Keap1, an intact actin-based cytoskeleton is required for inhibition of Nrf2-dependent transcription by Keap1 (51). In general, the BTB-Kelch proteins appear to provide critical molecular linkages between cytoskeletal organization and cellular physiology in response to environmental signals. We propose that the ability of BTB-Kelch proteins to function as substrate adaptor proteins for Cul3 is a conserved biochemical function that underlies their diverse biological roles in regulation of the cytoskeleton and cellular physiology.

Under normal conditions of cellular homeostasis, the ability of Keap1 to function as a substrate adaptor for Nrf2 insures that steady-state levels of Nrf2 are maintained at low, nearly undetectable, levels (17). However, perturbation of intracellular homeostasis by a wide variety of chemical compounds, including quinone-induced oxidative stress and sulforaphane, inhibits Keap1-dependent ubiquitination of Nrf2, increases steady-state levels of Nrf2 and activates expression of Nrf2-dependent genes (21). In our previous work, we found that a single cysteine residue in Keap1, Cys 151, is required for inhibition of Keap1-dependent ubiquitination of Nrf2 by both quinone-induced oxidative stress and sulforaphane (21). Furthermore, both agents decreased, but did not abolish, the ability of Keap1 to associate with Cul3 and Rbx1 (21). In these previous experiments, we found that serine substitution of Cys 151 completely abolished responsiveness of Keap1 to sulforaphane. However, the Keap1-C151S protein retained a low level of responsiveness to quinone-induced oxidative stress (24). In our present work, we

demonstrate that ubiquitination of Keap1 is increased by quinone-induced oxidative stress but not by sulforaphane. We find that ubiquitination and subsequent degradation of Keap1 is most pronounced following prolonged exposure of cells to oxidative stress, particularly in glutathione-deficient cells that are highly susceptible to oxidative stress. Serine substitution at Cys 151 does not prevent ubiquitination and degradation of Keap1 in response to quinone-induced oxidative stress (data not shown). Taken together, our results are consistent with a model in which the initial event for inhibition of Keap1 by both quinone-induced oxidative stress and sulforaphane is a chemical modification(s) on Cys 151 that decreases efficient assembly of Nrf2-bound Keap1 into a Cul3-dependent ubiquitin ligase complex. However, prolonged oxidative stress, particularly in cells that are depleted of glutathione, may result in other modifications to Keap1 that expose lysine residues within Keap1 for ubiquitination. Ubiquitination and subsequent degradation of Keap1 may be necessary for accumulation of Nrf2 to levels sufficient for mounting a sustained anti-oxidant counter response. Futhermore, our results point to a critical difference in how damaging (quinone-induced oxidative stress) and beneficial (sulforaphane) agents perturb the substrate adaptor function of Keap1 and suggest the possibility of developing novel chemopreventive agents with minimal deleterious side-effects.

Although the major function of substrate adaptor proteins is to bring specific substrates into cullin-based E3 ubiquitin ligase complexes such that the substrate becomes ubiquitinated, ubiquitination of substrate adaptor proteins is also of functional significance. The importance of substrate adaptor ubiquitination was first suggested by the demonstration that several yeast F-box proteins are ubiquitinated by the same Cul1-

dependent complex that carries out ubiquitination of their substrates (29,30). Alternatively, distinct ubiquitin ligase complexes can direct ubiquitination of specific substrate adaptor proteins (32,33), providing a mechanism for cross-talk between signaling pathways that control different aspects of cellular physiology. In our experiments, we find that ubiquitination of Keap1 is accomplished by the same Cul3-dependent ubiquitin ligase complex that also carries out ubiquitination of Nrf2. As quinone-induced oxidative stress does not dissociate Nrf2 from Keap1, our results suggest that the activity of the Keap1-Cul3-Rbx1 complex is altered such that Keap1, and not Keap1-associated Nrf2, is targeted for ubiquitination by the E2 enzyme that is recruited into the complex by Rbx1. A switch from substrate to substrate adaptor ubiquitination may be a general mechanism for controlling steady-state levels of both the substrate and substrate adaptor proteins.

A puzzling aspect of our results is the nature of cellular proteases that are responsible for degradation of Keap1. There is compelling evidence that the addition of multi-ubiquitin chains, linked through Lys 48 of ubiquitin, onto a protein will target it for degradation by the 26S proteosome (25). Keap1-dependent ubiquitination of Nrf2 results in degradation of Nrf2 by the proteosome, as inhibitors of the proteosome markedly increase steady-state levels of Nrf2 in the presence of Keap1. Indeed, Keap1-dependent multi-ubiquitination of Nrf2 does occur on Lys-48, although other lysine residues in ubiquitin can also be used (data not shown). In contrast, multi-ubiquitination onto Keap1 appears to require Lys-63 in ubiquitin. A second difference between Keap1 and Nrf2 is that proteosome inhibitors do not restore steady-state levels of either mutant Keap1 proteins that are highly ubiquitinated or of the wild-type Keap1 protein in cells exposed

to oxidative stress. In contrast, proteosome inhibitors are effective inhibitors of Nrf2 degradation. Our results suggest that degradation of Keap1 may not be accomplished by the 26S proteosome. Eukaryote cells contain a number of other proteolytic systems in addition to the proteosome. For example, a recent report has suggested that ubiquitination of the transcription factor c-Jun may target c-Jun for degradation by the lysosome (52). Our results, which indicate that degradation of ubiquitinated Keap1 is independent of the 26S proteosome, are consistent with the hypothesis that the nature of the ubiquitin linkage on protein-ubiquitin conjugates can target proteins for proteosome-independent degradative pathways. Our current work is focused on defining the nature of molecular signals that target Keap1 and other BTB-Kelch proteins for proteosome-independent degradation.

This chapter was reproduced with the expressed written permission of the American Society for Biochemistry and Molecular Biology.
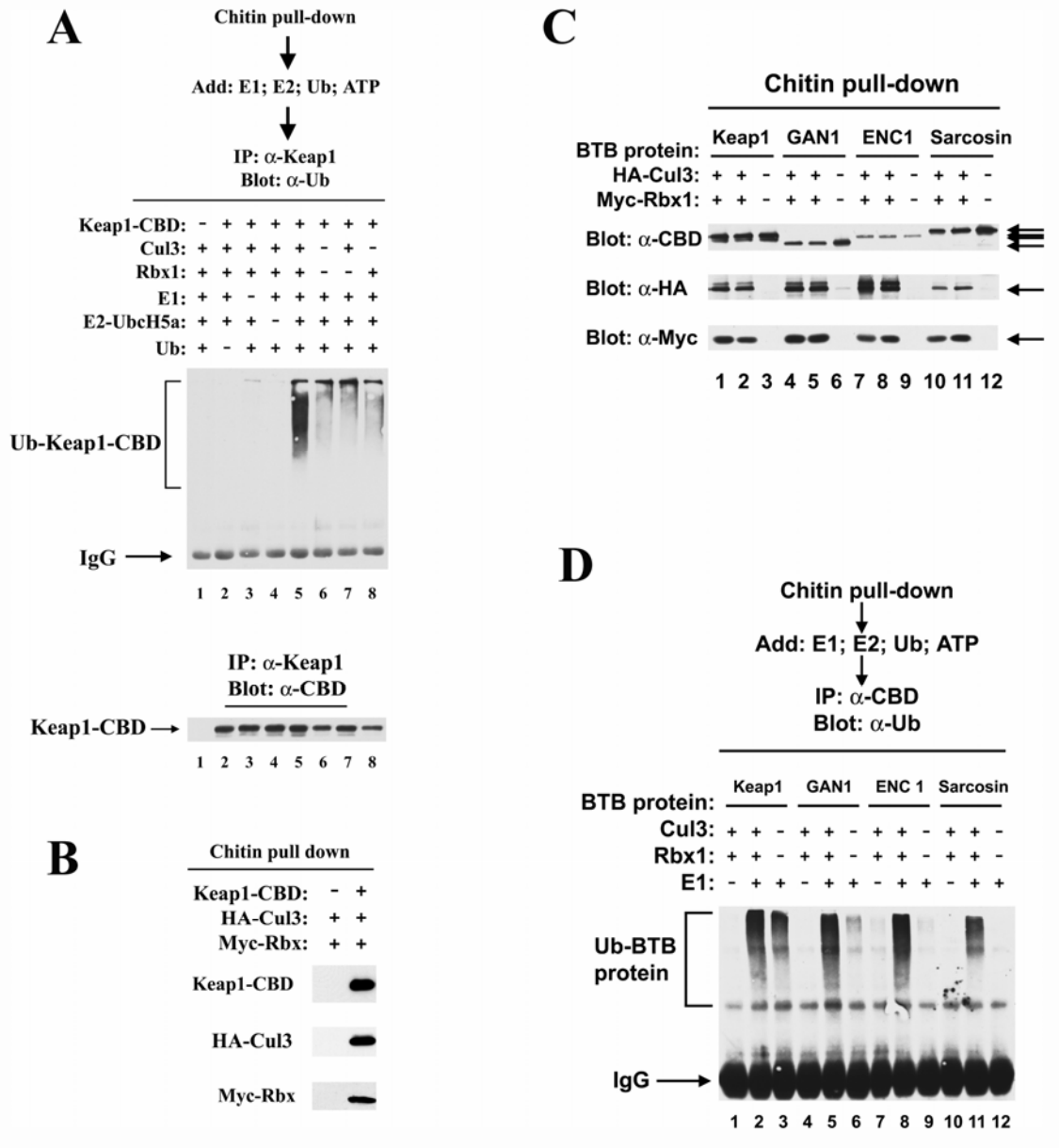
Figure III-1

Figure III-1. Autoubiquitination is a key feature for BTB-Kelch proteins that assemble into Cul3-RING ligase complexes. (A). Cell lysates from COS1 cells transfected with expression vectors for Keap1-CBD, HA-Cul3 and Myc-Rbx1 were incubated with chitin beads. Proteins bound to chitin beads were incubated with E1, E2-UbcH5a, ubiquitin and ATP. Following the reaction, proteins were eluted from the chitin beads by boiling and equivalent aliquots of the eluted proteins were either subjected to immunoblot analysis with anti-CBD antibodies (bottom panel), or immunoprecipitated with anti-Keap1 antibodies (top panel). The anti-Keap1 immunoprecipitates were subject to immunoblot analysis with anti-ubiquitin antibodies. (B) Cell lysates from COS1 cells transfected with expression vectors for Keap1-CBD, HA-Cul3 and Myc-Rbx1 were incubated with chitin beads. Proteins bound to chitin beads were analyzed by immunoblot analysis for Keap1 (top panel), HA-Cul3 (middle panel) or Myc-Rbx1 (bottom panel). (C) COS1 cells were co-transfected with CBD-tagged expression vectors for Keap1, GAN1, ENC1, or sarcosin, along with expression vectors for HA-Cul3 and Myc-Rbx1. Cell lysates were incubated with chitin beads. Proteins that associated with the chitin beads were eluted and analyzed by immunoblot with anti-CBD, anti-HA, and anti-Myc antibodies. (D) A portion of the chitin beads from (B) were incubated with E1, E2-UbvH5a, ubiquitin, and ATP. The reactions were terminated by boiling and subjected to immunoprecipitation with anti-CBD antibodies. Anti-CBD immunoprecipitates were analyzed by immunoblot with anti-ubiquitin antibodies.
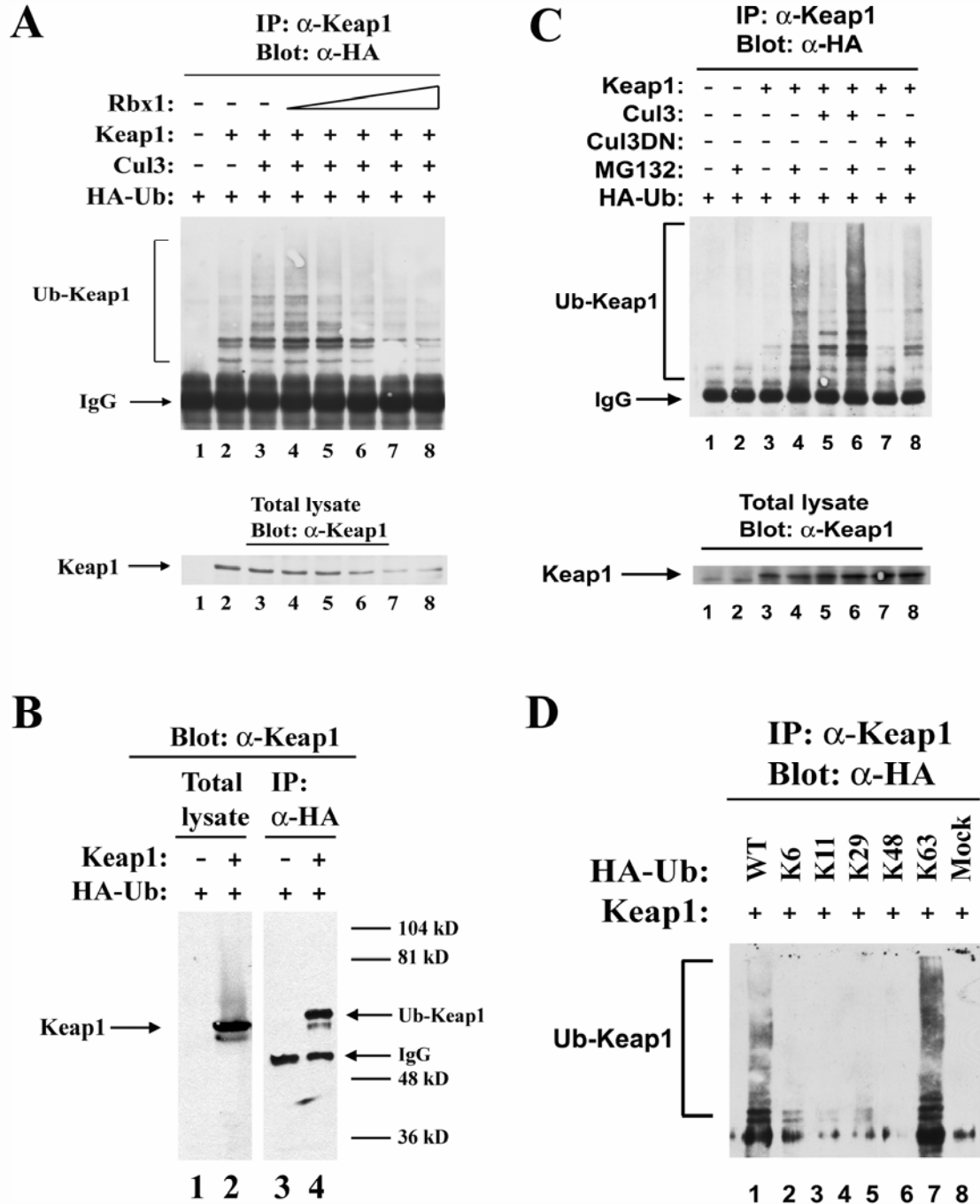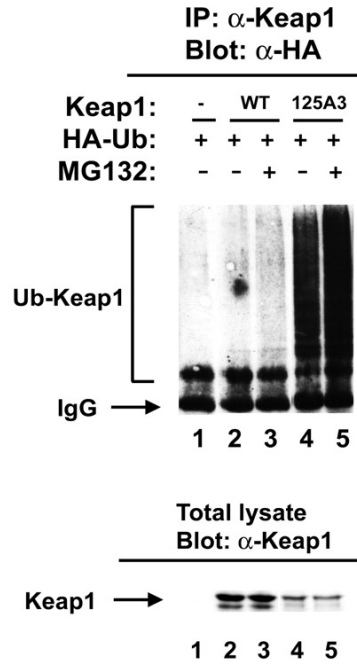
Figure III-2

Figure III-2. Autoubiquitination of Keap1 by a Cul3-Rbx1 subcomplex. (A) MDA-MB-231 cells were transfected with expression vectors for HA-ubiquitin, Keap1, and HA-Cul3 and increasing amounts of an expression vector for Rbx1. Cells were lysed under denaturing conditions and subjected to immunoblot analysis with Keap1 antibodies (bottom panel). Equivalent aliquots of each lysates were subjected to immunoprecipitation with anti-Keap1 antibodies. Anti-Keap1 immunoprecipitates were analyzed by immunoblot with anti-HA antibodies (top panel). (B) 293T cells were transfected with expression vectors for HA-ubiquitin and Keap1. Total lysates (left panel) or anti-HA immunoprecipitates (right panel) were analyzed by immunoblot with anti-Keap1 antibodies. The samples were analyzed in parallel on adjacent lanes. The left panel was exposed for a shorter time than the right panel. (C) MDA-MB-231 cells were transfected with expression vectors for HA-ubiquitin and Keap1, and the expression vector for either Cul3 or Cul3DN. Cells were either left untreated or treated with 10μM MG132 for 4 hours prior to lysis. Equivalent aliquots of each lysates were analyzed by immunoblot with anti-Keap1 antibodies (bottom panel) or subjected to immunoprecipitation with anti-Keap1 antibodies. Anti-Keap1 immunoprecipitates were analyzed by immunoblot with anti-HA antibodies (top panel). (D) Cell lysates from MDA-MB-231 cells transfected with expression vectors for Keap1 and the indicated wild-type or mutant HA-ubiquitin proteins were immunoprecipitated with anti-Keap1 antibodies. The immunoprecipitated proteins were analyzed by immunoblot with anti-HA antibodies.

Figure III-3

Figure III-3. Increased ubiquitination results in proteasome-independent degradation of Keap1. (A) MDA-MB-231 cells were transfected with expression vectors for either wild type or mutant Keap1 proteins and expression vectors for HA-ubiquitin. Cells were either left untreated or treated with MG132. Cells were lysed under the denaturing condition and equivalent aliquots were subjected to immunoblot analysis with anti-Keap1 antibodies (bottom panel) or to immunoprecipitation with anti-Keap1 antibodies (top panel). Anti-Keap1 immunoprecipitates were analyzed by immunoblot with anti-HA antibodies (top panel). (B) MDA-MB-231 cells transfected with expression vectors for either wild type or mutant Keap1 proteins were treated with DMSO, 2-Leu-Leu-Leu-B(OH)2 (1μM), Clasto-lactacystin- -lactone (10μM), or expoxomicin (1μM) for 4 hours prior to collection of cell lysates. Equivalent amounts of each cell lysate were analyzed by immunoblot with anti-Keap1 antibodies (top panel). The blot was stripped and reprobed with anti-tubulin antibodies (bottom panel).

Figure III-4

Figure III-4. Quinone-induced oxidative stress increases ubiquitination and turnover of Keap1. (A) MDA-MB-231 cells were transfected with expression vectors for HA-ubiquitin and Keap1. As indicated, the transfected cells were exposed to DMSO, 10μM Leptomycin B (LMB), 50μM tBHQ or 20 μM sulforaphane for 6 h or 16 h prior to cell lysis. Equivalent aliquots of cell lysates were subjected to immunoblot analysis with anti-Keap1 antibodies (bottom panel) or immunoprecipitated with anti-Keap1 antibodies. Anti-Keap1 immunoprecip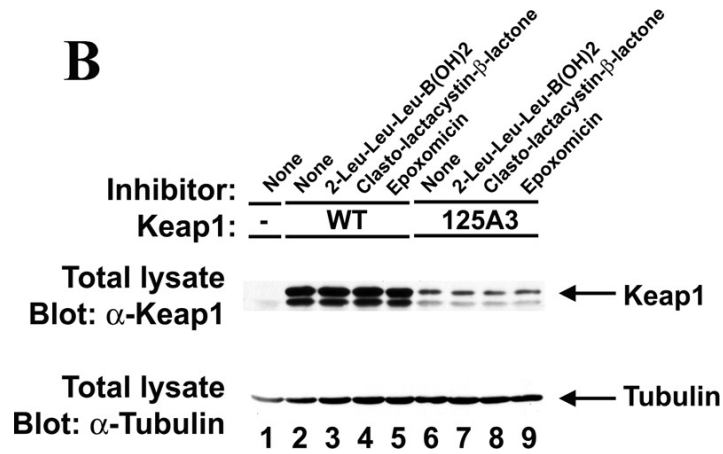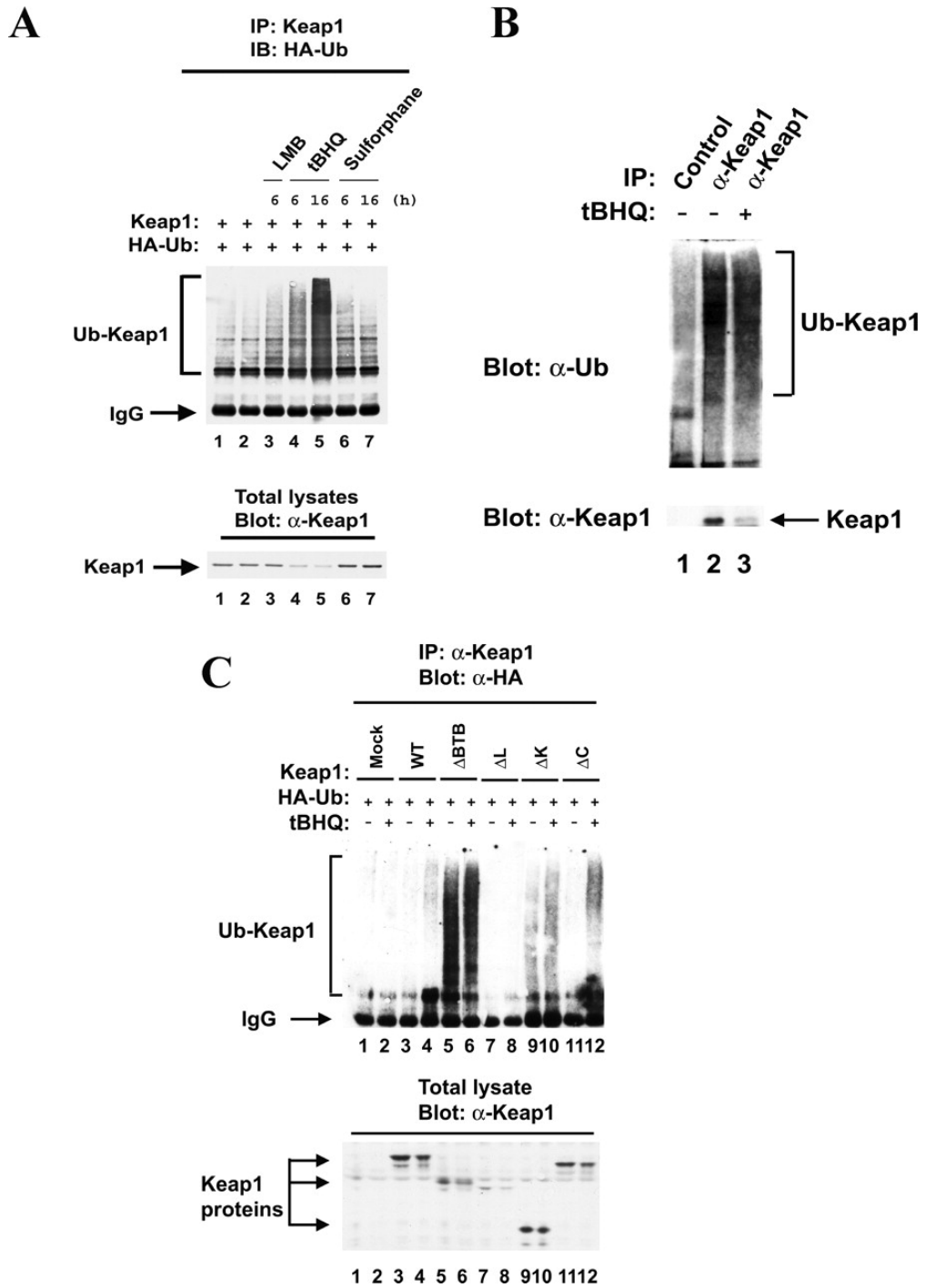itates were analyzed by immunoblot with anti-HA antibodies (top panel). (B) MDA-MB-231 cells were either left untreated or treated with 50μM tBHQ for 16 h prior to lysis under denaturing conditions. Equivalent amounts of cell lysates were immunoprecipitated with either anti-HA or anti-Keap1 antibodies conjugated to sepharose beads. The immunoprecipitated proteins were subjected to immunoblot analysis with anti-ubiquitin antibodies for detection of endogenous Keap1-ubiquitin conjugates (upper panel). The blot was stripped and re-probed with anti-Keap1 antibodies to detect levels of Keap1 (bottom panel). (C) MDA-MB-231 cells were transfected with expression vectors for HA-ubiquitin and the wild-type or mutant Keap1 proteins. The transfected cells were either left untreated or treated with 50μM tBHQ overnight prior to lysis under denaturing conditions. Equivalent aliquots of each lysate were subjected to immunoblot analysis with anti-Keap1 antibodies (bottom panel) or immunoprecipitation with anti-Keap1 antibodies. Anti-Keap1 immunoprecipitates were analyzed by immunoblot with anti-HA antibodies (top panel).

Figure III-5
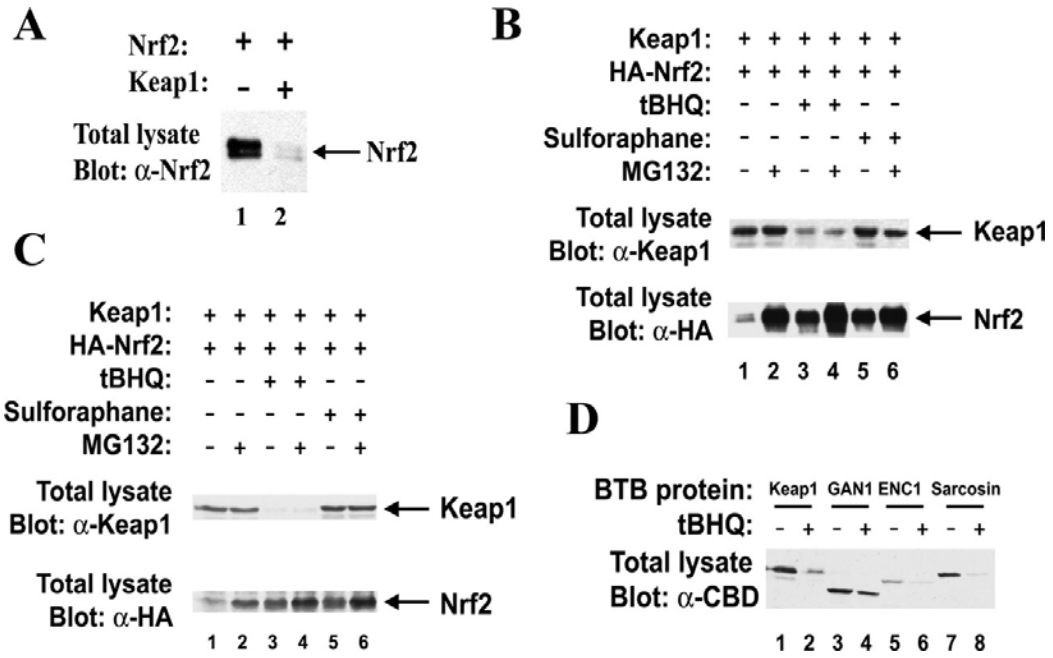
Figure III-5. Quinone-induced degradation of Keap1 is enhanced in cells deficient in glutathione biosynthesis. (A) Cell lysates from GCS-2 cells transfected with expression vectors for Keap1 and HA-Nrf2 were analyzed by immunoblot with anti-Nrf2 antibodies. (B) and (C) GCS-2 cells transfected with expression vectors for Keap1 and HA-Nrf2 were treated with either DMSO, 50μM tBHQ, or 20μM sulforaphane for 4 h (B) or 16 h (C). The cells were either left untreated or treated with 10μM MG132 for 4 h prior to cell lysis. Equivalent amounts of cell lysates were subjected to immunoblot analysis with anti-Keap1 antibodies (top panels) and anti-HA antibodies (bottom panels). (D) GCS-2 cells transfected with expression vectors for Keap1-CBD, GAN1-CBD, ENC1-CBD, or sarcosin-CBD were either left untreated or treated with 50μM tBHQ for 16 h. Equivalent amounts of cell lysates were subjected to immunoblot analysis with anti-CBD antibodies.

Figure III-6
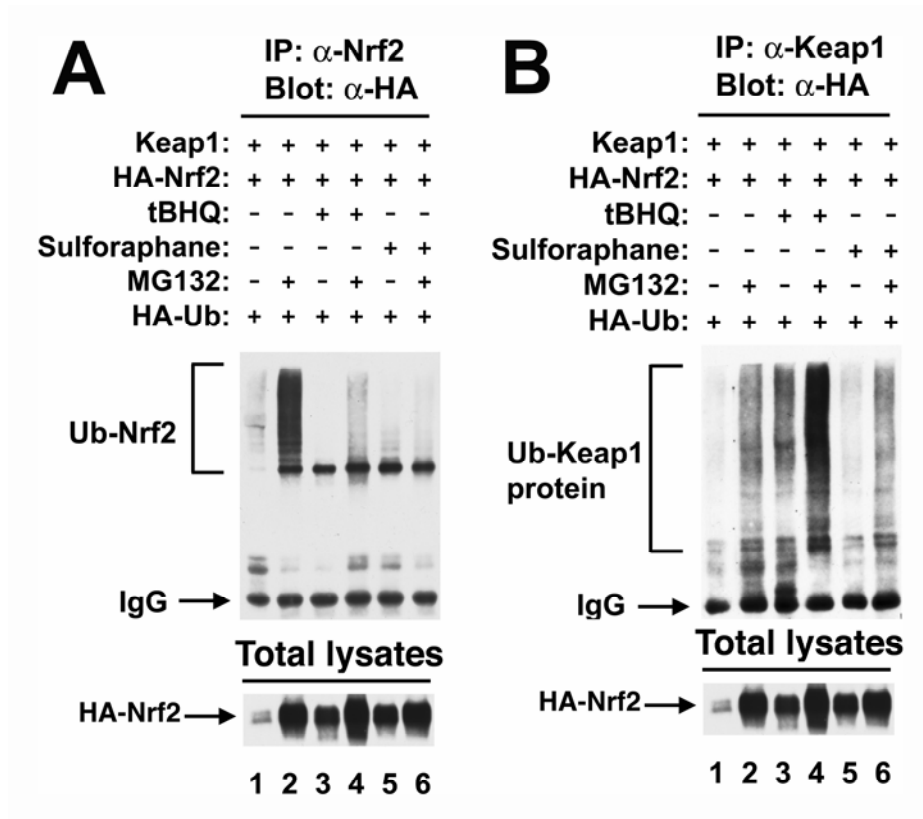
Figure III-6. Quinone-induced oxidative stress induces a switch in ubiquitination from substrate to substrate adaptor. GCS-2 cells were transfected with expression vectors for HA-ubiqutitin, HA-Nrf2, or Keap1. The cells were treated with DMSO, 50μM tBHQ, 20μM sulforaphane or 10μM MG132 for 4 h prior to cell lysis, as indicated. Lysates were collected under denaturing conditions and equivalent amounts of each cell lysate were immunoprecipitated with anti-Nrf2 antibodies (A) or with anti-Keap1 antibodies (B). The anti-Nrf2 and anti-Keap1 immunoprecipitates were analyzed by immunoblot with anti-HA antibodies.

REFERENCES

1.   Ames, B. N., and Shigenaga, M. K. (1993) in *Oxidants are a major contributor to cancer and aging* (Halliwell, B., and Aruoma, O. I., eds), pp. 1-15, Ellis Horwood, New York, NY
2.   Andreassi, M. G. (2003) *Mutat Res* **543**, 67-86
3.   Butterfield, D. A., Howard, B. J., and LaFontaine, M. A. (2001) *Curr Med Chem* **8**, 815-828
4.   Golden, T. R., Hinerfeld, D. A., and Melov, S. (2002) *Aging Cell* **1**, 117-123
5.   Rao, A. V., and Balachandran, B. (2002) *Nutr Neurosci* **5**, 291-309
6.   Kwak, M. K., Wakabayashi, N., Itoh, K., Motohashi, H., Yamamoto, M., and Kensler, T. W. (2003) *J Biol Chem* **278**, 8135-8145
7.   Thimmulappa, R. K., Mai, K. H., Srisuma, S., Kensler, T. W., Yamamoto, M., and Biswal, S. (2002) *Cancer Res* **62**, 5196-5203
8.   Nguyen, T., Sherratt, P. J., and Pickett, C. B. (2003) *Annu Rev Pharmacol Toxicol* **43**, 233-260
9.   Jaiswal, A. K. (2004) *Free Radic Biol Med* **36**, 1199-1207
10.   Ishii, T., Itoh, K., Takahashi, S., Sato, H., Yanagawa, T., Katoh, Y., Bannai, S., and Yamamoto, M. (2000) *J Biol Chem* **275**, 16023-16029
11.   Alam, J., Wicks, C., Stewart, D., Gong, P., Touchard, C., Otterbein, S., Choi, A. M., Burow, M. E., and Tou, J. (2000) *J Biol Chem* **275**, 27694-27702
12.   Dinkova-Kostova, A. T., Massiah, M. A., Bozak, R. E., Hicks, R. J., and Talalay, P. (2001) *Proc Natl Acad Sci U S A* **98**, 3404-3409
13.   Ramos-Gomez, M., Kwak, M.-K., Dolan, P. M., Itoh, K., Yamamoto, M., Talalay, P., and Kensler, T. W. (2001) *Proc. Nat. Acad. Sci USA* **98**, 3410-3415
14.   Talalay, P., and Fahey, J. W. (2001) *J Nutr* **131**, 3027S-3033S
15.   Itoh, K., Wakabayashi, N., Katoh, Y., Ishii, T., Igarashi, K., Engel, J. D., and Yamamoto, M. (1999) *Genes Dev* **13**, 76-86
16.   Dhakshinamoorthy, S., and Jaiswal, A. K. (2001) *Oncogene* **20**, 3906-3917
17.   Wakabayashi, N., Itoh, K., Wakabayashi, J., Motohashi, H., Noda, S., Takahashi, S., Imakado, S., Kotsuji, T., Otsuka, F., Roop, D. R., Harada, T., Engel, J. D., and Yamamoto, M. (2003) *Nat Genet*
18.   Prag, S., and Adams, J. C. (2003) *BMC Bioinformatics* **4**, 42
19.   Cullinan, S. B., Gordan, J. D., Jin, J., Harper, J. W., and Diehl, J. A. (2004) *Mol Cell Biol* **24**, 8477-8486
20.   Kobayashi, A., Kang, M. I., Okawa, H., Ohtsuji, M., Zenke, Y., Chiba, T., Igarashi, K., and Yamamoto, M. (2004) *Mol Cell Biol* **24**, 7130-7139
21.   Zhang, D. D., Lo, S. C., Cross, J. V., Templeton, D. J., and Hannink, M. (2004) *Mol Cell Biol* **24**, 10941-10953
22.   Furukawa, M., and Xiong, Y. (2005) *Mol Cell Biol* **25**, 162-171
23.   Li, X., Zhang, D., Hannink, M., and Beamer, L. J. (2004) *J Biol Chem* **279**, 54750-54758
24.   Zhang, D. D., and Hannink, M. (2003) *Mol Cell Biol* **23**, 8137-8151
25.   Pickart, C. M. (2001) *Annu Rev Biochem* **70**, 503-533

26. Deshaies, R. J. (1999) *Annu Rev Cell Dev Biol* **15**, 435-467
27. Cope, G. A., and Deshaies, R. J. (2003) *Cell* **114**, 663-671
28. Wolf, D. A., Zhou, C., and Wee, S. (2003) *Nat Cell Biol* **5**, 1029-1033
29. Galan, J. M., and Peter, M. (1999) *Proc Natl Acad Sci U S A* **96**, 9124-9129
30. Zhou, P., and Howley, P. M. (1998) *Mol Cell* **2**, 571-580
31. Li, Y., Gazdoiu, S., Pan, Z. Q., and Fuchs, S. Y. (2004) *J Biol Chem* **279**, 11074-11080
32. Bashir, T., Dorrello, N. V., Amador, V., Guardavaccaro, D., and Pagano, M. (2004) *Nature* **428**, 190-193
33. Wei, W., Ayad, N. G., Wan, Y., Zhang, G. J., Kirschner, M. W., and Kaelin, W. G., Jr. (2004) *Nature* **428**, 194-198
34. Wirbelauer, C., Sutterluty, H., Blondel, M., Gstaiger, M., Peter, M., Reymond, F., and Krek, W. (2000) *Embo J* **19**, 5362-5375
35. Liu, J., Furukawa, M., Matsumoto, T., and Xiong, Y. (2002) *Mol Cell* **10**, 1511-1518
36. Zheng, J., Yang, X., Harrell, J. M., Ryzhikov, S., Shim, E. H., Lykke-Andersen, K., Wei, N., Sun, H., Kobayashi, R., and Zhang, H. (2002) *Mol Cell* **10**, 1519-1526
37. Shi, Z. Z., Osei-Frimpong, J., Kala, G., Kala, S. V., Barrios, R. J., Habib, G. M., Lukin, D. J., Danney, C. M., Matzuk, M. M., and Lieberman, M. W. (2000) *Proc Natl Acad Sci U S A* **97**, 5101-5106
38. Stogios, P. J., and Prive, G. G. (2004) *Trends Biochem Sci* **29**, 634-637
39. Bomont, P., Cavalier, L., Blondeau, F., Ben Hamida, C., Belal, S., Tazir, M., Demir, E., Topaloglu, H., Korinthenberg, R., Tuysuz, B., Landrieu, P., Hentati, F., and Koenig, M. (2000) *Nat Genet* **26**, 370-374
40. Cullen, V. C., Brownlees, J., Banner, S., Anderton, B. H., Leigh, P. N., Shaw, C. E., and Miller, C. C. (2004) *Neuroreport* **15**, 873-876
41. Liang, X.-Q., Avraham, H. K., Jiang, S., and Avraham, S. (2004) *Oncogene* **23**, 5890-5990
42. Fujita, M., Furukawa, Y., Tsunoda, T., Tanaka, T., Ogawa, M., and Nakamura, Y. (2001) *Cancer Res* **61**, 7722-7726
43. Spence, H. J., Johnston, I., Ewart, K., Buchanan, S. J., Fitzgerald, U., and Ozanne, B. W. (2000) *Oncogene* **19**, 1266-1276
44. Suh, J. H., Shenvi, S. V., Dixon, B. M., Liu, H., Jaiswal, A. K., Liu, R. M., and Hagen, T. M. (2004) *Proc Natl Acad Sci U S A* **101**, 3381-3386
45. Sekhar, K. R., Crooks, P. A., Sonar, V. N., Friedman, D. B., Chan, J. Y., Meredith, M. J., Starnes, J. H., Kelton, K. R., Summar, S. R., Sasi, S., and Freeman, M. L. (2003) *Cancer Res* **63**, 5636-5645
46. Robinson, D. N., and Cooley, L. (1997) *J Cell Biol* **138**, 799-810
47. Kelso, R. J., Hudson, A. M., and Cooley, L. (2002) *J Cell Biol* **156**, 703-713
48. Bomont, P., and Koenig, M. (2003) *Hum Mol Genet* **12**, 813-822
49. Bruno, C., Bertini, E., Federico, A., Tonoli, E., Lispi, M. L., Cassandrini, D., Pedemonte, M., Santorelli, F. M., Filocamo, M., Dotti, M. T., Schenone, A., Malandrini, A., and Minetti, C. (2004) *Neurology* **62**, 13-16
50. Lu, S., Carroll, S. L., Herrera, A. H., Ozanne, B., and Horowits, R. (2003) *J Cell Sci* **116**, 2169-2178

51. Kang, M. I., Kobayashi, A., Wakabayashi, N., Kim, S. G., and Yamamoto, M. (2004) *Proc Natl Acad Sci U S A* **101**, 2046-2051
52. Fang, D., and Kerppola, T. K. (2004) *Proc Natl Acad Sci U S A* **101**, 14782-14787
53. Schnell, J. D., and Hicke, L. (2003) *J Biol Chem* **278**, 35857-35860
54. Conaway, R. C., Brower, C. S., and Conaway, J. W. (2002) *Science* **296**, 1254-1258
55. Pickart, C. M. (2001) *Mol Cell* **8**, 499-504

IV. CAND1-mediated substrate adaptor recycling is required for efficient repression of Nrf2 by Keap1.

ABSTRACT

The bZIP transcription factor Nrf2 controls a genetic program that protects cells from oxidative damage and maintains cellular redox homeostasis. Keap1, a BTB-Kelch protein, is the major upstream regulator of Nrf2. Keap1 functions as a substrate adaptor protein for a Cul3-dependent E3 ubiquitin ligase complex to repress steady-state levels of Nrf2 and Nrf2-dependent transcription. Cullin-dependent ubiquitin ligase complexes have been proposed to undergo dynamic cycles of assembly and disassembly that enable substrate adaptor exchange or recycling. In this report, we have characterized the importance of substrate adaptor recycling for regulation of Keap1-mediated repression of Nrf2. Assocation of Keap1 with Cul3 was decreased by ectopic expression of CAND1 and was increased by siRNA-mediated knockdown of CAND1. However, both ectopic overexpression and siRNA-mediated knockdown of CAND1 decreased the ability of Keap1 to target Nrf2 for ubiquitin-dependent degradation, resulting in stabilization of Nrf2 and activation of Nrf2-dependent gene expression. Neddylation of Cul3 on Lys 712 is required for Keap1-dependent ubiquitination of Nrf2 in vivo. However, the K712R mutant Cul3 molecule, which is not neddylated, can still assemble with Keap1 into a functional ubiquitin ligase complex in vitro. These results provide support for a model in which substrate adaptor recycling is required for efficient substrate ubiquitination by cullin-dependent E3 ubiquitin ligase complexes.

INTRODUCTION

Exposure of cells to reactive molecules, including reactive oxygen species and other chemically reactive compounds, can damage cellular macromolecules and compromise cellular functions (1, 2, 16, 20, 47). The coordinated induction of phase 2 genes provides an efficient mechanism for mammalian cells to neutralize reactive molecules, eliminate damaged macromolecules and restore cellular redox homeostasis (8, 22, 26, 33). Transcription of phase 2 genes is controlled, in large part, by the Nrf2 transcription factor (22, 33). The ability of Nrf2 to accumulate in the nucleus and bind DNA appears to be the rate-limiting step that controls expression of phase 2 genes.

Nrf2 is a member of the CNC subfamily of bZIP transcription factors (32). Nrf2 contains a N-terminal regulatory domain (Neh2), a central transactivation domain, and a C-terminal bZIP domain that is responsible for both nuclear localization and DNA-binding. The major upstream regulator of Nrf2 is a BTB-Kelch protein termed Keap1, which binds the Neh2 regulatory domain of Nrf2 via loops that extend out from the bottom face of the Kelch β-propellor domain (21, 27). Keap1 was initially regarded as a protein that sequestered Nrf2 in the cytoplasm (21). Subsequent work has revealed that Keap1 functions as a substrate adaptor protein for a Cul3-dependent E3 ubiquitin ligase that targets lysine residues within the Neh2 domain for ubiquitin conjugation (7, 14, 25, 26, 43). Ubiquitin conjugation onto specific N-terminal lysine residues marks Nrf2 for degradation by the 26S proteosome, such that Nrf2 is maintained at low steady-state levels under basal conditions (43). However, upon exposure to oxidative stress and reactive molecules, Nrf2 is no longer targeted for ubiquitin-dependent degradation (42, 43). Instead, Nrf2 accumulates in the nucleus and activates expression of phase 2 genes.

Cullin-dependent ubiquitin ligases are assembled around a common core complex consisting of one of six cullin proteins and a common RING finger protein, Rbx1 (also known as Roc1) (35). This core complex is used by a large number of substrate adaptor proteins that bring in specific substrates. Substrate adaptor proteins are modular in nature, having one domain that binds to the cullin protein and another domain that binds to small number of specific substrate proteins. These two modules can be encoded by two different polypeptides, as in the case of the Skp1/F-box protein complexes that are substrate adaptors for Cul1. Alternatively, as exemplified by Keap1, a substrate adaptor for Cul3, these two domains can be encoded by a single polypeptide.

A model that describes how Cullin-dependent ubiquitin ligases may be regulated by cycles of assembly and disassembly has been proposed (5). A central feature of this model is that the Cullin-Rbx1 core complex cycles between active and inactive states. The active complex contains a substrate adaptor protein with its bound substrate docked at the N-terminus of the Cullin protein. In this active complex, the Cullin protein is modified by Nedd8 conjugation on a conserved lysine residue (Lys 712 in Cul3). An ubiquitin-loaded E2 protein is recruited into the complex via protein-protein interactions with the Rbx1 subunit (9). The conjugated Nedd8 polypeptide may also facilitate E2 recruitment (24). The model proposes that the active complex is converted to an inactive complex in two steps. The first step is removal of the Nedd8 protein from the Cullin protein by one or more deneddylases, such as the CSN5 subunit of the COP9 signalosome (CSN) (6, 15, 29, 40). The second step is the association of a protein known as CAND1 (also termed TIP120A) with the deneddylated Cullin protein (17, 28, 45). CAND1 binds to both N-terminal and C-terminal sequences in Cul1, and blocks binding

of the substrate adaptor protein (17, 19, 28, 30, 45). Subsequent conjugation of Nedd8 onto the Cullin subunit by Ubc12, a Nedd8-specific E2 enzyme (5), is proposed to decrease the affinity of CAND1 for the Cullin protein, enabling another substrate adaptor protein (presumably with its bound substrate) to displace CAND1 and initiate another cycle of substrate ubiquitination (5, 35). A recent crystal structure of the CAND1:Cul1 complex, which showed that Lys 720 in Cul1 is located at the CAND1:Cul1 interface, has provided support for the notion that neddylation of Cul1 and binding of CAND1 are antagonistic (17). However, it is not clear if CAND1 is a global regulator of all cullin-dependent ubiquitin ligase complexes (28, 30, 45).

Regulation of cullin-dependent ubiquitin ligases by cycles of assembly and disassembly provides an attractive paradigm for considering how substrate adaptor proteins target their specific substrates for ubiquitin-dependent degradation. In the case of Keap1, we have proposed that cycles of assembly and disassembly of the Keap1:Cul3:Rbx1 complex allow Keap1 to act in a catalytic manner to efficiently target Nrf2 for degradation (43). To test this hypothesis, we have examined the role of CAND1 in Keap1-dependent ubiquitination of Nrf2. Our results indicate that CAND1-dependent substrate adaptor recycling is required for efficient repression of Nrf2 by Keap1 and support the notion that CAND1 is a global regulator of cullin-dependent ubiquitin ligases.

MATERIALS AND METHODS

Construction of recombinant DNA molecules. Plasmids expressing wild type Keap1, CBD-tagged Keap1, Nrf2, wild type Cul3, CBD-tagged GAN and sarcosin proteins have been previously described (43, 44). Mutant Cul3 cDNAs were generated by site-specific mutagenesis with standard overlap-extension techniques. The myc-Rbx1 expression vector was a gift from Dr. Joan Conaway (23). The Flag-CAND1 expression vector was a gift from Dr. Cecile M. Pickart (41). All the genes used in this study were sequenced in the context of the expression vectors used for the experiments.

Cell culture, transfections, and reporter gene assays. COS1, MDA-MB-231 and Hela cells were purchased from ATCC. CHO-K1 cells were obtained from Dr. Toshihiko Ezashi. The ts41 cells were obtained from Dr. Chuck Sherr. Cells were maintained in either Dulbecco's modified Eagle's medium (DMEM), Eagle's minimal essential medium (EMEM), or HAM's F-12 in the presence of 10% fetal bovine serum (FBS). Transfections of plasmid DNAs were performed with Lipofectamine Plus (Gibco BRL) according to the manufacturer's instructions. Transfections of siRNA nucleotides were performed with Oligofectamine^{TM} (Invitrogen) according to the manufacturer's instructions. All the siRNA nucleotides used in this study were obtained from Dharmacon as purified and annealed duplexes. The ARE TATA-Inr luciferase reporter plasmid pARE-Luc and a control plasmid encoding *Renilla* luciferase for transfection efficiency have been previously described (42). Reporter gene assays were performed using the Promega Dual-Light assay system as previously described (42).

Antibodies, immuprecipitation, and immunoblot analysis. The anti-Keap1 antibody has been described (42). Antibodies against Nrf2 (Santa Cruz), CAND1 (Santa Cruz),

Tubulin (Santa Cruz), Chitin binding domain (New England Biolabs), the Flag epitope (Sigma), the myc epitope (Santa Cruz), and the HA epitope (Covance) were purchased from commercial sources.

For detection of protein expression in total cell lysates, cells were lysed in sample buffer (50 mM Tris-HCl pH [6.8], 2% SDS, 10% Glycerol, 100 mM DTT, 0.1% bromophenol blue) at 24 to 48 hr post-transfection. For immunoprecipitation assays, cell extracts were prepared in lysis buffer (50 mM Hepes pH [7.9], 250 mM NaCl, 5 mM EDTA, 0.1% Triton X-100) containing 1 mM dithiothreitol (DTT), 1 mM phenylmethylsulfonyl fluoride (PMSF) and protease inhibitor cocktail (Sigma). In some cases, 10 mM N-ethylmaleimide (NEM) was included in the lysis solution to inactivate ubiquitin and nedd8 hydrolase activities. Soluble cell lysates were incubated with 2 μg of affinity-purified antibodies for 2 hr at 4°C, followed by incubation at 4°C with protein A-agarose beads (Sigma) for 2 hr. Unbound proteins were removed by washing four times with lysis buffer. The immunoprecipitated proteins were eluted in sample buffer by boiling for 5 minutes, electrophoresed through SDS-polyacrylamide gels, transferred to nitrocellulose membranes and subjected to immunoblot analysis.

In vivo ubiquitination assay. For detection of ubiquitinated Nrf2 proteins in vivo, cells were transfected with expression vectors for HA-tagged ubiquitin, Gal4-Neh2, and the indicated proteins. Cells were lysed by boiling in a buffer containing 2% SDS, 10 mM N-ethylmaleimide (NEM), 150 mM NaCl and 10 mM Tris-HCl pH [8.0]. This rapid lysis procedure inactivates cellular ubiquitin hydrolases and therefore preserves ubiquitin-substrate protein conjugates present in cells prior to lysis. Protein-protein interactions, including association of Nrf2 with Keap1, are also disrupted by this lysis procedure. For

179

immunoprecipitation, these lysates were diluted with 4 volumes of a buffer containing 150 mM NaCl, 10 mM Tris-HCl pH [8.0], 1 mM DTT and 1% Triton X-100. The diluted lysates were pre-cleared with protein A-agarose beads (Sigma) and incubated with 2 μg of anti-Gal4 antibodies. HA-ubiquitin conjugates in immunoprecipitated Gal4-Neh2 proteins were analyzed by immunoblot analysis with antibodies against the HA epitope.

In vitro ubiquitination assay. For detection of ubiquitinated Nrf2 and Keap1 proteins in vitro, cells were transfected with expression vectors for HA-Nrf2, Keap1-CBD, myc-Rbx1, and the wild-type or mutant HA-Cul3 proteins. Cells were lysed in buffer B (15 mM Tris-HCl pH [7.5], 500 mM NaCl, 0.25% NP-40) containing 1 mM dithiothreitol (DTT), 1 mM phenylmethylsulfonyl fluoride (PMSF) and protease inhibitor cocktail (Sigma). The lysates were pre-cleared with protein A-agarose beads prior to incubation with chitin beads (New England Biolabs) for four hours at 4 ^{o}C. Chitin beads were washed twice with buffer B, twice with buffer A (25 mM Tris-HCl [pH 7.5], 10% (v/v) glycerol, 1 mM EDTA, 0.01% NP-40 and 100 mM NaCl), and twice with reaction buffer (50 mM Tris-HCl [pH 7.5], 5 mM MgCl$_2$, 2 mM NaF, 0.6 mM DTT). The pellets were incubated with ubiquitin (300 pmol), E1 (2 pmol), E2-UbcH5a (10 pmol), and ATP (2 mM) in 1 x reaction buffer in a total volume of 30 μl for 1 hr at 37 ^{o}C. Ubiquitin, E1 and E2-UbcH5a were purchased from Boston Biochem. The chitin beads were pelleted by centrifugation (3,000 x g) and resuspended in 2% SDS, 150 mM NaCl, 10 mM Tris-HCl (pH8.0) and 1 mM DTT and boiled for 5 min to release bound proteins, inactivate any contaminating ubiquitin hydrolases and disrupt protein-protein interactions. The supernatant was diluted fivefold with buffer lacking SDS prior to immunoprecipitation

with anti-Nrf2 or anti-Keap1 antibodies. Immunoprecipitated proteins were subjected to

immunoblot analysis with anti-ubiquitin antibodies (Sigma).

RESULTS

CAND1 competes with Keap1 for binding to Cul3. To determine if CAND1 functions as a regulator of Keap1-dependent ubiquitination of Nrf2, we first determined the ability of CAND1 to associate with Cul3. COS1 cells were transfected with expression vectors for FLAG-tagged CAND1 and HA-tagged Cul3. Association between CAND1 and Cul3 was assessed by co-immunoprecipitation of cell lysates. The HA-tagged Cul3 protein was readily detected in anti-FLAG immunoprecipitates from co-transfected cells but not from singly-transfected cells (Fig. 1A, top panel, lane 3). Similarly, the FLAG-tagged CAND1 protein was only observed in anti-HA immunoprecipitates from co-transfected cells (Fig. 1A, second panel from top, lane 3). These results are consistent with the results reported by Min et al indicating the CAND1 is able to associate with several different human cullin proteins, including Cul3 (30).

CAND1 has been proposed to sequester the Cul1 protein in an inactive form that is unable to bind substrate adaptor proteins (5, 17, 45). Therefore, we determined if overexpression of CAND1 would perturb the ability of Keap1 to associate with Cul3. For these experiments, a Keap1 protein containing a C-terminal chitin-binding domain was expressed in COS1 cells along with Cul3 and association of Cul3 with Keap1 was measured following affinity purification of Keap1 on chitin beads. The level of Keap1-associated Cul3 was markedly reduced in cells co-transfected with an expression vector for FLAG-CAND1 (Fig. 1B, top panel, compare lanes 3 and 4). These results are consistent with the notion that CAND1 sequesters Cul3 away from Keap1.

Keap1 is one of 49 BTB-Kelch proteins encoded by the human genome (37). Several other BTB-Kelch proteins, including GAN and sarcosin, are able to associate with Cul3 and Rbx1 to form functional ubiquitin ligase complexes (13, 44). The ability of CAND1 to compete with either GAN or sarcosin for binding to Cul3 was determined. For these experiments, CBD-tagged GAN or sarcosin proteins were expressed in COS1 cells along with Cul3. Association of Cul3 with either GAN or sarcosin was measured following affinity purification with chitin beads. The amount of Cul3 that co-purified with either CBD-GAN or CBD-sarcosin was markedly reduced in cells co-transfected with an expression vector for FLAG-CAND1 (Fig. 1C, top panel, lanes 3 and 5). These results are consistent with the notion that CAND1 is a general regulator of Cul3-dependent E3 ubiquitin ligase complexes.

Increased CAND1 expression reduces Keap1-dependent ubiquitination of Nrf2 and increases steady-state levels of Nrf2. Keap1, as a substrate adaptor for Cul3, targets specific lysine residues within the N-terminal Neh2 domain of its substrate, the Nrf2 transcription factor, for ubiquitin conjugation (43). We therefore determined if increased levels of CAND1, which reduce association between Keap1 and Cul3, would also reduce Keap1-dependent ubiquitination of Nrf2. In the presence of Keap1 and Cul3, strong ubiquitin conjugation onto a Gal4-Neh2 fusion protein was observed in transfected MDA-MB-231 cells (Fig. 2A, top panel, lane 3). However, levels of ubiquitin conjugation onto Gal4-Neh2 were markedly reduced in the presence of increasing amounts of a co-transfected expression vector for CAND1 (Fig. 2A, top panel, lanes 4-7). In parallel experiments, the effect of CAND1 overexpression on steady-state levels of

Nrf2 was determined. In both MDA-MB-231 cells (Fig. 2B, top panel) and in HeLa cells (Fig. 2C, top panel), increased expression of CAND1 markedly increased steady-state levels of Nrf2 in the presence of co-expressed Keap1. Ectopic expression of CAND1 did not reduce binding of Nrf2 to Keap1 (data not shown). Rather, these results indicate that increased CAND1 expression, which reduces the ability of Keap1 to associate with Cul3, interferes with the ability of Keap1 to target Nrf2 for ubiquitin-dependent degradation.

CAND1 is required for efficient repression of Nrf2 by Keap1. To further evaluate the functional significance of CAND1 for Keap1-mediated regulation of Nrf2, a siRNA molecule against CAND1 was used to reduce levels of the endogenous CAND1 protein. Immunoblot analysis using an anti-CAND1 antibody confirmed that the anti-CAND1 siRNA molecule was effective in reducing expression of the endogenous CAND1 protein (Fig. 3A, second panel from bottom, lane 3). Increased association of Cul3 with Keap1 was observed in HeLa cells transfected with the anti-CAND1 siRNA as compared to cells transfected with a control siRNA molecule (Fig. 3A, top panel, compare lanes 2-4). The steady-state level of Keap1 was slightly reduced in the presence of the anti-CAND1 siRNA molecule (Fig. 3A, third panel from bottom, lane 3) and ubiquitin conjugation onto Keap1 was slightly increased (Fig. 3B, top panel, lane 3), presumably a consequence of increased association of Keap1 with Cul3. These results demonstrate that while ectopic overexpression of CAND1 results in reduced levels of association between Keap1 and Cul3 (Fig. 1B), siRNA-mediated knockdown of endogenous CAND1 results in increased levels of association between Keap1 and Cul3 (Fig. 3A).

Increased association between Keap1 and Cul3 might increase the ability of Keap1 to target Nrf2 for ubiquitin-dependent degradation. Therefore, steady-state levels of Nrf2 were determined in the absence or presence of siRNA molecules directed against CAND1. HeLa cells were transfected with expression vectors for Keap1 and Nrf2 along with siRNA molecules against Nrf2, Keap1 or CAND1. Co-expression of Keap1 and Nrf2 markedly reduced steady-state levels of Nrf2 (Fig. 3C, top panel, lanes 1 and 2). As expected, steady-state levels of Nrf2 were fully recovered in the presence of a siRNA molecule against Keap1 (Fig. 3C, top panel, lane 4). However, a significant increase in steady-state levels of Nrf2 was also observed following siRNA-mediated knockdown of endogenous CAND1 expression (Fig. 3C, top panel, lane 5). Thus, although reduced levels of CAND1 results in increased association of Keap1 with Cul3, the ability of Keap1 to efficiently target Nrf2 for ubiquitin-dependent degradation is decreased.

To determine if increased steady-state levels of Nrf2 in the presence of the anti-CAND1 siRNA results from decreased binding of Nrf2 to Keap1, the level of Keap1-associated Nrf2 was determined in the absence and presence of the anti-CAND1 siRNA molecule. Increased steady-state levels of Nrf2 were again observed in the presence of the anti-CAND1 siRNA molecule (Fig. 3D, second panel from top, compare lanes 1 and 2). A marked increase in Keap1-associated Nrf2 was also observed (Fig. 3D, top panel, compare lanes 1 and 2). Thus, decreased levels of CAND1 does not disrupt the ability of Keap1 to bind Nrf2. Rather, these results indicate that decreased levels of CAND1 disrupt the ability of Keap1 to efficiently target Nrf2 for ubiquitin-dependent degradation, and thereby increase steady-state levels of Keap1-associated Nrf2.

To confirm the importance of CAND1 for regulation of steady-state levels of Nrf2, steady-state levels of the endogenous Nrf2 protein was measured in HeLa cells transfected with siRNA molecules against Keap1 or CAND1. As expected, the siRNA molecule against Keap1 markedly increased steady-state levels of the endogenous Nrf2 protein (Fig. 4A, top panel, compare lanes 1 and 5). A marked increase in the steady-state levels of the endogenous Nrf2 protein was also observed in the presence of two different siRNA molecules against CAND1 (Fig. 4A, top panel, lanes 2 and 3). A control siRNA had no effect on steady-state levels of Nrf2 (Fig. 4A, top panel, lane 4).

Reporter gene assays were performed to determine if increased steady-state levels of Nrf2 resulted in increased Nrf2-dependent gene expression. A luciferase reporter gene controlled by a minimal promoter containing 4 copies of an antioxidant response element (ARE) was transfected into HeLa cells in the absence or presence of co-transfected siRNA molecules against Nrf2, Keap1 or CAND1. A low level of Nrf2-dependent reporter gene expression was observed in the cells transfected only with the reporter plasmid (Fig. 4B). This basal level of reporter gene expression was reduced by cotransfection of siRNA against Nrf2, confirming the validity of this assay as a measurement of transcription driven by the endogenous Nrf2 protein. Levels of reporter gene expression were increased 25-fold in the presence of a siRNA molecule against Keap1, while an siRNA molecule against CAND1 resulted in a 15-fold increase in Nrf2-dependent reporter gene expression (Fig. 4B).

Our results indicate a critical role for CAND1 in regulation of Keap1-mediated control over steady-state levels of Nrf2 and Nrf2-dependent transcription. Ectopic expression of CAND1 decreased the ability of Keap1 to assemble with Cul3 into a

186

functional E3 ubiquitin ligase complex, resulting in increased steady-state levels of Nrf2. On the other hand, decreased CAND1 expression, which increased complex formation between Keap1 and Cul3, also increased steady-state levels of Nrf2 and Nrf2-dependent gene expression. Taken together, these results indicate that an optimal level of CAND1 is required for efficient down-regulation of Nrf2 by Keap1. These results are consistent with a model in which CAND1-mediated cycles of assembly and disassembly of the Keap1-Cul3-Rbx1 E3 ubiquitin ligase complex are required for efficient control by Keap1 over steady-state levels of Nrf2 and Nrf2-dependent transcription.

Neddylation of Cul3 on Lys 712 is required for efficient Keap1-dependent ubiquitination of Nrf2 in vivo. Cyclical assembly and disassembly of Cullin-containing E3 ubiquitin ligase complexes has been suggested to involve both CAND1 and site-specific modification of the Cullin protein by the small ubiquitin-like protein, Nedd8 (5). The neddylated form of Cul3, which exhibits a slower mobility on SDS-polyacrylamide gels, can be readily observed following immunoblot detection of Cul3 in whole cell lysates (Fig. 1A, bottom panel). Neddylation of Cul3 occurs at a conserved C-terminal lysine residue (Lys 712 in human Cul3) and the biological importance of Nedd8 modification has been demonstrated for the Cul3 homologs in *D. melanogaster* and *C. elegans* (36, 46).

To determine if neddylation of Cul3 is required for Keap1-dependent ubiquitination of Nrf2, the ability of Keap1 to target Nrf2 for ubiquitination was characterized in the ts41 hamster ovary cell line. The ts41 cell line contains a temperature sensitive defect in the Nedd8 E1 activation enzyme (3, 34). As expected, the

slower migrating form of Cul3 was not detected in ts41 cells following a shift to the restrictive temperature of 40° C (Fig. 5A, second panel from top, lane 4). Increased association of CAND1 with Cul3 was also observed in ts41 cells at the restrictive temperature (Fig. 5A, top panel, lanes 2 and 4), consistent with the notion that CAND1 preferentially binds to the non-neddylated form of Cul3 (17, 19, 28, 45). In contrast, the neddylated form of Cul3 was readily detectable in wild-type Chinese hamster ovary cells grown at either 34° C or 40° C, and no changes in CAND1 association with Cul3 were observed (Fig. 5A, top panel, lanes 6 and 8). Ectopic expression of Keap1 and Cul3 markedly increased ubiquitination onto the Gal4-Neh2 fusion protein in both ts41 and wild-type cells grown at 34° C and in the wild-type cells grown at 40° C (Fig. 5B, lanes 1-4 and 9-16). However, Keap1-dependent ubiquitination of the Gal4-Neh2 protein was abolished in ts41 cells shifted to 40° C (Fig. 5B, lanes 5-8).

Neddylation of the human Cul3 protein is predicted to occur at Lys 712 located within a short stretch of amino acids that are highly conserved in other cullin proteins (Fig. 6A). Several amino acids in this region, including Lys 712, participate in direct contacts between Cul1 and CAND1 (17), suggesting that there may be an antagonistic relationship between modification of cullin proteins by Nedd8 and binding of cullin proteins to CAND1 (4, 17, 28, 31, 45). To further explore the functional significance of Cul3 neddylation and CAND1 association for efficient Keap1-dependent ubiquitination of Nrf2, a series of mutant Cul3 proteins were constructed. These mutations introduced either a single arginine substitution in place of Lys 712 or introduced two alanine substitutions at adjacent residues flanking Lys 712 (Fig. 6A). Modification of Cul3 by neddylation was abolished only by the K712R substitution (Fig. 6B, middle panel, lane

3). However, all of the mutant Cul3 proteins, including the K712R protein, were able to associate with CAND1 (Fig. 6B, upper panel), indicating that single or double amino acid substitutions within this conserved region are not sufficient to disrupt binding of Cul3 to CAND1.

All of the mutant Cul3 proteins were able to associate with Keap1 and Rbx1 (Fig. 7A and data not shown). Co-expression of the wild-type Cul3 protein with Keap1 markedly enhanced ubiquitination of the Gal4-Neh2 substrate protein (Fig. 6C, lanes 2-4) and markedly reduced steady-state levels of Nrf2 (Fig. 6D, lanes 1-3). However, only low levels of ubiquitin transfer onto the Gal4-Neh2 substrate protein was observed in the presence of the mutant K712R Cul3 protein (Fig. 6C, lane 5). Elevated steady state levels of Nrf2 were observed in the presence of the mutant K712R Cul3 protein (Fig. 6D, lane 4). Two other mutant Cul3 proteins, containing Ala or Met, respectively, at residue 712 were also impaired in their ability to repress steady-state levels of Nrf2 (data not shown). All of the other mutant Cul3 proteins were as effective as the wild-type Cul3 protein for supporting Keap1-dependent ubiquitination of Nrf2 and Keap1-mediated repression of steady-state levels of Nrf2 (Fig. 6C, lanes 6-11 and Fig. 6D, lanes 5-10). To confirm that the K712R mutant Cul3 protein is able to assemble into a functional E3 ubiquitin ligase complex with Keap1, in vitro ubiquitination assays were carried out following affinity purification of the complex from transfected cells. Both the wild-type and K712R mutant Cul3 proteins were able to form a complex with Keap1 and Rbx1 that could be affinity-purified from transfected cells (Fig. 7A, top two panels, lanes 3 and 4). Furthermore, following affinity purification of the quaternary Nrf2-Keap1-Cul3-Rbx1 complex from transfected cells, both the K712R mutant and the wild-type Cul3 proteins

189

were able to support ubiquitin transfer onto Nrf2 in vitro (Fig. 7B, lanes 3 and 4). Ubiquitin transfer onto Keap1 was also readily observed in vitro in the presence of either the K712R mutant or wild-type Cul3 (data not shown). Ubiquitin conjugation onto Nrf2 was not observed in reactions carried out in the absence of the E1 ubiquitin conjugation enzyme (Fig. 7B, lane 1). Importantly, only low levels of ubiquitin conjugation onto Nrf2 was observed in the absence of the co-expressed Cul3/Rbx1 subcomplex (Fig. 7B, lane 2), indicating that the robust ubiquitin conjugation activity observed in the presence of the K712R mutant protein is not simply due to co-purification of the endogenous Cul3/Rbx1 subcomplex with ectopically expressed Keap1-CBD. Thus, under the conditions of the in vitro assay, neddylation of Lys 712 is not required for the assembly of Cul3 into a functional ubiquitin ligase complex (Fig. 7B). However, neddylation of Cul3 is required to support efficient Keap1-dependent ubiquitination of Nrf2 in vivo (Fig. 6C).

DISCUSSION

The ability of Keap1 to function as a substrate adaptor protein for Cul3 and target Nrf2 for ubiquitin-dependent degradation has emerged as a major regulatory mechanism that regulates expression of cytoprotective phase 2 genes (7, 14, 25, 43). Cullin-dependent E3 ubiquitin ligases have been proposed to undergo cycles of assembly and disassembly that allow substrate adaptor recycling. Cyclical assembly and disassembly of cullin-dependent E3 ubiquitin ligase complexes is mediated, in part, by the antagonistic actions of Nedd8 modification of the cullin protein and association of cullin proteins with CAND1 (17, 31, 35). In the present work, we have used several independent experimental approaches to examine the role of substrate adaptor recycling for Keap1-mediated repression of Nrf2. Ectopic expression of CAND1 reduced the level of complex formation between Keap1 and Cul3 while siRNA-mediated knockdown of endogenous CAND1 expression increased complex formation between Keap1 and Cul3. However, both ectopic CAND1 expression and siRNA-mediated knockdown of endogenous CAND1 decreased the ability of Keap1 to target Nrf2 for ubiquitin-dependent degradation. Notably, a marked increase in Nrf2-dependent gene expression was observed following siRNA-mediated knockdown of CAND1 expression. Modification of Cul3 by Nedd8 at a conserved Lys acceptor residue is also required for Keap1-dependent ubiquitination in vivo. Taken together, these results are consistent with a model in which the ability of Keap1 to participate in multiple cycles of substrate adaptor exchange is a critical regulatory aspect of Keap1-mediated repression of Nrf2-dependent gene expression.

A key feature of this model is that physical release of Nrf2 from Keap1 is not required for activation of Nrf2-dependent transcription. Indeed, knockdown of CAND1 markedly increases the level of Keap1-associated Nrf2 yet also increases Nrf2-dependent transcription. Thus, decreasing the ability of Keap1 to efficiently target Nrf2 for ubiquitin-dependent degradation is sufficient to activate Nrf2-dependent gene expression. We propose that a decreased ability of Keap1 to target Nrf2 for ubiquitin-dependent degradation results in the accumulation of an excess of Nrf2 relative to Keap1 such that free Nrf2 proteins are able to localize to the nucleus and activate Nrf2-dependent gene expression.

The ability of Keap1 to act in a catalytic manner and target multiple Nrf2 proteins for ubiquitin-dependent degradation has important implications for how Nrf2 is able to escape Keap1-mediated repression following exposure of cells to oxidative stress and chemopreventive compounds. As Keap1 is able to sequester Nrf2 in the cytoplasm, it has been suggested that reactive molecules bind to Keap1 and cause the physical release of Nrf2 from Keap1. Consistent with this suggestion, direct binding of chemically reactive molecules to Keap1 has been demonstrated both in vitro and in vivo (10, 18). However, the importance of physical release of Nrf2 from Keap1 has not been clearly established. For example, although one report suggested that chemical inducers of Nrf2-dependent gene expression dissociate the Keap1-Nrf2 complex in vitro (10), a subsequent report suggested that reactive molecules simply alter the mobility of the complex in native polyacrylamide gels without causing the physical release of Nrf2 (18). In our previous work, we have demonstrated that association between Nrf2 and Keap1 in vivo is not decreased but is actually increased following exposure of cells to inducers of Nrf2-

192

dependent transcription (43). In a similar vein, we find that knockdown of CAND1, which markedly increases Nrf2-dependent gene expression, also increases the level of Keap1-associated Nrf2. Taken together, the available experimental evidence is most consistent with a model in which reactive molecules do not cause the physical release of Nrf2 from Keap1 but interfere with the ability of Keap1 to act in a catalytic manner to efficiently target Nrf2 for ubiquitin-dependent degradation.

Keap1 has been proposed to be a sensor of reactive molecules and oxidative stress, such that a redox-dependent modification of one or more cysteine residues in Keap1 is coupled to increased expression of Nrf2-dependent genes. Indeed, multiple cysteine residues in Keap1, including Cys 151, Cys 273 and Cys 288, can be modified by reactive molecules either in vivo and in vitro (10, 12, 18). Mutational analysis has revealed that Cys 273 and Cys 288, which are located in the central linker domain and participate in binding Zn^{+2} (11), are required for repression of Nrf2-dependent gene expression. In contrast, Cys 151, located in the N-terminal BTB domain, is specifically required for increased Nrf2-dependent gene expression following exposure of cells to oxidative stress (38, 42, 43). Mutant Keap1 proteins containing serine or alanine substitutions at either Cys 151, Cys 273 or Cys 288 are still able to bind Nrf2 (42). However, serine substitutions at Cys 273 and Cys 288, compromise the ability of Keap1 to target Nrf2 for ubiquitination because they reduce the ability of Keap1 to bind Cul3 (S.-C. Lo and M. Hannink, unpublished data). On the other hand, serine substitution at Cys 151 renders Keap1-dependent ubiquitination of Nrf2 resistant to inhibition by oxidative stress or chemopreventive compounds, presumably because modification of Cys 151 by chemopreventive compounds such as sulforaphane decreases the ability of

Keap1 to associate with Cul3 (43). Taken together, the current evidence is most consistent with a model in which modification of these (and perhaps other) cysteine residues in Keap1 would perturb the ability of Keap1 to assemble with Cul3 and target Nrf2 for ubiquitin-dependent degradation rather than inducing the release of Nrf2 from Keap1. An attractive feature of a model in which Keap1 acts in a catalytic manner to efficiently target Nrf2 for ubiquitin-dependent degradation is that modulating the catalytic efficiency of Keap1 by modification of one or more cysteine residues in Keap1 would allow a graded response of Nrf2-dependent gene expression following exposure of cells to oxidative stress and chemically reactive molecules.

This chapter was reproduced with the expressed written permission of the American Society for Microbiology.
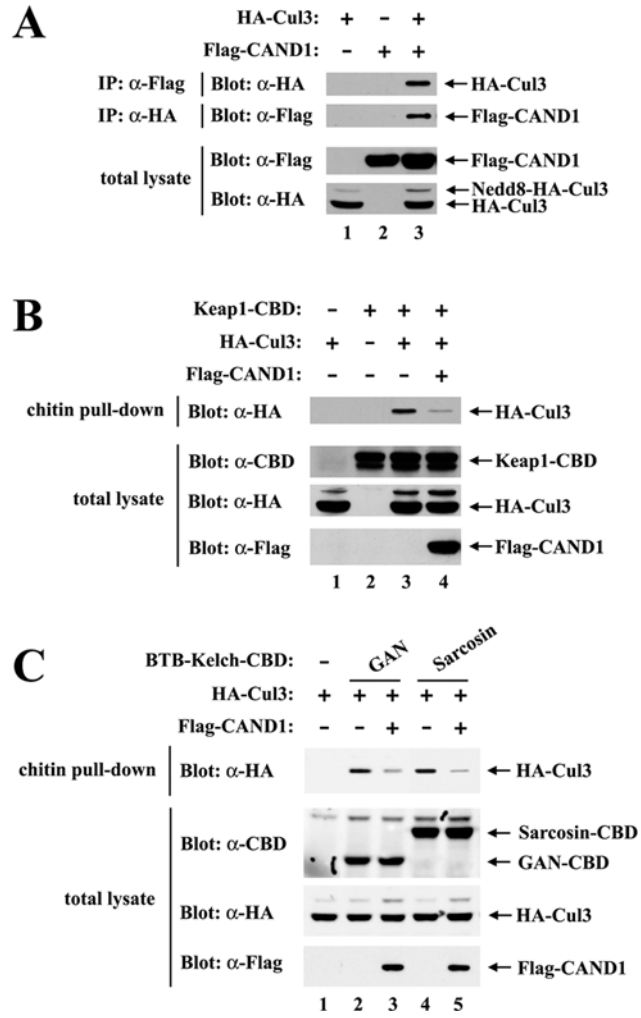
Figure IV-1

Figure IV-1. CAND1 competes with Keap1 for binding to Cul3. (A) Thirty-five-millimeter-diameter dishes of COS1 cells were transfected with 0.5 μg each of expression vectors for HA-Cul3 and Flag-CAND1 as indicated. Total cell lysates were analyzed by immunoblotting with anti-Flag and anti-HA antibodies (bottom two panels). Anti-Flag immunoprecipitates (IP) were subjected to immunoblot analysis using anti-HA antibodies (top panel). Anti-HA immunoprecipitates (IP) were subjected to immunoblot analysis using anti-Flag antibodies (second panel from the top). (B) Thirty-five-millimeter-diameter dishes of COS1 cells were transfected with 0.33 μg each of expression vectors for Keap1-CBD and HA-Cul3 as indicated. The Flag-CAND1 expression vector was either omitted (lanes 1 to 3) or included (lane 4). Total cell lysates were analyzed by immunoblotting with anti-CBD, anti-Flag, and anti-HA antibodies (bottom three panels). The lysates were incubated with chitin beads, pelleted by centrifugation (3,000 x g), and washed three times in the lysis buffer. Proteins that remained associated with the chitin beads were analyzed by immunoblotting with anti-HA antibodies (top panel). (C) Thirty-five-millimeter-diameter dishes of COS1 cells were transfected with expression vectors for HA-Cul3 (lanes 1 to 5) and GAN-CBD (lanes 2 and 3) or sarcosin-CBD (lanes 4 and 5). The Flag-CAND1 expression vector was either omitted (lanes 1, 2 and 4) or included (lanes 3 and 5). Cell lysates were analyzed by immunoblotting with the indicated antibodies (bottom three panels) or incubated with chitin beads. Proteins that remained associated with the chitin beads after extensive washing were analyzed by immunoblotting with anti-HA antibodies (top panel).
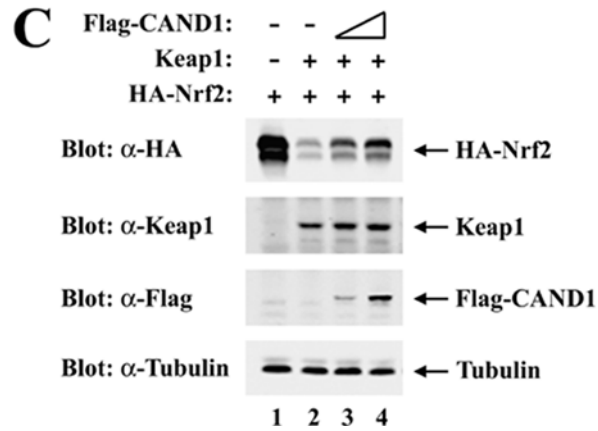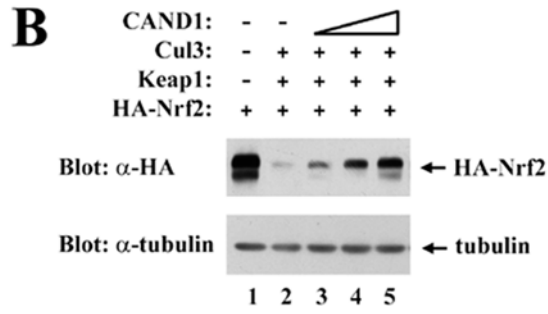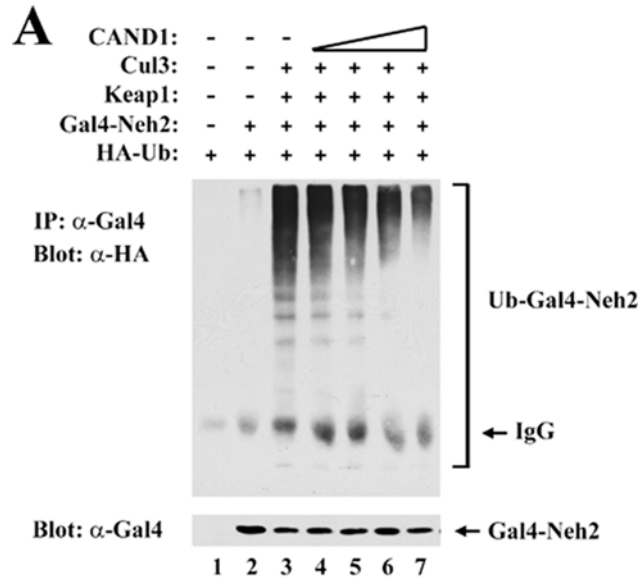
Figure IV-2

Figure IV-2. Increased CAND1 expression reduces Keap1-dependent ubiquitination and degradation of Nrf2. (A) Thirty-five-millimeter-diameter dishes of MDA-MB-231 cells were transfected with expression vectors for HA-Ub (0.4 μg), Gal4-Neh2 (0.4 μg, lanes 2 to 7), Keap1 (0.1 μg, lanes 3 to 7), Cul3 (0.1 μg, lanes 3 to 7), and CAND1 (from 0.0125 to 0.1 μg, lanes 4 to 7). The transfected cells were treated with MG132 for 5 h prior to cell lysis. Total cell lysates were analyzed by immunoblotting with anti-Gal4 antibodies (bottom panel). Anti-Gal4 immunoprecipitates were analyzed by immunoblotting with anti-HA antibodies (top panel). (B) Twenty-four-well plates of MDA-MB-231 cells were transfected with expression vectors for HA-Nrf2 (0.18 μg), Keap1 (0.018 μg, lanes 2 to 5), Cul3 (0.07 μg, lanes 2 to 5), and CAND1 (from 0.035 to 0.14 μg, lanes 3 to 5). Total cell lysates were subjected to immunoblot analysis with anti-HA (top panel) and anti-Tubulin (bottom panel) antibodies. (C) Twenty-four-well plates of HeLa cells were transfected with expression vectors for HA-Nrf2 (0.18 μg), Keap1 (0.018 μg, lanes 2 to 4), and Flag-CAND1 (0.035 to 0.14 μg, lanes 3 and 4). Total cell lysates were subjected to immunoblot analysis with anti-HA, anti-Keap1, anti-Flag, and anti-Tubulin antibodies as indicated.
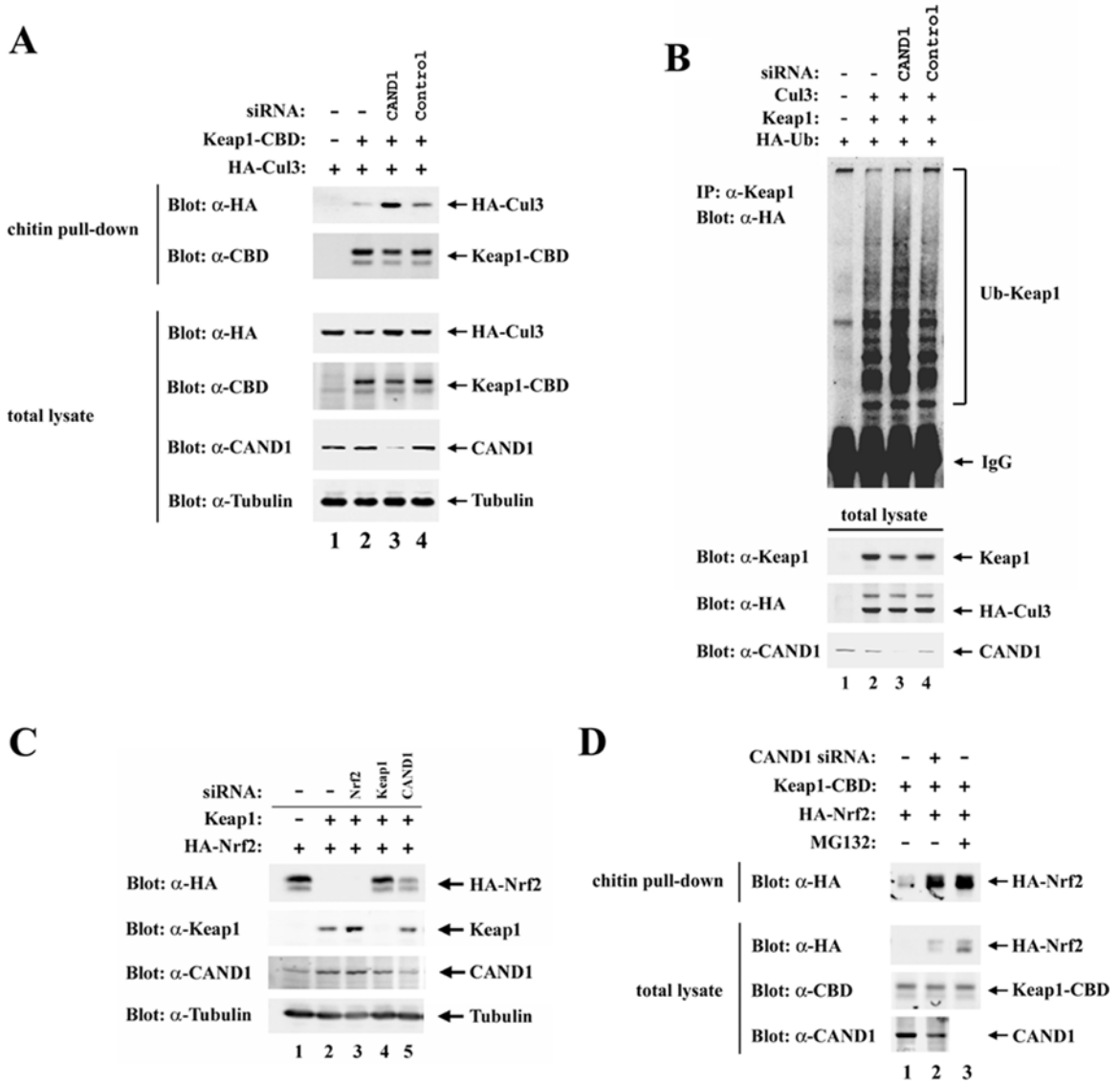
Figure IV-3

Figure IV-3. CAND1 is required for efficient repression of Nrf2 by Keap1. (A) HeLa cells were transfected with control (lane 4) or anti-CAND1 (lane 3) siRNA nucleotides (300 nM), allowed to recover for 24 h, and transfected with expression vectors for HA-Cul3 and Keap1-CBD (lanes 2 to 4). Cell lysates were immunoblotted with the indicated antibodies (bottom four panels) or incubated with chitin beads. Proteins that remained bound to the chitin beads after extensive washing were analyzed with the indicated antibodies (top two panels). (B) HeLa cells were transfected with control (lane 4) or anti-CAND1 (lane 3) siRNA nucleotides (100 nM), and transfected with expression vectors for HA-Ub, Keap1, and Cul3 as indicated. Cell lysates were collected after an additional 24 h and immunoblotted with the indicated antibodies (bottom three panels). Anti-Keap1 immunoprecipitates were analyzed by immunoblotting with anti-HA antibodies (top panel). (C) HeLa cells were transfected with anti-Nrf2 (lane 3), anti-Keap1 (lane 4), or anti-CAND1 (lane 5) siRNA nucleotides (50 nM), allowed to recover for 24 h and then transfected with expression vectors for HA-Nrf2 and Keap1 (lanes 2 to 5). Total cell lysates were collected and subjected to immunoblot analysis with the indicated antibodies. (D) HeLa cells were first mock transfected (lanes 1 and 3) or transfected with anti-CAND1 siRNA nucleotides (300 nM), allowed to recover for 24 h, and then transfected with expression vectors for HA-Nrf2 and Keap1-CBD. The transfected cells were either untreated (lanes 1 and 2) or treated with MG132 for 5 h prior to cell lysis. The lysates were incubated with chitin beads and levels of HA-Nrf2 proteins that remained bound to the chitin beads were determined by immunoblotting with anti-HA antibodies (top panel). Total lysates were analyzed by immunoblotting with the indicated antibodies (bottom three panels).

Figure IV-4
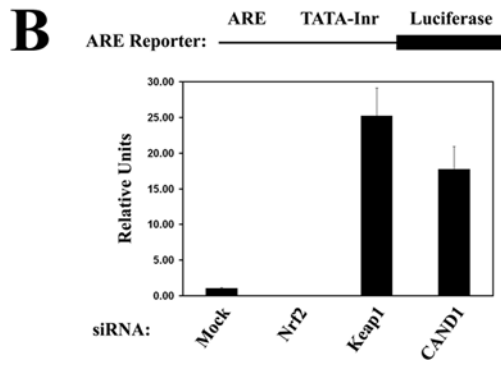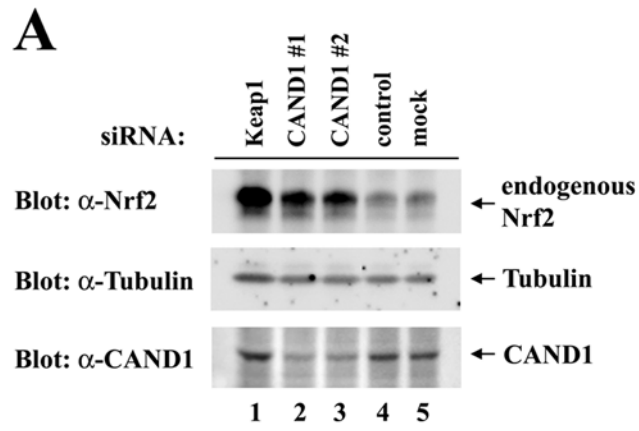
Figure IV-4. CAND1 is required for Nrf2 turnover, and contributes to repression of ARE-dependent gene expression. (A) Twenty-four-well plates of HeLa cells were transfected with 100 nM of control siRNA (lane 4) or siRNA nucleotides targeting Keap1 (lane 1) or CAND1 at different regions in CAND1 mRNA (lane 2 and 3). Levels of endogenous Nrf2 were determined by immunoblot analysis with anti-Nrf2 antibodies (top panel). Levels of CAND1 and Tubulin were analyzed by immunoblotting with the indicated antibodies (bottom two panels). (B) Twenty-four-well plates of HeLa cells were transfected with anti-Nrf2, anti-Keap1, or anti-CAND1 siRNA nucleotides (300 nM) as indicated and with an ARE-dependent firefly luciferase reporter gene construct (100 ng). A plasmid encoding *Renilla* luciferase (10 ng) was included as a control for transfection efficiency. The data shown represent the means and standard deviation of results from three independent experiments.

Figure IV-5
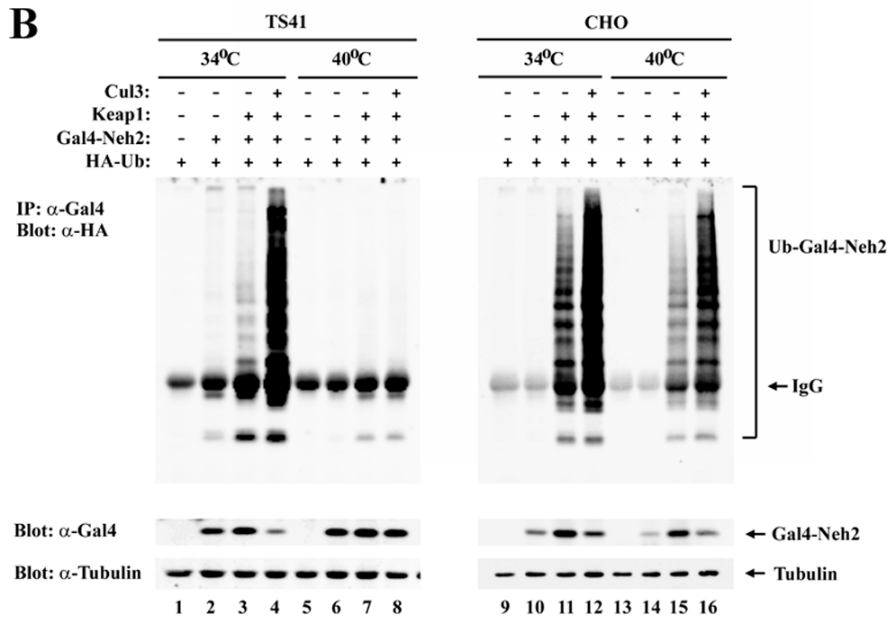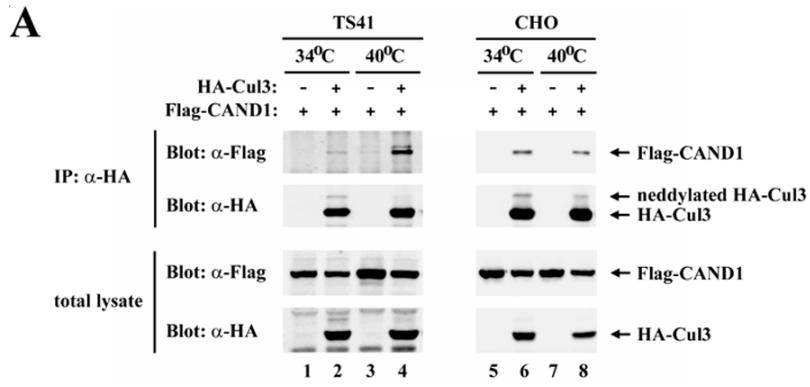
Figure IV-5. Nedd8 is required for ubiquitination of Nrf2 by a Keap1-Cul3 ligase complex. (A) Sixty-millimeter-diameter dishes of ts41 cells or wild-type CHO cells were cotransfected with 1.0 µg each of expression vectors for HA-Cul3 and Flag-CAND1 as indicated. The transfected cells were either kept at 34°C (lanes 1, 2, 5 and 6) or shifted to 40°C (lanes 3, 4, 7 and 8) for 24 h. Total cell lysates were analyzed by immunoblotting with anti-Flag and anti-HA antibodies (bottom two panels). Anti-HA immunoprecipitates (IP) were subjected to immunoblot analysis using anti-Flag and anti-HA antibodies (top two panels). (B) Sixty-millimeter-diameter dishes of ts41 cells or wild-type CHO cells were cotransfected with expression vectors for HA-Ub (0.7 µg), Gal4-Neh2 (0.8 µg), Keap1 (0.2 µg), and Cul3 (0.3 µg) as indicated. The transfected cells were either kept at 34°C (lanes 1 to 4, and 9 to 12) or shifted to 40°C (lanes 5 to 8, and 13 to 16) for 24 h, and were all treated with MG132 for 2.5 h prior to cell lysis. Total cell lysates were analyzed by immunoblotting with anti-Gal4 and anti-Tubulin antibodies (bottom two panels). Anti-Gal4 immunoprecipitates were analyzed by immunoblotting with anti-HA antibodies (top panel).

Figure IV-6

Figure IV-6. Neddylation of Cul3 on Lys 712 is required for efficient ubiquitination and degradation of Nrf2 by a Keap1-Cul3 ligase complex. (A) Sequence alignment of neddylation sites among five members of the cullin superfamily is shown. The conserved Lys residue for Nedd8 conjugation in the cullin proteins is indicated above the alignment by an arrow (39). Conserved residues in this region are indicated below the alignment by an asterisk (*). Residues in this region of Cul1 that make direct contacts with CAND1 are indicated above the alignment by the upper case symbol (^) (17). The conserved residues that were substituted with alanine or arginine in the Cul3 mutant proteins utilized in this report are illustrated. (B) COS1 cells were cotransfected with expression vectors for Flag-CAND1 and the mutant or wild-type HA-Cul3 proteins as indicated. Cell lysates were collected in the presence of 10 mM N-ethylmaleimide (NEM) and analyzed by immunoblotting with anti-Flag and anti-HA antibodies (bottom two panels). Anti-HA immunoprecipitates (IP) were subjected to immunoblot analysis using anti-Flag antibodies (top panel). (C) MDA-MB-231 cells were transfected with expression vectors for HA-Ub, Gal4-Neh2 (lanes 2 to 11), Keap1 (lanes 3 to 11), and the wild-type or mutant Cul3 proteins (lanes 4 to 11). The transfected cells were treated with MG132 for 2.5 h prior to cell lysis. Anti-Gal4 immunoprecipitates from cell lysates were analyzed by immunoblotting with anti-HA antibodies. (D) MDA-MB-231 cells were transfected with expression vectors for HA-Nrf2, myc-Rbx1 (lanes 2 to 10), Keap1 (lanes 2 to 10), and the wild-type or mutant Cul3 proteins (lanes 3 to 10). Total cell lysates were subjected to immunoblot analysis with anti-HA (top and middle panels) and anti-Tubulin (bottom panel) antibodies.

Figure IV-7
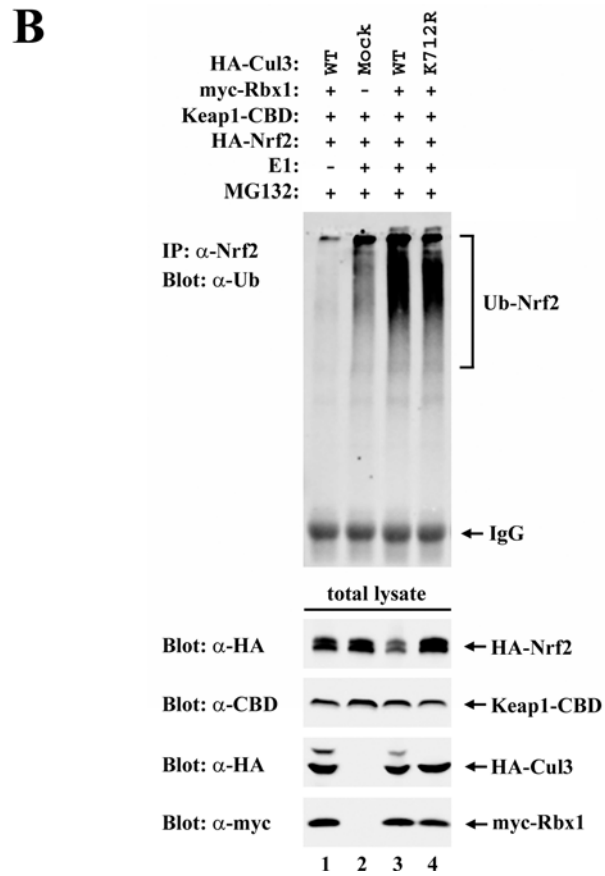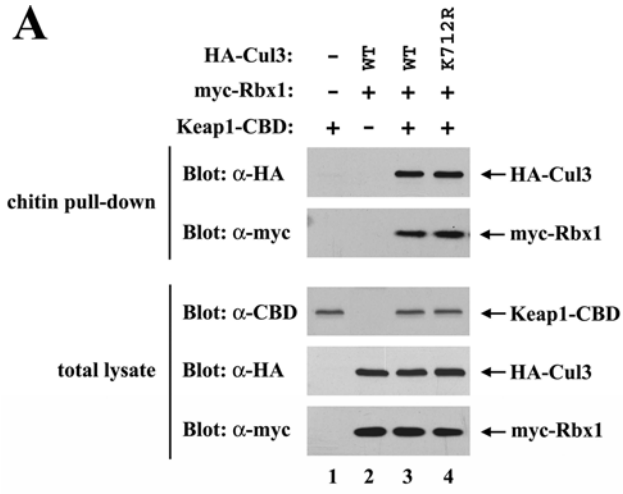
Figure IV-7. Catalytic activity of a Keap1-Cul3 ligase complex per se does not require neddylation on the Lys 712 of Cul3. (A) Thirty-five-millimeter-diameter dishes of COS1 cells were cotransfected with expression vectors for Keap1-CBD (0.3 µg, lanes 1, 3 and 4), myc-Rbx1 (0.1 µg, lanes 2 to 4), and the wild-type or mutant HA-Cul3 proteins (0.3 µg, lanes 2 to 4) as indicated. Cell lysates were analyzed by immunoblotting with the indicated antibodies (bottom three panels) or incubated with chitin beads. Proteins that remained bound to the chitin beads after extensive washing were analyzed by immunoblotting with the indicated antibodies (top two panels). (B) Sixty-millimeter-diameter dishes of COS1 cells were transfected with 0.5 µg each of the expression vectors for HA-Nrf2, Keap1-CBD, myc-Rbx1, and the wild-type or mutant HA-Cul3 proteins, as indicated in lanes 1 to 4. The transfected cells were treated with MG132 for 5 h prior to cell lysis. Lysates from three 60-mm-diameter dishes were pooled for each sample. One percent of the cell lysates were analyzed by immunoblotting with the indicated antibodies (bottom four panels) and the rest of the lysates were incubated with chitin beads. After washing, the chitin beads were incubated with E1, E2-UbcH5a, ubiquitin, and ATP. The E1 enzyme was omitted from one sample (lane 1). Subsequently, the chitin beads were pelleted and washed, and proteins that were eluted from the beads after boiling under denaturing conditions were immunoprecipitated with anti-Nrf2 antibodies and then analyzed by immunoblotting with anti-ubiquitin antibodies (top panel).

REFERENCES

1. **Ames, B. N., and M. K. Shigenaga.** 1993. DNA and Free Radicals, p. 1-15. *In* B. Halliwell and O. I. Aruoma (ed.), Oxidants are a major contributor to cancer and aging. Ellis Horwood, New York, NY.

2. **Ceconi, C., A. Boraso, A. Cargnoni, and R. Ferrari.** 2003. Oxidative stress in cardiovascular disease: myth or fact? Arch Biochem Biophys **420:**217-21.

3. **Chen, Y., D. L. McPhie, J. Hirschberg, and R. L. Neve.** 2000. The amyloid precursor protein-binding protein APP-BP1 drives the cell cycle through the S-M checkpoint and causes apoptosis in neurons. J Biol Chem **275:**8929-35.

4. **Chuang, H. W., W. Zhang, and W. M. Gray.** 2004. Arabidopsis ETA2, an apparent ortholog of the human cullin-interacting protein CAND1, is required for auxin responses mediated by the SCF(TIR1) ubiquitin ligase. Plant Cell **16:**1883-97.

5. **Cope, G. A., and R. J. Deshaies.** 2003. COP9 signalosome: a multifunctional regulator of SCF and other cullin-based ubiquitin ligases. Cell **114:**663-71.

6. **Cope, G. A., G. S. Suh, L. Aravind, S. E. Schwarz, S. L. Zipursky, E. V. Koonin, and R. J. Deshaies.** 2002. Role of predicted metalloprotease motif of Jab1/Csn5 in cleavage of Nedd8 from Cul1. Science **298:**608-11.

7. **Cullinan, S. B., J. D. Gordan, J. Jin, J. W. Harper, and J. A. Diehl.** 2004. The Keap1-BTB protein is an adaptor that bridges Nrf2 to a Cul3-based E3 ligase: oxidative stress sensing by a Cul3-Keap1 ligase. Mol Cell Biol **24:**8477-86.

8. **Davies, K. J.** 2000. Oxidative stress, antioxidant defenses, and damage removal, repair, and replacement systems. IUBMB Life **50:**279-89.

9. **Deffenbaugh, A. E., K. M. Scaglione, L. Zhang, J. M. Moore, T. Buranda, L. A. Sklar, and D. Skowyra.** 2003. Release of ubiquitin-charged Cdc34-S - Ub from the RING domain is essential for ubiquitination of the SCF(Cdc4)-bound substrate Sic1. Cell **114:**611-22.

10. **Dinkova-Kostova, A. T., W. D. Holtzclaw, R. N. Cole, K. Itoh, N. Wakabayashi, Y. Katoh, M. Yamamoto, and P. Talalay.** 2002. Direct evidence that sulfhydryl groups of Keap1 are the sensors regulating induction of phase 2 enzymes that protect against carcinogens and oxidants. Proc Natl Acad Sci U S A **99:**11908-13.

11. **Dinkova-Kostova, A. T., W. D. Holtzclaw, and N. Wakabayashi.** 2005. Keap1, the sensor for electrophiles and oxidants that regulates the phase 2 response, is a zinc metalloprotein. Biochemistry **44:**6889-99.

12. **Eggler, A. L., G. Liu, J. M. Pezzuto, R. B. van Breemen, and A. D. Mesecar.** 2005. Modifying specific cysteines of the electrophile-sensing human Keap1 protein is insufficient to disrupt binding to the Nrf2 domain Neh2. Proc Natl Acad Sci U S A **102:**10070-5.

13. **Furukawa, M., Y. J. He, C. Borchers, and Y. Xiong.** 2003. Targeting of protein ubiquitination by BTB-Cullin 3-Roc1 ubiquitin ligases. Nat Cell Biol **5:**1001-7.

14. **Furukawa, M., and Y. Xiong.** 2005. BTB Protein Keap1 Targets Antioxidant Transcription Factor Nrf2 for Ubiquitination by the Cullin 3-Roc1 Ligase. Mol Cell Biol **25:**162-71.

15. **Gan-Erdene, T., K. Nagamalleswari, L. Yin, K. Wu, Z. Q. Pan, and K. D. Wilkinson.** 2003. Identification and characterization of DEN1, a deneddylase of the ULP family. J Biol Chem **278:**28892-900.

16. **Golden, T. R., D. A. Hinerfeld, and S. Melov.** 2002. Oxidative stress and aging: beyond correlation. Aging Cell **1:**117-23.

17. **Goldenberg, S. J., T. C. Cascio, S. D. Shumway, K. C. Garbutt, J. Liu, Y. Xiong, and N. Zheng.** 2004. Structure of the Cand1-Cul1-Roc1 complex reveals regulatory mechanisms for the assembly of the multisubunit cullin-dependent ubiquitin ligases. Cell **119:**517-28.

18. **Hong, F., K. R. Sekhar, M. L. Freeman, and D. C. Liebler.** 2005. Specific patterns of electrophile adduction trigger keap1 ubiquitination and NRF2 activation. J Biol Chem.

19. **Hwang, J. W., K. W. Min, T. A. Tamura, and J. B. Yoon.** 2003. TIP120A associates with unneddylated cullin 1 and regulates its neddylation. FEBS Lett **541:**102-8.

20. **Imlay, J. A.** 2003. Pathways of oxidative damage. Annu Rev Microbiol **57:**395-418.

21. **Itoh, K., N. Wakabayashi, Y. Katoh, T. Ishii, K. Igarashi, J. D. Engel, and M. Yamamoto.** 1999. Keap1 represses nuclear activation of antioxidant responsive elements by Nrf2 through binding to the amino-terminal Neh2 domain. Genes Dev **13:**76-86.

22. **Jaiswal, A. K.** 2004. Nrf2 signaling in coordinated activation of antioxidant gene expression. Free Radic Biol Med **36:**1199-207.

23. **Kamura, T., D. M. Koepp, M. N. Conrad, D. Skowyra, R. J. Moreland, O. Iliopoulos, W. S. Lane, W. G. Kaelin, Jr., S. J. Elledge, R. C. Conaway, J. W. Harper, and J. W. Conaway.** 1999. Rbx1, a component of the VHL tumor suppressor complex and SCF ubiquitin ligase. Science **284:**657-61.

24. **Kawakami, T., T. Chiba, T. Suzuki, K. Iwai, K. Yamanaka, N. Minato, H. Suzuki, N. Shimbara, Y. Hidaka, F. Osaka, M. Omata, and K. Tanaka.** 2001. NEDD8 recruits E2-ubiquitin to SCF E3 ligase. Embo J **20:**4003-12.

25. **Kobayashi, A., M. I. Kang, H. Okawa, M. Ohtsuji, Y. Zenke, T. Chiba, K. Igarashi, and M. Yamamoto.** 2004. Oxidative stress sensor Keap1 functions as an adaptor for Cul3-based E3 ligase to regulate proteasomal degradation of Nrf2. Mol Cell Biol **24:**7130-9.

26. **Kobayashi, M., and M. Yamamoto.** 2005. Molecular mechanisms activating the nrf2-keap1 pathway of antioxidant gene regulation. Antioxid Redox Signal **7:**385-94.

27. **Li, X., D. Zhang, M. Hannink, and L. J. Beamer.** 2004. Crystal structure of the Kelch domain of human Keap1. J Biol Chem **279:**54750-8.

28. **Liu, J., M. Furukawa, T. Matsumoto, and Y. Xiong.** 2002. NEDD8 modification of CUL1 dissociates p120(CAND1), an inhibitor of CUL1-SKP1 binding and SCF ligases. Mol Cell **10:**1511-8.

29. **Lyapina, S., G. Cope, A. Shevchenko, G. Serino, T. Tsuge, C. Zhou, D. A. Wolf, N. Wei, and R. J. Deshaies.** 2001. Promotion of NEDD-CUL1 conjugate cleavage by COP9 signalosome. Science **292:**1382-5.

30. **Min, K. W., J. W. Hwang, J. S. Lee, Y. Park, T. A. Tamura, and J. B. Yoon.** 2003. TIP120A associates with cullins and modulates ubiquitin ligase activity. J Biol Chem **278:**15905-10.

31. **Min, K. W., M. J. Kwon, H. S. Park, Y. Park, S. K. Yoon, and J. B. Yoon.** 2005. CAND1 enhances deneddylation of CUL1 by COP9 signalosome. Biochem Biophys Res Commun **334:**867-74.

32. **Motohashi, H., T. O'Connor, F. Katsuoka, J. D. Engel, and M. Yamamoto.** 2002. Integration and diversity of the regulatory network composed of Maf and CNC families of transcription factors. Gene **294:**1-12.

33. **Nguyen, T., P. J. Sherratt, and C. B. Pickett.** 2003. Regulatory mechanisms controlling gene expression mediated by the antioxidant response element. Annu Rev Pharmacol Toxicol **43:**233-60.

34. **Osaka, F., H. Kawasaki, N. Aida, M. Saeki, T. Chiba, S. Kawashima, K. Tanaka, and S. Kato.** 1998. A new NEDD8-ligating system for cullin-4A. Genes Dev **12:**2263-8.

35. **Petroski, M. D., and R. J. Deshaies.** 2005. Function and regulation of cullin-RING ubiquitin ligases. Nat Rev Mol Cell Biol **6:**9-20.

36. **Pintard, L., T. Kurz, S. Glaser, J. H. Willis, M. Peter, and B. Bowerman.** 2003. Neddylation and deneddylation of CUL-3 is required to target MEI-1/Katanin for degradation at the meiosis-to-mitosis transition in C. elegans. Curr Biol **13:**911-21.

37. **Stogios, P. J., G. S. Downs, J. J. S. Jauhal, S. K. Nandra, and G. G. Prive.** 2005. Sequence and structural analysis of BTB domain proteins. Genome Biol **6**.

38. **Wakabayashi, N., A. T. Dinkova-Kostova, W. D. Holtzclaw, M. I. Kang, A. Kobayashi, M. Yamamoto, T. W. Kensler, and P. Talalay.** 2004. Protection against electrophile and oxidant stress by induction of the phase 2 response: fate of cysteines of the Keap1 sensor modified by inducers. Proc Natl Acad Sci U S A **101:**2040-5.

39. **Wu, K., A. Chen, and Z. Q. Pan.** 2000. Conjugation of Nedd8 to CUL1 enhances the ability of the ROC1-CUL1 complex to promote ubiquitin polymerization. J Biol Chem **275:**32317-24.

40. **Yamoah, K., K. Wu, and Z. Q. Pan.** 2005. In vitro cleavage of Nedd8 from cullin 1 by COP9 signalosome and deneddylase 1. Methods Enzymol **398:**509-22.

41. **You, J., M. Wang, T. Aoki, T. A. Tamura, and C. M. Pickart.** 2003. Proteolytic targeting of transcriptional regulator TIP120B by a HECT domain E3 ligase. J Biol Chem **278:**23369-75.

42. **Zhang, D. D., and M. Hannink.** 2003. Distinct cysteine residues in Keap1 are required for Keap1-dependent ubiquitination of Nrf2 and for stabilization of Nrf2 by chemopreventive agents and oxidative stress. Mol Cell Biol **23:**8137-51.

43. **Zhang, D. D., S. C. Lo, J. V. Cross, D. J. Templeton, and M. Hannink.** 2004. Keap1 is a redox-regulated substrate adaptor protein for a Cul3-dependent ubiquitin ligase complex. Mol Cell Biol **24:**10941-53.

44. **Zhang, D. D., S. C. Lo, Z. Sun, G. M. Habib, M. W. Lieberman, and M. Hannink.** 2005. Ubiquitination of Keap1, a BTB-Kelch substrate adaptor protein for Cul3, targets Keap1 for degradation by a proteasome-independent pathway. J Biol Chem **280:**30091-9.
45. **Zheng, J., X. Yang, J. M. Harrell, S. Ryzhikov, E. H. Shim, K. Lykke-Andersen, N. Wei, H. Sun, R. Kobayashi, and H. Zhang.** 2002. CAND1 binds to unneddylated CUL1 and regulates the formation of SCF ubiquitin E3 ligase complex. Mol Cell **10:**1519-26.
46. **Zhu, S., R. Perez, M. Pan, and T. Lee.** 2005. Requirement of Cul3 for axonal arborization and dendritic elaboration in Drosophila mushroom body neurons. J Neurosci **25:**4189-97.
47. **Zhu, X., A. K. Raina, H. G. Lee, G. Casadesus, M. A. Smith, and G. Perry.** 2004. Oxidative stress signalling in Alzheimer's disease. Brain Res **1000:**32-9.

V. STRUCTURE OF THE KEAP1:NRF2 INTERFACE PROVIDES MECHANISTIC INSIGHT INTO NRF2 SIGNALING

ABSTRACT

Keap1 is a BTB-Kelch substrate adaptor protein that regulates steady-state levels of Nrf2, a bZIP transcription factor, in response to oxidative stress. We have determined the structure of the Kelch domain of Keap1 bound to a 16-mer peptide from Nrf2 containing a highly conserved DxETGE motif. The Nrf2 peptide contains two short anti-parallel β strands connected by two overlapping type I β-turns stabilized by the aspartate and threonine residues. The β-turn region fits into a binding pocket on the top face of the Kelch domain and the glutamate residues form multiple hydrogen bonds with highly conserved residues in Keap1. Mutagenesis experiments confirmed the role of individual amino acids for binding of Nrf2 to Keap1 and for Keap1-mediated repression of Nrf2-dependent gene expression. Our results provide a detailed picture of how a BTB-Kelch substrate adaptor protein binds to its cognate substrate and will enable the rational design of novel chemopreventive agents.

INTRODUCTION

Eukaryote cells are constantly exposed to reactive molecules from endogenous and exogenous sources (Finkel and Holbrook, 2000; Jackson and Loeb, 2001). These molecules, including reactive oxygen species, electrophilic chemicals and heavy metals, damage biological macromolecules and impair normal cellular functions (Davies, 2000; Imlay, 2003). Oxidative damage has been implicated in diverse pathophysiological processes, including cancer, cardiovascular disease, diabetes and neurodegeneration (Ames and Shigenaga, 1993; Bonnefont-Rousselot, 2002; Ceconi et al., 2003; Ghanbari et al., 2004; Jackson and Loeb, 2001; Mhatre et al., 2004). Therapeutic approaches to protect against damage caused by reactive molecules would have broad ramifications for improving human health (Cash et al., 2002; Hamilton et al., 2004).

Eukaryote cells have evolved multiple protective mechanisms against reactive molecules. A major mechanism is the coordinated induction of enzymes that neutralize reactive molecules, eliminate damaged macromolecules and restore cellular redox homeostasis. In metazoan organisms, this cytoprotective response is controlled, in large part, by the Cap N' Collar (CNC) transcription factors, which constitute a unique subset within the bZIP transcription factor family (Mathers et al., 2004). In mammals, the CNC transcription factors include Nrf1, Nrf2, Nrf3, Bach1 and Bach2 (Motohashi et al., 2002). Phenotypic analysis of mice containing targeted deletions of individual or multiple CNC family members has revealed that Nrf1 and Nrf2 are the major regulators of cytoprotective gene expression (Leung et al., 2003; Yu and Kensler, 2005). Nrf1 and Nrf2 share a common domain structure, including a conserved N-terminal regulatory

domain termed Neh2, a central transactivation domain and a C-terminal bZIP domain required for heterodimer formation with members of the small Maf protein family, DNA-binding and both nuclear import and export (Bloom et al., 2002; Chan et al., 1993; Katoh et al., 2001; Li et al., 2005; Moi et al., 1994; Motohashi et al., 2002).

The Keap1 protein is the major negative regulator of cytoprotective gene expression (Dhakshinamoorthy and Jaiswal, 2001; Itoh et al., 1999). Keap1, a BTB-Kelch protein, is a substrate adaptor protein for a Cul3-dependent ubiquitin ligase complex (Cullinan et al., 2004; Kobayashi et al., 2004; Zhang et al., 2004). Under basal conditions, Keap1 targets Nrf2 for ubiquitin-dependent degradation and represses Nrf2-dependent gene expression (Wakabayashi et al., 2003; Zhang and Hannink, 2003). In cells exposed to reactive chemicals or oxidative stress, Nrf2 is no longer targeted for ubiquitin-dependent degradation (Kobayashi et al., 2006; Zhang and Hannink, 2003; Zhang et al., 2004). Instead, steady-state levels of Nrf2 increase, resulting in activation of Nrf2-dependent gene expression.

Keap1, as a substrate adaptor, bridges both Cul3 and Nrf2 using its N-terminal BTB and central linker domains to bind Cul3 and its C-terminal Kelch domain to bind the Neh2 domain of Nrf2 (Cullinan et al., 2004; Kobayashi et al., 2004; Zhang et al., 2004). Lysine residues within the Neh2 domain of Nrf2 are targeted for ubiquitin transfer mediated by the Cul3-associated Rbx1 protein and an ubiquitin-charged E2 protein (Zhang et al., 2004). Cyclical association and dissociation of this E3 ubiquitin ligase complex, mediated by the opposing actions of CAND1 and Cul3 neddylation, enables efficient ubiquitination of Nrf2 and repression of Nrf2-dependent gene expression (Lo and Hannink, 2006). This ubiquitin ligase complex is perturbed by reactive chemicals and

oxidative stress, which modify a number of reactive cysteine residues located in the BTB and linker domains of Keap1 (Dinkova-Kostova et al., 2002; Eggler et al., 2005; Hong et al., 2005a; Hong et al., 2005b; Wakabayashi et al., 2004; Zhang and Hannink, 2003).

We have determined structure of the Kelch domain of Keap1 bound to a peptide containing a conserved DxETGE motif located in the Neh2 domain of Nrf2. The binding pocket in Keap1 contains multiple charged and hydrophobic residues that contact the side-chains of the two glutamate residues and the peptide backbone. The DxETGE motif contains a β-turn region stabilized by the aspartate and threonine residues. Threonine phosphorylation prevents binding of the Nrf2-derived peptide to Keap1 and phosphomimetic mutations enable Nrf2 to escape Keap1-mediated repression. Keap1 dimerizes via its BTB domain and both Kelch domains within the Keap1 dimer are capable of independently binding to Nrf2. Our results provide insight into how Keap1 targets Nrf2 for ubiquitin-dependent degradation and will facilitate the rational design of novel therapeutic compounds that block binding of Nrf2 to Keap1.

MATERIALS AND METHODS

Recombinant DNA molecules and peptides. Eukaryote expression plasmids for the wild type Keap1, CBD-tagged Keap1, HA-tagged Nrf2 and Gal4-Neh2 proteins and the ARE-dependent reporter plasmid have been previously described (Zhang et al., 2004). The pET15b-based expression vector for the His-tagged Kelch domain of Keap1 has been described previously. Mutant Keap1 and Nrf2 cDNAs were generated by site-specific mutagenesis with standard overlap-extension techniques. All the genes used in this study were sequenced in the context of the expression vectors used for the experiments. Peptides were purchased from Sigma-Genosys and from Cell-tek and were supplied at greater than 95% purity following HPLC purification.

Cell culture, transfections, and reporter gene assays. COS1, MDA-MB-231, and HEK-293T cells were purchased from ATCC. Cells were maintained in either Dulbecco's modified Eagle's medium (DMEM) or Eagle's minimal essential medium (EMEM) in the presence of 10% fetal bovine serum (FBS). Transfections were performed with Lipofectamine Plus (Gibco BRL). Reporter gene assays were performed using the Promega Dual-Light assay system.

Antibodies, immuprecipitation, peptide competition and immunoblot analyses. The anti-Keap1 antibody has been described (Zhang and Hannink, 2003). Antibodies against Nrf2 (Santa Cruz), Chitin binding domain (New England Biolabs) and the HA epitope (Covance) were purchased from commercial sources. For immunoprecipitation, cell extracts were prepared in RIPA buffer (10 mM sodium phosphate pH [7.9], 150 mM

NaCl, 1% Triton X-100, 1% sodium deoxycholate, 0.1% Triton SDS) containing 1 mM dithiothreitol (DTT), 1 mM phenylmethylsulfonyl fluoride (PMSF) and protease inhibitor cocktail (Sigma). Soluble cell lysates were incubated with 2 μg of affinity-purified antibodies for 2 hr at 4°C followed by incubation at 4°C with protein A-agarose beads (Sigma) for 2 hr. Unbound proteins were removed by washing four times with lysis buffer. The immunoprecipitated proteins were eluted in sample buffer by boiling for 5 minutes, electrophoresed through SDS-polyacrylamide gels, transferred to nitrocellulose membranes and subjected to immunoblot analysis.

For peptide competition assay, COS1 cells were transfected with expression vectors for HA-Nrf2 and Keap1-CBD. The transfected cells were exposed to proteasome inhibitor MG132 for 4.5 h prior to cell lysis. Cell lysates were collected in ELB buffer (50 mM Hepes [pH 7.9], 250 mM NaCL, 0.1% Triton X-100, 5 mM EDTA) containing 1 mM DTT, 1 mM phenylmethylsulfonyl fluoride, protease inhibitor cocktail, and phosphatase inhibitors (1 mM EGTA, 1 mM Na3VO4, 100 mM NaF, 20 mM sodium pyrophosphate). The lysates (200 μg) were incubated with chitin bead at 4° C, pelleted by centrifugation (3,000 X g), and washed in ELB buffer. Proteins that remained associated with the chitin beads were further incubated with the peptides (10 ng, 100 ng, 1 μg, or 10 μg) at 4° C and, after several washes in ELB buffer, were analyzed by immunoblotting with anti-HA and anti-CBD antibodies.

Isothermal titration calorimetry. Isothermal titration calorimetry experiments were conducted at 25 °C in a MicroCal VP-ITC. The Kelch protein was dialyzed to equilibrium against the reaction buffer (50 mM Tris, pH 8.0, 100 mM NaCl, 5 mM DTT).

An aliquot of the dialysis reservoir was retained for preparing dilutions of the Kelch domain and peptide. Immediately prior to the experiment, the protein and peptide solutions were briefly degassed under vacuum. Additions (10 µL) of the peptide were made, at 4 min intervals, to samples of the Kelch domain contained in the 1.41 mL sample cell. In three experiments, a 5 µM solution of the Kelch domain was titrated with 50 µM peptide. In a fourth experiment, a 6.25 µM solution of the Kelch domain was titrated with 88 µM peptide. The integrated data from the four experiments were analyzed globally, employing a singe-site binding model, to extract estimates for the binding constant and binding enthalpy.

Crystallization and data collection. Purification of the Kelch domain was carried out as previously described (Li et al., 2004). Crystals were grown by hanging drop vapor diffusion at 4°C from 2 µl of a 1:3 molar ratio mixture of protein to peptide and 2 µl of well buffer.   Diffraction quality crystals grew within two days from a well buffer containing 0.2 M MgCl2, 0.1 M Tris HCl, and 30% w/v PEG 4000, at a protein concentration of 10 mg/ml. A single crystal was used to collect a 1.55 Å data set at $-180°$ C on beam line MBC 4.2.2 at the Advanced Light Source of Lawrence Berkeley National Laboratory. All data were indexed and integrated with d*Trek (Pflugrath, 1999). Data collection and refinement statistics are given in Table 3.

Structure solution and refinement. The structure of Kelch-peptide complex was determined by molecular replacement using MOLREP (Murshudov et al., 1997) and the structure of the Kelch domain (1U6D) as the search model. Refinement was performed with REFMAC 5.0 (Murshudov et al., 1999); progress was monitored by use of R_{free} and

5% of the data were set aside for cross-validation before refinement. Water molecules were placed in peaks greater than 3.0 σ in F_o-F_c maps and within hydrogen bonding distance to nitrogen or oxygen atoms of the protein, or other solvent atoms. TLS refinement (Winn et al., 2001) was performed with the protein and peptide as separate rigid bodies. Model building was done interactively using Coot (Emsley and Cowtan, 2004).

The final model of the protein consisted of 285 residues in the Kelch domain, 16 residues in the peptide, and 333 water molecules (Table 3). Residues are numbered according to the sequence of the intact Keap1 protein and Nrf2 proteins. Clear electron density was present for the backbone of all residues of the peptide; residues at the termini of the peptide are involved in crystal contacts with other molecules in the unit cell. Density for the side chains of five residues in the Kelch domain (Glu446, Arg447, Glu493, Gln528 and Lys551) and two in the peptide (T72 and E78) were not well defined and are represented as alanine residues. A total 17 residues have been modeled in two conformations, including one in the peptide (Q75). The model was evaluated by SFCHECK (Vaguine et al., 1999) and WHAT_CHECK (Hooft et al., 1996). Figures were prepared with PYMOL (De Lano, 2002). The coordinates have been deposited in the PDB with code 2FLU. The model has good geometry, with 91.6% of its residues in the most favored regions of the Ramachandran plot and 0.0% in the disallowed regions (Laskowski et al., 1993).

RESULTS

The structure of a complex between the Kelch domain of Keap1 and an Nrf2-derived peptide reveals how Nrf2 fits into the substrate binding pocket of Keap1.

The Kelch domain of Keap1 is a six-bladed β-propeller in which each blade of the propeller (I – VI) is comprised of four β-strands (A-D) (Figure 1A). (Li et al., 2004). The β-strands are connected by loops of varying lengths that project from the central core of the β-propeller. By convention (Wall et al., 1995), the short loops that connect either β-strands A and B (A-B) or β-strands C and D (C-D) define the bottom face of the β-propeller, while the longer loops that connect either β-strands D and A (D-A) or β-strands B and C (B-C) define the top face of the β-propeller.

The Neh2 domain contains two regions that are highly conserved from humans to flies (Figure 1B). One region, amino acids 17-32 in the human Nrf2 protein, contains a LxxQDxDLG motif (Katoh et al., 2005; McMahon et al., 2004). A second region, amino acids 77-82 in the human Nrf2 protein, contains a DxETGE motif (Kobayashi et al., 2002). Both of these motifs within Nrf2 bind to the same site in Keap1 but affinity of Keap1 for the DxETGE motif is approximately 100-fold higher than for the LxxQDxDLG motif (Tong et al., 2006).

To determine if the high-affinity DxETGE motif is sufficient for binding to Keap1, the ability of several different DxETGE-containing peptides to disrupt the Keap1-Nrf2 complex was determined. A complex between a Keap1 protein containing a C-terminal chitin-binding domain (Keap1-CBD) and a HA-tagged Nrf2 protein was isolated by affinity purification on chitin beads. The beads were incubated with increasing amounts of the peptides and levels of bound HA-Nrf2 determined. A marked reduction in

the amount of HA-Nrf2 that remained bound to the Keap1-CBD protein was observed following incubation with a 16-mer Nrf2-derived peptide containing amino acids 69 to 84, (AFFAQLQLDEETGEFL), (Figure 2A, lanes 11-14). A 14-mer peptide, containing amino acids 74 to 87 of Nrf2, (LQLDEETGEFLPIQ) was able to displace Nrf2 from Keap1 as effectively as the 16-mer (Figure 2A, lanes 7-10). A 10-mer Nrf2-derived peptide, containing amino acids 76 to 85 (LDEETGEFLP) was also able to displace Nrf2 from Keap1, although not quite as effectively as the two longer peptides (Figure 2A, lanes 3-6). This 10-mer peptide lacks one or more backbone interactions that stabilize the longer peptides (see Figure 4C). Isothermal titration calorimetry revealed that the 16-mer peptide bound to the Kelch domain of Keap1 with a K_d value of 20 nM (Figure 2B), in good agreement with the published K_d values ranging from 5 to 9 nM for binding of the Neh2 domain to the full-length Keap1 protein (Eggler et al., 2005; Tong et al., 2006).

The structure of the human Kelch domain bound to the 16-mer peptide was determined to 1.5 Å using X-ray crystallography (Figure 3). As predicted by our previous work (Li et al., 2004), and in agreement with the recent structural analysis of the mouse Kelch domain bound to a DxETGE-containing peptide (Padmanabhan et al., 2006), the Nrf2-derived peptide binds in the shallow pocket defined by the D-A and B-C loops on the top face of the Kelch domain (Figure 3). The peptide has two antiparallel β-strands connected by a turn region that has two overlapping type I β-turns (residues 77 to 80 and 78 to 81; Figure 4C). The turn region is stabilized by hydrogen bonds involving the side chains of D77 and T80 and the peptide backbone (Figure 4C). Complex formation buries 420 Å^2 of surface area on the Kelch β-propeller.

Glutamate residues E79 and E82 are the only peptide residues whose side chains make specific interactions with the Kelch domain (Figure 4A, Table 1). The carboxylate oxygen atoms of E79 contact the side chains of Arg415, Arg483, and Ser508, while the carboxylate oxygen atoms of E82 make hydrogen bonds with the side chains of Ser363, Asn382, and Arg380. The peptide backbone makes five contacts with the Kelch domain, four from the carbonyl oxygen atoms of E78, E79, T80, and F83, and one from a backbone amide group of F83 (Figure 4B).

Solvent molecules mediate additional contacts between the peptide and the Kelch domain (Table 2), enabling an additional contact between E79 and Arg415 and allowing E82 to interact with both Asn414 and Ser602. The carboxylate oxygen atom of D77 contacts two water molecules that make bridging hydrogen bonds with Arg415 and Arg380. The hydroxyl group of T80 utilizes a water molecule to interact with Arg380.

All six blades of the Kelch β-propeller contribute to complex formation (Table 1). Kelch domain residues that contact the side chains of the peptide are concentrated on one side of the binding pocket in blades II, III, IV, and V, while residues that contact backbone atoms of the peptide or participate in van der Waals interactions are located on the other side of the binding pocket in blades V, VI, I and II (Tables 1 and 2).

Side chains from six residues in Keap1 (Ser363, Asn382, Arg380, Arg415, Arg483, and Ser508) participate in hydrogen bond interactions with the carboxylate oxygen atoms from E79 and E82 in the peptide (Figure 4A). Some of these six residues also participate in other interactions with the peptide. For instance, the backbone amide of Asn382 interacts with the carbonyl oxygen of F83, and the side chains of both Arg415 and Arg380 form a hydrogen bond to a solvent water molecule that bridges to the

carboxylate oxygen of D77 (Table 2). Side chains from five additional residues in Keap1 participate in hydrogen bonding with the peptide backbone: these are Tyr334, Asn382, Gln530, Ser555 and Ser602 (Figure 4B). Finally, the side chains from seven residues in Keap1 participate in van der Waals interactions with the peptide, including Tyr 334, Asn387, Arg415, Ser508, Tyr525, Tyr572 and Phe577 (Table 1).

Identification of amino acids within the binding pocket of Keap1 that are required for binding to Nrf2. An extensive alanine-scan mutagenesis of Keap1 was performed to determine the contribution of specific amino acids in Keap1 for binding of Nrf2. Twelve Keap1 mutants that contained alanine substitutions for three or four adjacent residues within each B-C loop were constructed (Table 1). The ability of the mutant Keap1 proteins to bind Nrf2 was determined by co-immunoprecipation and their ability to repress Nrf2-dependent transcription was determined by a reporter gene assay using an ARE-dependent luciferase gene. Eight of the twelve mutant Keap1 proteins were impaired in their ability to bind to Nrf2 and to repress Nrf2-dependent gene transcription (Figures 5A and 5B).

The alanine-scan mutagenesis was refined in second set of mutant Keap1 proteins, in which 13 amino acids in the B-C loops, each with a surface-exposed side-chain, were individually mutated to alanine (Table 1). Substitution of individual alanine residues for Tyr334, Asn382, His436, Tyr525, and Tyr572 significantly disrupted the ability of Keap1 to bind Nrf2 and repress Nrf2-dependent transcription (Figures 5C and 5D). With the exception of His436, all of these residues were observed in the crystal structure to participate in contacts with the Nrf2-derived peptide (Figure 4 and Tables 1 and 2). It is

not clear why alanine substitution at His436 perturbed the ability of Keap1 to bind Nrf2, as the circular dichroic (CD) spectrum of the His436A Kelch domain is nearly identical to the CD spectrum of the wild-type Kelch domain (supplemental Figures 1 and 2). An additional residue, Phe478, was not required for binding to Nrf2 (Figure 5C), but was required for repression of Nrf2-dependent gene expression (Figure 5D). Further analysis revealed that this mutant was defective for directing ubiquitination onto Nrf2 (data not shown).

A third set of mutant Keap1 proteins were constructed in which six arginine residues and one lysine residue, all with surface-exposed side chains, were substituted with alanine residues (Table 1). This analysis identified three arginine residues (Arg380, Arg415, Arg483) that were required for binding to Nrf2 and for repression of Nrf2-dependent gene expression (Figures 5E and 5F). As seen in the crystal structure, the side-chains of these three arginine residues are involved in multiple contacts with the Nrf2-derived peptide (Figure 4 and Tables 1 and 2).

A final set of mutant Keap1 proteins were constructed that contained alanine residues individually substituted for four serine residues located in the D-A loops, Ser363, Ser508, Ser555 and Ser602 (Table 1). Although the side-chains of these serine residues are involved in hydrogen bond interactions with the Nrf2-derived peptide (Figure 4), individual alanine substitutions of these serine residues did not significantly reduce the ability of Keap1 to bind to Nrf2 or to repress Nrf2-dependent gene expression (Figures 5G and 5H).

Keap1 forms a homodimer capable of binding two Nrf2 molecules. The structure of the human Kelch domain bound to a 16-mer Nrf2-derived peptide and the recently published structure of the murine Kelch domain bound to a shorter Nrf2-derived peptide (Padmanabhan et al., 2006) indicate that the Kelch domain of Keap1 contains a single binding site for the DxETGE motif in Nrf2. As Keap1 dimerizes via its N-terminal BTB domain (Zipper and Mulcahy, 2002), the structural data is consistent with the notion that Keap1 and Nrf2 form a complex with a 2:2 stoichoimetry. However, several recent reports have suggested that the Keap1 dimer binds one Nrf2 polypeptide, resulting in a 2:1 stoichiometry (Eggler et al., 2005; Tong et al., 2006). As these in vitro biochemical experiments used high concentrations of purified proteins obtained from prokaryote expression systems, the stoichiometry of the Keap1:Nrf2 complex in the more complex environment of a eukaryote cell remains an open question.

To confirm that Keap1 exists as a dimer in eukaryote cells, a CBD-tagged Keap1 protein was co-expressed in HEK 293T cells along with an untagged Keap1 protein. The untagged Keap1 protein was pulled down with chitin beads only in the presence of CBD-tagged Keap1 (Figure 6A, second panel from top, compare lane 13 with lane 14). This result is consistent with a prior report that protein-protein interactions involving the N-terminal BTB domain enable Keap1 to form a homodimer (Zipper and Mulcahy, 2002), although the possibility that Keap1 forms higher order oligomeric structures in cells can not be ruled out. As expected, Nrf2 was pulled down with chitin beads in the presence of the CBD-tagged wild-type Keap1 protein (Figure 6A, top panel, lanes 11 and 12).

Next, we generated heterodimeric Keap1 complexes containing one wild-type Kelch domain and one mutant Kelch domain to determine if the presence of a single

functional Kelch domain in a Keap1 dimer would be sufficient to bind Nrf2. A CBD tag was appended to the mutant Keap1 protein such that two types of Keap1 dimers would be isolated on chitin beads: a Keap1 homodimer containing two mutant Kelch domains and a Keap1 heterodimer containing one wild-type and one mutant Kelch domain. Three mutant Keap1 proteins were used for this analysis, including two that were unable to bind Nrf2 on their own (Y334A and R415A) and one (Q337A) that was able to bind Nrf2 as well as the wild-type Keap1 protein. The ability of the homodimeric and heterodimeric complexes to bind Nrf2 was assessed by chitin pull-down followed by immunoblot analysis. As expected, no Nrf2 was pulled down with chitin beads in the presence of either the Keap1-Y334A and Keap1-R415A proteins (Figure 6A, upper panel, lanes 2 and 8). However, co-expression of the wild-type untagged Keap1 protein with either of these two mutant Keap1 proteins partially restored pulldown of Nrf2 (Figure 6A, upper panel, compare lanes 3, 9 and 12). Partial restoration of Nrf2 pulldown is expected, as only a portion of the dimeric Keap1 complexes isolated on chitin beads would have one wild-type Kelch domain with the remainder of the Keap1 complexes containing two non-functional Kelch domains. These results demonstrate that a single functional Kelch domain within the context of a Keap1 dimer is sufficient to bind Nrf2.

Finally, we asked if the Keap1 dimer is capable of binding two different Nrf2 proteins. The Neh2 domain of Nrf2 was fused onto the Gal4 DNA binding domain and co-expressed with HA-tagged full-length Nrf2 protein in the absence or presence of co-expressed Keap1. Cell lysates were immunoprecipitated with anti-HA antibodies and the resultant immunoprecipitates were probed for the presence of the Gal4-Neh2 protein using anti-Gal4 antibodies. The Gal4-Neh2 protein was only present in the anti-HA

immunoprecipitates in the presence of co-expressed Keap1 (Figure 6B, upper panel, compare lanes 2 and 3). Thus, the Keap1 protein functions as a bridge between the HA-Nrf2 protein and the Gal4-Neh2 protein. A single alanine substitution for T80 within the DxETGE motif of HA-Nrf2 abolished co-immunoprecipitation of the Gal4-Neh2 protein (Figure 6B, upper panel, lane 4). The Keap1-Y334A protein, which is not able to bind either HA-Nrf2 or Gal4-Neh2, is not able to bridge the two Nrf2 proteins (Figure 6B, upper panel, lane 5). Likewise, the isolated Kelch domain, which is not able to form a homodimer, is not able to bridge the two Nrf2 proteins although it readily binds to the HA-Nrf2 protein (Figure 6B, upper panel, lane 6). These results indicate that a Keap1 dimer is able to bridge two different DxETGE-containing proteins, consistent with the notion that Keap1 and Nrf2 can form a 2:2 stoichiometric complex.

Phosphorylation of the conserved threonine within the DxETGE motif in Nrf2 disrupts binding to Keap1. The crystal structure of the Nrf2-derived peptide bound to the Kelch domain revealed the presence of two overlapping type I β-turns, residues 77-80 and 78-81, in which the side-chains of D77 and T80, respectively, form hydrogen bonds with the peptide backbone. The threonine residue T80 was of particular interest, given the possibility that phosphorylation of this residue might interfere with formation of the β-turn and prevent binding of Nrf2 to Keap1.

Peptide competition experiments were carried out using 14-mer peptides that contained either an alanine or phosphothreonine in place of T80. A 14-mer peptide corresponding to amino acids 74 to 87 of Nrf2 that contained an alanine in place of T80 was unable to displace HA-Nrf2 from Keap1-CBD even at input peptide levels 100-fold

higher than needed for the wild-type peptide to displace Nrf2 from Keap1 (Figure 7A, compare lanes 3-6 with lanes 7-10). Likewise, a 14-mer peptide that contained a phosphothreonine residue in place of T80 was also unable to displace Nrf2 from Keap1 (Figure 7A, lanes 11-14).

To examine the importance of T80 for Keap1-mediated repression of Nrf2-dependent gene expression in cells, we characterized several mutant Nrf2 proteins in which T80 was altered to alanine, serine, or to the phosphomimetic glutamate or aspartate, respectively. Consistent with the peptide competition experiments, the T80A Nrf2 mutant protein did not bind Keap1 and was resistant to Keap1-mediated repression of Nrf2-dependent gene expression (Figure 7B, top panel, lane 2; Figure 7C). Nrf2 proteins containing either of the phosphomimetic substitutions (T80D and T80E) were also impaired in binding to Keap1 and were not subject to Keap1-mediated repression (Figure 7B, top panel, lanes 4 and 5; Figure 7C). In contrast, the T80S mutant Nrf2 protein behaved essentially like the wild-type Nrf2 protein, with only a slight reduction of binding of Nrf2 to Keap1 and Keap1-mediated repression (Figure 7B, top panel, lane 3; Figure 7C). These results indicate that the hydroxyl group of the serine residue is an effective substitute for the hydroxyl group of the threonine residue in stabilizing the β-turn of the DxETGE motif. In contrast, either the absence of the threonine hydroxyl group or the presence of a negative charge disrupts the β-turn region and likely prevents the flanking glutamate residues from interacting with their cognate residues in Keap1.

DISCUSSION

The ability of cullin-dependent ubiquitin ligase complexes to carry out protein ubiquitination in a highly specific and regulated manner derives from the ability of substrate adaptor proteins to recognize their substrates with high affinity and specificity. The substrate adaptor proteins for the Cul1 and Cul2 proteins have been intensively studied and structural analyses have provided a detailed understanding of their ability to recognize specific substrates (Hon et al., 2002; Min et al., 2002; Orlicky et al., 2003; Wu et al., 2003). Recent work has suggested that the BTB-Kelch proteins, defined by an N-terminal BTB domain and a C-terminal Kelch domain, function as substrate adaptor proteins for Cul3 (Cullinan et al., 2004; Furukawa and Xiong, 2005; Kobayashi et al., 2004; Kobayashi et al., 2006; Wang et al., 2005; Zhang et al., 2004; Zhang et al., 2005). In this report, we have determined the structure of the Kelch domain of human Keap1 bound to a 16-mer peptide derived from its substrate, Nrf2. Together with a structure of the Kelch domain of murine Keap1 bound to a 9-mer Nrf2-derived peptide published while this manuscript was under review (Padmanabhan et al., 2006), these structural studies provide a detailed picture of how Keap1 binds Nrf2.

Comparison of amino acid contacts between the Kelch domain and the Nrf2-derived peptide with functional analysis of mutant Keap1 proteins containing individual alanine substitutions indicates that charged residues and hydrophobic residues located in the binding pocket of Keap1 are the major contributors to the stability of the complex. In particular, the side chains of Tyr334, Arg380, Asn382, Arg415, Arg483, Tyr525, and Tyr572 in Keap1 each contact the Nrf2-derived peptide and individual alanine substitutions for these residues significantly impairs binding to Nrf2 and repression of

Nrf2-dependent gene expression. In contrast, individual alanine substitutions of four serine residues (Ser363, Ser508, Ser555 and Ser602) that directly contact the Nrf2-derived peptide did not significantly impair binding of Nrf2 or repression of Nrf2-dependent transcription. Thus, hydrogen bond contacts between these serine residues and Nrf2 do not contribute significantly to the overall stability of the Keap1:Nrf2 complex. Nevertheless, the overall agreement between our structural and functional studies indicate that the crystal structure of the complex between the Kelch domain of Keap1 and the Nrf2-derived peptide is an accurate representation of amino acid contacts between the full-length Keap1 and Nrf2 proteins.

Our structural and functional studies provide strong support for the notion that the DxETGE motif is the principal Keap1 binding site in Nrf2. The lysine residues in Nrf2 that are targeted for ubiquitination are located 10-30 amino acids on the N-terminal side of the DxETGE motif (Zhang et al., 2004). Binding of Nrf2 to Keap1 via the DxETGE motif would position these residues for ubiquitin transfer. A second Keap1 binding site in Nrf2, containing the consensus sequence LxxQDxDLG and located approximately 50 amino acids on the N-terminal side of the DxETGE motif, has recently been identified (Tong et al., 2006). The LxxQDxDLG motif binds in the substrate-binding pocket of the Kelch domain although the affinity of Keap1 for the LxxQDxDLG motif is approximately two orders of magnitude less than for the DxETGE motif. Yamamoto and coworkers have proposed a model in which one Nrf2 polypeptide, via both the DxETGE and the LxxQDxDLG motifs, bridges the two Kelch domains in the Keap1 homodimer (Tong et al., 2006). This model is supported by in vitro biochemical experiments using purified proteins that suggest a 2:1 stoichiometry of the Keap:Nrf2 complex (Eggler et

al., 2005; Tong et al., 2006). In contrast, our experiments, performed by ectopic expression of Keap1 and Nrf2 proteins in the complex intracellular milieu of a eukaryote cell, indicate that the two Kelch domains of a Keap1 homodimer are capable of binding independently to two different Nrf2 polypeptides, consistent with a 2:2 stoichiometry for the Keap:Nrf2 complex. A structure-based model of the Keap1:Cul3:Rbx1 complex suggests that the two Kelch domains in the Keap1 dimer are spatially separated (Stogios et al., 2005), consistent with the notion that each Kelch domain can independently present a substrate protein to the E2 conjugating enzyme recruited into the E3 ubiquitin ligase complex by Rbx1. As this structural model is largely based on computational modeling, detailed structural and functional analysis of the entire ubiquitin ligase complex is needed to provide further insight into how Keap1 presents Nrf2 as a substrate for ubiquitination.

Keap1 constitutively targets Nrf2 for ubiquitin-dependent degradation under basal conditions of cell growth. Following exposure of cells to electrophilic chemicals or overt oxidative stress, Nrf2 is able to escape Keap1-mediated degradation, accumulate in the nucleus and activate gene expression. The prevailing model for activation of Nrf2 is that reactive chemicals and oxidative stress modify one or more cysteine residues in Keap1 that are located in the BTB and linker domains (Dinkova-Kostova et al., 2002; Eggler et al., 2005; Hong et al., 2005a; Hong et al., 2005b; Wakabayashi et al., 2004; Zhang and Hannink, 2003). As a result, the ability of Keap1 to assemble into a functional E3 ubiquitin ligase complex with Cul3 is perturbed and Nrf2 is no longer efficiently targeted for ubiquitin-dependent degradation although Nrf2 remains associated with Keap1 (Kobayashi et al., 2006; Zhang and Hannink, 2003; Zhang et al., 2004). However, our present results indicate that phosphorylation of threonine residue T80 within the

DxETGE motif markedly decreases the ability of an Nrf2-derived peptide to compete with Nrf2 for binding to Keap1 in vitro. Futhermore, phosphomimetic mutants of Nrf2 escape Keap1-mediated repression in cells. As the side chain of T80 participates in hydrogen bonds that stabilize the β-turn which, in turn, enables the DxETGE motif to fit into the binding pocket of Keap1, phosphorylation of T80 is likely to perturb the conformation of the peptide so that is unable to fit into the binding site on Keap1. The bulky phosphoryl group may also provide steric hinderance. Although phosphorylation of T80 has not been demonstrated in vivo, an intriguing hypothesis is that phosphorylation of T80 may enable activation of Nrf2 in the absence of overt exposure to electrophilic compounds or oxidative stress. A detailed investigation of the phosphorylation status of T80 in Nrf2 in vivo will provide novel insights into the multiplicity of pathways that can lead to activation of Nrf2-dependent gene expression.

Keap1 is one of 49 BTB-Kelch proteins encoded by the human genome. Point mutations in the Kelch domain of several BTB-Kelch proteins, including Keap1, gigaxonin and ENC1, have been associated with human diseases (Figure 1A). In the case of Keap1, one gene variant (G364C) and one somatic mutation (G430C) have been associated with lung cancer (Padmanabhan et al., 2006). The G364C mutation is located in the A-D loop of blade I and likely disrupts the substrate binding pocket, while the G430C mutation is adjacent to the B strand in blade III and likely disrupts the structure of the Kelch domain. As expected, both of these mutant Keap1 proteins are impaired in their ability to bind Nrf2 (Padmanabhan et al., 2006). A number of disease-associated point mutations within the Kelch domains of both gigaxonin and ENC1 have been described (Bomont et al., 2000; Bomont et al., 2003; Kuhlenbaumer et al., 2002; Liang et al., 2004)

and it is likely that these mutations will perturb the association of gigaxonin and ENC1 with their respective substrate proteins. Furthermore, as the overall dimensions of the substrate binding pocket, formed by the D-A and the B-C loops, is likely to be very similar in other BTB-Kelch proteins, substrate(s) for other BTB-Kelch proteins may also utilize β-turn motifs to bind their cognate substrate adaptor. The Keap1 protein has emerged as a representative prototype for the BTB-Kelch proteins and a detailed understanding of the structure and function of Keap1 will continue to illuminate our understanding of this large and important family of human proteins.

This chapter was reproduced with the expressed written permission of European Molecular Biology Organization.

Table V-1

Blade[a]	Loop[b]	Amino acid[c]		Mutant Phenotype[d]	Nrf2 contact[e]
VI/I	D-A	S	602	+	T80 bb
I	B-C (N)	YFR	334-336	-	
I	B-C (C)	QSL	337-339	-	
I	B-C	Y	334	-	F83 bb
I	B-C	F	335	+	
I	B-C	R	336	+	
I	B-C	Q	337	+	
I/II	D-A	S	363	+	E82 sc
II	B-C (N)	NNSP	381-384	-	
II	B-C (C)	DGNT	385-388	+	
II	B-C	R	380	-	E82 sc
II	B-C	N	382	-	F83 bb; E82 sc
II	B-C	P	384	+	
II	B-C	N	387	+	
II/III	D-A	R	415	-	E79 sc; E79 vw; T80 vw
III	B-C (N)	SHG	431-433	+	
III	B-C (C)	CIH	434-436	-	
III	B-C	C	434	+	
III	B-C	H	436	-	
III/IV	D-A	R	459	+	
IV	B-C (N)	FDG	478-480	-	
IV	B-C (C)	TNR	481-483	-	
IV	B-C	F	478	-	
IV	B-C	R	483	-	E79 sc
IV/V	D-A	S	508	+	E79 sc
V	B-C (N)	YDG	525-527	-	
V	B-C (C)	ADQ	528-530	+	
V	B-C	Y	525	-	E79 vw
V	B-C	Q	530	+	E78 bb
V/VI	D-A	K	551	+	
V/VI	D-A	R	553	+	
V/VI	D-A	S	555	+	E79 bb
VI	B-C (N)	YDG	572-574	-	
VI	B-C (C)	HTF	575-577	+	
VI	B-C	Y	572	-	L76 vw; G81 vw
VI	B-C	F	577	+	G81 vw

Table V-1.

a: The six blades of the Kelch β-propeller are labeled I through VI.

b: The four β-strands of each blade of the Kelch β-propeller are labeled A through D.

c: The amino acid number of the indicated residue in the human Keap1 protein.

d: The ability of mutant Keap1 proteins containing an alanine substitution for the indicated amino acid to repress Nrf2-dependent transcription. A "+" indicates that the mutant Keap1 protein is equivalent to the wild-type Keap1 protein, while a "-" indicates that the mutant Keap1 protein is significantly impaired in terms of repression of Nrf2-dependent transcription.

e: Amino acids in Nrf2 contacted by the indicated residue in the human Keap1 protein. A "bb" indicates that the sidechain of the Keap1 residue contacts the backbone of the Nrf2 peptide; A "sc" indicates that the sidechain of the Keap1 residue contacts the sidechain of the Nrf2 residue; A "vw" indicates that the sidechain of the Keap1 residue participates in hydrophobic van der Waals interactions with the Nrf2 residue.

Table V-2

Peptide residue/ atom	Kelch residue/ atom	Distance (Å)	Bridging water	Distance (Å)	Kelch residue/ atom	Distance (Å)
D77 OD2			HOH 110	2.57	Arg415 NH1	2.76
			HOH 125	2.80	Arg380 NH1	2.90
E78 O	Gln530 NE2	2.98				
E79 O	Ser555 OG	2.59				
E79 OE1	Ser508 OG	2.63				
	Arg415 NH2	2.72				
	Arg415 NH1	3.04				
E79 OE2	Arg483 NH2	3.17				
	Arg483 NE	2.70				
			HOH 176	2.98	Arg415 NH1	3.14
T80 O	Ser602 OG	2.77				
T80 OG1			HOH 45	2.75	Arg380 NH1	3.04
E82 OE1	Asn382 ND2	2.98				
	Arg380 NH1	2.82				
	Arg380 NE	2.82				
E82 OE2	Ser363 OG	2.63				
			HOH 33	2.97	Asn414 OD1	2.80
			HOH 4	2.75	Ser602 OG	2.94
F83 O	Asn382 ND2	2.99				
F83 N	Try334 OH	3.34				

Table V-3

Data collection statistics	
Wavelength (Å)	1.239
Space group	$P2_12_12$
Cell (Å)	a= 76.76 b= 92.07 c= 46.31
No. molecules per asu	1
Resolution (Å)	36.42 -1.50
Mosaicity (°)	0.34
No. observations	321,494
No. unique reflections	50,551
Redundancy	6.3 (3.3)
R_{merge} (%)	7.7 (45.6)
Mean I/σ_I	11.1 (2.1)
Completeness (%)	94.7(64.6)
Refinement statistics	
Resolution range (Å)	36.0-1.50
[a]R_{cryst}	17.9
[b]R_{free}	19.9
Rmsd bond distance (Å)	0.009
Rmsd bond angle (°)	1.211
Total no. non-H atom in asu	2,728
No. of solvent molecules	333
Avg. peptide B-value ($Å^2$)	18.1
Avg. protein B-value ($Å^2$)	16.9
Avg. solvent B-value ($Å^2$)	30.2

Numbers in parentheses refer to statistics for outer resolution shell (1.55-1.50 Å).

[a]$R_{cryst} = \sum|F_o\text{-}F_c|/\sum|F_c|$ where F_o and F_c are observed and calculated structure factors, respectively.

[b]R_{free} is the R factor calculated from 5% of the reflections not included in refinement. No σ-cutoff of the data was used.
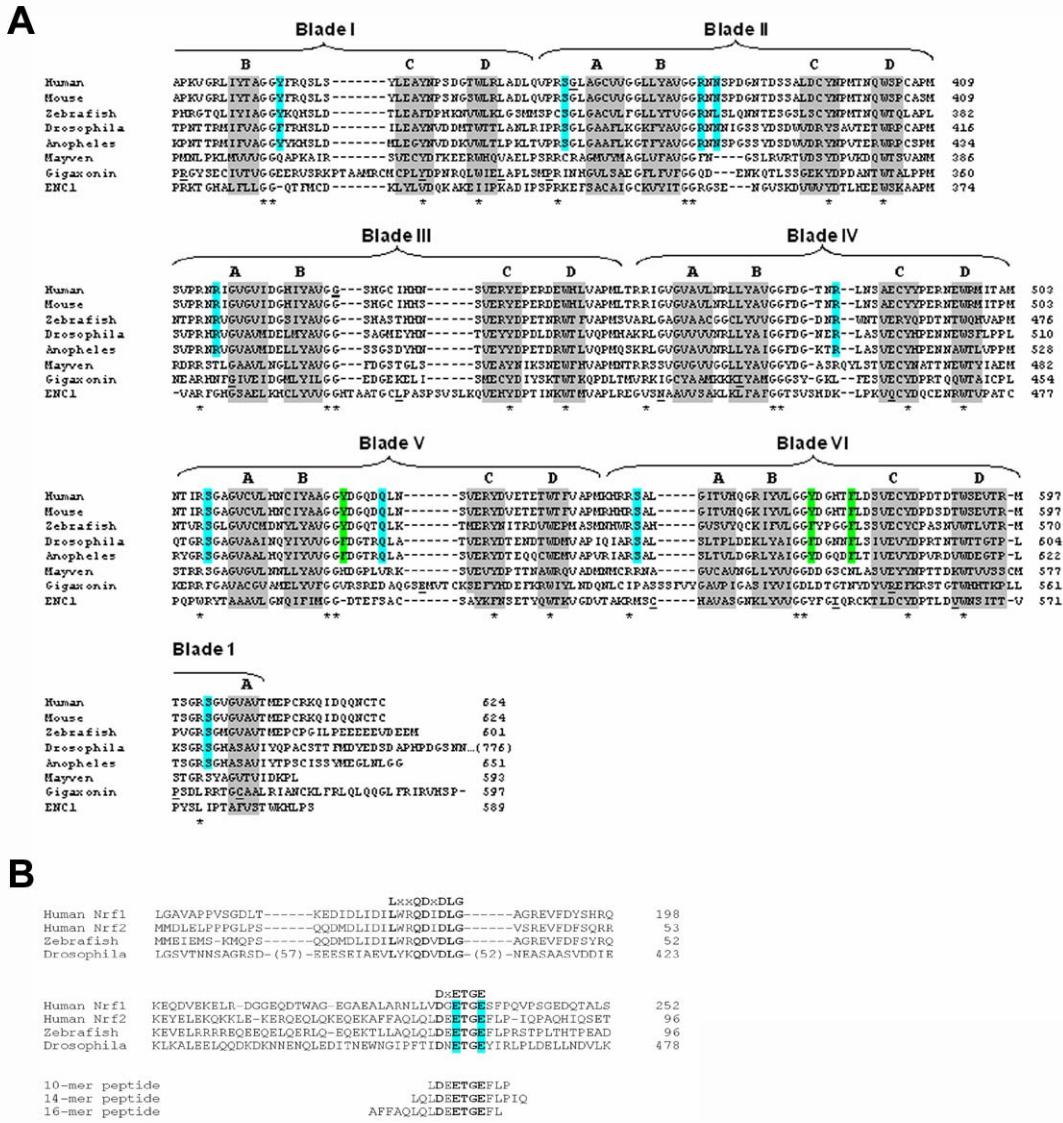
Figure V-1

Figure V-1. Sequence alignments among orthologues of Keap1 or Nrf2. (**A**) The sequence of the Kelch domains from the Keap1 protein of five different species (human, mouse, zebrafish, *Drosophila melanogaster* and *Anopheles gambia* are shown, along with the sequence of three human BTB-Kelch proteins, mayven, gigaxonin and ENC1. The six blades of the β-propeller structure are indicated above the alignment and the four β-strands (A-D) that comprise each blade are highlighted in gray. The A strand for blade I is located at the extreme C-terminus of the protein. Disease-associated mutations in Keap1, gigaxonin and ENC1 proteins are underlined in bold (Bomont et al., 2000; Bomont et al., 2003; Bruno et al., 2004; Kuhlenbaumer et al., 2002; Liang et al., 2004; Padmanabhan et al., 2006). Highly conserved residues that define the Kelch repeat are indicated by asteriks. Amino acids in Keap1 whose side chains contact the Nrf2-derived peptide in the crystal structure are highlighted in blue, while those amino acids that only make van der Waals contacts with the Nrf2-derived peptide are highlighted in green. (**B**) The Neh2 domain from the human Nrf1 and Nrf2 proteins are shown, along with the corresponding regions of Nrf2-related proteins from zebrafish and *Drosophila melanogaster*. Two conserved motifs that have been implicated in binding to Keap1 are shown. The glutamate residues of the DxETGE motif are highlighted in blue. The sequence of the three Nrf2-derived peptides used in our experiments is shown.

Figure V-2
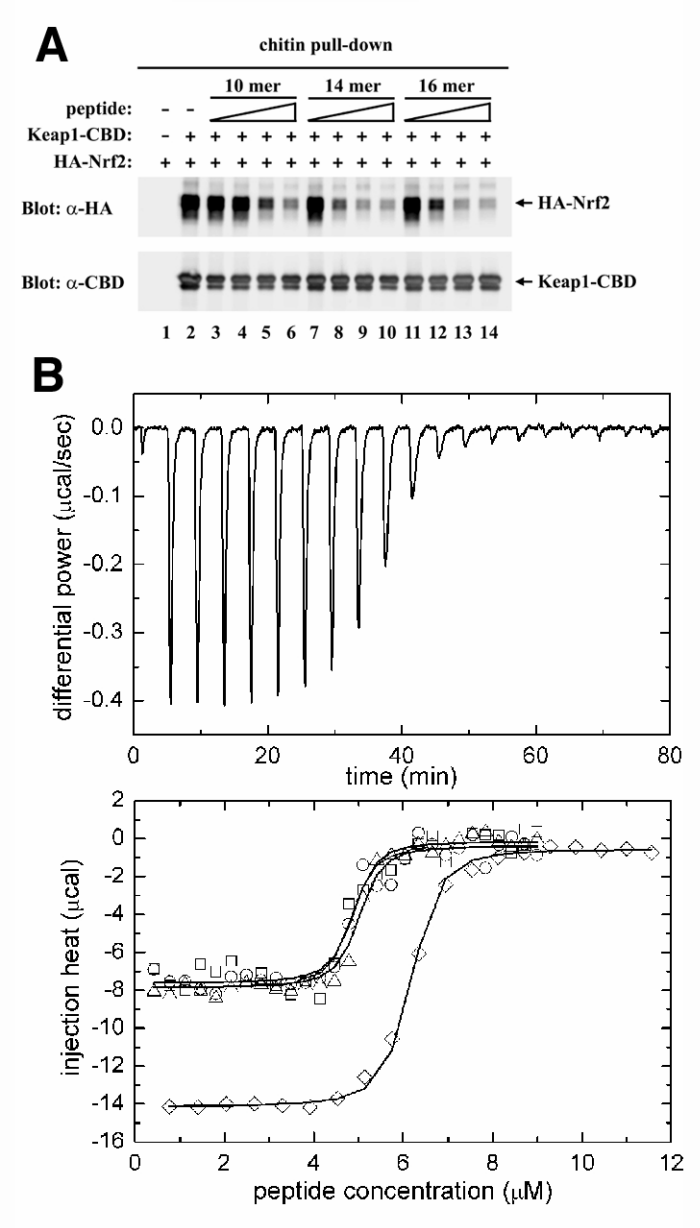
Figure V-2. Specific bindings between Keap1 and the Nrf2-derived peptides. (A). COS1 cells were transfected with expression vectors for Keap1-CBD and HA-Nrf2 and the Keap1:Nrf2 complex isolated on chitin beads. The beads were incubated with the indicated peptides, washed and proteins that remained bound to the beads were analyzed by immunoblot with anti-HA and anti-CBD antibodies. The amounts of peptides added to each sample were 10 ng (lanes 3, 7, 11), 100 ng (lanes 4, 8, 12), 1 µg (lanes 5, 9, 13) and 10 µg (lanes 6, 10, 14). **(B)** (Upper panel) Thermographs from a representative isothermal calorimetry experiment are shown, in which a 5 µM solution of the Kelch domain was titrated with 50 µM peptide are shown. (Lower panel) The fitted binding isotherms from four experiments are shown. Three experiments, (circles, squares and triangles), were perfomed using by titrating a 50 µM peptide solution into a 5 µM solution of the Kelch domain. A fourth experiment (diamonds) was performed by titrating an 88 µM solution of the peptide into a 6.25 µM solution of the Kelch domain.

Figure V-3
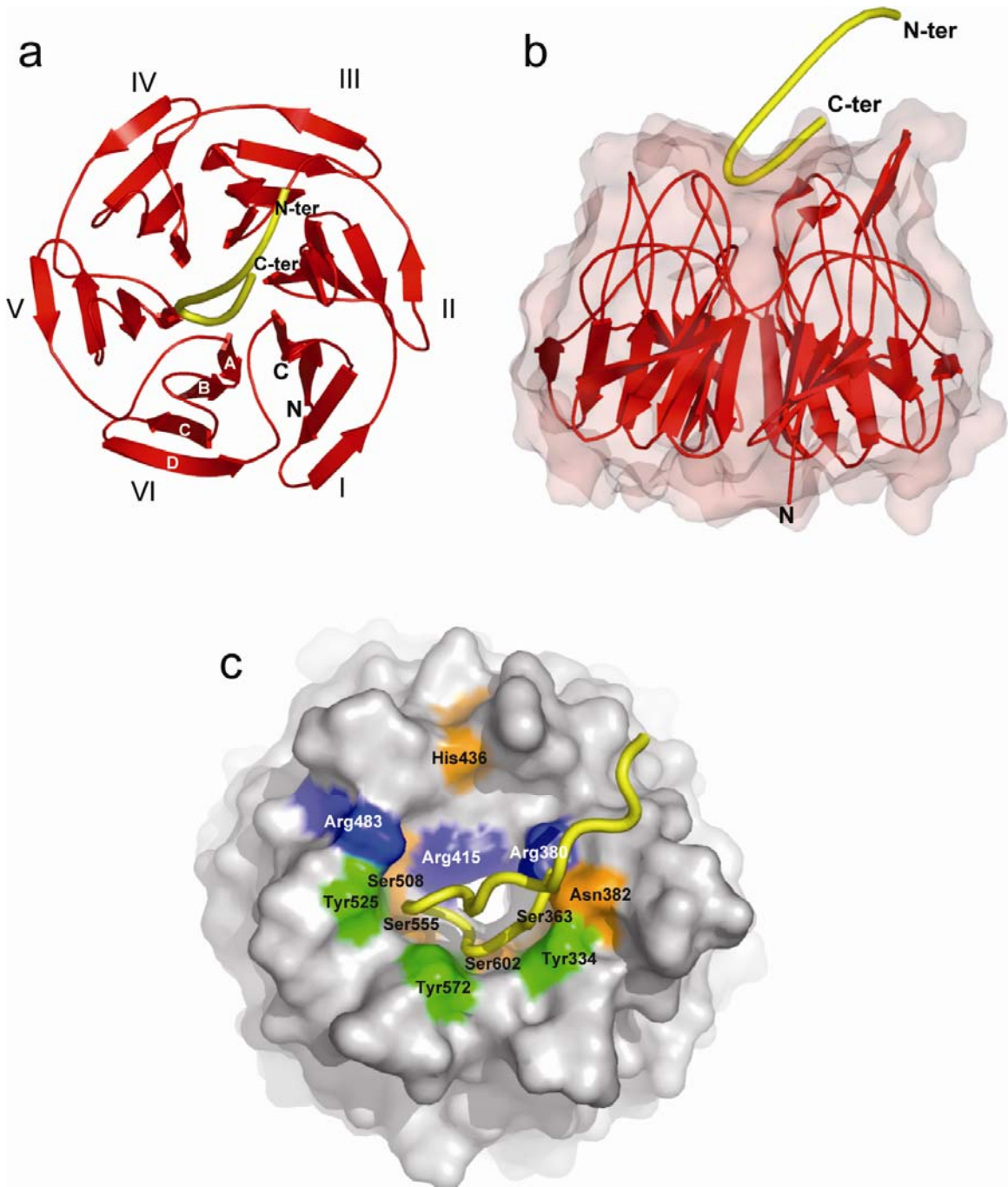
Figure V-3. Three-dimensional structure of the complex consisting of a Kelch β-propeller domain and an Nrf2-derived peptide. (**A**) A ribbon diagram of the Kelch β-propeller (red) and bound Nrf2 peptide (yellow tube). The termini of the peptide are labeled N-ter and C-ter; those of the Kelch domain are labeled N and C. The six blades of the β-propeller are labeled I-VI and the four β-strands found in each blade are labeled A-D (white font) on blade VI. (**B**) Side view of the Kelch domain, with a surface representation of the β-propeller. (**C**) A surface representation of the Kelch propeller (gray) and peptide (yellow tube). Selected residues are shown in blue (basic), orange (polar), and green (apolar).

Figure V-4
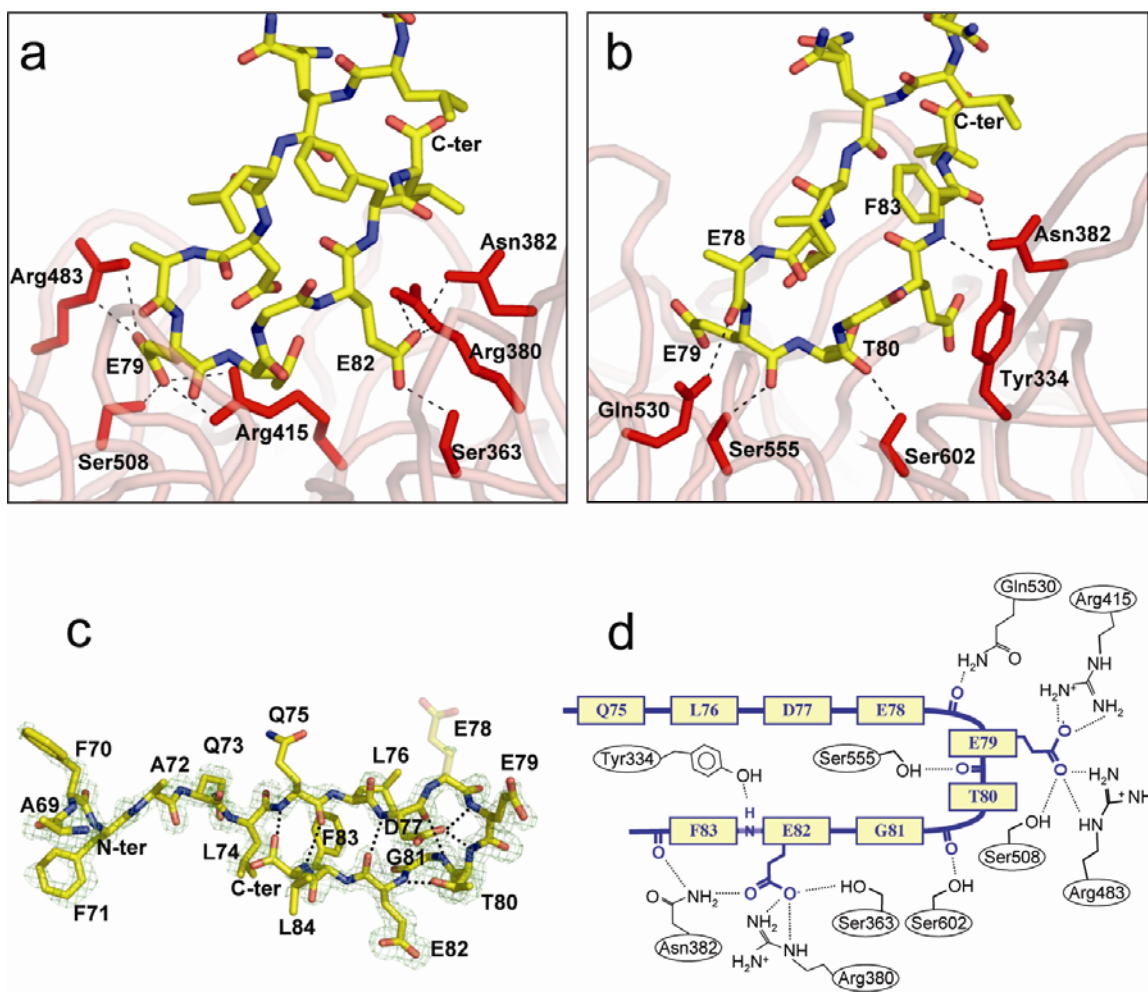
Figure V-4. Intermolecular and intramolecular contacts within the Kelch domain and the bound Nrf2 peptide. (**A**) Contacts between the side chain atoms of the Nrf2 peptide and residues in the Kelch domain. (**B**) Contacts between the backbone atoms of the peptide and residues of the Kelch domain. (**C**) A stick model of the Nrf2 peptide, with intramolecular hydrogen bonds highlighted. An F_o-F_c elecron density omit map, contoured at 2.5 σ for the vicinity of the peptide is shown in blue. Phases for the map were determined immediately following molecular replacement, prior to the inclusion of the peptide in the model. The side chain of E78 was not well ordered in the electron density maps and is shown as semi-transparent. (**D**) A schematic showing both backbone and side chain contacts to the Nrf2 peptide (yellow/blue) from interacting residues in the Kelch domain.

Figure V-5
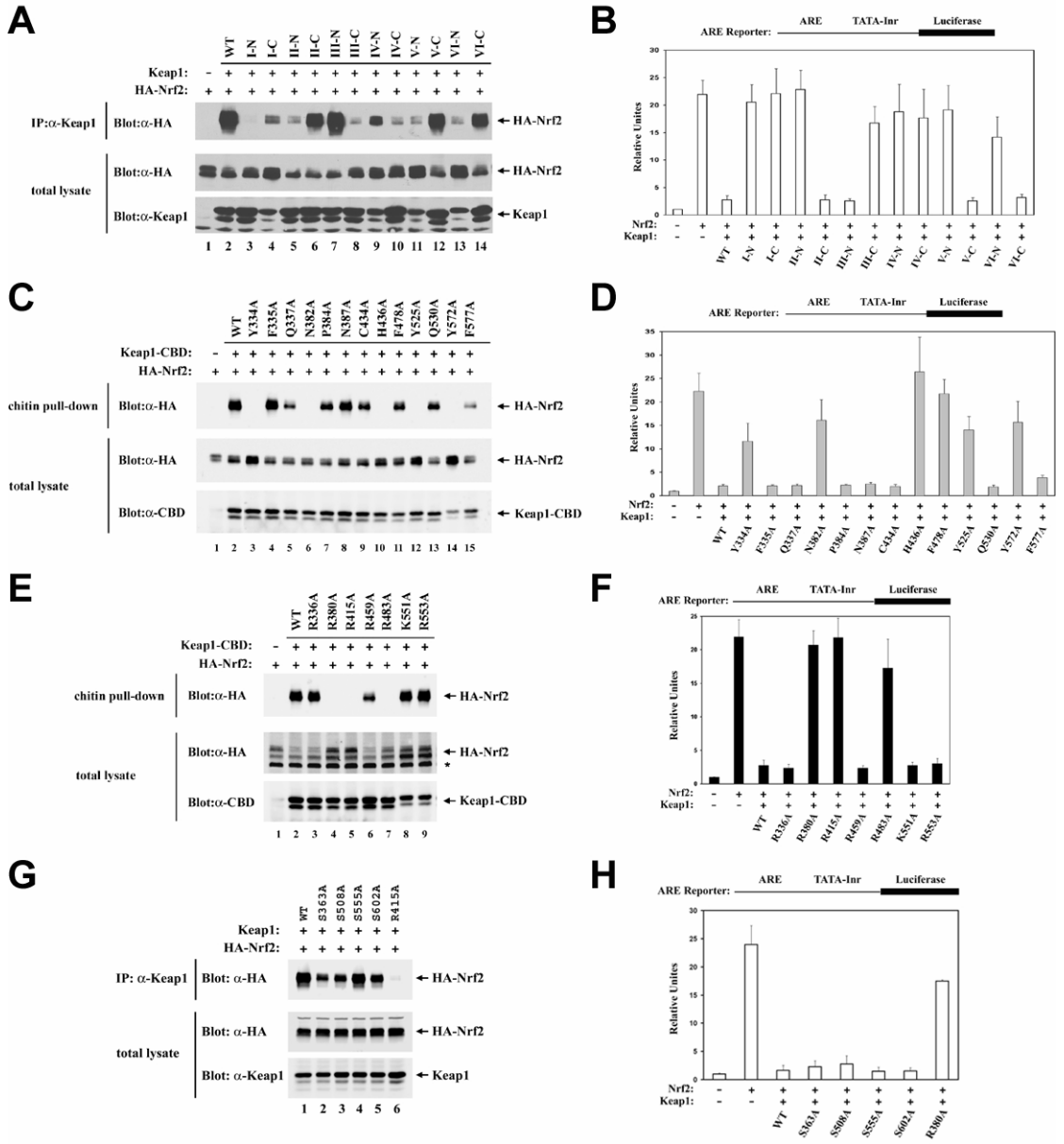
Figure V-5. Identification of amino acids within the Kelch domain of Keap1 that are required for binding to Nrf2. (**A**) COS1 cells were cotransfected with expression vectors for HA-Nrf2 and mutant Keap1 proteins as indicated. Total cell lysates were analyzed by immunoblot with anti-HA and anti-Keap1 antibodies (bottom two panels). Anti-Keap1 immunoprecipitates (IP) were subjected to immunoblot analysis using anti-HA antibodies (top panel). (**B**) MDA-MB-231 cells were transfected with expression vectors for HA-Nrf2 (100 ng) and mutant Keap1 proteins (50 ng) as indicated, and with an ARE-dependent firefly luciferase reporter gene construct (100 ng). A plasmid encoding *Renilla* luciferase (10 ng) was included as a control for transfection efficiency. The data shown represent the means and standard deviation of results from three independent experiments. (**C**) HEK 293T cells were transfected expression vectors for Keap1-CBD and mutant HA-Nrf2 proteins as indicated. Total cell lysates were analyzed by immunoblotting with anti-HA and anti-CBD antibodies (bottom two panels). The lysates were incubated with chitin beads, washed, and proteins that remained associated with the chitin beads were analyzed by immunoblotting with anti-HA antibodies (top panel). An asterisk (*) indicates a nonspecific protein detected by the antibody. (**D**) Reporter assays were formed as described in (B). (**E**) Pulldown assays were performed as described for (C). (**F**) Reporter assays were performed as described in (B). (**G**) Co-immunoprecipitation assays were performed as described in (A), except that the Keap1 and Nrf2 expression vectors were separately transfected into cells and cell lysates were mixed prior to the immunoprecipitation after input amounts were normalized to Nrf2 levels. (**H**). Reporter assays were performed as described in (B).

Figure V-6
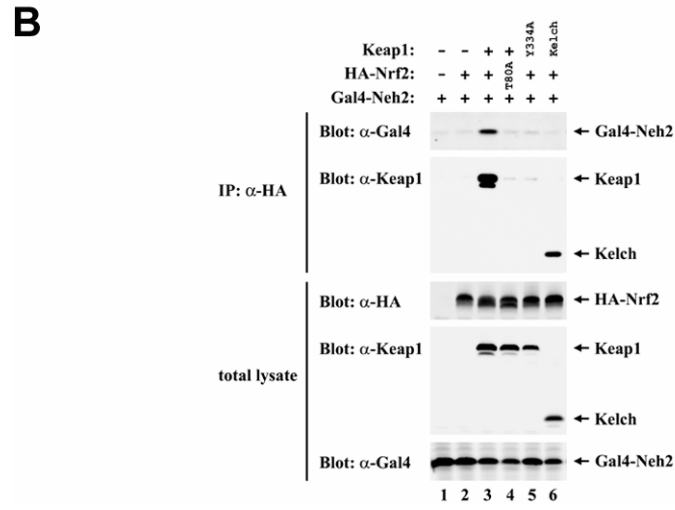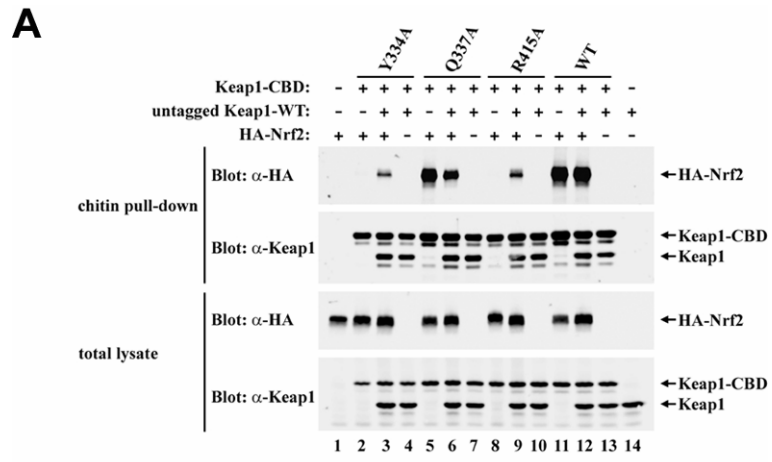
Figure V-6. Keap1 forms a homodimer capable of binding two Nrf2 molecules. (**A**) HEK 293T cells were transfected with expression vectors for the indicated Keap1 and Nrf2 proteins. Total cell lysates were analyzed by immunoblotting with anti-Keap1 and anti-HA antibodies (bottom two panels). Equivalent amounts of cell lysates were incubated with chitin beads, washed, and proteins that remained associated with the chitin beads were analyzed by immunoblotting with anti-HA and anti-Keap1 antibodies (top two panels). (**B**) HEK 293T cells were transfected with expression vectors for the indicated Keap1 and Nrf2 proteins. Total cell lysates were analyzed by immunoblotting with anti-HA, anti-Keap1 and anti-Gal4 antibodies (bottom three panels). Anti-HA immunoprecipitates were analyzed by immunoblotting with anti-Gal4 and anti-Keap1 antibodies (top two panels).

Figure V-7

A

chitin pull-down

| | | WT | T80A | p-Thr |

peptide:
Keap1-CBD:
HA-Nrf2:

Blot: α-HA → HA-Nrf2

Blot: α-CBD → Keap1-CBD

1 2 3 4 5 6 7 8 9 10 11 12 13 14

B

HA-Nrf2: WT T80A T80S T80D T80E
Keap1-CBD:

chitin pull-down
Blot: α-HA → HA-Nrf2
Blot: α-CBD → Keap1-CBD

total lysate
Blot: α-HA → HA-Nrf2
Blot: α-CBD → Keap1-CBD

1 2 3 4 5

C

ARE Reporter: —— ARE TATA-Inr Luciferase

Relative Unites

Keap1: - - + + + + +
Nrf2: - WT WT T80A T80S T80D T80E
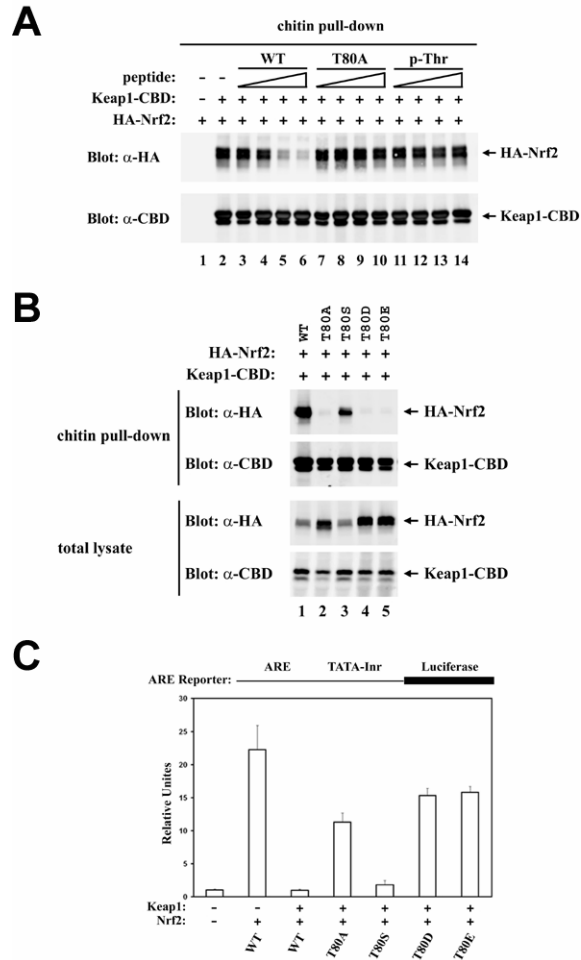
Figure V-7. Phosphorylation of the conserved threonine within the DxETGE motif in Nrf2 disrupts binding to Keap1. (**A**) COS1 cells were transfected with expression vectors for Keap1-CBD and HA-Nrf2 and the Keap1:Nrf2 complex isolated on chitin beads. The beads were incubated with the indicated peptides, washed, and proteins that remained bound to the beads were analyzed by immunoblot with anti-HA and anti-CBD antibodies. The amounts of peptides added to each sample were 10 ng (lanes 3, 7, 11), 100 ng (lanes 4, 8, 12), 1 μg (lanes 5, 9, 13) and 10 μg (lanes 6, 10, 14). (**B**) HEK 293T cells were transfected with expression vectors for the indicated Keap1 and Nrf2 proteins. Total cell lysates were analyzed by immunoblotting with anti-HA and anti-CBD antibodies (bottom two panels). Equivalent amounts of cell lysates were incubated with chitin beads, washed, and proteins that remained associated with the chitin beads were analyzed by immunoblotting with anti-HA and anti-CBD antibodies (top two panels). (**C**) Reporter assays were performed as described in Fig. 5B.

REFERENCES

Ames, B.N. and Shigenaga, M.K. (1993) DNA and Free Radicals. In Halliwell, B. and Aruoma, O.I. (eds.), *Oxidants are a major contributor to cancer and aging*. Ellis Horwood, New York, NY, pp. 1-15.

Bloom, D., Dhakshinamoorthy, S. and Jaiswal, A.K. (2002) Site-directed mutagenesis of cysteine to serine in the DNA binding region of Nrf2 decreases its capacity to upregulate antioxidant response element-mediated expression and antioxidant induction of NAD(P)H:quinone oxidoreductase1 gene. *Oncogene*, 21, 2191-2200.

Bomont, P., Cavalier, L., Blondeau, F., Ben Hamida, C., Belal, S., Tazir, M., Demir, E., Topaloglu, H., Korinthenberg, R., Tuysuz, B., Landrieu, P., Hentati, F. and Koenig, M. (2000) The gene encoding gigaxonin, a new member of the cytoskeletal BTB/kelch repeat family, is mutated in giant axonal neuropathy. *Nat Genet*, 26, 370-374.

Bomont, P., Ioos, C., Yalcinkaya, C., Korinthenberg, R., Vallat, J.M., Assami, S., Munnich, A., Chabrol, B., Kurlemann, G., Tazir, M. and Koenig, M. (2003) Identification of seven novel mutations in the GAN gene. *Hum Mutat*, 21, 446.

Bonnefont-Rousselot, D. (2002) Glucose and reactive oxygen species. *Curr Opin Clin Nutr Metab Care*, 5, 561-568.

Bruno, C., Bertini, E., Federico, A., Tonoli, E., Lispi, M.L., Cassandrini, D., Pedemonte, M., Santorelli, F.M., Filocamo, M., Dotti, M.T., Schenone, A., Malandrini, A. and Minetti, C. (2004) Clinical and molecular findings in patients with giant axonal neuropathy (GAN). *Neurology*, 62, 13-16.

Cash, A.D., Perry, G. and Smith, M.A. (2002) Therapeutic potential in Alzheimer disease. *Curr Med Chem*, 9, 1605-1610.

Ceconi, C., Boraso, A., Cargnoni, A. and Ferrari, R. (2003) Oxidative stress in cardiovascular disease: myth or fact? *Arch Biochem Biophys*, 420, 217-221.

Chan, J.Y., Han, X.L. and Kan, Y.W. (1993) Cloning of Nrf1, an NF-E2-related transcription factor, by genetic selection in yeast. *Proc Natl Acad Sci U S A*, 90, 11371-11375.

Cullinan, S.B., Gordan, J.D., Jin, J., Harper, J.W. and Diehl, J.A. (2004) The Keap1-BTB protein is an adaptor that bridges Nrf2 to a Cul3-based E3 ligase: oxidative stress sensing by a Cul3-Keap1 ligase. *Mol Cell Biol*, 24, 8477-8486.

Davies, K.J. (2000) Oxidative stress, antioxidant defenses, and damage removal, repair, and replacement systems. *IUBMB Life*, 50, 279-289.

De Lano, W.L. (2002) The PyMOL Molecular Graphics System. *In., DeLano Scientific, San Carlos, CA*.

Dhakshinamoorthy, S. and Jaiswal, A.K. (2001) Functional characterization and role of INrf2 in antioxidant response element-mediated expression and antioxidant induction of NAD(P)H:quinone oxidoreductase1 gene. *Oncogene*, 20, 3906-3917.

Dinkova-Kostova, A.T., Holtzclaw, W.D., Cole, R.N., Itoh, K., Wakabayashi, N., Katoh, Y., Yamamoto, M. and Talalay, P. (2002) Direct evidence that sulfhydryl groups of Keap1 are the sensors regulating induction of phase 2 enzymes that protect against carcinogens and oxidants. *Proc Natl Acad Sci U S A*, 99, 11908-11913.

Eggler, A.L., Liu, G., Pezzuto, J.M., van Breemen, R.B. and Mesecar, A.D. (2005) Modifying specific cysteines of the electrophile-sensing human Keap1 protein is insufficient to disrupt binding to the Nrf2 domain Neh2. *Proc Natl Acad Sci U S A*, 102, 10070-10075.

Emsley, P. and Cowtan, K. (2004) Coot: model-building tools for molecular graphics. *Acta Crystallogr D Biol Crystallogr*, 60, 2126-2132.

Finkel, T. and Holbrook, N.J. (2000) Oxidants, oxidative stress and the biology of ageing. *Nature*, 408, 239-247.

Furukawa, M. and Xiong, Y. (2005) BTB Protein Keap1 Targets Antioxidant Transcription Factor Nrf2 for Ubiquitination by the Cullin 3-Roc1 Ligase. *Mol Cell Biol*, 25, 162-171.

Ghanbari, H.A., Ghanbari, K., Harris, P.L., Jones, P.K., Kubat, Z., Castellani, R.J., Wolozin, B.L., Smith, M.A. and Perry, G. (2004) Oxidative damage in cultured human olfactory neurons from Alzheimer's disease patients. *Aging Cell*, 3, 41-44.

Hamilton, C.A., Miller, W.H., Al-Benna, S., Brosnan, M.J., Drummond, R.D., McBride, M.W. and Dominiczak, A.F. (2004) Strategies to reduce oxidative stress in cardiovascular disease. *Clin Sci (Lond)*, 106, 219-234.

Hon, W.C., Wilson, M.I., Harlos, K., Claridge, T.D., Schofield, C.J., Pugh, C.W., Maxwell, P.H., Ratcliffe, P.J., Stuart, D.I. and Jones, E.Y. (2002) Structural basis for the recognition of hydroxyproline in HIF-1 alpha by pVHL. *Nature*, 417, 975-978.

Hong, F., Freeman, M.L. and Liebler, D.C. (2005a) Identification of Sensor Cysteines in Human Keap1 Modified by the Cancer Chemopreventive Agent Sulforaphane. *Chem Res Toxicol*, 18, 1917-1926.

Hong, F., Sekhar, K.R., Freeman, M.L. and Liebler, D.C. (2005b) Specific patterns of electrophile adduction trigger keap1 ubiquitination and NRF2 activation. *J Biol Chem*, 280, 31768-31775.

Hooft, R.W., Sander, C. and Vriend, G. (1996) Positioning hydrogen atoms by optimizing hydrogen-bond networks in protein structures. *Proteins*, 26, 363-376.

Imlay, J.A. (2003) Pathways of oxidative damage. *Annu Rev Microbiol*, 57, 395-418.

Itoh, K., Wakabayashi, N., Katoh, Y., Ishii, T., Igarashi, K., Engel, J.D. and Yamamoto, M. (1999) Keap1 represses nuclear activation of antioxidant responsive elements by Nrf2 through binding to the amino-terminal Neh2 domain. *Genes Dev*, 13, 76-86.

Jackson, A.L. and Loeb, L.A. (2001) The contribution of endogenous sources of DNA damage to the multiple mutations in cancer. *Mutat Res*, 477, 7-21.

Katoh, Y., Iida, K., Kang, M.I., Kobayashi, A., Mizukami, M., Tong, K.I., McMahon, M., Hayes, J.D., Itoh, K. and Yamamoto, M. (2005) Evolutionary conserved N-terminal domain of Nrf2 is essential for the Keap1-mediated

degradation of the protein by proteasome. *Arch Biochem Biophys*, 433, 342-350.

Katoh, Y., Itoh, K., Yoshida, E., Miyagishi, M., Fukamizu, A. and Yamamoto, M. (2001) Two domains of Nrf2 cooperatively bind CBP, a CREB binding protein, and synergistically activate transcription. *Genes Cells*, 6, 857-868.

Kobayashi, A., Kang, M.I., Okawa, H., Ohtsuji, M., Zenke, Y., Chiba, T., Igarashi, K. and Yamamoto, M. (2004) Oxidative stress sensor Keap1 functions as an adaptor for Cul3-based E3 ligase to regulate proteasomal degradation of Nrf2. *Mol Cell Biol*, 24, 7130-7139.

Kobayashi, A., Kang, M.I., Watai, Y., Tong, K.I., Shibata, T., Uchida, K. and Yamamoto, M. (2006) Oxidative and Electrophilic Stresses Activate Nrf2 through Inhibition of Ubiquitination Activity of Keap1. *Mol Cell Biol*, 26, 221-229.

Kobayashi, M., Itoh, K., Suzuki, T., Osanai, H., Nishikawa, K., Katoh, Y., Takagi, Y. and Yamamoto, M. (2002) Identification of the interactive interface and phylogenic conservation of the Nrf2-Keap1 system. *Genes Cells*, 7, 807-820.

Kuhlenbaumer, G., Young, P., Oberwittler, C., Hunermund, G., Schirmacher, A., Domschke, K., Ringelstein, B. and Stogbauer, F. (2002) Giant axonal neuropathy (GAN): case report and two novel mutations in the gigaxonin gene. *Neurology*, 58, 1273-1276.

Laskowski, R.A., Moss, D.S. and Thornton, J.M. (1993) Main-chain bond lengths and bond angles in protein structures. *J Mol Biol*, 231, 1049-1067.

Leung, L., Kwong, M., Hou, S., Lee, C. and Chan, J.Y. (2003) Deficiency of the Nrf1 and Nrf2 transcription factors results in early embryonic lethality and severe oxidative stress. *J Biol Chem*, 278, 48021-48029.

Li, W., Jain, M.R., Chen, C., Yue, X., Hebbar, V., Zhou, R. and Kong, A.N. (2005) Nrf2 Possesses a redox-insensitive nuclear export signal overlapping with the leucine zipper motif. *J Biol Chem*, 280, 28430-28438.

Li, X., Zhang, D., Hannink, M. and Beamer, L.J. (2004) Crystal structure of the Kelch domain of human Keap1. *J Biol Chem*, 279, 54750-54758.

Liang, X.-Q., Avraham, H.K., Jiang, S. and Avraham, S. (2004) Genetic alterations of the NRP/B gene are associated with human brain tumors. *Oncogene*, 23, 5890-5990.

Lo, S.C. and Hannink, M. (2006) CAND1-Mediated Substrate Adaptor Recycling Is Required for Efficient Repression of Nrf2 by Keap1. *Mol Cell Biol*, 26, 1235-1244.

Mathers, J., Fraser, J.A., McMahon, M., Saunders, R.D., Hayes, J.D. and McLellan, L.I. (2004) Antioxidant and cytoprotective responses to redox stress. *Biochem Soc Symp*, 157-176.

McMahon, M., Thomas, N., Itoh, K., Yamamoto, M. and Hayes, J.D. (2004) Redox-regulated turnover of Nrf2 is determined by at least two separate protein domains, the redox-sensitive Neh2 degron and the redox-insensitive Neh6 degron. *J Biol Chem*, 279, 31556-31567.

Mhatre, M., Floyd, R.A. and Hensley, K. (2004) Oxidative stress and neuroinflammation in Alzheimer's disease and amyotrophic lateral sclerosis: common links and potential therapeutic targets. *J Alzheimers Dis*, 6, 147-157.

Min, J.H., Yang, H., Ivan, M., Gertler, F., Kaelin, W.G., Jr. and Pavletich, N.P. (2002) Structure of an HIF-1alpha -pVHL complex: hydroxyproline recognition in signaling. *Science*, 296, 1886-1889.

Moi, P., Chan, K., Asunis, I., Cao, A. and Kan, Y.W. (1994) Isolation of NF-E2-related factor 2 (Nrf2), a NF-E2-like basic leucine zipper transcriptional activator that binds to the tandem NF-E2/AP1 repeat of the beta-globin locus control region. *Proc Natl Acad Sci U S A*, 91, 9926-9930.

Motohashi, H., O'Connor, T., Katsuoka, F., Engel, J.D. and Yamamoto, M. (2002) Integration and diversity of the regulatory network composed of Maf and CNC families of transcription factors. *Gene*, 294, 1-12.

Murshudov, G.N., Vagin, A.A. and Dodson, E.J. (1997) Refinement of macromolecular structures by the maximum-likelihood method. *Acta Crystallogr D Biol Crystallogr*, 53, 240-255.

Murshudov, G.N., Vagin, A.A., Lebedev, A., Wilson, K.S. and Dodson, E.J. (1999) Efficient anisotropic refinement of macromolecular structures using FFT. *Acta Crystallogr D Biol Crystallogr*, 55 (Pt 1), 247-255.

Orlicky, S., Tang, X., Willems, A., Tyers, M. and Sicheri, F. (2003) Structural basis for phosphodependent substrate selection and orientation by the SCFCdc4 ubiquitin ligase. *Cell*, 112, 243-256.

Padmanabhan, B., Tong, K.I., Ohta, T., Nakamura, Y., Scharlock, M., Ohtsuji, M., Kang, M.I., Kobayashi, A., Yokoyama, S. and Yamamoto, M. (2006) Structural basis for defects of Keap1 activity provoked by its point mutations in lung cancer. *Mol Cell*, 21, 689-700.

Pflugrath, J.W. (1999) The finer things in X-ray diffraction data collection. *Acta Crystallogr D Biol Crystallogr*, 55 (Pt 10), 1718-1725.

Stogios, P.J., Downs, G.S., Jauhal, J.J.S., Nandra, S.K. and Prive, G.G. (2005) Sequence and structural analysis of BTB domain proteins. *Genome Biol*, 6, R82.

Tong, K.I., Katoh, Y., Kusunoki, H., Itoh, K., Tanaka, T. and Yamamoto, M. (2006) Keap1 recruits Neh2 through binding to ETGE and DLG motifs: characterization of the two-site molecular recognition model. *Mol Cell Biol*, 26, 2887-2900.

Vaguine, A.A., Richelle, J. and Wodak, S.J. (1999) SFCHECK: a unified set of procedures for evaluating the quality of macromolecular structure-factor data and their agreement with the atomic model. *Acta Crystallogr D Biol Crystallogr*, 55 (Pt 1), 191-205.

Wakabayashi, N., Dinkova-Kostova, A.T., Holtzclaw, W.D., Kang, M.I., Kobayashi, A., Yamamoto, M., Kensler, T.W. and Talalay, P. (2004) Protection against electrophile and oxidant stress by induction of the phase 2 response: fate of cysteines of the Keap1 sensor modified by inducers. *Proc Natl Acad Sci U S A*, 101, 2040-2045.

Wakabayashi, N., Itoh, K., Wakabayashi, J., Motohashi, H., Noda, S., Takahashi, S., Imakado, S., Kotsuji, T., Otsuka, F., Roop, D.R., Harada, T., Engel, J.D. and Yamamoto, M. (2003) Keap1-null mutation leads to postnatal lethality due to constitutive Nrf2 activation. *Nat Genet*.

Wall, M.A., Coleman, D.E., Lee, E., Iniguez-Lluhi, J.A., Posner, B.A., Gilman, A.G. and Sprang, S.R. (1995) The structure of the G protein heterotrimer Gi alpha 1 beta 1 gamma 2. *Cell*, 83, 1047-1058.

Wang, W., Ding, J., Allen, E., Zhu, P., Zhang, L., Vogel, H. and Yang, Y. (2005) Gigaxonin interacts with tubulin folding cofactor B and controls its degradation through the ubiquitin-proteasome pathway. *Curr Biol*, 15, 2050-2055.

Winn, M.D., Isupov, M.N. and Murshudov, G.N. (2001) Use of TLS parameters to model anisotropic displacements in macromolecular refinement. *Acta Crystallogr D Biol Crystallogr*, 57, 122-133.

Wu, G., Xu, G., Schulman, B.A., Jeffrey, P.D., Harper, J.W. and Pavletich, N.P. (2003) Structure of a beta-TrCP1-Skp1-beta-catenin complex: destruction motif binding and lysine specificity of the SCF(beta-TrCP1) ubiquitin ligase. *Mol Cell*, 11, 1445-1456.

Yu, X. and Kensler, T. (2005) Nrf2 as a target for cancer chemoprevention. *Mutat Res*, 591, 93-102.

Zhang, D.D. and Hannink, M. (2003) Distinct cysteine residues in Keap1 are required for Keap1-dependent ubiquitination of Nrf2 and for stabilization of Nrf2 by chemopreventive agents and oxidative stress. *Mol Cell Biol*, 23, 8137-8151.

Zhang, D.D., Lo, S.C., Cross, J.V., Templeton, D.J. and Hannink, M. (2004) Keap1 is a redox-regulated substrate adaptor protein for a Cul3-dependent ubiquitin ligase complex. *Mol Cell Biol*, 24, 10941-10953.

Zhang, D.D., Lo, S.C., Sun, Z., Habib, G.M., Lieberman, M.W. and Hannink, M. (2005) Ubiquitination of Keap1, a BTB-Kelch substrate adaptor protein for Cul3, targets Keap1 for degradation by a proteasome-independent pathway. *J Biol Chem*, 280, 30091-30099.

Zipper, L.M. and Mulcahy, R.T. (2002) The Keap1 BTB/POZ Dimerization Function Is Required to Sequester Nrf2 in Cytoplasm. *J Biol Chem*, 277, 36544-36552.

VI. PGAM5, a Bcl-X$_L$-interacting protein, is a novel substrate for the redox-regulated Keap1-dependent ubiquitin ligase complex

ABSTRACT

Keap1 is a BTB-Kelch substrate adaptor protein for a Cul3-dependent ubiquitin ligase complex that functions as a sensor for thiol-reactive chemopreventive compounds and oxidative stress. Inhibition of Keap1-dependent ubiquitination of the bZIP transcription factor Nrf2 enables Nrf2 to activate a cytoprotective transcriptional program that counters the damaging effects of oxidative stress. In this report, we have identified a member of the phosphoglycerate mutase family, PGAM5, as a novel substrate for Keap1. The N-terminus of the PGAM5 protein contains a conserved NxESGE motif that binds to the substrate-binding pocket in the Kelch domain of Keap1, while the C-terminal PGAM domain binds Bcl-X$_L$. Keap1-dependent ubiquitination of PGAM5 results in proteosome-dependent degradation of PGAM5. Quinone-induced oxidative stress and the chemopreventive agent sulforaphane inhibit Keap1-dependent ubiquitination of PGAM5. The identification of PGAM5 as a novel substrate of Keap1 suggests that Keap1 regulates both transcriptional and post-transcriptional responses of mammalian cells to oxidative stress.

INTRODUCTION

Diverse metabolic activities of eukaryote cells generate reactive oxygen species, which can damage biological macromolecules, including DNA, proteins, and lipids (1). Oxidative damage to biological macromolecules can alter multiple cellular functions and has been implicated in cancer, inflammation, cardiovascular and neurodegenerative diseases, and aging (2-6). Consequently, eukaryote cells have evolved multiple protective mechanisms against reactive molecules and oxidative stress. A comprehensive analysis of oxidative stress resistance in yeast has identified several core functions, including transcription, protein trafficking and vacuolar formation that are broadly required for oxidative stress resistance (7).

In mammals, the Keap1 protein has emerged as a major sensor for oxidative stress and electrophilic molecules. Keap1 is a BTB-Kelch protein that functions as a substrate adaptor protein for a Cul3-dependent E3 ubiquitin ligase complex. Under basal conditions of cellular redox homeostasis, the N-terminal BTB domain of Keap1 binds to Cul3 while the C-terminal Kelch domain of Keap1 binds to the bZIP transcription factor Nrf2 (8-10). This ubiquitin ligase complex conjugates ubiquitin onto specific lysine residues within the N-terminal Neh2 domain of Nrf2 and targets Nrf2 for degradation by the 26S proteosome. Cyclical association and dissociation of this E3 ubiquitin ligase complex is required for efficient ubiquitination of Nrf2 and repression of Nrf2-dependent gene expression (11). Reactive electrophilic chemicals and oxidative stress modify one or more cysteine residues located in the N-terminal BTB and central linker domains of Keap1 and disrupt formation of a functional E3 ubiquitin ligase complex (12-17).

Inhibition of Keap1-mediated ubiquitination of Nrf2 results in a marked increase in the steady-state level of Nrf2 and transcription of Nrf2-dependent genes. Induction of Nrf2-dependent genes represents a cytoprotective response to oxidative stress that neutralizes reactive molecules, eliminates damaged macromolecules, and restores cellular redox homeostasis (18-22).

Structural and functional analyses of Keap1 and Nrf2 have identified an evolutionarily conserved DxETGE motif in the N-terminal Neh2 domain of Nrf2 that binds in a shallow binding pocket on the top face of the Kelch domain of Keap1 (23-25). Although Nrf2 is the only known substrate for Keap1, the Kelch domain of Keap1 has been reported to bind several other proteins, including Nrf1, prothymosin alpha, and fetal Alz clone 1 (FAC1) (26-28). In general, substrate adaptors for cullin-dependent ubiquitin ligases often bind several substrates via a common recognition motif (29-32). For example, β-TrCP, a well-characterized substrate adaptor for Cul1, recognizes two substrate proteins, IκBα and β-catenin, after these proteins are phosphorylated on two serine residues embedded within a conserved sequence motif of DSGφXS (32,33).

In this report, we have identified a novel substrate of Keap1 encoded by the PGAM5 gene. The PGAM5 gene encodes two protein isoforms, PGAM5-L and PGAM5-S, which result from alternative splicing. Both PGAM5 isoforms contain an N-terminal region of approximately 100 amino acids, which includes a conserved NxESGE motif that is required for binding to Keap1, and a C-terminal phosphoglycerate mutase (PGAM) domain, which binds to Bcl-X_L (34). PGAM5 is ubiquitinated by a Keap1-dependent E3 ubiquitin ligase complex, which targets PGAM5 for proteosome-mediated degradation. Both quinone-induced oxidative stress and sulforaphane inhibit Keap1-

dependent ubiquitination and subsequent degradation of PGAM5. Our results establish PGAM5 as a novel substrate of Keap1 and support the notion that Keap1 regulates diverse cellular functions as part of a global response to oxidative stress.

MATERIALS AND METHODS

Construction of recombinant DNA molecules. The PGAM5-L cDNA (Accession number BG030775) and the PGAM5-S cDNA (Accession number BC008196) were obtained from ATCC and Open Biosystems, respectively. The PGAM5 expression vectors were constructed by cloning PCR-generated fragments containing the entire open reading frame of either PGAM5-L and PGAM5-S into the *BamHI/EcoRI* sites of pcDNA3 (Invitrogen), and the *NotI/SmaI* sites of pFLAG-CMV2 (Sigma). The mutant PGAM5-L cDNA containing alanines in place of Glu 79 and Ser 80 codons were generated by site-specific mutagenesis with standard overlap-extension techniques. Plasmids expressing wild type and the mutant Keap1, CBD-tagged Keap1, and Cul3 proteins have been previously described (10,11). The myc-Rbx1 expression vector was a gift from Dr. Joan Conaway (35). The Bxl-X$_L$ expression vector was a gift from Dr. Richard Youle (36). All the genes used in this study were sequenced in the context of the expression vectors used for the experiments.

Cell culture, transfections, and chemical reagents. COS1, HEK-293T, and Hela cells were purchased from ATCC. Cells were maintained in either Dulbecco's modified Eagle's medium (DMEM) or Eagle's minimal essential medium (EMEM) in the presence of 10% fetal bovine serum (FBS). Plasmid DNA transfections were performed with Lipofectamine Plus (Gibco BRL) according to the manufacturer's instructions. Lactacystin (*clasto*-lactacystin β-lactone) was purchased from Boston Biochem. Sulforaphane and tert-butylhydroquinone (tBHQ) were purchased from Sigma.

Immunofluorescence assays. Hela cells were grown on glass coverslips on 35 mm plates. Cells were transfected with 1.0 μg of the empty vector or the expression vectors for the FLAG-PGAM5 proteins. Cells were fixed with 100% methanol at -20ºC for 10 min. Fixed cells were incubated for 40 min with mouse anti-FLAG M2 antibodies (Sigma) in phosphate buffered saline (10 mM sodium phosphate [pH 8.0] and 150 mM NaCl) containing 10% (vol/vol) FBS. Coverslips were washed and incubated with fluorescein isothiocyanate-conjugated anti-mouse antibodies (Jackson Laboratories) for another 40 min. Coverslips were washed and incubated with To-pro-3 (Molecular Probes) for another 30 min. Coverslips were washed and mounted on glass slides. Images were obtained with a Bio-Rad Radiance 2000 confocal system coupled to an Olympus IX70 inverted microscope and a digital camera. The images were captured with ImagePro and transferred to Adobe Photoshop for construction of the figure.

Antibodies, immuprecipitation, and immunoblot analysis. The anti-Keap1 antibody has been described (17). Antibodies against tubulin (Santa Cruz), the chitin binding domain (New England Biolabs), ubiquitin (Sigma), the FLAG epitope (Sigma), the myc epitope (Santa Cruz Biotechnology), the HA epitope (Covance) and Bcl-X_L (L-19; Santa Cruz Biotechnology) were purchased from commercial sources.

For detection of protein expression in total cell lysates, cells were lysed in sample buffer (50 mM Tris-HCl [pH 6.8], 2% SDS, 10% Glycerol, 100 mM DTT, 0.1% bromophenol blue) at 24 to 48 hr post-transfection. For immunoprecipitation assays, cell extracts were prepared in RIPA buffer (10 mM sodium phosphate [pH 8.0], 150 mM NaCl, 1% Triton X-100, 1% sodium deoxycholate, 0.1% SDS) containing 1 mM

dithiothreitol (DTT), 1 mM phenylmethylsulfonyl fluoride (PMSF) and protease inhibitor cocktail (Sigma). Soluble cell lysates were incubated either with 2 μg of anti-FLAG M2 coupled to agarose (Sigma), or with 2 μg of affinity-purified antibodies for 2 hr at 4°C, followed by incubation at 4°C with protein A-agarose beads (Sigma) for 2 hr. Unbound proteins were removed by washing four times with lysis buffer. The immunoprecipitated proteins were eluted in sample buffer by boiling for 5 minutes, electrophoresed through SDS-polyacrylamide gels, transferred to nitrocellulose membranes and subjected to immunoblot analysis.

In vivo ubiquitination assay. For detection of ubiquitinated PGAM5-L proteins in vivo, cells were transfected with expression vectors for HA-tagged ubiquitin, FLAG-PGAM5-L, and the indicated proteins. Cells were lysed by boiling in a buffer containing 2% SDS, 10 mM N-ethylmaleimide (NEM), 150 mM NaCl and 10 mM Tris-HCl pH [8.0]. This rapid lysis procedure inactivates cellular ubiquitin hydrolases and therefore preserves ubiquitin-substrate protein conjugates present in cells prior to lysis.   Protein-protein interactions, including association of PGAM5-L with Keap1, are also disrupted by this lysis procedure. For immunoprecipitation, these lysates were diluted with 4 volumes of a buffer containing 150 mM NaCl, 10 mM Tris-HCl [pH 8.0], 1 mM DTT and 1% Triton X-100. The diluted lysates were pre-cleared with protein A-agarose beads (Sigma) and incubated with anti-FLAG M2 agarose (Sigma). HA-ubiquitin conjugates in immunoprecipitated FLAG-PGAM5-L proteins were analyzed by immunoblot analysis with antibodies against the HA epitope.

In vitro ubiquitination assay. For detection of ubiquitinated PGAM5-L proteins in vitro, cells were transfected with expression vectors for FLAG-PGAM5-L, Keap1-CBD, myc-Rbx1, and HA-Cul3 proteins. Cells were lysed in buffer B (15 mM Tris-HCl pH [7.5], 500 mM NaCl, 0.25% NP-40) containing 1 mM dithiothreitol (DTT), 1 mM phenylmethylsulfonyl fluoride (PMSF) and protease inhibitor cocktail (Sigma). The lysates were pre-cleared with protein A-agarose beads prior to incubation with chitin beads (New England Biolabs) for four hours at 4 ^{o}C. Chitin beads were washed twice with buffer B, twice with buffer A (25 mM Tris-HCl [pH 7.5], 10% [v/v] glycerol, 1 mM EDTA, 0.01% NP-40 and 100 mM NaCl), and twice with reaction buffer (50 mM Tris-HCl [pH 7.5], 5 mM MgCl$_2$, 2 mM NaF, 0.6 mM DTT). The pellets were incubated with ubiquitin (300 pmol), E1 (2 pmol), E2-UbcH5a (10 pmol), and ATP (2 mM) in 1 x reaction buffer in a total volume of 30 μl for 1 hr at 37 ^{o}C. Ubiquitin, E1 and E2-UbcH5a were purchased from Boston Biochem. The chitin beads were pelleted by centrifugation (3,000 x g) and resuspended in 2% SDS, 150 mM NaCl, 10 mM Tris-HCl [pH 8.0] and 1 mM DTT and boiled for 5 min to release bound proteins, inactivate any contaminating ubiquitin hydrolases and disrupt protein-protein interactions. The supernatant was diluted five-fold with buffer lacking SDS prior to immunoprecipitation with anti-FLAG M2 agarose. Immunoprecipitated proteins were subjected to immunoblot analysis with anti-ubiquitin antibodies (Sigma).

Mass spectrometry. Gel slices containing bands "A", "B" and "C" as indicated as in Fig. 1A were reduced, alkylated, and digested with trypsin. Tryptic peptides were desalted and subjected to MALDI-TOF mass spectrometry by the MU Proteomics Core

using a Voyager DEPro with a 20Hz 337-nm nitrogen laser (Applied Biosystems, Foster City, CA). The Mascot software package was used to match the mass of the peptides with predicted tryptic peptides generated from the translated human genome. Mowse scores of 74 and 172 were obtained for PGAM5 (band B) in two independent experiments. The cut-off values for statistical significance ($p < 0.05$) in these two experiments were 59 and 63, respectively. The matched peptides from the second experiment are shown in Table 1. A Mowse score of 59 was obtained for CH3L1 (Band A) in the first experiment (cut-off value at $p < 0.05$ was 59 in this experiment). Details of the mass spectrometry experiments are available upon request. We thank Dr. Beverly DaGue of the MU Proteomics Center for her careful analysis of the mass spectrometry data.

RESULTS

Identification of PGAM5 as an interaction partner of Keap1. To identify new Keap1-interacting proteins, the human Keap1 protein containing a C-terminal chitin-binding domain (CBD) was stably expressed in MDA-MB-231 cells, a human breast carcinoma-derived cell line. The Keap1-CBD protein was isolated from cell lysates using chitin beads and Keap1-associated proteins were visualized on silver-stained SDS-polyacrylamide gels. Three proteins, ranging in size from 30 to 39 kDa were found to co-purify with the Keap1-CBD protein in a specific and reproducible manner (Fig. 1A, lanes 3 and 4). Tryptic peptides from these three proteins were subjected to MALDI-TOF mass spectrometry. Band A (39 kDa) was tentatively identified as Chitinase-3-like protein 1 (CH3L1; NCBI accession number NP_001267), with a borderline Mowse score of 59 in one experiment (cut-off value for $p<0.05$ was 59; data not shown). Bands B and C (32 kDa and 30 kDa, respectively) were identified as phosphoglycerate mutase 5 (PGAM5; NCBI accession number NP_612642) in two independent experiments. The Mowse scores for Band B were 74 and 172, well above the cut-off values for statistical significance of 59 and 63, respectively. The position and sequence of the PGAM5-derived peptides identified by MALDI-TOF MS are given in Table 1.

A database search revealed the presence of two mRNA transcripts that originate from the PGAM5 gene located on chromosome 12. The proteins encoded by these mRNAs are identical from amino acid 1 to 239, with the shorter form (PGAM5-S) containing 16 additional C-terminal amino acids while the longer isoform (PGAM5-L) containing 50 additional C-terminal amino acids (Fig. 2A). Both isoforms of human

PGAM5 contain a PGAM domain (pfam00300), which begins at amino acid 98 and extends to the C-terminal end of the longer isoform. The PGAM5 isoforms are distant members of the phosphoglycerate mutase family, with their closest relatives being two proteins, termed STS-1 and STS-2, that do not have phosphoglycerate mutase activity but participate in receptor-mediated signal transduction pathways (37,38) (Fig. 2B). In particular, the phosphohistidine signature motif that is characteristic of PGAM domains with enzymatic activity is poorly conserved in PGAM5 (39)(Fig. 2D). A region within the PGAM domain of PGAM5 has previously been shown to bind to Bcl-X_L (34), and the ability of both isoforms of PGAM5 to associate with Bcl-X_L was confirmed by co-immunoprecipitation (Fig. 2E and data not shown).

To confirm association between Keap1 and the two PGAM5 isoforms, untagged or FLAG-tagged versions of both PGAM5-S and PGAM5-L were expressed in HEK-293T cells along with the Keap1-CBD protein. Proteins that bound to chitin beads were analyzed by SDS-PAGE and silver stain. Both PGAM5 isoforms bound to the Keap1-CBD protein (Fig. 1B, lanes 3-6). The presence of the N-terminal FLAG tag decreased the mobility of both PGAM5 isoforms, but did not perturb their ability to associate with Keap1-CBD (Fig. 1B, lanes 7 and 8). The ectopic untagged PGAM5-L protein co-migrated exactly with the endogenous 32 kDa Keap1-associated protein (Fig. 1B, compare lanes 1 and 3). In contrast, the mobility of the ectopic untagged PGAM5-S protein was slightly faster than the endogenous Keap1-associated protein of 30 kDa (Figure 1B, compare lanes 1 and 5). This result supports the identification of the Keap1-associated protein of 32 kDa as the PGAM5-L isoform and suggests that the Keap1-

associated protein of 30 kDa is not the PGAM5-S isoform but is derived from the 32 kDa protein by proteolysis during purification.

To verify the association of both isoforms of human PGAM5 with Keap1, reciprocal pull-down analyses of the proteins in transfected cells were performed. COS1 cells were transfected with expression vectors for untagged Keap and either of the FLAG-tagged PGAM5 isoforms. Cell lysates were immunoprecipitated with anti-FLAG antibodies and the resultant immunoprecipitates were probed for the presence of Keap1. The Keap1 protein was present in anti-FLAG immunoprecipitates of both PGAM5 isoforms (Fig. 1C, lanes 2 and 4).

The subcellular localization of both PGAM5 isoforms was determined by indirect immunofluorescence of Hela cells expressing the FLAG-tagged proteins. The PGAM5-L protein displayed diffuse cytoplasmic staining and a punctate nuclear staining, while the PGAM5-S protein displayed a punctate pattern in the cytoplasm (Fig. 3). A similar pattern was observed in COS1 cells (data not shown). Both PGAM isoforms co-localized with the Keap1 protein in the cytoplasm (data not shown). No nuclear staining of Keap1 was observed in our experiments. When co-expressed with Keap1, the cytoplasmic localization of both PGAM5-L and Keap1 shifted from a diffuse pattern to a punctate pattern (data not shown). Keap1 also displayed a punctate cytoplasmic pattern when co-expressed with PGAM5-S (data not shown). In subsequent experiments, we focused on the PGAM5-L isoform, as this isoform co-migrated with the 32 kDa protein identified as PGAM5 by mass spectrometry of tryptic peptides and is expressed at higher levels than the PGAM5-S isoform (Fig. 1B).

Identification of the interaction interface between Keap1 and pGAM5-L. The Keap1

protein possesses five discrete domains: the N-terminal region (N); an N-terminal Broad

complex, Tramtrack, and Bric-a-Brac domain (BTB); a central linker domain (Linker); a

C-terminal Kelch repeat domain (Kelch); and a C-terminal short tail (C). To determine

which domain(s) in Keap1 are responsible for binding to PGAM5, a series of mutant

Keap1 proteins containing a specific deletion of each individual domain were expressed

in HEK-293T cells along with FLAG-PGAM5-L proteins. Association of the mutant

Keap1 proteins and PGAM5-L was assessed by coimmunoprecipitation.   Only the

Keap1-ΔKelch protein did not associate with PGAM5-L (Fig. 4A, lane 5), indicating that

the Kelch domain of Keap1 is required for binding to PGAM5-L.

Previous structural and mutational studies have demonstrated that the Kelch

domain of Keap1 is a six-bladed β-propeller structure that contains a shallow pocket on

its top face that binds Nrf2 (23,25,40). The shallow pocket of Keap1 binds an Nrf2-

derived peptide containing a highly conserved DxETGE motif. Our previous analysis of

more than 30 Keap1 mutant proteins identified seven amino acids in Keap1 whose side

chains participate in direct contacts with the Nrf2-derived peptide and for which

individual alanine substitutions are sufficient to disrupt binding of Nrf2 to Keap1 (23).

These residues are: Tyr334, Arg380, Asn382, Arg415, Arg483, Tyr525, and Tyr572.

The charged residues are located at the base of the binding pocket while the hydrophobic

residues line the sides of the binding pocket. A set of mutant CBD-tagged Keap1 proteins

were characterized for their ability to bind pGAM5-L. Association of the endogenous

PGAM5-L protein with these mutant Keap1 proteins was determined by co-purification

on chitin beads followed by SDS-PAGE and visualization by silver stain. This analysis

revealed four amino acid residues, including Tyr334, Arg415, Arg483, and Tyr572, for which individual alanine substitutions significantly disrupted the ability of Keap1 to bind PGAM5-L (Fig. 4B, lanes 2 and 3; Fig. 4C, lanes 5 and 7).

The highly conserved DxETGE motif in Nrf2 is required for the association of Nrf2 with Keap1 (23-25). The side chains of the glutamate residues contact multiple residues in Keap1, including Arg380, Asn382, Arg415 and Arg483. The side chains of the asparate and threonine residues, on the other hand, interact with the backbone of the Nrf2-derived peptide and stabilize a β-turn region that enables the Nrf2-derived peptide to fit into the binding pocket on Keap1. Alanine substitution of the threonine residue within the DxETGE motif markedly reduces binding of Nrf2 to Keap1 and enables the mutant Nrf2 protein to escape Keap1-mediated repression (23). In contrast, serine substitution of this threonine residue does not disrupt the binding of Nrf2 to Keap1, suggesting that the hydroxyl group of the serine residue is an effective substitute for the hydroxyl group of the threonine residue. A NxE(S/T)GE motif, amino acids 77-82 in the human PGAM5 isoforms, is strongly conserved in mammals (Fig. 2C). To determine if the NxESGE motif in PGAM5-L is required for binding to Keap1, a mutant PGAM5-L protein was constructed in which two alanine substitutions were introduced in place of Glu79 and Ser80. FLAG-tagged versions of the wild-type and PGAM5-L-E79A/S80A mutant proteins were expressed in HEK-293T cells along with Keap1-CBD and association with Keap1 was assessed by immunoblot following affinity purification with chitin beads. The mutant PGAM5-L-E79A/S80A protein did not bind to Keap1-CBD (Fig. 4D, lane 3). The cytoplasmic localization (Fig. 3M) and association of PGAM5-L with Bcl-X_L (Fig. 4D) were not altered by the E79A/S80A mutation. Taken together,

these results indicate that four amino acids within the substrate binding pocket on the top face of the Kelch domain of Keap1 form critical contacts with the NxESGE motif in PGAM5-L and support the notion that Keap1 binds PGAM-L in a manner that is very similar to the way in which Keap1 binds Nrf2.

Keap1 targets PGAM5-L for ubiquitin-dependent degradation. Binding of Nrf2 to Keap1 results in the ubiquitination of specific lysine residues in Nrf2 by a Cul3-dependent ubiquitin ligase complex, leading to the proteosome-dependent degradation of Nrf2 (8-10). Several experimental approaches were used to determine if PGAM5-L is also a substrate for Keap1-dependent ubiquitination. In one set of experiments, an in vivo ubiquitination analysis was performed, in which expression vectors for FLAG-PGAM5-L, Keap1 and HA-ubiquitin were transfected into COS1 cells. Cell lysates were collected under strongly denaturing conditions to eliminate non-covalent protein-protein interactions and the presence of HA-ubiquitin conjugation onto the FLAG-PGAM5-L protein was measured by anti-HA immunoblot analysis of anti-FLAG immunoprecpitates. A low level of ubiquitin conjugation was observed in the absence of co-expressed Keap1 (Fig. 5A, lane 2). Coexpression of Keap1 resulted in a marked increase in ubiquitin conjugation onto PGAM5-L, including a distinct band with apparent molecular weight of 40 kDa and a prominent ladder comprised of multiple bands of higher apparent molecular weight (Fig. 5A, lane 3). Ubiquitin conjugation onto the mutant PGAM5-L-E79A/S80A protein was not observed (Fig. 5A, lane 4), consistent with the inability of the mutant PGAM5-L protein to associate with Keap1 (Fig. 4A, lane

3). Mutant Keap1 proteins defective in binding to PGAM5-L were likewise defective in directing ubiquitin conjugation of PGAM5-L (data not shown).

In a second set of experiments, the ability of Keap1 to recruit PGAM5-L into a Cul3-dependent ubiquitin ligase complex capable of targeting PGAM5-L for ubiquitination was determined. Expression vectors for FLAG-tagged PGAM5-L, Keap1, HA-Cul3, and Myc-Rbx1 were cotransfected into COS1 cells. Cell lysates were immunoprecipitated with anti-FLAG antibodies and analyzed for the presence of Keap1, Cul3 and Rbx1 by immunoblotting with specific antibodies. Coimmunoprecipitation of either Cul3 and Rbx1 was markedly enhanced in the presence of co-expressed Keap1 (Fig. 5B, compare lanes 2 and 3), consistent with the notion that Keap1 bridges the interaction between PGAM5-L and the Cul3:Rbx1 complex. Furthermore, co-expression of Cul3 and Rbx1 markedly increased Keap1-dependent ubiquitination of PGAM5-L (Fig. 5C, compare lanes 2 - 4). Finally, the quaternary PGAM5-L:Keap1-CBD:Cul3:Rbx1 complex was purified from transfected cells using chitin beads and the ability of this complex to support ubiquitin conjugation onto PGAM5-L was determined. Ubiquitin conjugation onto PGAM5-L was readily observed in the presence of E1 activating enzyme, the UbcH5 E2 conjugating enzyme, ubiquitin and ATP (Fig. 5D, lane 2). Ubiquitin conjugation onto PGAM5-L was not observed with reactions carried out in the absence of the E1 ubiquitin-activating enzyme (Fig. 5D, lane1), confirming that conjugation of ubiquitin onto PGAM5-L occurred in vitro. A low level of ubiquitin conjugation onto PGAM5-L was observed in the absence of the Cul3/Rbx1 subcomplex (Fig. 5D, lane 3), presumably due to copurification of trace amount of the endogenous Cu3:Rbx1 subcomplex with ectopically expressed Keap1-CBD protein.

To determine if the ubiquitination of pGAM5-L by Keap1 alters the stability of the PGAM5-L protein, the steady-state levels of the wild-type and E79A/S80A mutant PGAM5-L proteins in the absence and presence of Keap1 were compared. Both proteins were expressed at comparable levels in HeLa cells in the absence of Keap1 (Fig. 6A, compare lanes 1 and 4). However, co-expression of Keap1 markedly decreased steady-state levels of the wild-type but not the mutant PGAM5-L protein (Fig. 6A, compare lanes 2 and 3 with lanes 5 and 6). The half-life of the PGAM5-L protein in the absence or presence of Keap1 was determined in a cycloheximide pulse-chase experiment. Transfected HeLa cells were treated with cycloheximide to block protein synthesis and the level of the PGAM5-L protein was determined at time points following addition of cycloheximide. The half-life of the ectopically expressed PGAM5-L protein was 75 hours in the absence of co-expressed Keap1, but was reduced to 6 hours in the presence of coexpressed Keap1 (Figs. 6B and 6C).

To confirm that Keap1 targets PGAM5-L for degradation by the 26S proteosome, the ability of the proteosome-specific inhibitor, *clasto*-lactacystin β-lactone (lactacystin), to block Keap1-dependent degradation and increase steady-state levels of PGAM5-L was determined. HeLa cells transfected with expression vectors for PGAM5-L and Keap1 were exposed to either DMSO or lactacystin, followed by cycloheximide to block protein synthesis. The level of PGAM5-L was determined at 0, 2, 6 and 8 hours following cycloheximide treatment. As before, the level of PGAM5-L was reduced in the presence of cycloheximide (Fig. 6D, lanes 1-4). However, levels of PGAM5-L did not decrease in the presence of lactacystin (Fig. 6D, lanes 5-8). Taken together, these experiments

demonstrate that Keap1-mediated ubiquitination of PGAM5-L protein targets the PGAM5-L protein for degradation by the proteosome.

Keap1-dependent ubiquitination of pGAM5-L is blocked by sulforaphane and quinone-induced oxidative stress. Several reports have demonstrated that oxidative stress and thiol-reactive chemopreventive compounds block the ability of Keap1 to target Nrf2 for ubiquitin-dependent degradation (10,17,41). As a result, steady-state levels of Nrf2 are increased and transcription of Nrf2-dependent target genes is increased. As Keap1 binds the PGAM5-L protein and targets the PGAM5-L protein for ubiquitin-dependent degradation, the ability of both overt quinone-induced oxidative stress and sulforaphane, a chemopreventive isothiocyanate compound, to inhibit Keap1-dependent ubiquitination of PGAM5-L was determined. Both quinone-induced oxidative stress and sulforaphane markedly diminished Keap1-dependent ubiquitination of PGAM5-L (Fig. 7A, lanes 3 and 4) and increased steady-state levels of PGAM5-L (Fig. 7B, lanes 3-8). Treatment of cells with either lactacystin or sulforaphane also increased the amount of the endogenous PGAM5 that was associated with Keap1-CBD (Fig. 7C).

Inhibition of Keap1-dependent ubiquitination of Nrf2 by electrophilic molecules and oxidative stress has been suggested to occur through modification of one or more cysteine residues in Keap1 (10,12,14-17). In previous work, we have identified a single cysteine residue, C151, located in the BTB domain of Keap1 that is required for inhibition of Keap1-dependent ubiquitination of Nrf2 by both quinone-induced oxidative stress and sulforaphane (10,17). Direct modification of C151 in Keap1 by iodoacetamide in vitro has been demonstrated (15). In agreement with importance of Cys 151 for

inhibition of Keap1-dependent substrate ubiquitination, the ability of the Keap1-C151S mutant protein to target PGAM5-L for ubiquitin conjugation (Fig. 7A, lanes 5-7) was resistant to inhibition by either oxidative stress or sulforaphane.

DISCUSSION

The ability of Keap1 to function as a redox-sensitive substrate adaptor protein for a Cul3-based E3 ubiquitin ligase has emerged as a major regulatory mechanism that governs downstream cellular responses to oxidative stress. In the present work, we have identified a member of the phosphoglycerate mutase family, PGAM5, as an interaction partner for Keap1. Human cells express two isoforms of human PGAM5 proteins, PGAM5-L and PGAM5-S, both of which bind to Keap1. We provide several lines of evidence that the PGAM5-L protein is a substrate of a Keap1-dependent ubiquitin ligase complex. First, PGAM5-L contains a conserved NxE(S/T)GE motif that is required for binding to Keap1. As PGAM5-L and PGAM5-S only differ at their C-termini, it is likely that PGAM5-S also uses this motif to bind Keap1. Second, co-expression of Keap1 with PGAM-L in cells markedly increases ubiquitin conjugation onto PGAM5-L and Keap1-dependent ubiquitination of PGAM5-L by a Cul3:Rbx1-dependent E3 ubiquitin ligase complex can be reconstituted in vitro. Third, co-expression of Keap1 decreases steady-state levels of PGAM5-L, which are recovered by inhibition of the 26S proteosome. Finally, Keap1-dependent ubiquitination of PGAM5-L is impaired by both quinone-induced oxidative stress and sulforaphane, resulting in elevated levels of PGAM5-L. Mutation of a single cysteine residue in the BTB-domain of Keap1, C151, confers resistance to inhibition by oxidative stress and sulforaphane of Keap1-dependent ubiquitination of PGAM5-L Taken together, these results indicate that PGAM5-L joins Nrf2 on a short list of bona fide substrates for a Keap1-dependent ubiquitin ligase complex.

The NxE(S/T)GE motif present in PGAM5 is similar in sequence to the conserved DxETGE motif in Nrf2 that binds Keap1 (24). The crystal structure of a Nrf2-derived peptide containing the DxETGE motif bound to the Kelch domain of Keap1 reveals that the hydroxyl residue of the threonine residue stabilizes a type I β-turn that enables the two glutamate side chains to contact multiple residues in Keap1 (23,25). A serine residue, but not an alanine residue, can substitute for the threonine residue in the Nrf2-derived DxETGE motif (23). It is likely that the serine residue in the NxESGE motif in PGAM5-L forms a similar type I β-turn that fits into the binding pocket in Keap1 and enables the side-chains of the flanking glutamate residues to contact specific residues in Keap1. In support of this notion, two arginine residues, Arg415 and Arg483, which participate in direct contacts with the corresponding glutamate residues in Nrf2 (23,25) , are required for binding of PGAM5-L. Taken together, our mutational data indicate that PGAM5-L binds to Keap1 in a manner that is similar, though not identical, to the way in which Nrf2 binds to Keap1. In particular, the number of critical contacts formed between Nrf2 and Keap1 appear to be greater than the number of critical contacts formed between PGAM5-L and Keap1. Two other proteins, prothymosin alpha and FAC1, also interact with Keap1 in a way that suggests these two proteins may also be substrates of Keap1 (27,42). However, neither prothymosin alpha nor FAC1 have an D/NxE(S/T)GE-like motif, suggesting that binding pocket on the Kelch domain of Keap1 may recognize several different binding motifs.

Although both Nrf2 and PGAM5-L are substrates for Keap1-dependent ubiquitination and are subsequently degraded by the 26S proteosome, PGAM5-L is a more abundant protein with longer half-life than Nrf2. Keap1-dependent ubiquitination

of Nrf2 results in a rapid turnover of Nrf2, with a half-life of approximately 30 minutes under basal conditions (17). In contrast, PGAM5-L has a half-life under basal conditions of approximately 6 hours when co-expressed with Keap1. This marked difference in the rate of protein turnover between Nrf2 and PGAM5-L likely reflects the rate at which multi-ubiquitination chains are added to Nrf2 or PGAM5-L. Several factors, including the affinity of the respective substrate proteins for Keap1 and the spatial orientation of the targeted lysine residues in the substrate, will contribute to the rate at which a given substrate acquires multi-ubiquitination chains. The importance of processivity of ubiquitin ligase complexes for determining the relative rates of substrate degradation has been suggested by a recent study of the anaphase-promoting complex (APC). The APC has several different substrates that are degraded in a temporal manner during progression through mitosis and G1, and the processivity of APC towards the different substrates has been suggested to determine the temporal order of substrate degradation (43).

PGAM5 is a member of the phosphoglycerate mutase superfamily. In humans, the phosphoglycerate mutase superfamily consists of at least ten distinct protein-encoding genes defined by the presence of the evolutionarily conserved PGAM domain (pfam00300). These genes can be divided into three groups based on sequence similarities and known functions (Fig. 2B). One group includes two genes that encode enzymes with known phosphoglycerate mutase activity (PGAM1 and PGAM2) and one gene that encodes an enzyme with diphosphoglycerate mutase activity (BPGM). This group also includes several pseudogenes, at least one of which is expressed (44). A second group of four genes encode isozymes of the bifunctional 6-phosphofructo-2-kinase /fructose-2,6-bisphosphatase enzyme (PFKFB). This group includes the TIGAR

279

protein, encoded by p53-inducible gene, that may contribute to dysregulation of glycolysis and apoptosis in cancer cells (45). A third group of proteins includes two related proteins, termed STS-1 and STS-2, and PGAM5. STS-1 and STS-2, which associate with the Cbl ubiquitin ligase, contain a ubiquitin-associated motif and an SH3 domain in addition to a C-terminal PGAM domain and have been implicated in regulation of T-cell receptor signaling and endocytosis of the receptor tyrosine kinases (37,38).

A common feature of phosphoglycerate mutase, diphosphoglycerate mutase and the 6-phosphofructo-2-kinase /fructose-2,6-bisphosphatase enzymes is the use of a phosphohistidine intermediate to mediate the transfer of phosphate to carbon atoms of their respective substrates (39). This catalytic histidine residue is embedded within a highly conserved signature motif of [LIVM]xRHG[EQ]x(Y)xN (Prosite PS00175) (39). The catalytic histidine residue is present in the proteins encoded by the third group of PGAM-domain containing proteins, although the C-terminal Asn residue in this signature motif, which is part of the active site of PGAM1 (39), has not been conserved in STS-1, STS-2 and PGAM5 (Fig. 2D). The PGAM domains in STS-1 and STS-2 do not appear to have phosphotransfer activity towards phosphoglycerate (43,46). Rather, the PGAM domains in STS-1 and STS-2 function as protein-protein interaction domains that enable the STS proteins to form dimers (38). Preliminary results suggest that the PGAM5 isoforms also form dimers (unpublished data). As the phosphohistidine signature motif of PGAM5 is the most divergent of all PGAM-domain containing proteins, it is likely that the PGAM5 proteins, like STS-1 and STS-2, will function as a mediators of protein-protein interactions rather than as a metabolic enzymes.

Our results confirm a previous report that identified PGAM5 as a Bcl-X_L-binding protein using in vitro mRNA display and peptide binding analysis (34). Bcl-X_L is a member of the Bcl-2 protein family that contains both anti-apoptotic (Bcl-2, Bcl-X_L, etc.) and pro-apoptotic members (Bax, Bak, Bad, etc.). A balance between the actions of anti-apoptotic and pro-apoptotic members is essential to maintain tissue homeostasis in multicellular organisms. The formation of homodimeric and heterodimeric complexes between Bcl-2 family members, mediated in large part by the conserved BH3 domain, regulates the activity of the Bcl-2 proteins. For example, BH3-derived peptides from the BH3-only proteins BID or BIM are able to induce oligomerization of the pro-apoptotic BAX or BAK proteins, with subsequent induction of apoptosis (47). These BH3-derived peptides bind in a hydrophobic cleft located on the surface of the Bcl-2 family proteins. A PGAM5-derived peptide, amino acids 125 to 156, has been shown to bind Bcl-X_L (34). However, binding of the PGAM5-derived peptide to Bcl-X_L was not competed by a peptide derived from the BH3 domain of Bak, although a Bim-derived BH3 peptide was a very effective competitor for the Bak-derived BH3 peptide (34). This result suggests that the PGAM5 proteins bind outside of the groove in Bcl-X_L that binds BH3 domains and are not likely to directly compete with BH3-only proteins for binding to Bcl-X_L. Although it remains to be determined if binding of PGAM5 to Bcl-X_L will modulate the balance between cell survival and death in response to changes in redox homeostasis, the PGAM5 proteins provide an intriguing molecular link between oxidative stress and apoptosis.

In summary, we have identified PGAM5 as a novel substrate for a redox-regulated Keap1-dependent ubiquitin ligase. The possibility that PGAM5 proteins may

modulate oxidative stress-induced apoptosis is under active investigation by our laboratory.

This chapter was reproduced with the expressed written permission of the American Society for Biochemistry and Molecular Biology.

Table VI-1

Position and sequence of PGAM5 peptides[a]		Mr (calculated)[b]	Mr (measured)[c]
33-52	AGGDAEPRPAEPPAWAGGAR[d]	1931.92	1931.90
53-64	PGPGVWDPNWDR[d]	1394.64	1395.64
65-74	REPLSLINVR	1195.70	1195.68
66-74	EPLSLINVRK	1039.60	1039.59
99-104	HIFLIR	797.49	797.49
105-116	HSQYHVDGSLEK	1398.65	1398.65
105-118	HSQYHVDGSLEKDR	1669.78	1669.76
119-125	TLTPLGR	765.45	765.44
126-134	EQAELTGLR	1015.53	1015.52
153-162	AIETTDIISR	1117.69	1117.60
170-176	VSTDLLR	802.45	802.44
177-203	EGAPIEPDPPVSHWKPEAVQYYEDGARIEAAFR	3036.43	3036.35
204-209	IEAAFR	705.38	705.38
210-214	NYIHR	701.36	701.36
219-235	QEEDSYEIFICHANVIR	2121.98	2121.98

a: The position and sequence of PGAM5-derived peptides identified by MALDI-TOF MS.
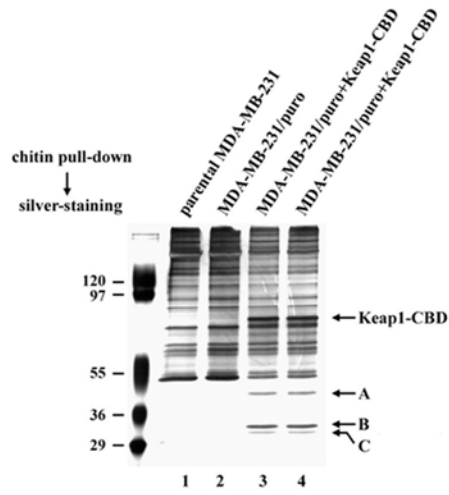
b: The calculated mass of the indicated PGAM5-derived peptides.

c: The observed mass of the indicated PGAM5-derived peptides by mass spectrometry.
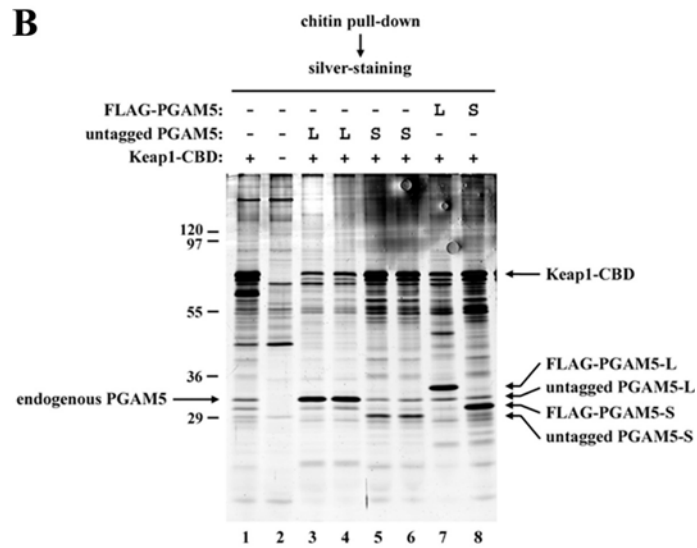
d: The amino acid composition of the indicated peptides was confirmed by MS/MS. These two peptides were only observed in band B of Fig. 1A. All other peptides were observed in both bands B and C.
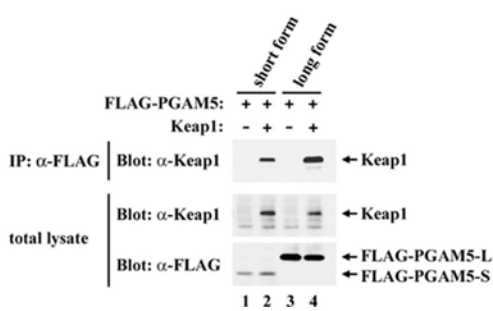
Figure VI-1

Figure VI-1. Identification of PGAM5 as an interaction partner of Keap1. (A) MDA-MB-231 cells that stably express the wild type Keap1-CBD proteins were generated by co-transfection of pBABE-puro and subsequent selection for puromycin resistance. MDA-MB-231 cells stably transfected with pBABE-puro alone were generated in parallel as a control cell line. Lysates from these cells were subjected to affinity purification using chitin beads. Proteins that remained associated with the chitin beads after extensive washing were analyzed by SDS-PAGE and visualized by silver stain. (B) Sixty-millimeter-diameter dishes of MDA-MB-231 cells were transfected with 2.0 µg of either an empty vector (lane 2) or an expression vector for Keap1-CBD (lane 1). Thirty-five-millimeter-diameter dishes of HEK-293T cells (lanes 3-8) were singly or co-transfected with 0.5 µg each of expression vectors for Keap1-CBD and FLAG-tagged or untagged versions of both PGAM5-L and PGAM5-S as indicated. Keap1-CBD proteins were purified from cell lysates from the singly transfected MDA-MB-231 cells (lanes 1 and 2) or the co-transfected HEK-293T cells (lanes 3-8) with chitin beads. Proteins remained bound to the chitin beads after extensive washing were analyzed by SDS-PAGE and visualized by silver stain. (C) Thirty-five-millimeter-diameter dishes of COS1 cells were transfected with 0.5 µg each of expression vectors for Keap1 and FLAG-tagged version of either PGAM5-S or PGAM5-L as indicated. Total cell lysates were analyzed by immunoblotting with anti-FLAG and anti-Keap1 antibodies (bottom two panels). Anti-FLAG immunoprecipitates (IP) were subjected to immunoblot analysis using anti-Keap1 antibodies (top panel).
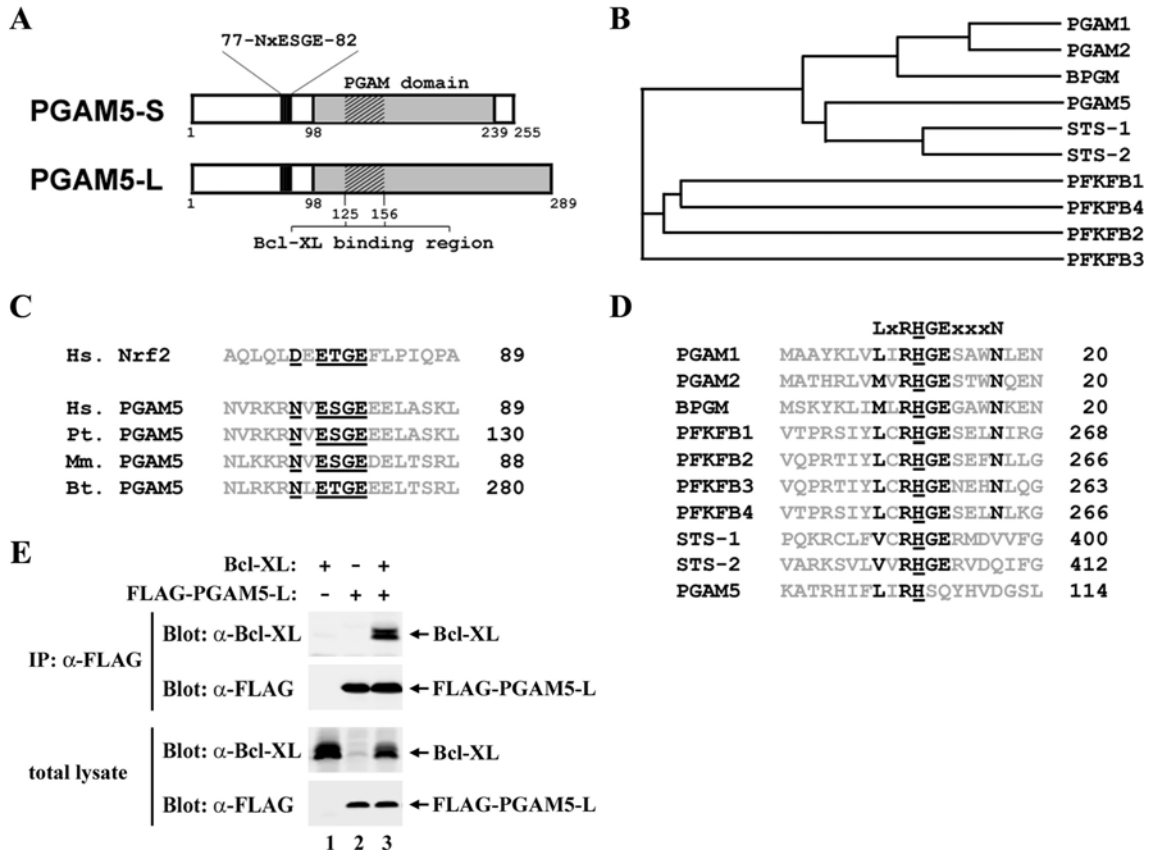
Figure VI-2

Figure VI-2. Featured domains and motifs in PGAM5, a member in phosphoglycerate mutase family. (A) The two isoforms of PGAM5 are depicted, with relevant regions of the proteins indicated. The two isoforms are identical up to amino acid 239 and have different C-termini as the result of alternative splicing. The NxESGE motif is located between amino acids 77-82 and the Bcl-X_L interaction region is located between amino acids 125 and 156. The PGAM domain extends from amino acid 98 to the C-terminus (amino acid 289) of the PGAM5-L isoform. (B) The relationship between ten human proteins that contain a PGAM domain is depicted by a cladogram generated using the ClustalW program at European Bioinformatics Institute website (http://www.ebi.ac.uk/). The protein sequences were obtained from the Swiss Institute of Bioinformatics website (http://ca.expasy.org/) using the following accession numbers in parentheses: PGAM1 (P18669); PGAM2 (P15259); BPGM (P07738); STS-1 (Q96IG9); STS-2 (P57075); PGAM5 (Q96HS1); PFKFB1 (P16118); PFKFB2 (O60825); PFKFB3 (Q16875); PFKFB4 (Q16877). Several PGAM1-derived pseudogenes, including an expressed pseudogene termed PGAM4 (Q8N0Y7), were not included in this analysis (44). (C) Mammalian PGAM5 proteins contain a conserved NxE(S/T)GE motif that is similar to the conserved DxETGE motif in the human Nrf2 protein (Q16236). The NCBI accession numbers for the indicated PGAM5 proteins are in parentheses. Hs., Homo sapiens (NP_612642); Pt., Pan troglodytes (XP_509498); Mm., Mus musculus (NP_082549); Bt., Bos Taurus (XP_585405). The numbers on the right indicate the number of the last amino acid shown. (D) Alignment of ten PGAM domain-containing proteins showing the conservation of residues surrounding the phosphohistidine signature motif ([LIVM]xRHG[EQ]x(Y)xN; Prosite PS00175) for the

phosphoglycerate mutase family, as described on the Swiss Institute of Bioinformatics website.   A simplified version of signature motif (LxRHGExxxN) is shown in the Figure, with the conserved residues in bold and the histidine that forms a phosphohistidine intermediate underlined (39).   The numbers on the right indicate the number of the last amino acid shown in each protein.   (E). Thirty-five-millimeter-diameter dishes of HEK-293T cells were cotransfected with expression vectors for FLAG-PGAM5-L and Bcl-X$_L$. Total cell lysates were analyzed by immunoblotting with anti-FLAG and anti-Bcl-X$_L$ antibodies (bottom two panels).   Anti-FLAG immunoprecipitates (IP) were subjected to immunoblot analysis using anti-Bcl-X$_L$ and anti-FLAG antibodies (top two panels).
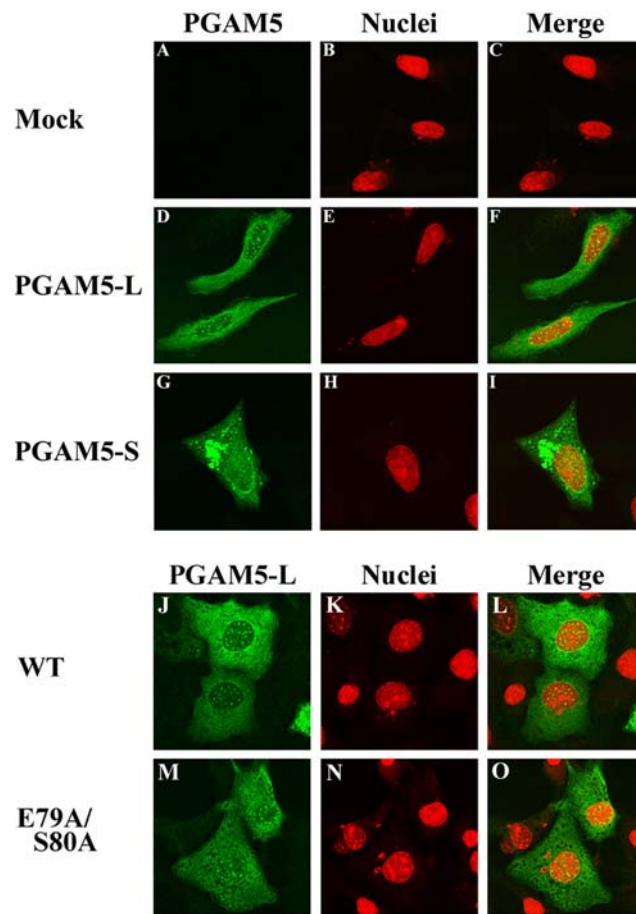
Figure VI-3

289

Figure VI-3. Subcellular localization of N-terminal FLAG-tagged PGAM5 isoforms.

(A-I) Thirty-five-millimeter-diameter dishes of Hela cells growing on coverslips were transfected with an empty expression vector (panels A, B, and C) or expression vectors for FLAG-PGAM5-L (panels D, E, and F) or FLAG-PGAM5-S (panels G, H, and I). The cellular localization of the PGAM5 proteins was determined by indirect immunofluorescence with anti-FLAG antibodies (panels A, D, and G). Nuclei were stained with Topro3 (panels B, E, and H). Merged images were shown on the right (panels C, F, and I). (J-O) Thirty-five-millimeter-diameter dishes of COS1 cells growing on coverslips were transfected with expression vectors for the wild type (panels J, K, and L) or mutant (panels M, N, and O) FLAG-PGAM5-L. The cellular localization of the PGAM5 proteins was determined by indirect immunofluorescence with anti-FLAG antibodies (panels J and M). Nuclei were stained with propidium iodide (panels K and N). Merged images were shown on the right (panels L and O).
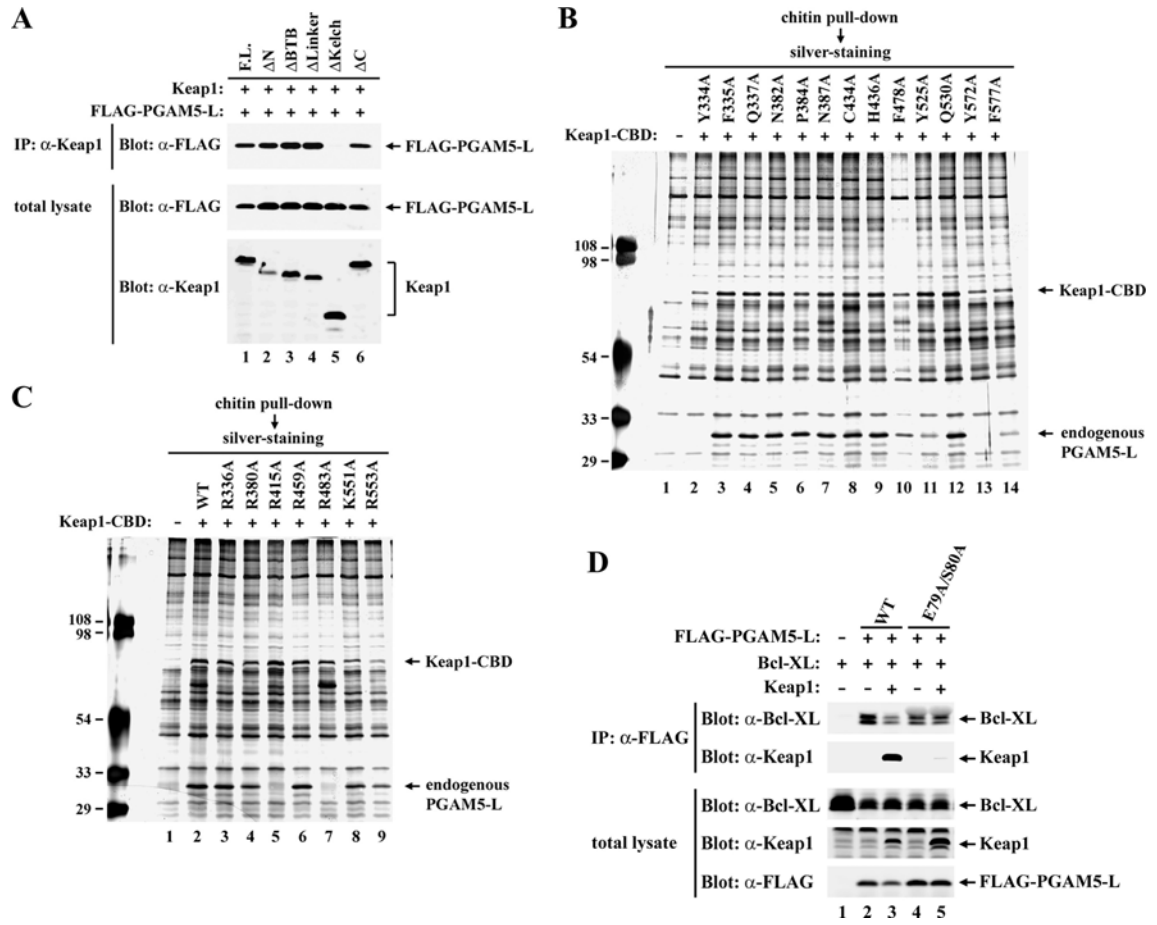
Figure VI-4

Figure VI-4. Identification of the interaction interface between Keap1 and PGAM5.

(A) Thirty-five-millimeter-diameter dishes of HEK-293T cells were cotransfected with expression vectors for FLAG-PGAM5-L and the full-length (F.L.) or mutant Keap1 proteins containing a specific deletion of each individual domain in Keap1 as indicated. Total cell lysates were analyzed by immunoblotting with anti-FLAG and anti-Keap1 antibodies (bottom two panels). Anti-Keap1 immunoprecipitates (IP) were subjected to immunoblot analysis using anti-FLAG antibodies (top panel). (B) Thirty-five-millimeter-diameter dishes of Hela cells were transfected with expression vectors for the wild type or mutant Keap1-CBD proteins as indicated. Cell lysates were incubated with chitin beads and proteins that remained bound after extensive washing were analyzed by SDS-PAGE and visualized by silver stain. (C) Pull-down assays were performed for the indicated Keap1 proteins as described for panel B. (D) Thirty-five-millimeter-diameter dishes of COS1 cells were cotransfected with expression vectors for Bcl-X_L (0.4 μg), Keap1 (0.4 μg) and the wild type or mutant FLAG-PGAM5-L (0.2 μg) proteins as indicated. Total cell lysates were analyzed by immunoblotting with anti-FLAG, anti-Keap1 and anti-Bcl-X_L (L-19) antibodies (bottom three panels). Anti-FLAG immunoprecipitates (IP) were analyzed by immunoblotting with anti-Bcl-X_L (L-19) and anti-Keap1 antibodies (top two panels).
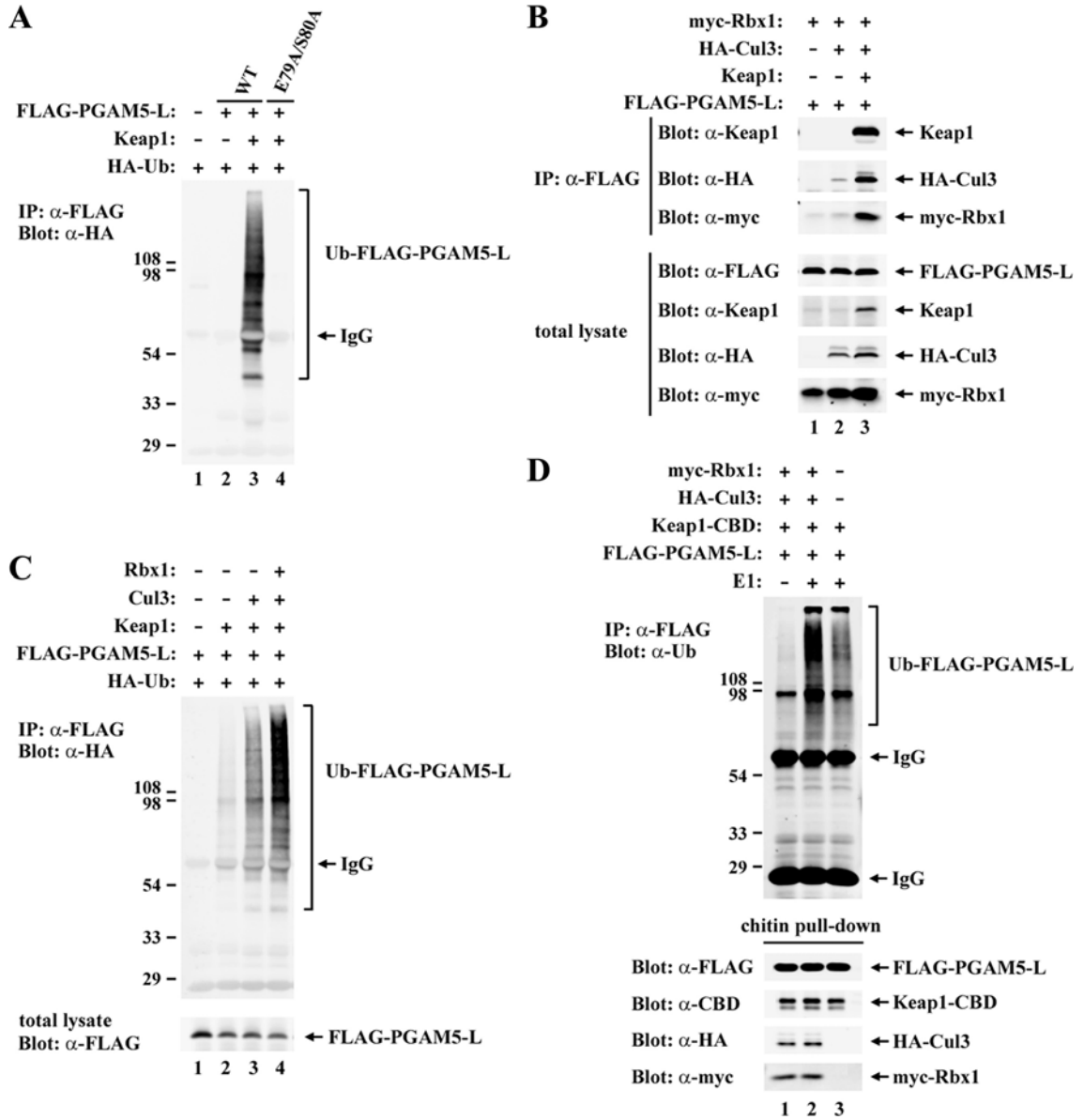
Figure VI-5

Figure VI-5. PGAM5-L is targeted for ubiquitination by a Keap1-dependent Cul3-RING ligase. (A) COS1 cells were transfected with expression vectors as indicated. Anti-FLAG immunoprecipitates (IP) were analyzed by immunoblot with anti-HA antibodies. (B) COS1 cells were transfected with expression vectors for Keap1, HA-Cul3, and myc-Rbx1 as indicated. An expression vector for FLAG-PGAM5-L was separately transfected into cells. Cell lysates were mixed prior to immunoblotting with the indicated antibodies (bottom four panels), or immunoprecipitation with anti-FLAG M2 agarose beads. Anti-FLAG immunoprecipitates (IP) were analyzed by immunoblot with the indicated antibodies (top three panels). This procedure enabled input cell lysates to be normalized to input levels of FLAG-PGAM5-L prior to the immunoprecipitation. (C) COS1 cells were transfected with expression vectors for HA-Ub, FLAG-PGAM5-L, Keap1, Cul3, and Rbx1 as indicated. Total cell lysates were analyzed by immunoblotting with anti-FLAG antibodies (bottom panel). Anti-FLAG immunoprecipitates (IP) were analyzed by immunoblot with anti-HA antibodies (top panel). (D) COS1 cells were transfected with expression vectors for FLAG-PGAM5-L, Keap1-CBD, HA-Cul3, and myc-Rbx1 as indicate. Lysates were pooled for each sample and incubated with chitin beads. After washing, the chitin beads were incubated with E1, E2-UbcH5a, ubiquitin, and ATP. The E1 enzyme was omitted from one sample (lane 1). Subsequently, the chitin beads were pelleted and washed, and proteins that were eluted from the beads under denaturing conditions were split into two sets of samples. One set was immunoprecipitated with anti-FLAG M2 agarose beads and then analyzed by immunoblotting with anti-ubiquitin antibodies (top panel). The other set was subjected to immunoblot analysis with the indicated antibodies (bottom four panels).
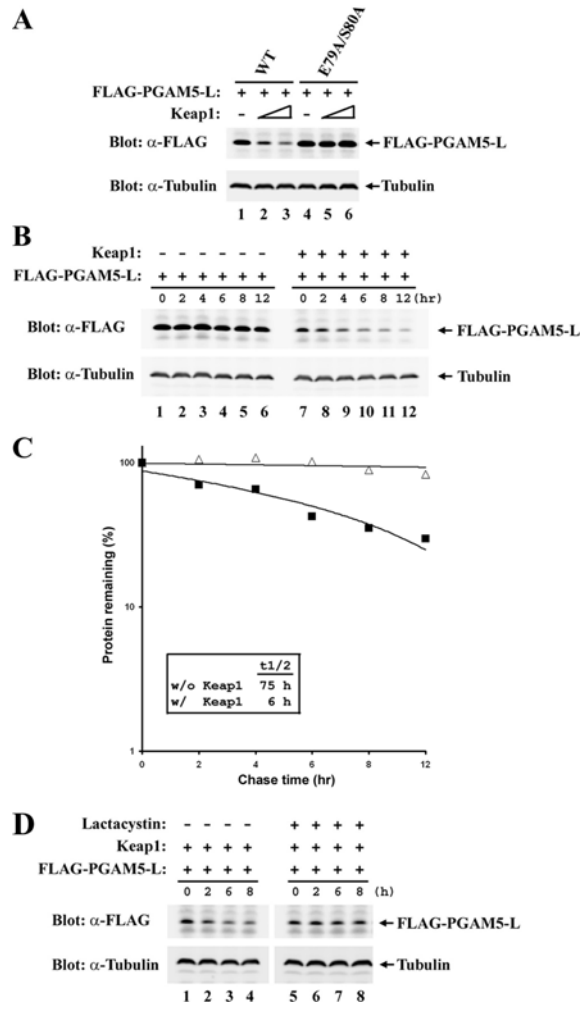
Figure VI-6

Figure VI-6. Keap1 targets PGAM5-L for a proteasome-mediated degradation. (A) Twenty-four-well plates of Hela cells were transfected with expression vectors for the wild type or mutant FLAG-PGAM5-L proteins (0.2 μg) along with an empty expression vector (lanes 1 and 4) or expression vectors for Keap1 (0.02 or 0.2 μg; lanes 2, 3, 5, and 6). Total cell lysates were subjected to immunoblot analysis with anti-FLAG and anti-Tubulin antibodies. (B) Thirty-five-millimeter-diameter dishes of Hela cells were transfected with an expression vector for FLAG-PGAM5-L (0.8 μg), along with an empty vector (lanes 1-6) or an expression vector for Keap1 (0.2 μg, lanes 7-12). Cells were treated with 50 μg/ml cycloheximide. Total cell lysates were collected at the indicated time points following cycloheximide treatment and subjected to immunoblot analysis with anti-FLAG and anti-Tubulin antibodies. (C) The relative intensities of FLAG-PGAM5-L were quantified by using the Multi Gauge software (FUJIFILM) and plotted on a semi-log graph. The amount of FLAG-PGAM5-L present at the beginning of cycloheximide treatment was set at 100. The half-life of PGAM5-L proteins in the presence (closed square) and absence (open triangle) of Keap1 are indicated in the inset. (D) Thirty-five-millimeter-diameter dishes of Hela cells were transfected with expression vectors for FLAG-PGAM5-L (0.68 μg) and Keap1 (0.34 μg). Cells were treated with solvent only (DMSO; 20 μl) (lanes 1-4) or 10 μM *clasto*-lactacystin β-lactone (Lactacystin) (lanes 5-8) 1 h prior to and during the cycloheximide treatment (50 μg/ml). Total cell lysates were collected at the indicated time points following cycloheximide treatment and subjected to immunoblot analysis with anti-FLAG and anti-Tubulin antibodies.
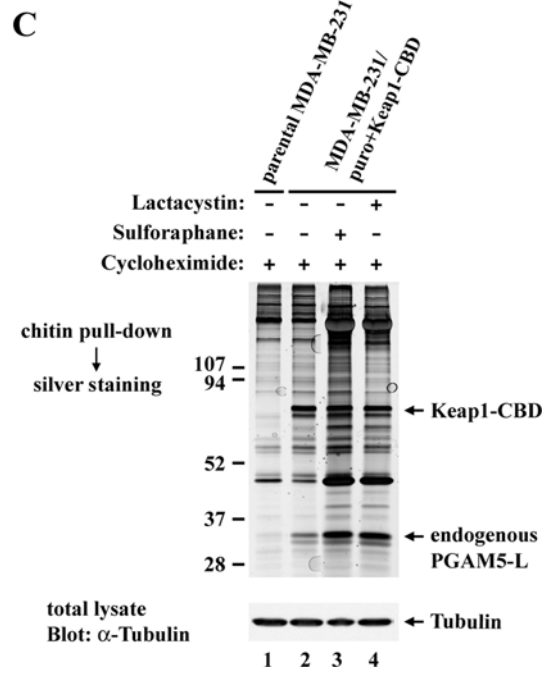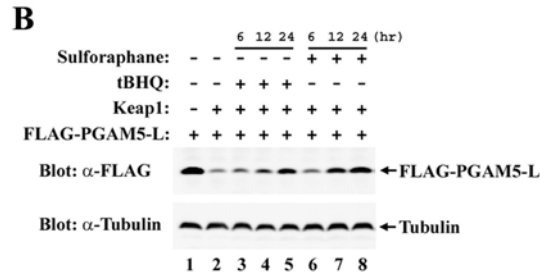
Figure VI-7
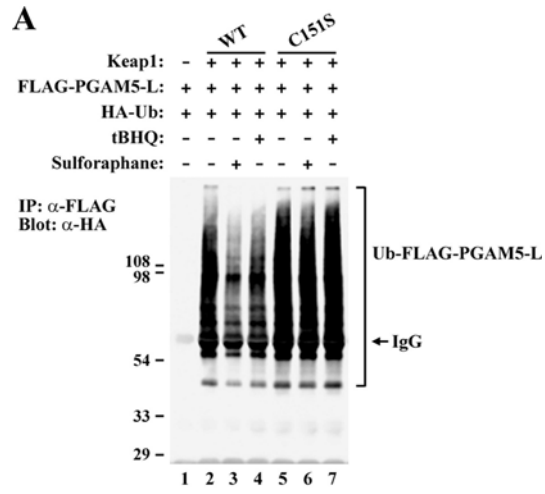
Figure VI-7. Keap1-dependent ubiquitination of PGAM5-L is inhibited by sulforaphane and quinone-induced oxidative stress. (A) Sixty-millimeter-diameter dishes of COS1 cells were transfected with expression vectors for HA-Ub (0.6 μg), FLAG-PGAM5-L (0.7 μg), and the wild type or mutant Keap1 proteins (0.7 μg) as indicated. The cells were either untreated (lanes 1, 2 and 5) or treated with 25 μM sulforaphane (lanes 3 and 6) or 50 μM tBHQ (lanes 4 and 7) for 4.5 h prior to cell lysis under strongly denaturing conditions. Anti-FLAG immunoprecipitates (IP) were analyzed by immunoblot with anti-HA antibodies. (B) Thirty-five-millimeter-diameter dishes of Hela cells were transfected with expression vectors for FLAG-PGAM5-L (0.68 μg) and Keap1 (0.34 μg). The cells were either untreated (lanes 1 and 2) or treated with 25 μM sulforaphane (lanes 6-8) or 50 μM tBHQ (lanes 3-5) for the indicated time periods prior to cell lysis. Total cell lysates were analyzed by immunoblotting with anti-FLAG and anti-Tubulin antibodies. (C) One-hundred-millimeter-diameter dishes of MDA-MB-231 cells that stably express the wild type Keap1-CBD protein were treated with DMSO (lanes 1 and 2), or 5 μM Sulforaphane for 16 hours (lane 3), or 10 μM *clasto*-lactacystin β-lactone (Lactacystin, lane 4) for one hour as indicated. All the cells were further treated with cycloheximide (50 μg/ml) for six additional hours prior to lysis to block new protein synthesis. Cells were lysed in RIPA buffer and the lysates were incubated with chitin beads, pelleted by centrifugation (3,000 X g), and washed three times in the lysis buffer. Proteins that remained associated with the chitin beads were analyzed by SDS-PAGE and visualized by silver stain (top panel). Total cell lysates were analyzed by immunoblotting with anti-Tubulin antibodies (bottom panel).

REFERENCES

1. **Imlay, J. A. (2003)** *Annu Rev Microbiol* **57, 395-418**
2. **Nunomura, A., Perry, G., Aliev, G., Hirai, K., Takeda, A., Balraj, E. K., Jones, P. K., Ghanbari, H., Wataya, T., Shimohama, S., Chiba, S., Atwood, C. S., Petersen, R. B., and Smith, M. A. (2001)** *J Neuropathol Exp Neurol* **60(8), 759-767**
3. **Andreassi, M. G. (2003)** *Mutat Res* **543(1), 67-86**
4. **Nathan, C. (2002)** *Nature* **420(6917), 846-852**
5. **Jackson, A. L., and Loeb, L. A. (2001)** *Mutat Res* **477(1-2), 7-21**
6. **Ames, B. N., and Shigenaga, M. K. (1993) DNA and Free Radicals. In: Halliwell, B., and Aruoma, O. I. (eds).** *Oxidants are a major contributor to cancer and aging***, Ellis Horwood, New York, NY**
7. **Ahmad, S., Anderson, W. L., and Kitchin, K. T. (1999)** *Cancer Lett* **139(2), 129-135**
8. **Cullinan, S. B., Gordan, J. D., Jin, J., Harper, J. W., and Diehl, J. A. (2004)** *Mol Cell Biol* **24(19), 8477-8486**
9. **Kobayashi, A., Kang, M. I., Okawa, H., Ohtsuji, M., Zenke, Y., Chiba, T., Igarashi, K., and Yamamoto, M. (2004)** *Mol Cell Biol* **24(16), 7130-7139**
10. **Zhang, D. D., Lo, S. C., Cross, J. V., Templeton, D. J., and Hannink, M. (2004)** *Mol Cell Biol* **24(24), 10941-10953**
11. **Lo, S. C., and Hannink, M. (2006)** *Mol Cell Biol* **26(4), 1235-1244**
12. **Hong, F., Freeman, M. L., and Liebler, D. C. (2005)** *Chem Res Toxicol* **18(12), 1917-1926**
13. **Hong, F., Sekhar, K. R., Freeman, M. L., and Liebler, D. C. (2005)** *J Biol Chem* **280(36), 31768-31775**
14. **Dinkova-Kostova, A. T., Holtzclaw, W. D., Cole, R. N., Itoh, K., Wakabayashi, N., Katoh, Y., Yamamoto, M., and Talalay, P. (2002)** *Proc Natl Acad Sci U S A* **99(18), 11908-11913**
15. **Eggler, A. L., Liu, G., Pezzuto, J. M., van Breemen, R. B., and Mesecar, A. D. (2005)** *Proc Natl Acad Sci U S A* **102(29), 10070-10075**
16. **Wakabayashi, N., Dinkova-Kostova, A. T., Holtzclaw, W. D., Kang, M. I., Kobayashi, A., Yamamoto, M., Kensler, T. W., and Talalay, P. (2004)** *Proc Natl Acad Sci U S A* **101(7), 2040-2045**
17. **Zhang, D. D., and Hannink, M. (2003)** *Mol Cell Biol* **23(22), 8137-8151**
18. **Shen, G., Xu, C., Hu, R., Jain, M. R., Nair, S., Lin, W., Yang, C. S., Chan, J. Y., and Kong, A. N. (2005)** *Pharm Res*
19. **Lee, J. M., Calkins, M. J., Chan, K., Kan, Y. W., and Johnson, J. A. (2003)** *J Biol Chem* **278(14), 12029-12038**
20. **Thimmulappa, R. K., Mai, K. H., Srisuma, S., Kensler, T. W., Yamamoto, M., and Biswal, S. (2002)** *Cancer Res* **62(18), 5196-5203**
21. **Mathers, J., Fraser, J. A., McMahon, M., Saunders, R. D., Hayes, J. D., and McLellan, L. I. (2004)** *Biochem Soc Symp* **(71), 157-176**
22. **Kwak, M. K., Wakabayashi, N., Itoh, K., Motohashi, H., Yamamoto, M., and Kensler, T. W. (2003)** *J Biol Chem* **278(10), 8135-8145**

23. Lo, S. C., Li, X., Henzl, M. T., Beamer, L. J., and Hannink, M. (2006) *Embo J* 25(15), 3605-3617

24. Kobayashi, M., Itoh, K., Suzuki, T., Osanai, H., Nishikawa, K., Katoh, Y., Takagi, Y., and Yamamoto, M. (2002) *Genes Cells* 7(8), 807-820

25. Padmanabhan, B., Tong, K. I., Ohta, T., Nakamura, Y., Scharlock, M., Ohtsuji, M., Kang, M. I., Kobayashi, A., Yokoyama, S., and Yamamoto, M. (2006) *Mol Cell* 21(5), 689-700

26. Strachan, G. D., Morgan, K. L., Otis, L. L., Caltagarone, J., Gittis, A., Bowser, R., and Jordan-Sciutto, K. L. (2004) *Biochemistry* 43(38), 12113-12122

27. Karapetian, R. N., Evstafieva, A. G., Abaeva, I. S., Chichkova, N. V., Filonov, G. S., Rubtsov, Y. P., Sukhacheva, E. A., Melnikov, S. V., Schneider, U., Wanker, E. E., and Vartapetian, A. B. (2005) *Mol Cell Biol* 25(3), 1089-1099

28. Wang, W., and Chan, J. Y. (2006) *J Biol Chem*

29. Orlicky, S., Tang, X., Willems, A., Tyers, M., and Sicheri, F. (2003) *Cell* 112(2), 243-256

30. Petroski, M. D., and Deshaies, R. J. (2005) *Nat Rev Mol Cell Biol* 6(1), 9-20

31. Sakamoto, K. M., Kim, K. B., Verma, R., Ransick, A., Stein, B., Crews, C. M., and Deshaies, R. J. (2003) *Mol Cell Proteomics* 2(12), 1350-1358

32. Winston, J. T., Strack, P., Beer-Romero, P., Chu, C. Y., Elledge, S. J., and Harper, J. W. (1999) *Genes Dev* 13(3), 270-283

33. Wu, G., Xu, G., Schulman, B. A., Jeffrey, P. D., Harper, J. W., and Pavletich, N. P. (2003) *Mol Cell* 11(6), 1445-1456

34. Hammond, P. W., Alpin, J., Rise, C. E., Wright, M., and Kreider, B. L. (2001) *J Biol Chem* 276(24), 20898-20906

35. Kamura, T., Koepp, D. M., Conrad, M. N., Skowyra, D., Moreland, R. J., Iliopoulos, O., Lane, W. S., Kaelin, W. G., Jr., Elledge, S. J., Conaway, R. C., Harper, J. W., and Conaway, J. W. (1999) *Science* 284(5414), 657-661

36. Jeong, S. Y., Gaume, B., Lee, Y. J., Hsu, Y. T., Ryu, S. W., Yoon, S. H., and Youle, R. J. (2004) *Embo J* 23(10), 2146-2155

37. Carpino, N., Turner, S., Mekala, D., Takahashi, Y., Zang, H., Geiger, T. L., Doherty, P., and Ihle, J. N. (2004) *Immunity* 20(1), 37-46

38. Kowanetz, K., Crosetto, N., Haglund, K., Schmidt, M. H., Heldin, C. H., and Dikic, I. (2004) *J Biol Chem* 279(31), 32786-32795

39. Jedrzejas, M. J. (2000) *Prog Biophys Mol Biol* 73(2-4), 263-287

40. Li, X., Zhang, D., Hannink, M., and Beamer, L. J. (2004) *J Biol Chem* 279(52), 54750-54758

41. Kobayashi, A., Kang, M. I., Watai, Y., Tong, K. I., Shibata, T., Uchida, K., and Yamamoto, M. (2006) *Mol Cell Biol* 26(1), 221-229

42. Strachan, G. D., Ostrow, L. A., and Jordan-Sciutto, K. L. (2005) *Biochem Biophys Res Commun* 336(2), 490-495

43. Rape, M., Reddy, S. K., and Kirschner, M. W. (2006) *Cell* 124(1), 89-103

44. Betran, E., Wang, W., Jin, L., and Long, M. (2002) *Mol Biol Evol* 19(5), 654-663

45. Bensaad, K., Tsuruta, A., Selak, M. A., Vidal, M. N., Nakano, K., Bartrons, R., Gottlieb, E., and Vousden, K. H. (2006) *Cell* 126(1), 107-120

46.   Carpino, N., Kobayashi, R., Zang, H., Takahashi, Y., Jou, S. T., Feng, J., Nakajima, H., and Ihle, J. N. (2002) *Mol Cell Biol* 22(21), 7491-7500

47.   Letai, A., Bassik, M. C., Walensky, L. D., Sorcinelli, M. D., Weiler, S., and Korsmeyer, S. J. (2002) *Cancer Cell* 2(3), 183-192

VII. REGULATION OF ANTI-OXIDANT GENE EXPRESSION BY A MITOCHONDRIAL-LOCALIZED COMPLEX CONTAINING KEAP1, NRF2 AND PGAM5

ABSTRACT

Eukaryote cells balance production of reactive oxygen species (ROS) with levels of anti-oxidant enzyme activity to maintain cellular redox homeostasis. Mitochondria are a major source of ROS, while many anti-oxidant genes are regulated by the Nrf2 transcription factor. Keap1, a redox-regulated substrate adaptor for a cullin-based ubiquitin ligase, regulates steady-state levels of Nrf2. In this report, we demonstrate that a significant fraction of the endogenous Keap1-Nrf2 complex is tethered to the outer membrane of mitochondria through association with PGAM5, a member of the phosphoglycerate mutase family. The dimeric Keap1 protein simultaneously binds both PGAM5 and Nrf2 through their conserved E(S/T)GE motifs to form a ternary complex. This ternary complex of PGAM5, Keap1 and Nrf2 provides a direct molecular link between mitochondria and Nrf2-dependent regulation of nuclear anti-oxidant gene expression. Ternary complex formation between a dimerized substrate adaptor and two different substrates represents a novel mechanism for regulation of cullin-based ubiquitin ligases.

INTRODUCTION

Oxidative stress has been implicated in diverse pathophysiological processes, including cancer, neurodegenerative diseases, and aging (1, 16, 35, 62). Oxidative stress is often viewed as an imbalance between levels of reactive oxygen species (ROS) and the ability of cells to counteract ROS-mediated oxidative damage to biological macromolecules (13). ROS are also essential molecular components of signal transduction pathways that control cell fate decisions and perturbation of these pathways can contribute to the pathological consequences of oxidative stress (27). Mitochondria are a major source of endogenous ROS production and perturbation of mitochondrial function has been linked to increased ROS production and, ultimately, adverse pathophysiological consequences (1, 5, 13, 16, 26, 27, 35, 55, 62).

In mammals, the bZIP transcription factor Nrf2 is a major regulator of cytoprotective genes which encode enzymes that neutralize reactive molecules, eliminate damaged macromolecules and restore cellular redox homeostasis (44). Nrf2-dependent gene expression is increased by diverse stimuli, including increased mitochondrial ROS production arising from pharmacological inhibition of electron transport complex I or II (3, 44, 45, 49). Nrf2 nullizygous mice develop normally but several indices of oxidative damage are increased in aged female mice, coincident with the development of symptoms that resemble systemic lupus erythromatosus in humans (36, 40, 61). Extensive analysis of Nrf2 nullizygous mice has demonstrated that Nrf2-dependent genes provide protection from ROS generated by diverse cellular stresses (32).

A BTB-Kelch protein termed Keap1 is the major negative regulator of Nrf2 (10, 23, 59). Mice that lack Keap1 contain elevated levels of nuclear Nrf2 protein and increased levels of Nrf2-dependent gene expression (59). Keap1 is a substrate adaptor for an E3 ubiquitin ligase complex that assembles around a Cul3 scaffold protein (8, 28, 33, 64). The N-terminal BTB and central linker domains of Keap1 bind to Cul3 while the C-terminal Kelch domain of Keap1 binds to Nrf2 (33, 39, 46, 64). This E3 ubiquitin ligase complex directs the covalent attachment of ubiquitin onto specific lysine residues within the N-terminal Neh2 domain of Nrf2 (64). Cyclical assembly and disassembly of this E3 ubiquitin ligase complex is required for efficient ubiquitination of Nrf2 and repression of Nrf2-dependent gene expression (37). Reactive electrophiles modify highly reactive cysteine residues within Keap1 and perturb formation of a functional ubiquitin ligase complex (11, 12, 14, 19, 21, 22, 63, 64). As a result, steady-state levels of Nrf2 increase, along with a marked increase in levels of Nrf2-dependent genes (11, 12, 22, 63). Keap1, as a potent repressor of Nrf2-dependent gene expression and a direct target for reactive molecules, functions as a molecular sensor for ROS and electrophilic chemicals.

Keap1 was initially characterized as a cytoplasmic actin-associated protein (23, 28). Keap1 has also been localized to specialized adherens junctions and focal adhesions (56). More recently, several reports have demonstrated that both Keap1 and Nrf2 shuttle between the nucleus and the cytoplasm (29, 43, 58). Different subcellular compartments have different redox potentials and different oxidant-generating complexes are confined to discrete subcellular locations (18, 53). The molecular and spatial relationship(s) between Keap1 and the subcellular locations of ROS formation is a critical unanswered question.

The human phosphoglycerate mutase family contains at by least ten distinct proteins that share a structurally conserved PGAM domain (24). Most members of this family, including PGAM1, PGAM2, 2,3-bisphosphoglycerate mutase (BPGM), and the four members of the 6-phosphofructo-2-kinase/fructose-2,6-biphosphatase (PFKFB) family, are metabolic enzymes that mediate phosphotransfer via a histidine residue located within a highly conserved motif in the PGAM domain (24). Several other members of this family, including STS-1, STS-2 and PGAM5, contain a divergent catalytic motif (38). Neither STS-1 nor STS-2 have phosphoglycerate mutase activity, although a recent report indicated that STS-1 has phosphotransferase activity towards other substrates (4, 9, 34). PGAM5 was first identified as a $Bcl-X_L$-interacting protein and subsequently identified as a protein that bound to Keap1 (17, 38). The PGAM5 gene, located on chromosome 12 in humans, encodes two protein isoforms, PGAM5-L (32 kDa) and PGAM5-S (28 kDa), generated by alternative splicing of a 3' exon. Both isoforms of PGAM5 contain a conserved N-terminal NxESGE motif. This motif bears striking resemblance to the DxETGE motif in Nrf2 that binds to a shallow pocket located on the top face of Kelch domain of Keap1 (39, 46). Indeed, amino acids in Keap1 that make critical contacts with the DxETGE motif from Nrf2 are required for binding of PGAM5 to Keap1. PGAM5, like Nrf2, can be modified by ubiquitin conjugation in a Keap1-dependent manner (38).

In this report, we demonstrate that PGAM5 contains an N-terminal mitochondrial targeting sequence that is necessary and sufficient for localization of PGAM5 to the outer membrane of mitochondria. Co-immunoprecipitation and co-localization experiments revealed the presence of a ternary complex containing Nrf2, Keap1 and PGAM5 that is

305

localized to mitochondria. This ternary complex of PGAM5, Keap1 and Nrf2 contributes to repression of Nrf2-dependent gene expression, as siRNA-mediated knockdown of PGAM5 increased expression of an Nrf2-dependent reporter gene. Our results suggest a model in which PGAM5, by anchoring the Keap1-Nrf2 complex to outer membrane of mitochondria, facilitates coordination between mitochondrial function and regulation of Nrf2-dependent anti-oxidant gene expression.

MATERIALS AND METHODS

Construction of recombinant DNA molecules. The PGAM5-L cDNA (Accession number BG030775), the PGAM5-S cDNA (Accession number BC008196) and mutant PGAM5-L-E79A/S80A cDNA have been described previously (38). The deletion mutant of PGAM5-L-Δ2-25 (codons 2 to 25) in pcDNA3 and in pCMV-Tag4A was constructed by PCR and standard recombinant DNA techniques. The expression vectors for GFP fusion proteins containing N-terminal PGAM5-derived sequences were constructed by cloning PCR-generated fragments into the *XhoI/BamHI* sites of pEGFP-N1. Plasmid expression vectors for both wt and mutant Keap1 and Nrf2 have been previously described (39). The Mito-GFP expression vector was a gift from Dr. Seamus J. Martin. The pEGFP-N1 empty vector was a gift from Dr. Marc C. Johnson. All the genes used in this study were sequenced in the context of the expression vectors used for the experiments.

Cell culture, transfections, and reportor gene assays. COS1, HeLa, MDA-MB-231, HEK-293T cells were purchased from ATCC. Cells were maintained in either Dulbecco's modified Eagle's medium (DMEM) or Eagle's minimal essential medium (EMEM) in the presence of 10% fetal bovine serum (FBS). Transfections of plasmid DNA were performed with Lipofectamine 2000 or Lipofectamine Plus (Invitrogen) according to the manufacturer's instruction. Transfections of small interfering RNA (siRNA) nucleotides were performed with Oligofectamine (Invitrogen) according to the manufacturer's instructions. All siRNA nucleotides used in this study were obtained from Dharmacon as

307

purified and annealed duplexes. The antioxidant response element (ARE) TATA-Inr luciferase reporter plasmid pARE-Luc and a control plasmid encoding *Renilla* luciferase for transfection efficiency have been previously described (37). Reporter gene assays were performed using a Promega dual-light assay system.

Antibodies, immunoprecipitation and immunoblot analysis. The PGAM domain (codons 89 to 289) of PGAM5-L protein was expressed in *Escherichia coli* as a His$_6$-tagged protein and purified by metal–chelate chromatography. Care was taken to maintain reducing conditions during all stages of the purification and subsequent use of the purified PGAM domain of PGAM5 protein. Antibodies were generated in chickens against the PGAM domain by Alpha Diagnostics (San Antonio, TX) and affinity-purified over a column containing immobilized His-PGAM5 (89-289) protein with reagents obtained from Pierce. Specificity of the anti-PGAM5 (89-289) antibodies was confirmed by immunoblotting, immunoprecipitation, and immunocytochemistry techniques. The affinity-purified anti-PGAM5 antibodies were able to bind both native and denatured PGAM5 isoforms. The affinity-purified anti-Keap1 antibody has been described previously (63). Antibodies against Cytochrome c (6H2.B4, BD Pharmingen), COXIV (10G8, Molecular Probes), TOM20 (FL-145, Santa Cruz), Tubulin (TU-02, Santa Cruz), the chitin binding domain (New England Biolabs), the FLAG epitope (Sigma), the HA epitope (Covance), and Nrf2 (H-300, Santa Cruz) were purchased from commercial sources.

For detection of protein expression in total cell lysates, cells were lysed in sample buffer (50 mM Tris-HCl [pH 6.8], 2% SDS, 10% Glycerol, 100 mM DTT, 0.1%

bromophenol blue) at 24 to 48 hr post-transfection. For immunoprecipitation assays, cell extracts were prepared in RIPA buffer (10 mM sodium phosphate [pH 8.0], 150 mM NaCl, 1% Triton X-100, 1% sodium deoxycholate, 0.2% SDS) containing 1mM dithiothreitol (DTT), 1mM phenylmethylsulfonyl fluoride (PMSF) and protease inhibitor cocktail (Sigma). Soluble cell lysates were incubated with either antibodies immobilized to agarose beads or with affinity-purified antibodies for 2 hr at 4°C, followed by incubation at 4°C with protein A-agarose beads (Sigma) or with anti-chicken IgY-agarose (*gallus* Immunotech Inc.) for two hours. Unbound proteins were removed by washing four times with lysis buffer. The immunoprecipitated proteins were eluted in sample buffer by boiling for 5 minutes, electrophoresed through SDS-polyacrylamide gels, transferred to nitrocellulose membranes and subjected to immunoblot analysis.

Immunofluorescence assays. Cells were grown on glass coverslips on 35-mm-diameter plates. Cells were either non-tranfected or transfected with 1.0 μg of the empty vector, or the indicated expression vectors. Cells were fixed with 3.7% formaldehyde in culture media at 37ºC for 15 min and incubated with 0.1 M glycine in phosphate buffered saline (10 mM sodium phosphate [pH 8.0] and 150 mM NaCl) at room temperature for 5 min to quench autofluorescence. Cells were permeabilized in 0.2% Triton X-100 in phosphate buffered saline at room temperature for 10 min. Fixed cells were incubated at room temperature for 60 min with affinity-purified primary antibodies as indicated in phosphate buffered saline containing 10% (vol/vol) FBS. Coverslips were washed and incubated with anti-chicken, anti-mouse, or anti-rabbit antibodies conjugated with either Alexa Fluor 488 or Alexa Fluor 568 (Molecular Probes), and with Hoechst 33258 for

another 60 min. GFP expression was visualized by direct fluorescence. Coverslips were washed and mounted in ProLong Gold (Molecular Probes) on glass slides. Images were obtained with a Zeiss Meta NLO 2-photon laser scanning confocal microscopy system at the MU Cytology Core. The images were captured with LSM 510 META, and transferred to Adobe Photoshop for construction of the figure.

In vivo ubiquitination assays. For detection of ubiquitinated PGAM5 proteins in vivo, cells were lysed by boiling and sonication in a buffer containing 2% SDS, 10 mM N-ethylmaleimide (NEM), 150 mM NaCl and 10 mM Tris-HCl pH [8.0]. This rapid lysis procedure inactivates cellular ubiquitin hydrolases and preserves ubiquitin-substrate protein conjugates present in cells prior to lysis. Protein-protein interactions, including association of Keap1 with PGAM5-FLAG, are also disrupted by this lysis procedure. Lysates were diluted with 4 volumes of a buffer containing 150 mM NaCl, 10 mM Tris-HCl pH [8.0], 1 mM DTT and 1% Triton X-100 prior to immunoprecipitation. The diluted lysates were pre-cleared with protein A-agarose beads (Sigma) and incubated with anti-FLAG M2 agarose (Sigma). HA-ubiquitin conjugates in immunoprecipitated PGAM5-L-FLAG proteins were analyzed by immunoblot analysis with antibodies against the HA epitope.

PGAM5 is a nuclear-encoded mitochondria-resident protein. The PGAM5 gene encodes two distinct protein isoforms that differ at their C-termini due to alternative splicing of a 3' exon (Fig. 1A). A polyclonal antibody generated against amino acids 89-289 of the PGAM5-L protein was used to characterize expression and subcellular localization of the endogenous PGAM5 proteins. Although the antibody recognizes both the ectopically expressed PGAM5-L and PGAM5-S proteins, only the 32kDa PGAM5-L isoform was detected by immunoblot analysis of lysates from several different cultured cell lines (Fig. 1B and data not shown). The subcellular localization of the endogenous PGAM5 protein in COS1 cells was determined by indirect immunofluorescence using the affinity-purified anti-PGAM5 antibody. No staining was observed with the pre-immune antisera, while a reticular-tubular pattern of cytoplasmic staining was observed with the anti-PGAM5 antibody (Fig. 1C, compare panels b and e). Confocal microscopy analysis revealed that PGAM5 co-localized with several different mitochondrial resident proteins, including cytochrome c (Fig. 1C, panels d-f; data not shown). No colocalization was observed with protein disulphide isomerase, a marker for the endoplasmic reticulum (data not shown). A similar pattern of PGAM5 staining and colocalization with cytochrome c was observed in HeLa, HEK293T, and MDA-MB-231 cells (Fig. 1C, panels g-l, and data not shown).

Examination of the amino acid sequence of PGAM5 by MITOPRED revealed a potential mitochondrial targeting sequence, including the presence of a short stretch of amino acids with the potential of forming a transmembrane α-helix (amino acids 9-29)

and a candidate matrix processing peptidase (MPP) cleavage site (between amino acids 33 and 34) (Fig. 1A) (15, 42). The subcellular localization of a mutant PGAM5 protein (PGAM5-L-Δ2-25), containing a deletion of amino acids 2 to 25, was determined by confocal microscopy using reduced laser intensity so that only the strong signal from the ectopic PGAM5-L-Δ2-25 and Mito-GFP proteins was detected (Fig. 2A, compare panels a, b, d and e). The PGAM5-L-Δ2-25 protein displayed diffuse cytoplasmic staining while the Mito-GFP protein was efficiently targeted to mitochondria (Fig. 2A; panels a-c). Fusion of the first 35 or 45 amino acids of PGAM5 onto GFP was sufficient to target GFP to mitochondria, while a GFP fusion protein containing the first 25 amino acids of PGAM5 was diffusely localized in the cytoplasm and nucleus (Fig. 2B; panels d-i). Taken together, these results demonstrate that PGAM5 contains an N-terminal mitochondrial targeting sequence that localizes PGAM5 to mitochondria.

Several different classes of mitochondrial targeting sequences have been identified (42). Although many mitochondrial targeting sequences are cleaved after transit of the polypeptide across the inner membrane, a number of mitochondrial proteins, such as Bcl-X_L, contain uncleaved mitochondrial targeting sequences that also function to anchor the protein to the cytosolic side of the outer membrane (25, 30). Both PGAM5-L and PGAM5-S migrated as a tight doublet during SDS-PAGE, with the predominant species migrating slower than the corresponding PGAM5-Δ2-25 deletion mutant (Fig. 2C). Mass spectrometry of tryptic peptides from the slower migrating form of the endogenous PGAM5-L protein purified from MDA-MB-231 cells identified a peptide that corresponding to amino acids 5-32 of PGAM5 (Table 1). Addition of proteinase K to a mitochondrial-enriched subcellular fraction from Hela cells resulted in proteolytic

digestion of the endogenous PGAM5-L protein (data not shown). Taken together, these data indicate that the mitochondrial targeting sequence of PGAM5-L is not cleaved but anchors the protein in the outer membrane of mitochondria such that the PGAM domain is cytoplasmic.

Mitochondrial morphology is altered by overexpression of PGAM5 isoforms. Ectopic expression of the PGAM5 isoforms revealed that both PGAM5-S and PGAM5-L colocalized with cytochrome c oxidase IV (COXIV) (Fig. 3A). However, profound differences in the morphology of mitochondria were observed in the transfected cells expressing either of the two PGAM5 isoforms. In particular, while mitochondria in mock-transfected COS1 cells displayed a typical reticular-tubular morphology (Fig. 1C), ectopic expression of the PGAM5-S protein resulted in the formation of disconnected punctuate mitochondria distributed throughout the cytoplasm (Fig. 3A, panels a-c). In contrast, ectopic expression of the PGAM5-L protein resulted in the clustering of mitochondria around the nucleus (Fig. 3A, panels d-f). Confocal analysis of COXIV and TOM20 localization in PGAM5-L-expressing cells revealed that the perinuclear mitochondrial aggregates are not giant fused mitochondria but are aggregates of individual mitochondria (Fig. 3B, panels a-f).

These dramatic alterations in mitochondrial morphology caused by overexpression of the PGAM5 isoforms, were quantified in COS1 cells transiently transfected with the Mito-GFP expression vector along with expression vectors for either of the PGAM5 isoforms. The co-transfected cells were scored for their mitochondrial morphology as being either tubular, intermediate (both tubular and fragmented),

313

fragmented or aggregated (see Fig. 3C for representative images of each morphology). More than 95% of COS1 cells that only expressed the Mito-GFP protein displayed either tubular or intermediate mitochondria (Fig. 3D). In contrast, more than 80% of the cells that expressed the PGAM5-S protein displayed exclusively fragmented mitochondria, while more than 80% of the cells that expressed the PGAM5-L protein displayed perinuclear aggregates of mitochondria (Fig. 3D).

Similar perturbations of mitochondrial morphology were observed in Hela cells transfected with expression vectors for the PGAM5-S or PGAM5-L. Mitochondrial membrane potential is preserved despite these dramatic alterations in mitochondrial morphology, as the fragmented mitochondria observed in PGAM5-S-expressing cells and the aggregated mitochondria observed in PGAM5-L-expressing cells were both readily stained by Mitotracker Red (data not shown). Ectopic expression of the PGAM5-L or PGAM5-S proteins did not induce cytochrome c release in either COS1 or HeLa cells. Taken together, these results suggest that the PGAM5 isoforms may be novel regulators of mitochondrial movement, a possibility that is currently under active investigation.

PGAM5 anchors Keap1 to mitochondria. We have previously characterized PGAM5 as a Keap1-interacting protein and a candidate substrate for a Keap1-dependent E3 ubiquitin ligase complex (38). To confirm physical interactions between the endogenous Keap1 and PGAM5 proteins, anti-Keap1 immunoprecipitates from HeLa cell lysates were subjected to immunoblot analysis with anti-PGAM5 antibodies. The endogenous PGAM5 protein was present in anti-Keap immunoprecipitates but not in parallel immunoprecipitates performed with pre-immune rabbit sera (Fig. 4A, lanes 1 and 2).

314

Likewise, the endogenous Keap1 protein was specifically detected in anti-PGAM5 immunoprecipitates from HEK293T cell lysates (Fig. 4A, lanes 3 and 4). Confocal microscopy analysis of HeLa cells using anti-Keap1 antibodies revealed a reticulo-tubular staining pattern that colocalized with both cytochrome c and PGAM5 (Fig. 4B, panels d and h). Large punctate bodies that did not co-localize with mitochondria were also observed with the anti-Keap1 antibody. Taken together, the co-immunoprecipitation and co-localization experiments indicate that a significant fraction of the endogenous Keap1 protein co-localizes with the endogenous PGAM5-L protein at mitochondria.

PGAM5 contains a conserved NxESGE motif (amino acids 77-82) that is required for binding to Keap1 (Fig. 1A) (38). To determine if localization of Keap1 to mitochondria requires binding to PGAM5, the localization of ectopic Keap1 protein in the absence or presence of either wt or mutant PGAM5-L proteins was determined. Ectopic Keap1 was diffusely localized throughout the cytoplasm but was completely relocalized to perinuclear mitochondria clusters when co-expressed with the PGAM5-L protein (Fig. 4C, panel a-f). In contrast, Keap1 remains distributed throughout the cytoplasm when co-expressed with the mutant PGAM5-L-E79A/S80A protein that is localized to mitochondria but defective in binding to Keap1 (Fig. 4C, panels g-l).

To determine if Keap1 is able to direct ubiquitination onto PGAM5, an in vivo ubiquitinatin analysis was performed, in which COS1 cells were transfected with expression vectors for HA-ubiquitin, Keap1, and C-terminal FLAG-tagged PGAM5-L. The C-terminal FLAG-tagged PGAM5-L protein, like the untagged PGAM5-L protein, was localized to mitochondria (data not shown). A C-terminal FLAG-tagged PGAM5-L-Δ2-25 mutant protein, which was localized to the cytoplasm (data not shown), was

analyzed in parallel. Cell lysates were collected under denaturing conditions to eliminate non-covalent protein-protein interactions, and levels of ubiquitin conjugation onto the PGAM5-L-FLAG protein were measured by anti-HA immunoblot analysis of anti-FLAG immunoprecipitates. A modest level of ubiquitin conjugation onto the wt PGAM5-L protein was observed in the presence of co-expressed Keap1, while strong Keap1-dependent ubiquitin conjugation onto the mutant PGAM5-L-Δ2-25 protein was observed (Fig. 4D, lanes 3 and 6). Co-expression of Keap1 did not reduce steady-state levels of the wt PGAM5-L protein but significantly reduced steady-state levels of the mutant PGAM5-L-Δ2-25 protein in both COS1 and Hela cells (Figs. 4D and 4E). Similar results were obtained with the untagged wt and mutant PGAM5-L proteins (data not shown). Thus, mitochondrial-localized PGAM5 is a substrate for Keap1-dependent ubiquitination but is not efficiently targeted for degradation, while mislocalization of PGAM5-L to the cytoplasm results in efficient ubiquitin-dependent degradation.

Keap1 mediates assembly of a mitochondria complex that contains both PGAM5 and Nrf2. Keap1 is a BTB-Kelch protein, and has been shown to form a homo-dimeric complex through its N-terminal BTB domain (6, 41, 67). Crystallographic analysis has demonstrated that an isolated Kelch domain can bind an Nrf2-derived peptide containing the DxETGE motif (39, 46). Mutational analysis has confirmed the functional importance of amino acid contacts observed in the crystal structure for Keap1 and Nrf2 interactions in vivo (39). A Keap1 dimer is able to bind two different Nrf2 molecules at the same time, consistent with a 2:2 stoichiometry for the Keap1:Nrf2 complex (39). However, Nrf2 has also been reported to form a 2:1 complex with Keap1, using two

different amino acid motifs, the DLG motif (amino acid residues 17-32) and the DxETGE motif to bind to Keap1 (41, 54).

We first determined if PGAM5-L, like Nrf2, is able to bind to a Keap1 heterodimer containing one functional and one mutant Kelch domain. A chitin-binding domain (CBD) was appended onto the C-terminus of mutant and wt Keap1 proteins. The presence of the CBD tag did not perturb formation of a heterodimeric complex with untagged wt Keap1 (Fig. 5A, lane 7). Two mutant Keap1 proteins (Y334A and Q337A) containing single amino acid substitutions were used in this experiment, only one of which (Y334A) is impaired in binding to PGAM5-L (Fig. 5A, compare lanes 2, 4 and 6). Co-expression of the untagged wild-type Keap1 protein with the mutant CBD-tagged Keap1-Y334A protein markedly increased the level of the PGAM5-L protein that was pulled down with chitin beads (Fig. 5A, lanes 2 and 3). Thus PGAM5-L, like Nrf2, binds to a dimeric Keap1 complex.

As both Nrf2 and PGAM5 utilize similar ETGE-containing motifs to bind the Kelch domain of Keap1, we considered the possibility that a Keap1 dimer might bind both Nrf2 and PGAM5 to form a ternary complex. To examine this possibility, HA-Nrf2 was expressed in COS1 cells along with PGAM5 and Keap1, and the presence of PGAM5 and Keap1 in anti-HA immunoprecipitates was determined. Indeed, both PGAM5 and Keap1 were readily detected in anti-HA immunoprecipitates following ectopic expression of all three proteins (Fig. 5B, lane 6). PGAM5 was also detected, albeit at reduced levels, in anti-HA immunoprecipitates in the absence of ectopic Keap1 (Fig. 5B, lane 5), presumably due to ability of endogenous Keap1 to bridge HA-Nrf2 and PGAM5. In HEK293T cells, which contain higher levels of endogenous Keap1 than

COS1 cells, the endogenous PGAM5 protein was readily detected in anti-Nrf2 immunoprecipitates but absent from control immunoprecipitates (Fig. 5C, lanes 1 and 2).

To determine if the ternary complex of Keap1, PGAM5 and Nrf2 is localized to mitochondria, COS1 cells were transfected with various combinations of expression vectors for Keap1, PGAM5-L and Nrf2 and the subcellular localization of the proteins was determined by confocal microscopy. Mitochondria were visualized by co-expression of Mito-GFP, and nuclei were visualized by DAPI staining. The HA-Nrf2 protein, when expressed alone, was predominantly nuclear and was shifted to the cytoplasm by co-expression of Keap1 (Fig. 5D, panels a-f). Co-expression of HA-Nrf2 and PGAM5-L did not alter either the predominant nuclear localization of HA-Nrf2 or the localization of PGAM5-L to perinuclear clusters of mitochondria (Fig. 5D, panels g-i). However, coexpression of Keap1 with both PGAM5-L and HA-Nrf2 dramatically shifted the localization of HA-Nrf2 from the nucleus to perinuclear mitochondrial clusters. Taken together, these results indicate that Keap1, PGAM5-L and Nrf2 form a ternary complex at mitochondria.

Reporter gene assays were performed to determine if PGAM5 participates in regulation of Nrf2-dependent gene expression. A luciferase reporter gene controlled by a minimal promoter containing four copies of an ARE was transfected into Hela cells, in which expression of endogenous Nrf2, Keap1, or PGAM5 were individually reduced by siRNA molecules. A low level of ARE-dependent reporter gene expression was observed in cells transfected with only the reporter construct, which was further reduced by siRNA against Nrf2. As expected, reporter gene expression was markedly increased by an anti-Keap1 siRNA (Fig. 5E). Reporter gene expression was also strongly increased by any of

three different anti-PGAM5 siRNA molecules (Fig. 5E and data not shown). These

siRNAs reduced steady-state levels of the endogenous PGAM5 protein by 40-60% (Fig.

5F, middle panel, lanes 1-3). Cotransfection of siRNA against both Nrf2 and PGAM5

reduced reporter gene expression to baseline levels, confirming that Nrf2 is responsible

for activation of ARE-dependent gene expression following siRNA-mediated knockdown

of PGAM5 (data not shown). While steady-state levels of Nrf2 were increased in cells

transfected with the anti-Keap1 siRNA, siRNA-mediated knockdown of PGAM5 did not

significantly increase steady-state levels of Nrf2 (Fig. 5F, top panel, compare lanes 1-3

with 5-7). Taken together, these results demonstrate that PGAM5 contributes to

repression of Nrf2-dependent gene expression by localizing the Keap1/Nrf2 complex to

the outer mitochondrial membrane.

DISCUSSION

Mitochondria are highly dynamic organelles that have critical roles in several aspects of cellular physiology, including ATP generation and regulation of programmed cell death (5). Mitochondria can be a major source of ROS, particularly when efficient transfer of electrons to oxygen during oxidative phosphorylation is disrupted (26, 55). Disruption of mitochondrial function and subsequent generation of ROS has been implicated in both cancer and neurodegenerative diseases (1, 2, 66). For example, mutations in either DJ1 or PINK, both of which are mitochondrial proteins, are responsible for two different monogenic forms of Parkinson's (1). Complex I inhibitors such as rotenone or 1-methyl-4-phenyl-1,2,5,6-tetrahydropyridine (MPP+) are widely used in animal models of Parkinson's and oxidative damage to complex 1 has been demonstrated in Parkinson's (20, 31, 48). Increased ROS production resulting from inhibition of complex I has been associated with activation of Nrf2-dependent anti-oxidant genes (45), while loss of DJ1 results in decreased steady-state levels of Nrf2 and reduced Nrf2-dependent gene expression (7). Our results, which demonstrate the existence and functional importance of a mitochondrial-localized complex containing PGAM5, Keap1 and Nrf2, provide a molecular framework for signal transduction pathways that connect mitochondrial-derived ROS and regulation of anti-oxidant gene expression in the nucleus.

Keap1 is generally regarded as a critical molecular sensor for ROS and electrophilic chemicals. However, the molecular and spatial relationships between the endogenous Keap1 protein and subcellular locations of ROS generation are poorly

understood. Our experiments indicate that there are at least two pools of Keap1; one pool that is tethered to the outer membrane of mitochondria through a physical association with PGAM5 and another pool that is localized to discrete cytoplasmic dots. In our hands, treatment of Hela cells with leptomycin B (LMB), an inhibitor of protein export from the nucleus, does not perturb the mitochondrial pool of Keap1, but results in the translocation of these cytoplasmic Keap1-containing dots into the nucleus (data not shown). Our observation that a portion of the endogenous Keap1 protein undergoes LMB-dependent nuclear accumulation is in agreement with several recent reports that ectopically expressed Keap1 and Nrf2 are shifted to the nucleus in LMB-treated cells (29, 43, 58). Keap1 has also been reported to localize to other subcellular compartments, including peripheral focal adhesions and specialized adherens junctions (56, 57). As Nrf2 is activated in response to a diverse array of cellular stresses (32), we suggest that the presence of Keap1 at multiple subcellular locations enables activation of Nrf2 in response to different types of cellular stress.

Although the ability of Keap1 to dimerize via its N-terminal BTB domain has been established (6, 41, 67), the importance of Keap1 dimerization for binding of Nrf2 and repression of Nrf2-dependent gene expression remains controversial. Structural analyses of complexes between the Kelch domain of Keap1 and several different Nrf2-derived peptides have demonstrated that the two glutamic acid residues within the NxETGE motif of Nrf2 form multiple contacts with positively charged residues in a shallow binding pocket located on the top face of the Kelch domain (39, 46). The importance of these amino acid contacts for binding of Nrf2 to Keap1 has been confirmed in a detailed mutagenesis study involving more than 30 single and multiple amino acid

321

substitutions in both Keap1 and Nrf2 (39). Biophysical studies have suggested the existence of a second motif in Nrf2 that also binds to the Kelch domain of Keap1, leading to a model in which the Keap1 dimer forms a 2:1 complex with a single molecule of Nrf2 (41, 54). However, a Keap1 dimer can bind two different Nrf2 molecules at the same time, suggesting that Keap1 and Nrf2 may form a 2:2 complex (39). Our previous identification of PGAM5 as a Keap1-binding protein revealed the existence of a conserved DxESGE motif in PGAM5 that binds to Keap1 in a manner very similar to that previously described for the NxETGE motif in Nrf2 (38). In our present experiments, we demonstrate, by both colocalization and co-immunoprecipitation, that Keap1 forms a bridge between PGAM5 and Nrf2 to form a complex of three proteins with a 1:2:1 stoichiometry. The ability of Keap1 to bridge PGAM5 and Nrf2 is a critical determinant for localization of Nrf2 to the outer membrane of mitochondria. Keap1 may utilize other binding modes, including formation of a 2:1 complex, to regulate Nrf2 at other subcellular locations. In this respect, several other candidate substrates for Keap1, including prothymosin-α and FAC1 (29, 50), have been identified and it will be of interest to determine if these proteins form higher-order complexes with Keap1 and Nrf2 that contribute to regulation of Nrf2-dependent gene expression.

Dimerization of substrate adaptor proteins for cullin-based ubiquitin ligases appears to be a general phenomenon, as several different substrate adaptors for both Cul1 (Cdc4, Fbw7 and Skp2) and Cul3 (Keap1, KLHL9 and KLHL13) form homodimeric or heterodimeric complexes (6, 39, 41, 47, 51, 52, 60, 65, 67). Formation of dimeric substrate adaptor complexes may facilitate efficient ubiquitination of a single substrate (52, 65). Our results, which demonstrate that the subcellular localization of Keap1 is

determined, in part, by its ability to simultaneously bind two different substrates, reveal a

novel aspect of substrate adaptor dimerization with important functional consequences.

Table VII-1

Position and sequence of PGAM5 peptides[a]		Mr (calculated)[b]	Mr (measured)[c]
5-32	QALQLAACGLAGGSAAVLFSAVAVGKPR	2682.46	2682.50
65-74	REPLSLINVR	1195.70	1195.73
66-74	EPLSLINVR	1039.60	1039.63
99-104	HIFLIR	797.49	797.51
105-116	HSQYHVDGSLEK	1398.65	1398.70
119-125	TLTPLGR	756.45	756.46
126-134	EQAELTGLR	1015.53	1015.56
135-141	LASLGLK	700.45	700.46
153-169	AIETTDIISRHLPGVCK	1909.01	1908.93
163-169	HLPGVCK	809.42	809.51
170-176	VSTDLLR	802.45	802.48
204-209	IEAAFR	705.38	705.39
219-235	QEEDSYEIFICHANVIR	2121.98	2122.04

a: The position and sequence of PGAM5-derived peptides identified by MALDI-TOF MS. The

MOWSE score in this experiment was 74, with a statistical significance cut-off of 63.

b: The calculated mass of the indicated PGAM5-derived peptides.

c: The observed mass of the indicated PGAM5-derived peptides by mass spectrometry.
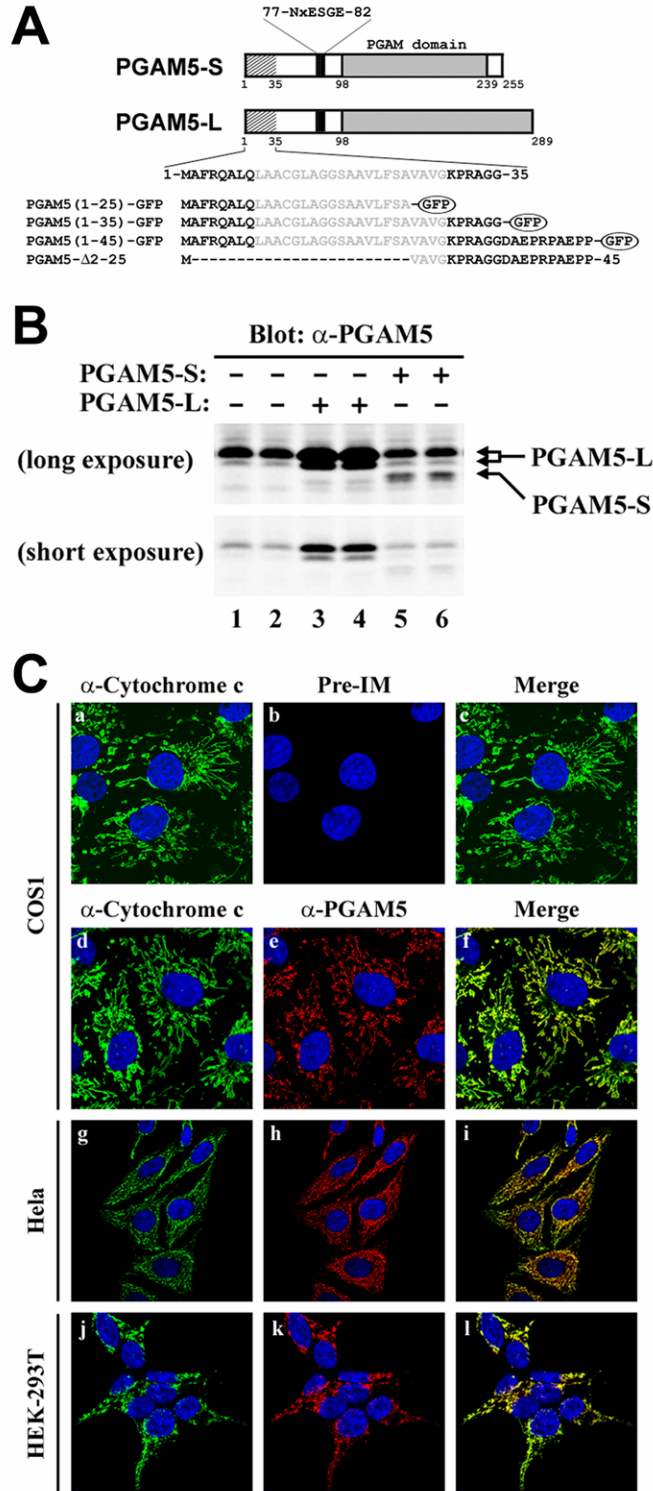
Figure VII-1

Figure VII-1. PGAM5 is a mitochondrial protein. *(A)* The two PGAM5 isoforms are depicted. Relevant landmarks include a putative transmembrane helix (amino acids 9-29), a conserved NxESGE motif that binds Keap1 (amino acids 77-82) and the PGAM domain (beginning at amino acid 98). The two isoforms have different C-terminal sequences beginning at amino acid 239. The amino acid sequence of the N-terminus of PGAM5 is shown, along with the amino acids used to make several GFP fusion proteins and the region deleted in the PGAM5-D2-25 protein. *(B)* Hela cells were transfected with an empty vector (lanes 1 and 2), or expression vectors for either of the untagged PGAM5 isoforms as indicated (lanes 3-6). Total lysates were analyzed by immunoblot with anti-PGAM5 antibodies. The relative positions of the PGAM5-L and PGAM5-S proteins are indicated by the arrows on the right side. Two different exposures of the same immunoblot are shown. *(C)* The cellular localization of the endogenous PGAM5 protein in COS1 (a-f), HeLa (g-i), or HEK-293T (j-l) was determined by indirect immunofluorescence using pre-immune (panel b) or affinity-purified anti-PGAM5 antibodies (panels e, h and k). Mitochondria were visualized with anti-cytochrome c antibodies (panels a, d, g and j). Nuclei were visualized by staining with Hoechst 33258. Merged images are shown on the right (panels c, f, i and l).
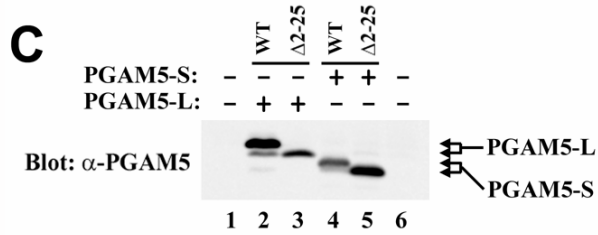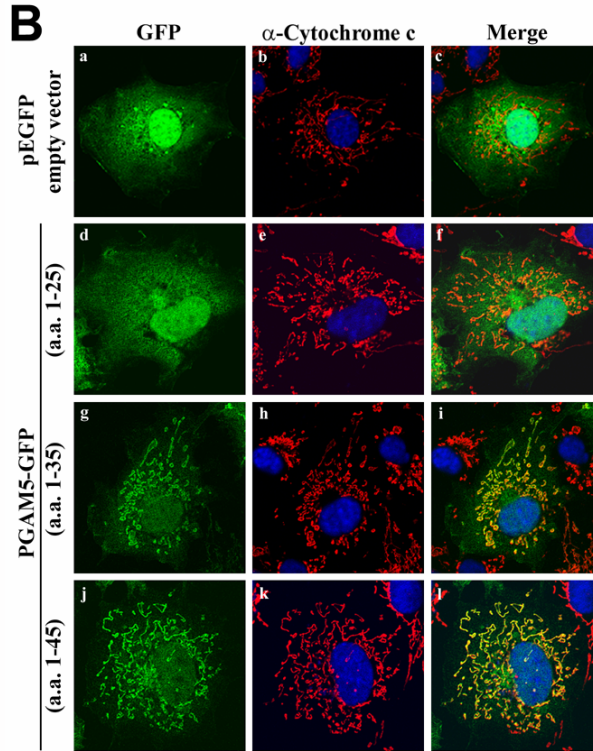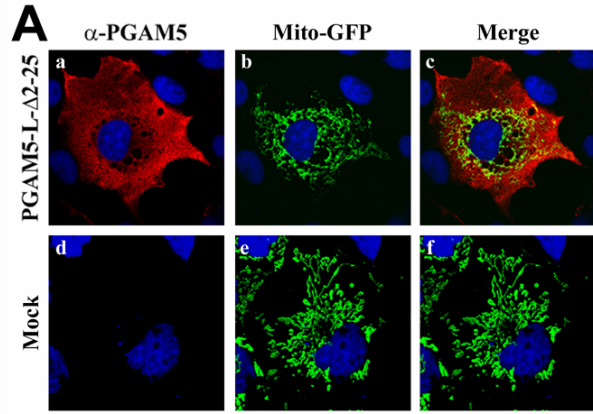
Figure VII-2

Figure VII-2. N-terminal sequences target PGAM5 to mitochondria. *(A)* COS1 cells growing on coverslips were transfected with an expression vector for Mito-GFP along with either an empty vector (bottom panels) or an expression vector for PGAM5-L-Δ2-25 (top panels). The cellular localization of the PGAM5-L-Δ2-25 mutant protein was determined by indirect immunofluorescence with anti-PGAM5 antibodies (panels a and d). Mitochondria were visualized by Mito-GFP fluorescence (panels b and e). Nuclei were stained with Hoechst 33258. Merged images were shown on the right (panels c and f). *(B)* COS1 cells were transfected with an expression vector for GFP (panels a-c), or with expression vectors for the indicated GFP fusion proteins (panels d-l). The cellular localization of GFP and the GFP fusion proteins was determined by direct fluorescence. Mitochondria were visualized by indirect immunofluorescence with anti-cytochrome c antibodies (panels b, e, h and k). Nuclei were stained with Hoechst 33258 (all panels). Merged images were shown on the right (panels c, f, i, and l). *(C)* Cell lysates from COS1 cells either mock-transfected (lane 1) or transfected with expression vectors for the indicated proteins (lanes 2-5) were analyzed by immunoblot with anti-PGAM5 antibodies. The wt and mutant PGAM5 proteins are indicated by the arrows on the right side.
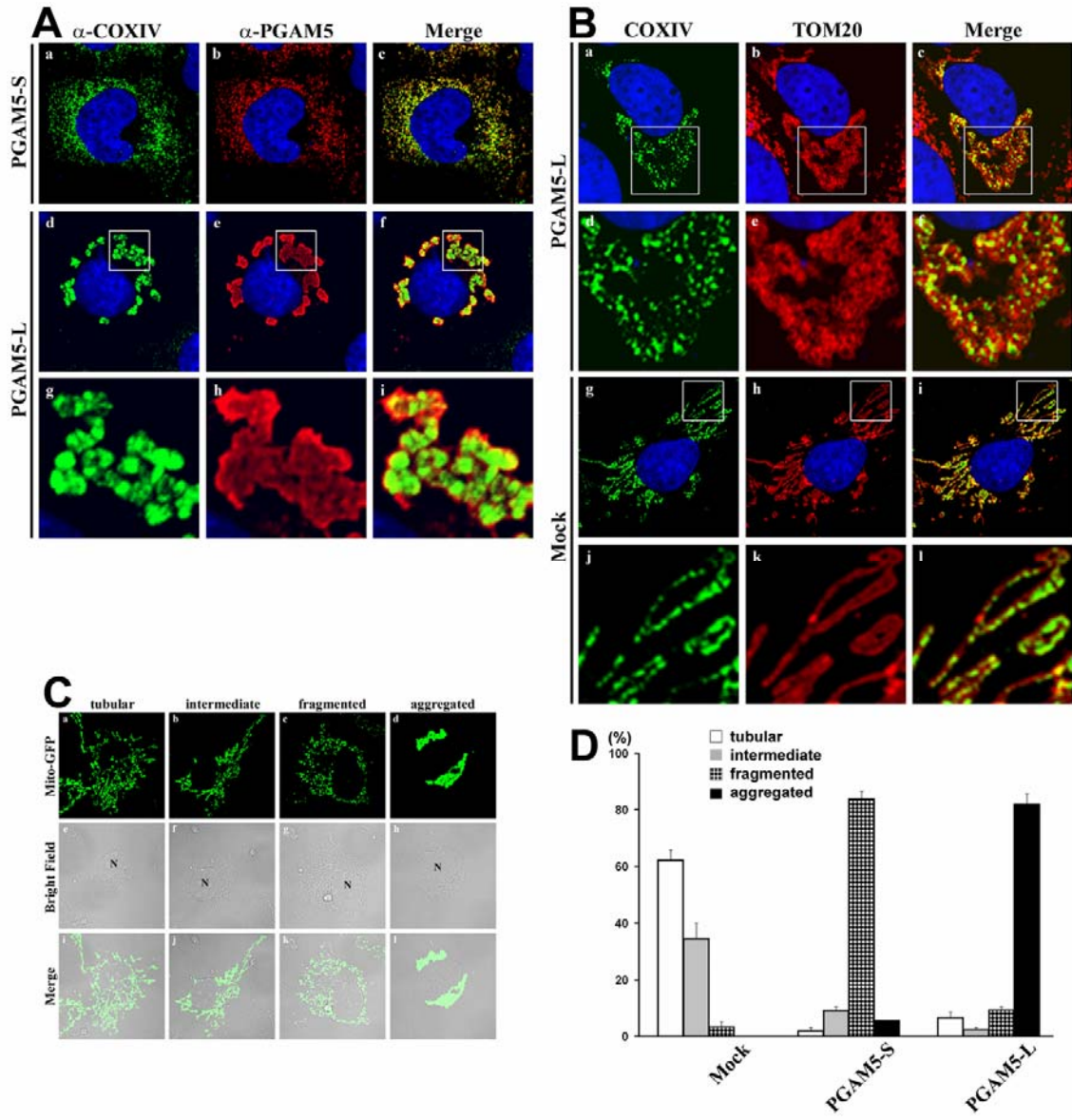
Figure VII-3

Figure VII-3. Ectopic expression of PGAM5 isoforms alter mitochondrial morphology. *(A)* COS1 were transfected with expression vectors for PGAM5-S or PGAM5-L as indicated. The cellular localization of the overexpressed PGAM5 proteins was determined by indirect immunofluorescence using anti-PGAM5 antibodies (panels b, e and h). Mitochondria were visualized by indirect immunofluorescence with anti-COXIV antibodies (panels a, d and g). Nuclei were stained with Hoechst 33258. Merged images were shown on the right (panels c, f and i). The region within the white squares in panels d-f are shown under higher magnification in panels g-i. *(B)* Spatial relation between inner mitochondrial membranes (IMM) and outer mitochondrial membranes (OMM). COS1 cells transfected with an expression vector for PGAM5-L (panels a-f) or mock transfected (panels g-l) were analyzed by double-labeled indirect immunofluorescence with anti-COXIV and anti-TOM20 antibodies. The region within the white squares in panels a-c and g-i are shown under higher magnification in panels d-f and j-l, respectively. Nuclei were stained with Hoechst 33258. Merged images are shown on the right. *(C)* Tubular, intermediate, fragmented and aggregated mitochondria in PGAM5-expressing COS1 cells were shown by the distribution of Mito-GFP (panels a-d). Bright-field microscopic images were shown in the middle (panels e-h). Merged images were shown on the bottom (panels i-l). *(D)* Percentage of cells displaying each of the four different types of mitochondrial morphology in COS1 cells transfected with an empty vector (Mock) or expression vectors for PGAM5-S or PGAM5-L. At least 200 cells were evaluated in each experiment. The mean and standard deviation from the mean for three independent experiments are shown.
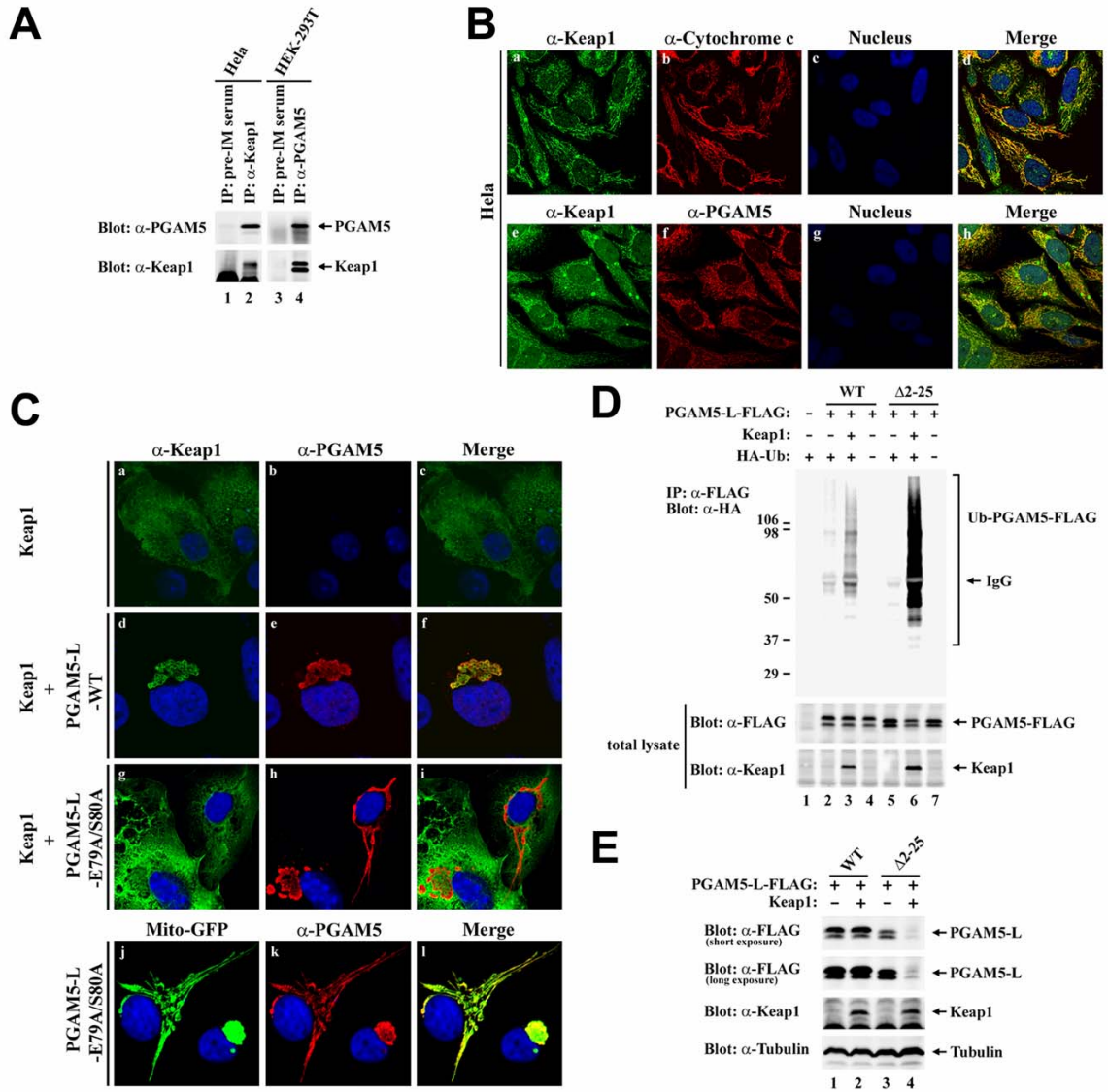
Figure VII-4

Figure VII-4. PGAM5 recruits Keap1 to mitochondria. *(A)* Anti-Keap1 immunoprecipitates from HeLa cell lysates (lane 2) and anti-PGAM5 immunoprecipitates from HEK-293T cell lysates (lane 4) were subjected to immunoblot analysis with anti-PGAM5 (top panel) and anti-Keap1 antibodies (bottom panel). Pre-immune rabbit and chicken serum were used as negative controls for the anti-Keap1 and anti-PGAM5 antibodies, respectively (lanes 1 and 3). *(B)* The cellular localization of the endogenous Keap1 protein in HeLa cells was determined by indirect immunofluorescence with affinity-purified anti-Keap1 antibodies against the full-length Keap1 (panels a and e). Mitochondria were visualized by indirect immunofluorescence using anti-Cytochrome c antibodies (panel b). PGAM5 was detected by indirect immunofluorescence using affinity-purified anti-PGAM5 antibodies (panel f). Nuclei were stained with Hoechst 33258. Merged images were shown on the right (panels d and h). *(C)* COS1 cells were transfected with expression vectors for Keap1, untagged wild-type PGAM5-L, mutant PGAM5-L-E79A/S80A and Mito-GFP as indicated. The cellular localization of the ectopic Keap1 and PGAM5-L proteins was determined by indirect immunofluorescence with anti-Keap1 (panels a, d, and g) and anti-PGAM5 antibodies (panels b, e, h and k). Mito-GFP was visualized by direct fluorescence (panel j). Nuclei were stained with Hoechst 33258. Merged images are shown on the right (panels c, f, i and l). *(D)* COS1 cells were transfected with expression vectors as indicated. Anti-FLAG immunoprecipitates (IP) were analyzed by immunoblot with anti-HA antibodies (top panel). Total lysates were analyzed by immunoblot with antibodies as indicated (bottom two panels). *(E)* Hela cells were transfected with expression vectors as indicated. Total lysates were analyzed by immunoblot with antibodies as indicated.
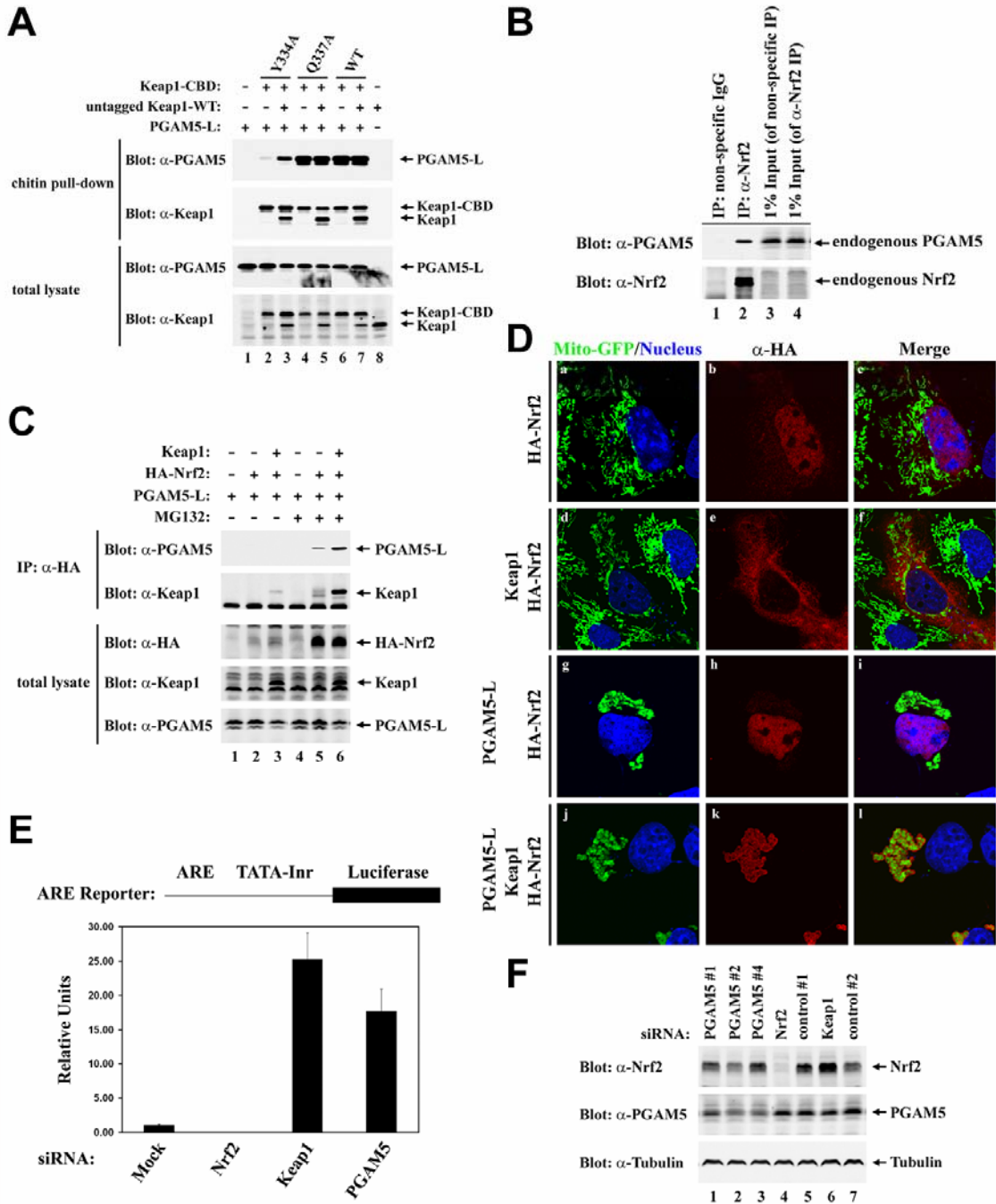
Figure VII-5

Figure VII-5. Nrf2, Keap1 and PGAM5 form a ternary complex at mitochondria.

(A) HEK-293T cells were transfected with expression vectors for PGAM5-L (0.2 μg), untagged wild-type Keap1 (0.4 μg), and wild-type or mutant Keap1-CBD proteins (0.4 μg) as indicated. Cell lysates were incubated with chitin beads and proteins that remained bound after extensive washing were subjected to immunoblot analysis with anti-PGAM5 and anti-Keap1 antibodies (top two panels). Total cell lysates were analyzed by immunoblot with anti-PGAM5 and anti-Keap1 antibodies (bottom two panels). *(B)* COS1 cells were transfected with expression vectors for HA-Nrf2 (1.6 μg), Keap1 (1.6 μg), and PGAM5-L (0.8 μg) as indicated. The transfected cells were treated with 10 μM MG132 or DMSO (0.1%) for 5 h prior to lysis. Anti-HA immunoprecipitates (IP) were analyzed by immunoblot with anti-PGAM5 and anti-Keap1 antibodies (top two panels). Total lysates were analyzed by immunoblot with anti-HA, anti-Keap1, and anti-PGAM5 antibodies (bottom three panels). *(C)* Anti-Nrf2 immunoprecipitates from 9.5 mg of HEK-293T cell lysates (lane 2) were subjected to immunoblot analysis with anti-PGAM5 (top panel) and anti-Nrf2 antibodies (bottom panel). A non-specific polyclonal antibody from rabbit was used as a negative control for IP (lane 1). Total lysates (95 μgm) were analyzed by immunoblot in parallel (lanes 3 and 4). *(D)* COS1 cells were transfected with an expression vector for Mito-GFP (0.15 μg), along with expression vectors for HA-Nrf2 (0.3 μg), Keap1 (0.3 μg), and PGAM5-L (0.15 μg) as indicated. The cellular localization of HA-Nrf2 was determined by indirect immunofluorescence with anti-HA antibodies (panels b, e, h and k). Mitochondria were visualized by distribution of Mito-GFP (panels a, d, g and j). Nuclei were stained with Hoechst 33258. Merged images are shown on the right (panels c, f, i and l). *(E)* Hela cells were transfected an ARE-dependent firefly

334

luciferase reporter gene construct (0.1 µg) and with siRNA nucleotides (300 nM) against

Nrf2, Keap1, or PGAM5 as indicated. A plasmid encoding *Renilla* luciferase (0.01 µg)

was included as a control for transfection efficiency. The data shown are the mean and

standard deviation from the mean from three independent experiments. *(F)* Hela cells

were transfected with siRNA nucleotides (300 nM) against Nrf2, Keap1, or PGAM5 as

indicated. Total lysates were analyzed by immunoblot with anti-Nrf2 (top panel), anti-

PGAM5 (middle panel), and anti-Tubulin antibodies (bottom panel).

REFERENCES

1. **Abou-Sleiman, P. M., M. M. Muqit, and N. W. Wood.** 2006. Expanding insights of mitochondrial dysfunction in Parkinson's disease. Nat Rev Neurosci **7:**207-19.

2. **Brandon, M., P. Baldi, and D. C. Wallace.** 2006. Mitochondrial mutations in cancer. Oncogene **25:**4647-62.

3. **Calkins, M. J., R. J. Jakel, D. A. Johnson, K. Chan, Y. W. Kan, and J. A. Johnson.** 2005. Protection from mitochondrial complex II inhibition in vitro and in vivo by Nrf2-mediated transcription. Proc Natl Acad Sci U S A **102:**244-9.

4. **Carpino, N., S. Turner, D. Mekala, Y. Takahashi, H. Zang, T. L. Geiger, P. Doherty, and J. N. Ihle.** 2004. Regulation of ZAP-70 activation and TCR signaling by two related proteins, Sts-1 and Sts-2. Immunity **20:**37-46.

5. **Chan, D. C.** 2006. Mitochondria: dynamic organelles in disease, aging, and development. Cell **125:**1241-52.

6. **Chew, E. H., T. Poobalasingam, C. J. Hawkey, and T. Hagen.** 2007. Characterization of cullin-based E3 ubiquitin ligases in intact mammalian cells--evidence for cullin dimerization. Cell Signal **19:**1071-80.

7. **Clements, C. M., R. S. McNally, B. J. Conti, T. W. Mak, and J. P. Ting.** 2006. DJ-1, a cancer- and Parkinson's disease-associated protein, stabilizes the antioxidant transcriptional master regulator Nrf2. Proc Natl Acad Sci U S A **103:**15091-6.

8. **Cullinan, S. B., J. D. Gordan, J. Jin, J. W. Harper, and J. A. Diehl.** 2004. The Keap1-BTB protein is an adaptor that bridges Nrf2 to a Cul3-based E3 ligase: oxidative stress sensing by a Cul3-Keap1 ligase. Mol Cell Biol **24:**8477-86.

9. **Davies, L., I. P. Anderson, P. C. Turner, A. D. Shirras, H. H. Rees, and D. J. Rigden.** 2007. An unsuspected ecdysteroid/steroid phosphatase activity in the key T-cell regulator, Sts-1: surprising relationship to insect ecdysteroid phosphate phosphatase. Proteins **67:**720-31.

10. **Dhakshinamoorthy, S., and A. K. Jaiswal.** 2001. Functional characterization and role of INrf2 in antioxidant response element-mediated expression and antioxidant induction of NAD(P)H:quinone oxidoreductase1 gene. Oncogene **20:**3906-17.

11. **Dinkova-Kostova, A. T., W. D. Holtzclaw, R. N. Cole, K. Itoh, N. Wakabayashi, Y. Katoh, M. Yamamoto, and P. Talalay.** 2002. Direct evidence that sulfhydryl groups of Keap1 are the sensors regulating induction of phase 2 enzymes that protect against carcinogens and oxidants. Proc Natl Acad Sci U S A **99:**11908-13.

12. **Eggler, A. L., G. Liu, J. M. Pezzuto, R. B. van Breemen, and A. D. Mesecar.** 2005. Modifying specific cysteines of the electrophile-sensing human Keap1 protein is insufficient to disrupt binding to the Nrf2 domain Neh2. Proc Natl Acad Sci U S A **102:**10070-5.

13. **Finkel, T., and N. J. Holbrook.** 2000. Oxidants, oxidative stress and the biology of ageing. Nature **408:**239-47.

14. **Gao, L., J. Wang, K. R. Sekhar, H. Yin, N. F. Yared, S. N. Schneider, S. Sasi, T. P. Dalton, M. E. Anderson, J. Y. Chan, J. D. Morrow, and M. L. Freeman.** 2007. Novel n-3 fatty acid oxidation products activate Nrf2 by destabilizing the association between Keap1 and Cullin3. J Biol Chem **282:**2529-37.

15. **Guda, C., P. Guda, E. Fahy, and S. Subramaniam.** 2004. MITOPRED: a web server for the prediction of mitochondrial proteins. Nucleic Acids Res **32:**W372-4.

16. **Halliwell, B.** 2007. Oxidative stress and cancer: have we moved forward? Biochem J **401:**1-11.

17. **Hammond, P. W., J. Alpin, C. E. Rise, M. Wright, and B. L. Kreider.** 2001. In vitro selection and characterization of Bcl-X(L)-binding proteins from a mix of tissue-specific mRNA display libraries. J Biol Chem **276:**20898-906.

18. **Hansen, J. M., Y. M. Go, and D. P. Jones.** 2006. Nuclear and mitochondrial compartmentation of oxidative stress and redox signaling. Annu Rev Pharmacol Toxicol **46:**215-34.

19. **He, X., M. G. Chen, G. X. Lin, and Q. Ma.** 2006. Arsenic induces NAD(P)H-quinone oxidoreductase I by disrupting the Nrf2 x Keap1 x Cul3 complex and recruiting Nrf2 x Maf to the antioxidant response element enhancer. J Biol Chem **281:**23620-31.

20. **Hoglinger, G. U., W. H. Oertel, and E. C. Hirsch.** 2006. The rotenone model of parkinsonism--the five years inspection. J Neural Transm Suppl**:**269-72.

21. **Hong, F., M. L. Freeman, and D. C. Liebler.** 2005. Identification of Sensor Cysteines in Human Keap1 Modified by the Cancer Chemopreventive Agent Sulforaphane. Chem Res Toxicol **18:**1917-1926.

22. **Hong, F., K. R. Sekhar, M. L. Freeman, and D. C. Liebler.** 2005. Specific patterns of electrophile adduction trigger keap1 ubiquitination and NRF2 activation. J Biol Chem **280:**31768-75.

23. **Itoh, K., N. Wakabayashi, Y. Katoh, T. Ishii, K. Igarashi, J. D. Engel, and M. Yamamoto.** 1999. Keap1 represses nuclear activation of antioxidant responsive elements by Nrf2 through binding to the amino-terminal Neh2 domain. Genes Dev **13:**76-86.

24. **Jedrzejas, M. J.** 2000. Structure, function, and evolution of phosphoglycerate mutases: comparison with fructose-2,6-bisphosphatase, acid phosphatase, and alkaline phosphatase. Prog Biophys Mol Biol **73:**263-87.

25. **Jeong, S. Y., B. Gaume, Y. J. Lee, Y. T. Hsu, S. W. Ryu, S. H. Yoon, and R. J. Youle.** 2004. Bcl-x(L) sequesters its C-terminal membrane anchor in soluble, cytosolic homodimers. Embo J **23:**2146-55.

26. **Jones, D. P.** 2006. Disruption of mitochondrial redox circuitry in oxidative stress. Chem Biol Interact **163:**38-53.

27. **Jones, D. P.** 2006. Redefining oxidative stress. Antioxid Redox Signal **8:**1865-79.

28. **Kang, M. I., A. Kobayashi, N. Wakabayashi, S. G. Kim, and M. Yamamoto.** 2004. Scaffolding of Keap1 to the actin cytoskeleton controls the function of Nrf2 as key regulator of cytoprotective phase 2 genes. Proc Natl Acad Sci U S A **101:**2046-51.

29. **Karapetian, R. N., A. G. Evstafieva, I. S. Abaeva, N. V. Chichkova, G. S. Filonov, Y. P. Rubtsov, E. A. Sukhacheva, S. V. Melnikov, U. Schneider, E.**

E. Wanker, and A. B. Vartapetian. 2005. Nuclear oncoprotein prothymosin alpha is a partner of Keap1: implications for expression of oxidative stress-protecting genes. Mol Cell Biol **25:**1089-99.

30. **Kaufmann, T., S. Schlipf, J. Sanz, K. Neubert, R. Stein, and C. Borner.** 2003. Characterization of the signal that directs Bcl-x(L), but not Bcl-2, to the mitochondrial outer membrane. J Cell Biol **160:**53-64.

31. **Keeney, P. M., J. Xie, R. A. Capaldi, and J. P. Bennett, Jr.** 2006. Parkinson's disease brain mitochondrial complex I has oxidatively damaged subunits and is functionally impaired and misassembled. J Neurosci **26:**5256-64.

32. **Kensler, T. W., N. Wakabayashi, and S. Biswal.** 2006. Cell Survival Responses to Environmental Stresses Via the Keap1-Nrf2-ARE Pathway. Annu Rev Pharmacol Toxicol.

33. **Kobayashi, A., M. I. Kang, H. Okawa, M. Ohtsuji, Y. Zenke, T. Chiba, K. Igarashi, and M. Yamamoto.** 2004. Oxidative stress sensor Keap1 functions as an adaptor for Cul3-based E3 ligase to regulate proteasomal degradation of Nrf2. Mol Cell Biol **24:**7130-9.

34. **Kowanetz, K., N. Crosetto, K. Haglund, M. H. Schmidt, C. H. Heldin, and I. Dikic.** 2004. Suppressors of T-cell receptor signaling Sts-1 and Sts-2 bind to Cbl and inhibit endocytosis of receptor tyrosine kinases. J Biol Chem **279:**32786-95.

35. **Kregel, K. C., and H. J. Zhang.** 2007. An integrated view of oxidative stress in aging: basic mechanisms, functional effects, and pathological considerations. Am J Physiol Regul Integr Comp Physiol **292:**R18-36.

36. **Li, J., T. D. Stein, and J. A. Johnson.** 2004. Genetic dissection of systemic autoimmune disease in Nrf2-deficient mice. Physiol Genomics **18:**261-72.

37. **Lo, S. C., and M. Hannink.** 2006. CAND1-Mediated Substrate Adaptor Recycling Is Required for Efficient Repression of Nrf2 by Keap1. Mol Cell Biol **26:**1235-44.

38. **Lo, S. C., and M. Hannink.** 2006. PGAM5, a Bcl-XL-interacting protein, is a novel substrate for the redox-regulated Keap1-dependent ubiquitin ligase complex. J Biol Chem **281:**37893-903.

39. **Lo, S. C., X. Li, M. T. Henzl, L. J. Beamer, and M. Hannink.** 2006. Structure of the Keap1:Nrf2 interface provides mechanistic insight into Nrf2 signaling. Embo J **25:**3605-17.

40. **Ma, Q., L. Battelli, and A. F. Hubbs.** 2006. Multiorgan autoimmune inflammation, enhanced lymphoproliferation, and impaired homeostasis of reactive oxygen species in mice lacking the antioxidant-activated transcription factor Nrf2. Am J Pathol **168:**1960-74.

41. **McMahon, M., N. Thomas, K. Itoh, M. Yamamoto, and J. D. Hayes.** 2006. Dimerization of substrate adaptors can facilitate cullin-mediated ubiquitylation of proteins by a "tethering" mechanism: a two-site interaction model for the Nrf2-Keap1 complex. J Biol Chem **281:**24756-68.

42. **Neupert, W., and J. M. Herrmann.** 2007. Translocation of proteins into mitochondria. Annu Rev Biochem **76:**723-49.

43. **Nguyen, T., P. J. Sherratt, P. Nioi, C. S. Yang, and C. B. Pickett.** 2005. Nrf2 controls constitutive and inducible expression of ARE-driven genes through a

dynamic pathway involving nucleocytoplasmic shuttling by Keap1. J Biol Chem **280:**32485-92.

44. **Nguyen, T., P. J. Sherratt, and C. B. Pickett.** 2003. Regulatory mechanisms controlling gene expression mediated by the antioxidant response element. Annu Rev Pharmacol Toxicol **43:**233-60.

45. **Osburn, W. O., N. Wakabayashi, V. Misra, T. Nilles, S. Biswal, M. A. Trush, and T. W. Kensler.** 2006. Nrf2 regulates an adaptive response protecting against oxidative damage following diquat-mediated formation of superoxide anion. Arch Biochem Biophys **454:**7-15.

46. **Padmanabhan, B., K. I. Tong, T. Ohta, Y. Nakamura, M. Scharlock, M. Ohtsuji, M. I. Kang, A. Kobayashi, S. Yokoyama, and M. Yamamoto.** 2006. Structural basis for defects of Keap1 activity provoked by its point mutations in lung cancer. Mol Cell **21:**689-700.

47. **Petroski, M. D., and R. J. Deshaies.** 2005. Function and regulation of cullin-RING ubiquitin ligases. Nat Rev Mol Cell Biol **6:**9-20.

48. **Schmidt, W. J., and M. Alam.** 2006. Controversies on new animal models of Parkinson's disease pro and con: the rotenone model of Parkinson's disease (PD). J Neural Transm Suppl:273-6.

49. **Shih, A. Y., S. Imbeault, V. Barakauskas, H. Erb, L. Jiang, P. Li, and T. H. Murphy.** 2005. Induction of the Nrf2-driven antioxidant response confers neuroprotection during mitochondrial stress in vivo. J Biol Chem **280:**22925-36.

50. **Strachan, G. D., K. L. Morgan, L. L. Otis, J. Caltagarone, A. Gittis, R. Bowser, and K. L. Jordan-Sciutto.** 2004. Fetal Alz-50 clone 1 interacts with the human orthologue of the Kelch-like Ech-associated protein. Biochemistry **43:**12113-22.

51. **Sumara, I., M. Quadroni, C. Frei, M. H. Olma, G. Sumara, R. Ricci, and M. Peter.** 2007. A Cul3-based E3 ligase removes Aurora B from mitotic chromosomes, regulating mitotic progression and completion of cytokinesis in human cells. Dev Cell **12:**887-900.

52. **Tang, X., S. Orlicky, Z. Lin, A. Willems, D. Neculai, D. Ceccarelli, F. Mercurio, B. H. Shilton, F. Sicheri, and M. Tyers.** 2007. Suprafacial Orientation of the SCF(Cdc4) Dimer Accommodates Multiple Geometries for Substrate Ubiquitination. Cell **129:**1165-76.

53. **Terada, L. S.** 2006. Specificity in reactive oxidant signaling: think globally, act locally. J Cell Biol **174:**615-23.

54. **Tong, K. I., Y. Katoh, H. Kusunoki, K. Itoh, T. Tanaka, and M. Yamamoto.** 2006. Keap1 recruits Neh2 through binding to ETGE and DLG motifs: characterization of the two-site molecular recognition model. Mol Cell Biol **26:**2887-900.

55. **Turrens, J. F.** 2003. Mitochondrial formation of reactive oxygen species. J Physiol **552:**335-44.

56. **Velichkova, M., J. Guttman, C. Warren, L. Eng, K. Kline, A. W. Vogl, and T. Hasson.** 2002. A human homologue of Drosophila kelch associates with myosin-VIIa in specialized adhesion junctions. Cell Motil Cytoskeleton **51:**147-64.

57. **Velichkova, M., and T. Hasson.** 2003. Keap1 in adhesion complexes. Cell Motil Cytoskeleton **56:**109-19.

58. **Velichkova, M., and T. Hasson.** 2005. Keap1 regulates the oxidation-sensitive shuttling of Nrf2 into and out of the nucleus via a Crm1-dependent nuclear export mechanism. Mol Cell Biol **25:**4501-13.

59. **Wakabayashi, N., K. Itoh, J. Wakabayashi, H. Motohashi, S. Noda, S. Takahashi, S. Imakado, T. Kotsuji, F. Otsuka, D. R. Roop, T. Harada, J. D. Engel, and M. Yamamoto.** 2003. Keap1-null mutation leads to postnatal lethality due to constitutive Nrf2 activation. Nat Genet **35:**238-45.

60. **Wimuttisuk, W., and J. D. Singer.** 2007. The Cullin3 ubiquitin ligase functions as a Nedd8-bound heterodimer. Mol Biol Cell **18:**899-909.

61. **Yoh, K., K. Itoh, A. Enomoto, A. Hirayama, N. Yamaguchi, M. Kobayashi, N. Morito, A. Koyama, M. Yamamoto, and S. Takahashi.** 2001. Nrf2-deficient female mice develop lupus-like autoimmune nephritis. Kidney Int **60:**1343-53.

62. **Zana, M., Z. Janka, and J. Kalman.** 2007. Oxidative stress: a bridge between Down's syndrome and Alzheimer's disease. Neurobiol Aging **28:**648-76.

63. **Zhang, D. D., and M. Hannink.** 2003. Distinct cysteine residues in Keap1 are required for Keap1-dependent ubiquitination of Nrf2 and for stabilization of Nrf2 by chemopreventive agents and oxidative stress. Mol Cell Biol **23:**8137-51.

64. **Zhang, D. D., S. C. Lo, J. V. Cross, D. J. Templeton, and M. Hannink.** 2004. Keap1 is a redox-regulated substrate adaptor protein for a Cul3-dependent ubiquitin ligase complex. Mol Cell Biol **24:**10941-53.

65. **Zhang, W., and D. M. Koepp.** 2006. Fbw7 isoform interaction contributes to cyclin E proteolysis. Mol Cancer Res **4:**935-43.

66. **Zhu, X., M. A. Smith, G. Perry, and G. Aliev.** 2004. Mitochondrial failures in Alzheimer's disease. Am J Alzheimers Dis Other Demen **19:**345-52.

67. **Zipper, L. M., and R. T. Mulcahy.** 2002. The Keap1 BTB/POZ Dimerization Function Is Required to Sequester Nrf2 in Cytoplasm. J Biol Chem **277:**36544-52.

VIII.   SUMMARY AND FUTURE DIRECTIONS

SUMMARY

Eukaryote cells are constantly exposed to reactive molecules from endogenous and exogenous sources. These molecules, including reactive oxygen species, electrophilic chemicals, and heavy metals, damage biological macromolecules and impair normal cellular functions. Oxidative damage derived from these molecules has been implicated in diverse pathophysiological processes, including cancer, cardiovascular disease, diabetes and neurodegeneration. Multiple protective mechanisms have evolved in eukaryote cells to combat these reactive molecules and oxidative stress. Among them, one major mechanism is the coordinated induction of enzymes that neutralize reactive molecules, eliminate damaged macromolecules and restore cellular redox homeostasis. In metazoan organisms, this cytoprotective response is mainly controlled by the Cap N' Collar (CNC) transcription factors, which constitute a subset within the bZIP transcription factor superfamily. In mammals, the Nrf2 transcription factor in the CNC family has merged as the key regulator of cytoprotective gene expression. Nrf2 activates transcription of an array of cytoprotective genes at both constitutive and inducible manners that operate in accordance to the regulation of Nrf2 itself. The Nrf2 transcription factor is mainly controlled by its upstream repressor Keap1. Keap1 is a BTB-Kelch protein that binds the Neh2 regulatory domain of Nrf2 via the Kelch β-propeller domain. Under redox homeostatic conditions, Nrf2 is kept largely inactive by Keap1, such that the constitutive Nrf2-dependent gene expression exhibits minimal basal levels. Upon exposure of cells to reactive molecules and oxidative stress, Keap1 undergoes a cysteine-

dependent biochemical transformation that in turn releases the repression of Nrf2, resulting in a burst activation of Nrf2-dependent gene expression.

The overall objective of the research presented in this dissertation was to focus on understanding the mechanisms by which Keap1 regulates Nrf2, with the ultimate goal of manipulating the Nrf2-Keap1 system to develop novel antioxidant compounds to counteract the damaging consequences of oxidative stress. Towards this end, the results presented in the first half of this dissertation have demonstrated the following key points: (1) the Nrf2 transcription factor is a labile protein that is subject to constitutive degradation by Keap1 in a proteasome-dependent manner; (2) Keap1 functions as a substrate adaptor in an E3 ubiquitin ligase complex that assembles around the Cul3-RING catalytic core complex; (3) in cells maintained under redox homeostatic conditions, this Keap1-dependent Cul3-RING ubiquitin ligase efficiently targets Nrf2 for polyubiquitin conjugation and subsequent proteolysis by 26S proteasome; (4) in cells exposed to quinone-induced oxidative stress and sulforaphane, a chemopreventive isothiocyanate compound, Keap1-dependent Cul3-RING ligases are subject to various modes of modulation, such as autoubiquitination of Keap1, or reduced binding between Keap1 and Cul3, that all lead to inhibition of Keap1-dependent ubiquitination and degradation of Nrf2; (5) covalent modification of the conserved Lys712 within Cul3 by a ubiquitin-like protein Nedd8 is required for efficient ubiquitination of Nrf2 *in vivo*; (6) CAND1, a Cul3-binding protein, competes with Keap1 for binding of Cul3, whereby CAND1 governs dynamic cycles of assembly and disassembly of the Keap1-dependent Cul3-RING ligase that are crucial for efficient degradation of Nrf2. Taken together, these

342

results have established a revolutionary point of view in the mechanistic studies of Nrf2-Keap1 system. The progression of the mechanistic studies of Nrf2-Keap1 system had been hindered in early days by a simplistic and blindly-accepted dogma. In this dogma, it was proposed that Nrf2 is repressed by Keap1 via physical sequestration in cytoplasm, and is de-repressed upon stress signals via physical liberation from binding of Keap1. In contrast, our results have taken this regulatory mechanism onto a more sophisticated and realistic level, in which Nrf2 is repressed by Keap1 via ubiquitin-dependent degradation, and is de-repressed as a result of modulation of the Keap1-dependent E3 ubiquitin ligase by a variety of mechanistic modes.

In addition, the results presented in the second half of this dissertation have demonstrated the following critical points: (1) a number of crucial amino acid residues located within the substrate-binding pocket of Kelch β-propeller domain of Keap1 recognize and make key contacts with the conserved (D/N)xE(T/S)GE motifs in cognate substrate proteins, such as Nrf2 and PGAM5; (2) Keap1 functions as a homodimer, in which two substrate-binding pockets can simultaneously accommodate two cognate substrate proteins; (3) PGAM5 is a bona fide Keap1-interacting protein that is delivered to mitochondrial outer membrane via an N-terminal mitochondrial targeting signal sequence; (4) when mislocalized in cytoplasm, PGAM5 is subject to ubiquitin-mediated degradation by a Keap1-dependent Cul3-RING ligase; (5) when residing at mitochondrial outer membrane, PGAM5 functions to modulate Nrf2-dependent gene expression via assembly of a mitochondrial ternary complex consisting of one PGAM5, one Keap1 homodimer, and one Nrf2. Taken together, these results suggest that Keap1 homodimer

nucleates formation of a signalosome containing one substrate and one substrate-like protein, which in turn modulates the function of the adjacent substrate. In addition, mitochondrial localized PGAM5-Keap1-Nrf2 signaling complex provides a novel molecular link between an Nrf2-dependent nuclear cytoprotective program and a signaling machinery of mitochondrial stress.

FUTURE DIRECTIONS

A. Characterization of physical and functional interaction of Keap1-SQSTM1/p62 complex.

A.1. To determine the regions in SQSTM1/p62 that binds Kelch domain of Keap1.

SQSTM1/p62 is a multi-domain protein and functions as molecular scaffold for assembly of multi-protein signaling complexes (signalosomes) in diverse pathways associated with cellular stress responses, survival, and inflammation (for review, see [1]). A number of proteins in these signalosomes have been shown to directly associate with SQSTM/p62, and the protein domains that mediate these interaction have been identified. For example, atypical protein kinase C (aPKC) isoforms, such as λ/ιPKC and ζPKC, binds to N-terminal PB1 domain of SQSTM1/p62 [2]; death receptor-interacting protein RIP binds to the ZZ type zinc finger domain (ZZ domain) of SQSTM1/p62 [3]; cell adhesion protein Ajuba binds to the regions following the ZZ domain of SQSTM1/p62 [4]; RING-type E3 ubiquitin ligase TRAF6 binds to the regions preceding the first PEST

sequence of SQSTM1/p62 [5];.K63-linked polyubiquitin chains bind to C-terminal UBA domain of SQSTM1/p62 [6]. Our preliminary results showed that the UBA domain of SQSTM1/p62 is dispensable for binding of Keap1, suggesting that ubiquitin conjugation of Keap1 is not required for interaction between Keap1 and SQSTM1/p62 [7]. However, it remains unclear how they interact physically. To determine which regions in SQSTM1/p62 direct binding with Keap1, a comprehensive pull-down analysis will be carried out, in which we will examine the binding between Kelch domain of Keap1 and a series of both N-terminal and C-terminal deletion mutant proteins of SQSTM1/p62. Internal deletion mutants of SQSTM1/p62 will be subsequently examined to confirm regions in SQSTM1/p62 that are necessary and sufficient for binding of Keap1. Identification of Keap1-interacting motifs in SQSTM1/p62 will provide valuable information for further investigation of potential signalosomes in which Keap1-SQSTM1/p62 complex is engaged.

A.2. To determine the role of SQSTM1/p62 in Keap1-dependent regulation of Nrf2.

Studies have shown that expression of SQSTM1/p62 is significantly up-regulated upon exposure of microphages to stress signals, including electrophilic chemicals, ROS, and heavy metals, suggesting an important regulatory role for SQSTM1/p62 in response to oxidative stress [8, 9]. One recent report suggested that SQSTM1/p62 may function as a positive regulator for Nrf2, based upon the observation that ectopically expressed SQSTM1/p62 caused activation of Nrf2-dependent gene expression [10]. However, the physiological relevance of this observation is not clear, as overexpression of

SQSTM1/p62 often causes formation of super-sized sequestosome bodies that may have a global impact on cellular functions. In contrast, it has been suggested that expression of SQSTM1/p62 is positively regulated by Nrf2, as expression of SQSTM1/p62 is activated by stress to a lesser degree in Nrf2-deficient microphages than in wild-type microphages [8]. However, the residual activation of SQSTM1/p62 gene expression by stress was still observed, suggesting that stress-induced expression of SQSTM1/p62 can also be achieved in an Nrf2-independent manner [8]. In brief, Nrf2 can partially activate expression of SQSTM/p62 via a mechanism that is yet to be identified. A critical question awaits to be addressed is whether (1) Nrf2 functions as a transcription factor directly in gene expression of SQSTM1/p62 that then functions downstream of cytoprotective processes, or (2) induction of SQSTM1/p62 is carried out in a feedback manner indirectly upon high abundance of Nrf2, such that SQSTM1/p62 functions to promote removal of Nrf2 proteins that were induced to cope with stress at the front line and are no linger needed.

Early sequencing studies of the 5' flanking region of the STAP gene (mouse homologue of SQSTM1/p62) revealed multiple consensus motifs for binding of several transcription factors, including Sp1, AP-1, NF-E2, MyoD, and NF-κB [11]. A comprehensive *in vivo* and *in vitro* analysis on promoter regions of SQSTM1/p62 will determine if Nrf2 indeed functions to directly activate transcription of the human SQSTM1/p62 gene. If, however, Nrf2 does not play a major role in transcription activation of SQSTM1/p62 per se, it would be interesting to determine the mechanisms of

how elevated levels of Nrf2 transduce signals to specific transcription factors for gene expression of SQSTM1/p62.

We hypothesize that binding of SQSTM1/p62 with Keap1 would promote destruction of Nrf2 during the period of post-stabilization (post-induction) of Nrf2 by stress signals. The idea is that upon stress signals, the processivity of Nrf2 ubiquitination decreases as the result of its re-positioning in cognate CRL, in which substrate adaptor Keap1 homodimer undergoes conformational change via modification of thiol groups in cysteine residues. The subsequent binding of SQSTM1/p62 onto Kelch domain of Keap1 would somehow function to compensate this decrease in processivity of Nrf2 ubiquitination, such that destruction of Nrf2 is restored once oxidative stress is neutralized and oxidative damage is eliminated. To examine the core idea in this hypothesis, we will first generate pools of stabilized Nrf2 proteins in vivo by various stress signals. The half-lives of these Nrf2 proteins will then be compared in wild-type and in SQSTM1/p62-knockout cells, upon removal of these stress signals. The results, in which SQSTM1/p62-knockout cells exhibit longer half-life of Nrf2 than wild-type cells shortly after removal of stress signals, would support our hypothesis that SQSTM1/p62 plays a crucial role for efficient turnover of Nrf2 once stress is eliminated and Nrf2 is no longer of immediate use.

To further investigate this hypothesis, we propose two plausible models to explain how SQSTM1/p62 promotes Nrf2 destruction in a cooperative manner with the sub-active Keap1 that has just undergone oxidative modification and failed to maintain a

conformation in favor of optimal positioning of Nrf2. In the first model, we propose that SQSTM1/p62 functions as an accessory protein for Nrf2 orientation in Keap1-dependent Cul3-RING ligases. The notion is that even though Keap1-bound Nrf2 has been deviated from the optimal positioning due to conformational rearrangement of Keap1 homodimer, subsequent binding of SQSTM1/p62 onto this Nrf2-bound Kelch domain of Keap1 will re-adjust binding orientation of Nrf2, such that Nrf2 is optimally poised again for productive ubiquitin transfer, hence regains its high processivity. The hallmark in this model is that SQSTM1/p62 and Nrf2 simultaneously bind Kelch domain(s) of oxidative modified Keap1 homodimer. Pull-down analysis will be carried out to confirm the presence of both Nrf2 and SQSTM1/p62 in the same complex with Keap1. In addition, in vitro ubiquitin conjugation analysis of Nrf2 and three-dimensional structure of this complex will provide definitive validation for this model.

In the second model, we propose that SQSTM1/p62 functions as a pseudosubstrate in Keap1-dependent Cul3-RING ligases that enhances, or restores processivity of Nrf2 ubiquitination by pre-engaging hyper-neddylated and thus highly active CRLs. Consistent with the characteristics of pseudosubstrate hnRNP-U in β-TrCP/E3RS-dependent Cul1-RING ligases [12], our preliminary data have shown several pseudosubstrate properties for SQSTM1/p62, in that (1) SQSTM1/p62 overall binds to the same site in Kelch domain of Keap1 as Nrf2 does, yet with a low affinity, via a non-conventional (D/N)xE(T/S)GE motif; (2) SQSTM1/p62 was hardly subjected to Keap1-mediated ubiquitination and degradation; (3) SQSTM1/p62 and the true substrate Nrf2 largely reside in distinct subcellular compartments, as we did not observe significant

localization of endogenous Nrf2 proteins at sequestosome bodies, even in the presence of the proteasome-inhibitor MG132 [7]. To further demonstrate a pseudosubstrate role for SQSTM1/p62, several critical analyses will be carried out. First, we will determine if SQSTM1/p62 assembles into Keap1-dependent Cul3-RING ligases. Secondly, we will determine if SQSTM1/p62 are indeed engaged to Keap1-dependent Cul3-RING ligases that are predominantly hyper-neddylated. Importantly, to determine if pre-engagement of SQSTM1/p62 with Keap1 promotes kinetics in ubiquitination of subsequently bound Nrf2, we will examine *in vitro* ubiquitination of Nrf2 by Keap1-dependent Cul3-RING ligases that are pre-incubated with SQSTM1/p62. Lastly, deciphering mechanisms of how SQSTM1/p62 increases neddylation of bound Cul3 will provide novel insights into current research on regulation of CRLs by pseudosubstrates.

A.3. To determine the role of SQSTM1/p62-Keap1 complex in autophagy.

Autophagy is a cellular process, in which subcellular membranes undergo dynamic rearrangement to package macromolecules and organelles for subsequent lysosomal degradation. In general, autophagy occurs constitutively at basal levels in most tissues. In addition, high levels of autophagy can be induced upon environmental stress, such as nutrient depletion and pathogen invasion. The significance of autophagy has been broadly implicated in multiple physiological processes, including cell differentiation, tissue remodeling, cellular defense, cell survival, and programmed cell death. Defects in autophagy have been shown in a number of pathological conditions, such as

neurodegenerative diseases, cardiomyopathies, cancer, and aging (for review, see [13-16]).

As defined by the mechanistic routes to the final destination in lysosomes, autophagy can be divided into three classes, macroautophagy, microautophagy, and chaperon-mediated autophagy. Macroautophagy is an evolutionary conserved process that has been found in virtually all eukaryotes. Thus, the term 'autophagy' is often used to refer to macroautophagy. In macroautophagy, de novo formation of double- or multi-membrane bound structures, termed autophagosomes, is carried out to sequester intracellular macromolecules or organelles. Subsequent fusion of autophagosomes with lysosomes results in formation of autolysosomes, in which the proteins and organelles are degraded and/or recycled for further usage by cells. Autophagy is a multi-step process that is accomplished by a sophisticated machinery involving a large number of protein and lipid players. Yeast genetic studies have identified approximately 20 autophagy-related genes (ATGs) that are evolutionarily conserved throughout eukaryotes. However, given the more complex organismal development and stress-induced adaptation, many more protein players are involved in autophagy process and its regulation in higher eukaryotes (fore review, see [17-19]).

Although autophagy was thought to non-selectively target cellular proteins and organelles for digestion, increasing lines of evidence have demonstrated that it can also operate locally at a selective fashion. Recent studies have indicated a role of SQSTM1/p62 in autophagy, in that the small-sized subtype of sequestosome bodies is in

essence double-membrane bilayered autophagosome, and that SQSTM1/p62 directly interacts with LC3 (Atg8), one of the critical components in autophagy machinery [20, 21]. Additionally, our preliminary data showed that in the presence of mitochondrial Keap1-PGAM5 complexes, mitochondria can be studded with sequestosome bodies that are otherwise scattered in cytoplasm, indicating that Keap1 together with mitochondrial PGAM5 may recruit SQSTM1/p62-containing autophagosomes to specific groups of mitochondria for selective digestion [7]. We propose that under oxidative stress, certain pools of mitochondrial PGAM5-Keap1 complexes, in which cysteine residues of Keap1 are modified on site with ROS released from local damaged mitochondria, transduce signals to recruit SQSTM1/p62-dependent autophagy for selective clearance of these damaged mitochondria. Given the dynamic localization of Keap1 and its potential role as a molecular sensor for various oxidative stress signals, verification and characterization of the functions of Keap1 in local autophagy will provide insights into mechanisms underlying the selective mode of autophagy induction.

Indeed, a recent study suggested that ROS arising locally upon short-term starvation can function as signaling molecules for induction of local autophagy, and addition of antioxidants counteract the ROS-induced autophagy [22, 23]. In this study, human cysteine protease Atg4 was shown to be the direct target for these signaling ROS molecules. One of the major functions of Atg4(s) is to catalytically remove the lipid modification of Atg8(s) that is otherwise required for autophagosome formation. Thus, inactivation of Atg4 via oxidation of a critical cysteine residue that is required for its protease activity would lead to increased lipidation of Atg8(s) for autophagy onset.

Interestingly, catalytic cysteine residues in other autophagy enzymes, such as Atg3, Atg7, and Atg10, did not seem to be affected by these starvation-generated local ROS, suggesting that redox-regulation of autophagy can be accomplished differentially and specifically. Thus, identification of connections between various pools of local ROS and their corresponding protein targets in autophagy processes would provide valuable groundwork for further manipulation of autophagy, and for potential drug discovery in autophagy-related pathological conditions.

B. Comprehensive characterization of PGAM5.

B.1. To explore functionalities of PGAM5 by using a wide spectrum of approaches.

PGAM5 is a nuclear-encoded, mitochondrial-resident protein [24]. It belongs to the phosphoglycerate mutase family, in which members share a structurally-related yet functionally-divergent PGAM domain. Homologues of PGAM5 are widely found in mammals. Based on published results of the high-throughput microarray-based analysis from GENEVESTIGATOR and the in situ hybridization-based analysis from Allen Brain Atlas, PGAM5 is ubiquitously expressed in a variety of cell types. Consistent with our preliminary immunoblot assay of mouse tissues, PGAM5 is particularly expressed at high levels in placenta, brain, and spleen. However, little is known about the biochemical functions and physiological roles of PGAM5.

Genetic approaches will be utilized to further investigate biological roles of PGAM5. First, we propose to generate PGAM5$^{-/-}$ mice by using an ES cell line containing a gene trap insertion into the mouse PGAM5 locus, and examine the phenotypic abnormalities that these mice might show. Secondly, we will generate PGAM5-knockout cell lines by stable transfection of pSilencer vectors that express PGAM5-specific hairpin siRNAs. A number of cellular parameters and processes that are related to mitochondrial functions will be assessed in these PGAM5-silencing cell lines, in comparison with parental as well as stable control cells. For example, growth rates of the cells will be measured by cellular colony formation assays; cell viabilities over a time period will be determined upon exposure of cells to various stress signals, and apoptotic signals; mitochondrial ultra-structures, including overall morphology, distribution, and cristae organization, will be inspected for abnormality by electron microscopy; mitochondrial homeostasis and oxidative capacity will be examined, such as mitochondrial membrane potential, rate of O2 consumption, and ATP production; cellular redox homeostasis will be assessed by measuring cellular levels of ROS, and GSH/GSSG ratio; intracellular calcium homeostasis will also be examined. In parallel, we will generate stable cell lines that express high levels of PGAM5, and determine the impact of increased abundance of PGAM5 on cellular processes listed above.

To investigate the biochemical functions of PGAM5, we will first seek to identify interaction partners of PGAM5 by using yeast two-hybrid screening, and by proteomic analysis of anti-FLAG immunoprecipitates containing C-terminal FLAG-tagged PGAM5. Additionally, we will confirm physical interaction between PGAM5 and several known

binding candidates, including RhoBTBs, PLZF (ZBTB16), and TRAF2. Based on the personal communication with Dr. Rory Geyer at Mayo Clinic, PGAM5 was found in RhoBTB-containing immunoprecipitates from HeLa cell lysates. The RhoBTB proteins (RhoBTB1 and RhoBTB2) are atypical Rho GTPases that comprise an N-terminal Rho GTPase domain and two tandem BTB domains. However, the functions of RhoBTBs are not known. As several GTPase proteins have been shown to function in mitochondrial morphogenesis, it is of great interests to determine if RhoBTBs can be tethered to mitochondria via binding of PGAM5, and relay signals for communication between mitochondria and other intracellular events [25]. Furthermore, a yeast two-hybrid mating-based, systematic protein matrix-generated map of protein-protein interactions has indicated that PGAM5 may physically interact with PLZF (promyelocytic leukemia zinc finger protein), SETDB1, and HSPA1B (heat shock 70 kDa protein 1) [26]. The SETDB1 proteins are histone-lysine methyltransferases that function in heterochromatin and euchromatin remodeling, while the PLZF proteins are BTB domain-containing zinc finger-type transcription factors that are involved in physiological development, cell proliferation, differentiation, and apoptosis [27-32]. Investigation of potential interactions of PGAM5 with PLZF and/or SETDB1 may uncover an unexpected signaling pathway in nuclear-mitochondrial communication. Lastly, PGAM5 contains a putative TRAF2-binding motif (amino acids 217-220). TRAF2 is a critical adaptor protein in TNF-Rs (tumor necrosis factor receptor)-induced signaling cascades that lead to activation of NFκB or JNK, and apoptosis [33-35]. Studies have shown that upon TNF-R2 signaling, TRAF2 binds to c-IAP1 (cellular inhibitor of apoptosis protein), and translocates to a Triton X-100 insoluble cellular compartment that displays round punctae-like

354

morphology [36]. It would be interesting to determine if this compartment is linked to mitochondria via TRAF2-PGAM5 complex formation, and to examine the functional implication behind.

B.2. To determine phosphatase activity of PGAM5, and to identify its substrate(s)

PGAM5 belongs to the phosphoglycerate mutase family. The PGAM domains in certain family members confer phosphatase activities. The enzyme active site is constructed by a catalytic triad consisting of two conserved histidine residues, and a third variant amino acid residue. Thus, these protein members also belong to the histidine phosphatase superfamily, in which the catalytic histidine residue forms a phospho-histidine intermediate during removal of phosphate group from substrates. A key feature of histidine phosphatases is that the histidine catalytic core is conserved, while the adjacent substrate-binding site varies dramatically in size and chemical property, such that histidine phosphatases can catalyze cleavage of phosphates from diverse classes of substrates [37-39]. The best-characterized members in the phosphoglycerate mutase family, PGAM1/2 (phosphglycerate mutase 1/2) and PFKFBs (6-phosphofructo-2-kinase/ fructose-2, 6-biphosphatases), are histidine phosphatases that function as metabolic enzymes and mediate phosphate transfer in different carbohydrate substrates. However, the ability to carry out such phospho-carbohydrate metabolism was not observed in other members in the family, including STS-1 and STS-2, even though they contain the conserved histidine residues that can presumably form the catalytic triad [40].

355

Recent studies have demonstrated that STS-1 exhibits specific phosphatase activity toward non-carbohydrate substrates, including phospho-steroids and phospho-Tyrosines in a number of proteins [41, 42], suggesting that members in the phosphoglycerate mutase family may mediate phosphate trasfer for a variety of classes of substrates, and thereby exert divergent physiological roles. In addition, MINPPs (multiple inositol poly-phosphate phosphatases) are histidine phosphatases, and belong to a distinct subgroup of inositol phosphate phosphatases. The MINPP enzymes function to cleave phosphate from multiple inositol poly-phosphate substrates, such as inositol tetrakisphosphates, inositol pentakisphosphates, and inositol hexakisphosphates. Interestingly, the consensus sequences flanking the catalytic histidine residue in MINPPs share high similarity with those in phosphoglycerate mutase family members, raising the possibility that certain members in the phosphoglycerate mutase family may exhibit phosphatase activity toward inositol poly-phosphate substrates [43, 44]. PGAM5 contains a putative catalytic triad, in which the flanking sequence of the catalytic histidine residue is semi-consensus, suggesting that PGAM5 may confer phosphatase activity toward substrates that are distinct from the known substrates for other phosphoglycerate mutase family members. We propose to determine the potential phosphatase activity of PGAM domain in PGAM5, and to further identify the specific substrates. PGAM domains of PGAM5 will be expressed in S2 Drosophila cell lines, and purified via chromatography. In vitro phosphatase assays will then be carried out to examine the phosphatase activity of the PGAM domains toward the generic substrate *p*-nitrophenyl phosphate (pNPP), and a number of putative substrates, such as steroid derivatives, various inositol poly-phosphates, and peptides containing phospho-Tyr, phospho-Ser or phospho-Thr.

In parallel, we propose to determine three dimensional structure of the PGAM domain of human PGAM5. The obtained structure will subsequently be subject to structural alignment with all the histidine phosphatases of known structure and known substrates throughout species. The notion is that PGAM5 is likely to share the same category of substrates with the histidine phosphatases whose substrate-binding pockets highly resemble to the predicted substrate-binding pocket of PGAM5, structurally and chemical property-wise. A short list of the substrate candidates will be determined from the alignment analysis. Furthermore, we will carry out a structural modeling for tentative substrate binding, in which each substrate candidate from the list will be manually docked into the substrate-binding pocket and the adjacent catalytic core of PGAM5 for the best fit in conformation and binding properties. The most favored substrate candidates obtained from these analyses will be assayed for their phosphate catalysis by purified PGAM5 proteins in *in vitro* systems described earlier.

B.3. To determine the mechanisms underlying the functional interaction between mitochondrial PGAM5 and Nrf2-dependent gene expression

PGAM5 contains an N-terminal mitochondrial targeting sequence that enables steady-state localization of PGAM5 at mitochondrial outer membrane [24]. PGAM5 can recruit Nrf2 and Keap1 to mitochondria, where it forms a ternary complex with one Keap1 homodimer and one Nrf2, resulting in a 1:2:1 binding stoichiometry [24]. An intriguing idea is that this ternary complex facilitates the first line communication

between mitochondrial ROS production and a nuclear cytoprotection program against oxidative damage. Indeed, studies have shown that Nrf2-dependent gene expression was increased by excessive production of mitochondrial ROS arising from inhibition of mitochondrial respiratory chain. Under these conditions, nuclear translocation of Nrf2 was also observed [45]. However, it remains obscure how nuclear translocation of Nrf2 and subsequent expression of ROS-scavenging enzymes are readily induced by mitochondrial ROS before massive diffusion of ROS occurs and concomitant cellular damage has spiraled out of control. Our results showed that siRNA-mediated knockdown of PGAM5 resulted in an increase in Nrf2-dependent gene expression, suggesting an important functional interaction between mitochondrial protein PGAM5 and nuclear transcription factor Nrf2. Interestingly, this increase in Nrf2-dependent gene expression is likely achieved by nuclear translocation of Nrf2 rather than by stabilization of Nrf2, as steady-state levels of Nrf2 were not altered [24].

To address the potential role of mitochondrial PGAM5 in Nrf2-dependent cytoprotection against mitochondrial stress, we propose that (1) under cellular redox homeostatic conditions, a subpopulation of Nrf2-Keap1 complex is physically retained at mitochondria via interaction with mitochondrial PGAM5; (2) In response to mitochondrial stress, excessive mitochondrial ROS produced is conveniently sensed by the neighboring Keap1 that has been tethered by PGAM5 at mitochondria, and readily enables bound Nrf2 to translocate into nucleus and activate transcription. The notion is that the mitochondrial-localized subpopulation of Nrf2 is dispensable in maintaining

basal levels of antioxidant gene expression, but is pivotal for rapid and efficient response to locally increased levels of ROS caused by mitochondrial stress.

To verify this hypothesis, subcellular distribution of endogenous Nrf2 and Keap1 will first be examined under redox homeostatic conditions in the presence and absence of endogenous PGAM5. Secondly, mitochondrial stress will be introduced in vivo by pharmacological inhibition of electron transport complex I or II. Under these conditions, levels of Nrf2 and Keap1 in the mitochondria versus in the nucleus will be measured and compared. As it is possible that relocalization of Nrf2 functions as the first line defense to mitochondrial ROS, while stabilization of Nrf2 as the second line defense, this analysis will be carried out over a time course, in which we predicted to observe an early nuclear translocation of Nrf2 followed by a later stabilization of Nrf2 in all compartments. Furthermore, the role of PGAM5 in the efficiency of Nrf2-Keap1 system to respond to mitochondrial stress will be assessed by measuring an Nrf2-dependen reporter gene expression over a time course in the presence and absence of PGAM5.

Lastly, a critical question in this model needed to be carefully examined is whether (1) mitochondrial Keap1 translocates along with bound Nrf2 into nucleus upon mitochondrial stress, or (2) Keap1 stays at mitochondria, while Nrf2 is discharged from Keap1 and translocates into nucleus. We currently favor the first model, in which we hypothesize that ROS induces conformational change within Keap1 homodimer, such that the distance between two substrate-binding pockets in Kelch domains decreases, and is no longer able to accommodate both PGAM5 and Nrf2. As a result, Keap1 homodimer

is released from mitochondrial PGAM5, and translocates with bound Nrf2 into nucleus. If, however, mitochondrial retention of Keap1, instead of nuclear translocation of Keap1 occurs, we will then generate a chimeric Keap1 protein that contains an intrinsic mitochondrial targeting sequence, and determine if this mitochondrial-localized chimeric Keap1 can bypass the requirement of mitochondrial PGAM5 for rapid response of Nrf2-dependent gene expression to mitochondrial stress.

B.4. To determine the roles of PGAM5 in mitochondrial dynamics.

Mitochondria are highly dynamic organelles that undergo constant trafficking and morphogenesis. Mitochondrial morphogenesis is a morphology-shaping process, in which individual units of mitochondria frequently fuse and divide (also termed 'fission') to form a network at a dynamic equilibrium. Thus, the morphology of mitochondrial network is dictated by the relative rate between mitochondrial fusion and fission. Decreasing the relative rate of fusion leads to mitochondrial fragmentation, whereas decreasing the relative rate of fission results in mitochondrial elongation and interconnection. Mitochondrial network often displays diverse morphology in various types of cells, or in the same type of cells with different physiological demands, suggesting that mitochondrial morphogenesis may exert particular biological functions. Indeed, studies have indicated that elongated mitochondria may enable rapid transmission of membrane potential across significant distances in mitochondrial network, while mitochondrial fragmentation may facilitate deliver of mitochondria to subcellular loci where the ATP is temporally in high demands. It is likely that mitochondrial morphology is modulated to

optimize its temporal functionality at a dynamic fashion, such that mitochondria can be efficiently fine tuned to cope with cellular demands and environmental stress. Impaired mitochondrial morphogenesis can contribute to pathophysiological conditions, such as autosomal dominant optic atrophy (ADOA), neurodegeneration, aging, and programmed cell death [46-50].

Studies over the past half decade have identified the essential machinery and demonstrated the principle mechanisms of mitochondrial morphogenesis. In mammals, essential players that mediate mitochondrial fusion process include mitofusin1 (Mfn1), mitofusin2 (Mfn2), and optic atrophy 1 (OPA1). Mfn1 and Mfn2 are dynamin-related GTPases that localize at mitochondrial outer membranes, and form homo- and heterodimers with each other during mitochondrial tethering and fusion. OPA1 is also a dynamin-related GTPase that localizes in the mitochondrial intermembrane space, and participates in mitochondrial inner membrane fusion and cristae remodeling. On the other hand, two essential players that mediate mitochondrial fission process are FIS1 and dynamin-related GTPase protein DRP1. FIS1 is a tail-anchored mitochondrial protein that is distributed throughout mitochondrial outer membrane, and functions to recruit DRP1 from cytoplasm. DRP1 localizes at specific foci of mitochondrial outer membrane where it forms a ring-like structure around mitochondria via polymerization, and is thought to catalyze mitochondrial fission through membrane constriction [46, 49, 50]. In addition, a growing number of mitochondrial-resident proteins have been shown to modulate mitochondrial morphology. These modulators each contain distinct biochemical structures and properties, indicating that mitochondrial morphogenesis can be regulated

361

at multiple levels via different mechanisms. For example, Rho-family GTPase Miro, pro-apoptotic proteins BAX and BAK, rhomboid protease PARL, and RING-domain E3 ubiquitin ligase MARCH-V (MITOL) have been demonstrated to modulate mitochondrial morphology via direct regulation of essential players in the morphogenesis machinery described above [51-55].

The human PGAM5 gene encodes two distinct protein isoforms that differ at their C-termini due to alternative splicing. Our results showed that ectopic expression of PGAM5-S (short) isoform protein resulted in dramatic fragmentation of mitochondria in a number of cell lines that normally displayed elongated and interconnected mitochondrial network, suggesting a potential role of PGAM5 in modulation of mitochondrial morphology [24]. To determine if PGAM5 functions to regulate mitochondrial morphogenesis, mitochondrial fragmentation by overexpressed PGAM5-S proteins will first be confirmed at the dynamic levels by monitoring changes in mitochondrial morphology in real time under time-lapse confocal microscopy. Secondly, a series of pull-down analysis will be carried out to verify physical interactions between PGAM5 and each of the essential protein components in mitochondrial fusion and fission machinery, including Mfn1, Mfn2, FIS1, and DRP1. Moreover, to determine if mitochondrial fragmentation by PGAM5-S is due to reduced rate of fusion, mitochondrial fusion activity will be directly measured by a polyethylene glycol (PEG) cell fusion assay [56]. In this assay, cells expressing mitochondrial-localized dsRed will be co-cultured, and subsequently fused to cells expressing mitochondrial-localized GFP. Cycloheximide will be included to stop de novo synthesis of fluorescent molecules, such that the yellow

mitochondria are (colocalization of dsRed and GFP is) resulted solely from the fusion between dsRed-containing mitochondria and GFP-containing mitochondria. The mitochondrial fusion activity in the fused cells will be then quantified by measuring the percentage of the fused cells displaying fused, partially fused, or unfused mitochondria. Lastly, we propose to also perform fluorescence recovery after photobleaching (FRAP) assays to confirm PGAM5-mediated reduction of mitochondrial fusion activity in a quantitative manner [53].

In addition to mitochondrial morphogenesis, mitochondrial trafficking is another key factor that governs dynamics of this organelle. Mitochondrial trafficking is a highly diverse and complex process, in that mitochondria move at different speed, change directions spontaneously, and make stops for different time periods along their trajectory. In principle, mitochondria move along microtubules and actin microfilaments by molecular motor protein ATPases, including kinesin(s) and dynein. Movement of mitochondria toward the plus ends of microtubules (anterograde transport) is carried out by kinesin motors, while movement towards the minus ends of microtubules (retrograde transport) is accomplished by dynein motors. Importantly, a set of adaptor and scaffolding proteins, such as Miro and Milton, function to link mitochondria with cytoskeletal trajectory during mitochondrial trafficking by mediating physical interactions between motor proteins and the cargo proteins that reside at mitochondrial outer membranes [57-60].

Mitochondrial trafficking is subject to exquisite regulations, such that distribution of mitochondrial subpopulations varies in response to multiple cellular cues, including intracellular local energy requirements, and local stimulation by extracelluar growth factors [61-63]. An increasing number of modulator proteins have been identified in regulation of mitochondrial distribution in cells [64, 65]. Although the exact mechanisms underlying are yet to be determined, several parameters in mitochondrial trafficking process have been shown that when altered by these modulator proteins, resulted in dramatic redistribution of mitochondria. These parameters include phosphorylation status, conformational changes, activities, and abundances of motor proteins, and association among motor proteins, adaptor proteins, and cargo proteins [66-68]. For example, KIF5B is a member of the kinesin superfamily. It functions to mediate anterograde transport of mitochondria toward cell periphery. Studies have shown that in cells that were depleted of KIF5B proteins, mitochondria appeared accumulating around nucleus as a combinatorial result of the defective anterograde transport by kinesin and the remaining retrograde transport by dynein [69]. Our results showed that ectopic expression of PGAM5-L (long) isoform resulted in the clustering of fragmented mitochondria at peri-nuclear regions, rather than widely distribution throughout cytoplasm, suggesting that PGAM5 may also function in mitochondrial trafficking [24]. It is likely that PGAM5 plays dual roles in morphogenesis and trafficking of mitochondria, such that a drastic increase in levels of PGAM5 due to overexpression shifts the equilibriums in both processes and in turn results in polarized morphology and distribution of mitochondria. In a similar tone, studies have indicated that Rho-family GTPase Miro may have such dual roles in mitochondrial morphogenesis and trafficking [51, 70]. Further investigation in

the biochemical functions and interacting proteins of Miro and PGAM5 in mitochondrial trafficking process will provide valuable insights into mechanisms underlying the regulation of mitochondrial dynamics.

REFERENCES

1.   Geetha, T. and M.W. Wooten, *Structure and functional properties of the ubiquitin binding protein p62.* FEBS Lett, 2002. **512**(1-3): p. 19-24.

2.   Sanchez, P., et al., *Localization of atypical protein kinase C isoforms into lysosome-targeted endosomes through interaction with p62.* Mol Cell Biol, 1998. **18**(5): p. 3069-80.

3.   Sanz, L., et al., *The interaction of p62 with RIP links the atypical PKCs to NF-kappaB activation.* Embo J, 1999. **18**(11): p. 3044-53.

4.   Feng, Y. and G.D. Longmore, *The LIM protein Ajuba influences interleukin-1-induced NF-kappaB activation by affecting the assembly and activity of the protein kinase Czeta/p62/TRAF6 signaling complex.* Mol Cell Biol, 2005. **25**(10): p. 4010-22.

5.   Sanz, L., et al., *The atypical PKC-interacting protein p62 channels NF-kappaB activation by the IL-1-TRAF6 pathway.* Embo J, 2000. **19**(7): p. 1576-86.

6.   Seibenhener, M.L., et al., *Sequestosome 1/p62 is a polyubiquitin chain binding protein involved in ubiquitin proteasome degradation.* Mol Cell Biol, 2004. **24**(18): p. 8055-68.

7.   Lo, S.-C., M. Hannink, *Characterization of physical and functional interactions between Keap1 and SQSTM1/p62. (unpublished work).* 2007.

8.   Ishii, T., et al., *Transcription factor Nrf2 coordinately regulates a group of oxidative stress-inducible genes in macrophages.* J Biol Chem, 2000. **275**(21): p. 16023-9.

9.   Ishii, T., et al., *Low micromolar levels of hydrogen peroxide and proteasome inhibitors induce the 60-kDa A170 stress protein in murine peritoneal macrophages.* Biochem Biophys Res Commun, 1997. **232**(1): p. 33-7.

10.   Liu, Y., et al., *A genomic screen for activators of the antioxidant response element.* Proc Natl Acad Sci U S A, 2007. **104**(12): p. 5205-10.

11. Okazaki, M., et al., *Cloning, expression profile, and genomic organization of the mouse STAP/A170 gene.* Genomics, 1999. **60**(1): p. 87-95.

12. Davis, M., et al., *Pseudosubstrate regulation of the SCF(beta-TrCP) ubiquitin ligase by hnRNP-U.* Genes Dev, 2002. **16**(4): p. 439-51.

13. Shintani, T. and D.J. Klionsky, *Autophagy in health and disease: a double-edged sword.* Science, 2004. **306**(5698): p. 990-5.

14. Lum, J.J., R.J. DeBerardinis, and C.B. Thompson, *Autophagy in metazoans: cell survival in the land of plenty.* Nat Rev Mol Cell Biol, 2005. **6**(6): p. 439-48.

15. Levine, B., *Eating oneself and uninvited guests: autophagy-related pathways in cellular defense.* Cell, 2005. **120**(2): p. 159-62.

16. Kondo, Y., et al., *The role of autophagy in cancer development and response to therapy.* Nat Rev Cancer, 2005. **5**(9): p. 726-34.

17. Ohsumi, Y., *Molecular dissection of autophagy: two ubiquitin-like systems.* Nat Rev Mol Cell Biol, 2001. **2**(3): p. 211-6.

18. Reggiori, F. and D.J. Klionsky, *Autophagy in the eukaryotic cell.* Eukaryot Cell, 2002. **1**(1): p. 11-21.

19. Levine, B. and D.J. Klionsky, *Development by self-digestion: molecular mechanisms and biological functions of autophagy.* Dev Cell, 2004. **6**(4): p. 463-77.

20. Bjorkoy, G., et al., *p62/SQSTM1 forms protein aggregates degraded by autophagy and has a protective effect on huntingtin-induced cell death.* J Cell Biol, 2005. **171**(4): p. 603-14.

21. Pankiv, S., et al., *p62/SQSTM1 binds directly to Atg8/LC3 to facilitate degradation of ubiquitinated protein aggregates by autophagy.* J Biol Chem, 2007. **282**(33): p. 24131-45.

22. Scherz-Shouval, R., et al., *Reactive oxygen species are essential for autophagy and specifically regulate the activity of Atg4.* Embo J, 2007. **26**(7): p. 1749-60.

23. Liu, Z. and M.J. Lenardo, *Reactive oxygen species regulate autophagy through redox-sensitive proteases.* Dev Cell, 2007. **12**(4): p. 484-5.

24. Lo, S.-C., M. Hannink, *PGAM5 anchors Keap1-Nrf2 complex at mitochondria, and regulates Nrf2-dependent gene expression. (submitted).* 2007.

25. Aspenstrom, P., A. Fransson, and J. Saras, *Rho GTPases have diverse effects on the organization of the actin filament system.* Biochem J, 2004. **377**(Pt 2): p. 327-37.

26. Stelzl, U., et al., *A human protein-protein interaction network: a resource for annotating the proteome.* Cell, 2005. **122**(6): p. 957-68.

27. Schultz, D.C., et al., *SETDB1: a novel KAP-1-associated histone H3, lysine 9-specific methyltransferase that contributes to HP1-mediated silencing of euchromatic genes by KRAB zinc-finger proteins.* Genes Dev, 2002. **16**(8): p. 919-32.

28. Ayyanathan, K., et al., *Regulated recruitment of HP1 to a euchromatic gene induces mitotically heritable, epigenetic gene silencing: a mammalian cell culture model of gene variegation.* Genes Dev, 2003. **17**(15): p. 1855-69.

29. Bernardo, M.V., et al., *Identification of apoptosis-related PLZF target genes.* Biochem Biophys Res Commun, 2007. **359**(2): p. 317-22.

30. Hong, S.H., et al., *SMRT corepressor interacts with PLZF and with the PML-retinoic acid receptor alpha (RARalpha) and PLZF-RARalpha oncoproteins associated with acute promyelocytic leukemia.* Proc Natl Acad Sci U S A, 1997. **94**(17): p. 9028-33.

31. Guidez, F., et al., *Histone acetyltransferase activity of p300 is required for transcriptional repression by the promyelocytic leukemia zinc finger protein.* Mol Cell Biol, 2005. **25**(13): p. 5552-66.

32. McConnell, M.J., et al., *Growth suppression by acute promyelocytic leukemia-associated protein PLZF is mediated by repression of c-myc expression.* Mol Cell Biol, 2003. **23**(24): p. 9375-88.

33.   Rothe, M., et al., *TRAF2-mediated activation of NF-kappa B by TNF receptor 2 and CD40.* Science, 1995. **269**(5229): p. 1424-7.

34.   Habelhah, H., et al., *Ubiquitination and translocation of TRAF2 is required for activation of JNK but not of p38 or NF-kappaB.* Embo J, 2004. **23**(2): p. 322-32.

35.   Fotin-Mleczek, M., et al., *Apoptotic crosstalk of TNF receptors: TNF-R2-induces depletion of TRAF2 and IAP proteins and accelerates TNF-R1-dependent activation of caspase-8.* J Cell Sci, 2002. **115**(Pt 13): p. 2757-70.

36.   Wu, C.J., et al., *TNF-alpha induced c-IAP1/TRAF2 complex translocation to a Ubc6-containing compartment and TRAF2 ubiquitination.* Embo J, 2005. **24**(10): p. 1886-98.

37.   Rigden, D.J., *Unexpected catalytic site variation in phosphoprotein phosphatase homologues of cofactor-dependent phosphoglycerate mutase.* FEBS Lett, 2003. **536**(1-3): p. 77-84.

38.   Rigden, D.J., et al., *Structure and mechanism of action of a cofactor-dependent phosphoglycerate mutase homolog from Bacillus stearothermophilus with broad specificity phosphatase activity.* J Mol Biol, 2002. **315**(5): p. 1129-43.

39.   Hamada, K., et al., *Crystal structure of the protein histidine phosphatase SixA in the multistep His-Asp phosphorelay.* Genes Cells, 2005. **10**(1): p. 1-11.

40.   Kowanetz, K., et al., *Suppressors of T-cell receptor signaling Sts-1 and Sts-2 bind to Cbl and inhibit endocytosis of receptor tyrosine kinases.* J Biol Chem, 2004. **279**(31): p. 32786-95.

41.   Davies, L., et al., *An unsuspected ecdysteroid/steroid phosphatase activity in the key T-cell regulator, Sts-1: surprising relationship to insect ecdysteroid phosphate phosphatase.* Proteins, 2007. **67**(3): p. 720-31.

42.   Mikhailik, A., et al., *A phosphatase activity of Sts-1 contributes to the suppression of TCR signaling.* Mol Cell, 2007. **27**(3): p. 486-97.

43.   Chi, H., et al., *Multiple inositol polyphosphate phosphatase: evolution as a distinct group within the histidine phosphatase family and chromosomal*

localization of the human and mouse genes to chromosomes 10q23 and 19. Genomics, 1999. **56**(3): p. 324-36.

44. Caffrey, J.J., et al., *The human and rat forms of multiple inositol polyphosphate phosphatase: functional homology with a histidine acid phosphatase up-regulated during endochondral ossification.* FEBS Lett, 1999. **442**(1): p. 99-104.

45. Shih, A.Y., et al., *Induction of the Nrf2-driven antioxidant response confers neuroprotection during mitochondrial stress in vivo.* J Biol Chem, 2005. **280**(24): p. 22925-36.

46. Youle, R.J. and M. Karbowski, *Mitochondrial fission in apoptosis.* Nat Rev Mol Cell Biol, 2005. **6**(8): p. 657-63.

47. Chan, D.C., *Mitochondria: dynamic organelles in disease, aging, and development.* Cell, 2006. **125**(7): p. 1241-52.

48. Chen, H., J.M. McCaffery, and D.C. Chan, *Mitochondrial fusion protects against neurodegeneration in the cerebellum.* Cell, 2007. **130**(3): p. 548-62.

49. Okamoto, K. and J.M. Shaw, *Mitochondrial morphology and dynamics in yeast and multicellular eukaryotes.* Annu Rev Genet, 2005. **39**: p. 503-36.

50. Hoppins, S., L. Lackner, and J. Nunnari, *The machines that divide and fuse mitochondria.* Annu Rev Biochem, 2007. **76**: p. 751-80.

51. Fransson, A., A. Ruusala, and P. Aspenstrom, *Atypical Rho GTPases have roles in mitochondrial homeostasis and apoptosis.* J Biol Chem, 2003. **278**(8): p. 6495-502.

52. Cipolat, S., et al., *Mitochondrial rhomboid PARL regulates cytochrome c release during apoptosis via OPA1-dependent cristae remodeling.* Cell, 2006. **126**(1): p. 163-75.

53. Karbowski, M., et al., *Role of Bax and Bak in mitochondrial morphogenesis.* Nature, 2006. **443**(7112): p. 658-62.

54. Nakamura, N., et al., *MARCH-V is a novel mitofusin 2- and Drp1-binding protein able to change mitochondrial morphology.* EMBO Rep, 2006. **7**(10): p. 1019-22.

55. Yonashiro, R., et al., *A novel mitochondrial ubiquitin ligase plays a critical role in mitochondrial dynamics.* Embo J, 2006. **25**(15): p. 3618-26.

56. Chen, H., et al., *Mitofusins Mfn1 and Mfn2 coordinately regulate mitochondrial fusion and are essential for embryonic development.* J Cell Biol, 2003. **160**(2): p. 189-200.

57. Chang, D.T. and I.J. Reynolds, *Mitochondrial trafficking and morphology in healthy and injured neurons.* Prog Neurobiol, 2006. **80**(5): p. 241-68.

58. Rice, S.E. and V.I. Gelfand, *Paradigm lost: milton connects kinesin heavy chain to miro on mitochondria.* J Cell Biol, 2006. **173**(4): p. 459-61.

59. Glater, E.E., et al., *Axonal transport of mitochondria requires milton to recruit kinesin heavy chain and is light chain independent.* J Cell Biol, 2006. **173**(4): p. 545-57.

60. Hollenbeck, P.J. and W.M. Saxton, *The axonal transport of mitochondria.* J Cell Sci, 2005. **118**(Pt 23): p. 5411-9.

61. Chada, S.R. and P.J. Hollenbeck, *Nerve growth factor signaling regulates motility and docking of axonal mitochondria.* Curr Biol, 2004. **14**(14): p. 1272-6.

62. Miller, K.E. and M.P. Sheetz, *Axonal mitochondrial transport and potential are correlated.* J Cell Sci, 2004. **117**(Pt 13): p. 2791-804.

63. Morris, R.L. and P.J. Hollenbeck, *The regulation of bidirectional mitochondrial transport is coordinated with axonal outgrowth.* J Cell Sci, 1993. **104 (Pt 3**): p. 917-27.

64. De Vos, K.J., et al., *Expression of phosphatidylinositol (4,5) bisphosphate-specific pleckstrin homology domains alters direction but not the level of axonal transport of mitochondria.* Mol Biol Cell, 2003. **14**(9): p. 3636-49.

65.   Gross, S.P., et al., *A determinant for directionality of organelle transport in Drosophila embryos.* Curr Biol, 2003. **13**(19): p. 1660-8.

66.   Sheetz, M.P., *Motor and cargo interactions.* Eur J Biochem, 1999. **262**(1): p. 19-25.

67.   Reilein, A.R., et al., *Regulation of molecular motor proteins.* Int Rev Cytol, 2001. **204**: p. 179-238.

68.   De Vos, K., et al., *Tumor necrosis factor induces hyperphosphorylation of kinesin light chain and inhibits kinesin-mediated transport of mitochondria.* J Cell Biol, 2000. **149**(6): p. 1207-14.

69.   Tanaka, Y., et al., *Targeted disruption of mouse conventional kinesin heavy chain, kif5B, results in abnormal perinuclear clustering of mitochondria.* Cell, 1998. **93**(7): p. 1147-58.

70.   Frederick, R.L., et al., *Yeast Miro GTPase, Gem1p, regulates mitochondrial morphology via a novel pathway.* J Cell Biol, 2004. **167**(1): p. 87-98.

VITA

Shih-Ching (Joyce) Lo was born in April, 1979 in Taipei, Taiwan. She received her B.S. in Life Sciences at Tsing-Hua University-Taiwan in June, 2001. She joined the Biochemistry Department at University of Missouri-Columbia in August, 2001, and received her Ph.D. in Biochemistry in October, 2007.